L'intérêt de l'imagerie dynamique 4-Dimensions dans la prise en charge chirurgicale des instabilités scapho-lunaires

Lionel Athlani

École Doctorale BioSE (Biologie-Santé-Environnement)

Thèse

Présentée et soutenue publiquement pour l'obtention du titre de

DOCTEUR DE l'UNIVERSITE DE LORRAINE

Mention : « Sciences de la Vie et de la Santé »

par **Lionel ATHLANI**

L'intérêt de l'imagerie dynamique 4-Dimensions dans la prise en charge chirurgicale des instabilités scapho-lunaires

Le 26 Mars 2021

Membres du jury :

Rapporteurs :

Madame Isabelle AUQUIT-AUCKBUR, Professeur, Université de Rouen, France
Monsieur Jean-Yves BEAULIEU, Professeur, Université de Genève, Suisse

Examinateurs :

Monsieur Gilles DAUTEL, Professeur, Université de Lorraine, France
Madame Marie FARUCH-BILFELD, Professeur, Université de Toulouse, France
Monsieur Pedro Augusto GONDIM TEIXEIRA, Professeur, Université de Lorraine, France (directeur de thèse)
Monsieur Didier MAINARD, Professeur, Université de Lorraine, France

---

Laboratoire IADI, INSERM U1254, CIC-IT Nancy, Université de Lorraine, Bâtiment Recherche, CHRU de Nancy Brabois, 5 Rue du Morvan, 54500 Vandœuvre-lès-Nancy.

École Doctorale BioSE (Biologie-Santé-Environnement)

Thèse

Présentée et soutenue publiquement pour l'obtention du titre de

DOCTEUR DE l'UNIVERSITE DE LORRAINE

Mention : « Sciences de la Vie et de la Santé »

par **Lionel ATHLANI**

L'intérêt de l'imagerie dynamique 4-Dimensions dans la prise en charge chirurgicale des instabilités scapho-lunaires

Le 26 Mars 2021

Membres du jury :

Rapporteurs :

Madame Isabelle AUQUIT-AUCKBUR, Professeur, Université de Rouen, France
Monsieur Jean-Yves BEAULIEU, Professeur, Université de Genève, Suisse

Examinateurs :

Monsieur Gilles DAUTEL, Professeur, Université de Lorraine, France
Madame Marie FARUCH-BILFELD, Professeur, Université de Toulouse, France
Monsieur Pedro Augusto GONDIM TEIXEIRA, Professeur, Université de Lorraine, France (directeur de thèse)
Monsieur Didier MAINARD, Professeur, Université de Lorraine, France

---

Laboratoire IADI, INSERM U1254, CIC-IT Nancy, Université de Lorraine, Bâtiment Recherche, CHRU de Nancy Brabois, 5 Rue du Morvan, 54500 Vandœuvre-lès-Nancy.

REMERCIEMENTS

À l'issue de la rédaction de ce travail de recherche, je suis convaincu que la thèse est loin d'être un travail solitaire. En effet, je n'aurais jamais pu réaliser ce travail doctoral sans le soutien d'un grand nombre de personnes dont la générosité, la bonne humeur et l'intérêt manifesté à l'égard de ma recherche m'ont permis de mener à bien ce projet doctoral.

En premier lieu, je tiens à remercier chaleureusement Monsieur le Professeur Jacques FELBLINGER, directeur du *Laboratoire IADI*, pour m'avoir donné l'opportunité de rejoindre son équipe et travailler au sein de ce magnifique laboratoire. J'ai été sensible à ses qualités humaines d'écoute, de grande disponibilité et son soutien sans faille.

Je souhaiterais exprimer ma gratitude à Monsieur le Professeur Pedro TEIXEIRA, mon directeur de thèse et ami, pour la confiance qu'il m'a accordée en acceptant d'encadrer ce travail doctoral, pour ses multiples conseils et pour toutes les heures qu'il a consacré à diriger cette recherche. Je le remercie pour son accueil chaleureux à chaque fois que j'ai sollicité son aide, ainsi que ses nombreux encouragements. Je trouve que nous formons un super binôme et j'espère que nous continuerons notre partenariat.

Mes remerciements vont également aux membres de mon jury pour avoir accepté d'évaluer mon travail et m'apporter de nouvelles pistes de réflexion.

Aux professeurs Isabelle AUQUIT-AUCKBUR et Jean-Yves BEAULIEU, vont mes remerciements pour avoir accepté la fonction de rapporteur.

Je remercie Madame le Professeur Isabelle AUQUIT-AUCKBUR, pour vos encouragements et votre message de sympathie lors de ma candidature pour devenir membre du Collège Français des Enseignants en Chirurgie de la Main. J'apprécie votre enthousiasme pour la formation des jeunes chirurgiens de la main. Votre motivation est communicative.

J'aimerais remercier chaleureusement Monsieur le Professeur Jean-Yves BEAULIEU, pour son accueil au sein de son unité durant mon année de mobilité. Je souhaiterais vous exprimer ma gratitude pour toutes les attentions que vous portez à mon égard afin que mon année puisse se dérouler à merveille. C'est un immense plaisir d'échanger quotidiennement avec vous sur la chirurgie de la main. J'apprécie énormément votre ouverture d'esprit, votre disponibilité, vos connaissances et votre enthousiasme à chaque projet de recherche que nous concevons et réalisons. C'est pour moi une chance de travailler à vos côtés et je suis heureux de vous compter parmi les membres de mon jury.

Monsieur le Professeur Gilles DAUTEL, Cher Maître, j'aimerais vous remercier chaleureusement pour l'attention, l'enthousiasme et l'intérêt que vous manifestez constamment à l'égard de chacune de mes idées et chacun de mes projets. J'espère que vous apprécierez ce travail de thèse qui reflète au mieux l'évolution de notre réflexion sur l'instabilité scapho-lunaire et son traitement. Comme vous le savez, j'affectionne tout particulièrement le projet « SLIC » et suis heureux d'avoir pu travailler avec vous et Nicolas, sur le développement, l'évaluation et la diffusion de cette technique chirurgicale. J'ai adoré parcourir la France et l'Europe à vos côtés pour communiquer sur nos travaux scientifiques et pouvoir pousser notre réflexion encore plus loin. Je suis particulièrement reconnaissant pour l'enseignement chirurgical que vous m'avez transmis, mais aussi votre goût de l'excellence et votre envie constante de faire avancer notre belle spécialité chirurgicale.

Je remercie Madame le Professeur Marie FARUCH-BILFELD, pour avoir participé à mon comité de suivi de thèse et avoir apporté son analyse de spécialiste en imagerie ostéo-articulaire. Vous me faites l'honneur de participer à ce jury et je vous en remercie.

Monsieur le Professeur Didier MAINARD, je tiens à vous témoigner ma reconnaissance pour votre disponibilité et vos nombreux conseils concernant mon projet professionnel. Je vous remercie pour l'honneur que vous me faites en participant à ce jury.

Je remercie Monsieur le Professeur François SIRVEAUX, pour l'aide apportée à la réalisation de mon projet professionnel. J'apprécie le fait que vous preniez régulièrement des nouvelles de son avancée. Je vous remercie d'avoir participé à mon comité de suivi de thèse et m'avoir donné de nombreux conseils pour mener à terme ce projet doctoral.

Un grand merci à Gabriela HOSSU pour son aide précieuse dans l'analyse méthodologique et statistique de nos différentes études. Merci pour tes conseils avisés.

Un grand merci à Nicolas WEBER pour son aide précieuse à la réalisation des dispositifs de recherche de ce travail de thèse. J'ai adoré concevoir à tes côtés notre dispositif de guidage du mouvement du poignet. Merci pour ta disponibilité et ton efficacité.

Un grand merci à Marine KREBS du laboratoire d'anatomie, à Frédérique GROUBATCH-JOINEAU et Marion LUCAS de l'École de chirurgie, pour leur aide précieuse dans la réalisation de mes études anatomiques.

Je tiens également à remercier les docteurs Nicolas PAUCHARD, Romain DETAMMAECKER, Yoan-Kim DE ALMEIDA, Jonathan GRANERO et Aymeric RAUCH pour leur participation active dans les différentes études de ce travail doctoral. J'ai été extrêmement sensible à votre motivation à l'égard de mon travail.

Ces remerciements seraient incomplets si je n'en adressais pas à l'ensemble de mes collègues du *Laboratoire IADI*. Merci de m'avoir permis de réaliser mon travail de recherche dans un environnement convivial et propice au développement de compétences scientifiques. Je me réjouis de faire partie de votre famille !

Je voudrais remercier l'ensemble des équipes médicales et paramédicales du *Centre Chirurgical Émile Gallé et du Service d'imagerie Guilloz, du CHRU de Nancy*, pour leur collaboration dans la réalisation de nos différentes études.

Ma reconnaissance va également à ceux qui ont plus particulièrement assuré le soutien affectif de ce travail doctoral : ma famille, ma belle-famille et mes amis.

Enfin, j'adresse mille et mille mercis à Lucie, ma compagne, ma moitié, pour son soutien de tous les jours, pour sa présence et son écoute, pour sa patience et pour son amour. Je suis tellement heureux d'avoir croisé ta route et de t'avoir rencontré. Je t'envoie tout mon amour !

RÉSUMÉ

L'instabilité scapho-lunaire est difficile à diagnostiquer et à traiter. En l'absence de traitement, elle évolue vers l'arthrose du poignet. Au stade statique, le diagnostic est évident lorsqu'une analyse radiographique minutieuse est effectuée, mais le choix du traitement chirurgical n'est pas aussi simple. Au stade dynamique, le diagnostic est plus difficile à poser sur la base unique de méthodes d'imagerie statiques (radiographies, tomodensitométrie ou IRM), ce qui justifie qu'une arthroscopie exploratoire puisse être nécessaire avant le traitement chirurgical. Bien qu'il s'agisse d'une procédure invasive, l'arthroscopie est considérée par de nombreuses équipes chirurgicales comme le gold standard pour explorer l'espace articulaire scapho-lunaire. L'imagerie dynamique, telle que le scanner dynamique quatre dimensions (4DCT), peut analyser les modifications des espaces articulaires du carpe lors des mouvements du poignet. Au vu des résultats de notre étude prospective, le 4DCT est apparu comme un outil pertinent multiparamétrique quantitatif et reproductible pour le diagnostic et le pronostic de l'instabilité scapho-lunaire suspectée, y compris pour les patients présentant des résultats radiographiques douteux. Les valeurs anormales des paramètres cinématiques semblent indiquer des changements biomécaniques significatifs dans les poignets dissociés. De plus, l'analyse 4DCT a démontré une correspondance avec l'analyse dynamique arthroscopique de l'espace articulaire scapho-lunaire. Plusieurs techniques de ligamentoplastie ont été décrites pour traiter l'instabilité scapho-lunaire réductible, chronique et sans lésions chondrales. Leur objectif commun est de corriger les anomalies radiologiques afin de prévenir des risques d'arthrose. Ces procédures ont servi de base à plusieurs études cliniques, et si ces dernières partagent de bons résultats cliniques similaires, l'aspect radiographique est très variable, où la récidive des anomalies radiologiques est fréquente. Ainsi, nous avons mis au point la ligamentoplastie scapho-lunaire et inter-carpienne (SLIC) qui utilise un transplant libre de Palmaris Longus pour reconstruire le complexe scapho-lunaire. Avec un suivi à court et moyen terme, nous rapportons des résultats cliniques et radiologiques satisfaisants, et aucun cas d'arthrose. Dans une étude cadavérique, nous avons évalué en 4DCT cette ligamentoplastie et fourni des preuves supplémentaires de son efficacité dans la réduction de l'instabilité scapho-lunaire et la restauration de la stabilité articulaire de ce couple. Nous avons également décrit une nouvelle capsulotomie comme approche dorsale de l'articulation du poignet, et ses avantages sur la préservation des structures anatomiques, en particulier des fibres des ligaments extrinsèques dorsaux. Enfin, nous avons conçu un dispositif de guidage des mouvements du poignet, afin d'augmenter la reproductibilité et l'homogénéité du mouvement lors de l'acquisition d'imageries dynamiques.

ABSTRACT

Scapholunate instability is challenging to diagnose and to treat. If left untreated, it contributes to the development of wrist osteoarthritis. In the static stage, diagnosis is obvious when a careful radiographic analysis is performed, but the choice of surgical treatment is not as straightforward. In the dynamic stage, diagnosis is harder to make solely based on static imaging methods (radiographs, CT or MR arthrogram), which means exploratory arthroscopy may be required prior to surgical treatment. Despite it is an invasive procedure, arthroscopy is considered by many surgical teams, as the gold standard to explore the scapholunate joint space. Dynamic imaging, such as the four-dimensional computed tomography (4DCT), can analyze changes in the carpal joint spaces during wrist movements. Given our prospective study's findings, 4DCT appeared as a quantitative multiparametric and reproductible relevant tool for the diagnosis and prognosis of suspected scapholunate instability, including for patients with questionable radiography findings. Abnormal kinematic parameters values seem to be indicative of significant biomechanical changes in the dissociated wrists. Moreover, 4DCT analysis demonstrated correspondence with the arthroscopic dynamic analysis of the scapholunate joint space. Several ligamentoplasty techniques have been described to treat chronic reducible scapholunate instability without chondral lesions. Their common objective is to correct radiological anomalies in order to prevent risk of osteoarthritis. These procedures have served as the basis for several clinical studies and while all the latter share similar good clinical results, the radiographic aspect varies widely, with frequently the recurrence of radiological anomalies. Thus, we described the scapholunate intercarpal ligamentoplasty (SLIC) which uses a free Palmaris Longus graft to reconstruct the scapholunate complex. At short to mid-term follow-up, we report satisfactory clinical and radiological results, and no osteoarthritis wrist case. In a cadaver study, we reported the 4DCT evaluation of that ligamentoplasty and provided additional evidence of its effectiveness in reducing scapholunate instability and restoring scapholunate joint stability. We also described a new capsulotomy-based dorsal approach to the wrist joint, and its advantages with regards to preserving anatomical structures, especially the dorsal extrinsic ligaments fibers. Finally, we designed a device for guiding wrist movements in order to increase the reproducibility and homogeneity of the movement during dynamic imaging acquisition.

TABLE DES MATIÈRES

ABRÉVIATIONS

4DCT	*Four dimensional CT (Scanner dynamique quatre dimensions)*
CT	*Computerized tomography (Tomodensitométrie)*
DCSS	*Dorsal Capsulo-Scapholunate Septum (Septum capsulo-scapho-lunaire dorsal)*
DIC	*Dorsal intercarpal (Inter-carpien dorsal)*
DISI	*Dorsal Intercaled Segment Instability*
DRC	*Dorsal radiocarpal (Radio-carpien dorsal)*
DRU	*Déviation radio-ulnaire*
Gy	*Gray*
ISL	*Instabilité scapho-lunaire*
LCA	*Lunocapitate angle (Angle capito-lunaire)*
LIOSL	*Ligament inter-osseux scapho-lunaire*
PRSA	*Posterior radioscaphoid angle (Angle postérieur radio-scaphoïdien)*
RLC	*Radio-lunaire court*
RLL	*Radio-lunaire long*
RSA	*Radioscaphoid angle (Angle radio-scaphoïdien)*
RSC	*Radio-scapho-capital*
Se	*Sensibilité*
SLA	*Scapholunate angle (Angle scapho-lunaire)*
SLAC	*Scapho Lunate Advanced Collapse*
SLG	*Scapholunate gap (Espace scapho-lunaire)*
Sp	*Spécificité*
SPS	*Subluxation postéro-latérale du scaphoïde*
STT	*Scapho-trapézo-trapézien*
Sv	*Sievert*
T	*Tesla*

TABLE DES FIGURES

Figure 10. Méthode de mesure radiographique du PRSA (Gondim Teixeira et al., 2016). Le point le plus postérieur du scaphoïde (C) est sélectionné. Puis, les bords postérieurs (A) et antérieurs (B) de la fossette scaphoïdienne du radius sont identifiés. Deux lignes sont ensuite tracées, l'une du point A au point C et l'autre du point A au point B. L'angle formé par ces deux lignes correspond au PRSA (ici valeur de 105°).

Figure 11. IRM de poignet droit objectivant une lésion du LIOSL. A : Incidence axiale en pondération T1 mettant en évidence un hyper-signal dans la portion dorsale du LIOSL (flèche indiquant la localisation de la rupture LIOSL). B : Incidence axiale en pondération T2 fat-sat mettant en évidence un hypo-signal de cette même lésion LIOSL (flèche indiquant la localisation de la rupture LIOSL). C : Incidence coronale en pondération T2 révélant par hypo-signal une rupture du LIOSL (indiquée par la pointe de la flèche).

Figure 12. Schémas et vues arthroscopiques d'un poignet au niveau de l'articulation médio-carpienne. Le testing de la congruence articulaire scapho-lunaire est réalisé par le crochet du palpeur. A : Le crochet est introduit dans l'espace entre le scaphoïde (1) et le lunatum (3). La tête du capitatum est visible en haut (2), de même que le Ligament RSC (4). B : Sous l'effet du mouvement de torsion appliqué au crochet, un diastasis se démasque entre le scaphoïde (1) et le lunatum (3). L'articulation scapho-lunaire s'ouvre et les reliquats ligamentaires (5) deviennent visibles au niveau de l'articulation radio-carpienne.

Figure 13. Représentation graphique tridimensionnelle d'un poignet droit, au niveau de la première rangée du carpe, expliquant la positivité du test arthroscopique de Corella et al., (2013) en cas d'ISL. A-B-C : En vue latérale, la pression externe sur le tubercule du scaphoïde (flèche verte) entraine la SPS (C). D-E-F : Vues axiales de la même manœuvre (flèches vertes) entrainant un déplacement dorsal du pôle proximal du scaphoïde. La manœuvre se révèle positive lorsqu'elle entraine un déplacement scaphoïdien de proximal en distal (aspect de marche d'escalier au niveau de l'interligne scapho-lunaire), une translation radiale du scaphoïde par rapport au lunatum (diastasis) ainsi qu'une bascule dorsale du pôle proximal du scaphoïde.

Figure 14. Radiographies de face en position neutre (A) puis en inclinaison ulnaire (B) d'un poignet gauche. Vues per-opératoires (B et C) après arthrotomie dorsale du poignet de type Berger et al., (1995). L'ISL suspectée en radiographie standard (A – flèche rouge) s'est confirmée en per-opératoire (B – flèche blanche). On note la bonne mobilité du scaphoïde avec sa reverticalisation lors du cliché radiographique en inclinaison ulnaire (C – flèche rouge), et la confirmation de la réductibilité de l'ISL en per-opératoire (D – flèche blanche).

Figure 15. Schémas représentant les techniques de Brunelli modifiée par Van Den Abbeele (Van Den Abbeele et al., 1998) et de Garcia-Elias (Garcia-Elias et al., 2006) qui utilisent une bandelette de Flexor Carpi Radialis laissée pédiculée en distal.

Figure 16. Reconstructions 3D à partir d'acquisitions en 4DCT mettant en évidence une ISL. A : Vue dorsale du carpe avec présence d'un diastasis scapho-lunaire (flèche) et d'une projection dorsale du pôle proximal du scaphoïde (S). Le lunatum (L) présente un aspect de bascule dorsale ou DISI. B : Vue latérale du carpe avec présence d'une SPS responsable d'un contact entre le pôle proximal du scaphoïde et la berge dorsale du radius (Carr et al., 2018).

Figure 17. Coupes scanographiques sagittales et reconstruction 3D à partir d'acquisitions en 4DCT d'un poignet en position neutre (A) puis en inclinaison radiale maximale (B). A : En position neutre, on note un scaphoïde centré par rapport à la glène radiale. B : En inclinaison radiale maximale, apparaît une SPS responsable d'un contact entre le pôle proximal du scaphoïde et la berge dorsale du radius (Kakar et al., 2016).

Figure 18. Évaluation tridimensionnelle du déplacement du scaphoïde après section des stabilisateurs ligamentaires du complexe scapho-lunaire (Mat Jais et al., 2017).

Figure 19. Photographies illustrant la procédure d'acquisition en 4DCT. A. Le patient, protégé par un tablier de plomb, est assis à côté du scanner, son poignet est en position neutre, placé sur la table du scanner et reposant sur des coussinets en mousse. B. La capture d'écran d'une tablette montre l'amplitude et la vitesse de déplacement en DRU du poignet (à droite), et la vision directe de l'installation du patient (à gauche) (Rauch et al., 2018).

Figure 20. Plans de référence et position des points repères utilisés pour effectuer les mesures des SLG (A), LCA (B) et PRSA (C), sur des images scanographiques multiplanaires. A : Pour la construction du SLG, deux marqueurs ont été placés sur le scaphoïde et le lunatum, à hauteur de la distance la plus courte entre ces deux os, dans le plan axial passant par la styloïde radiale (flèche fine) et la styloïde ulnaire (flèche épaisse) (Abou Arab et al., 2018). B : Pour la construction du LCA, deux marqueurs ont été placés sur les cornes palmaire et dorsale du lunatum, et deux autres marqueurs ont été positionnés le long du grand axe du capitatum, dans le plan sagittal situé le plus près du centre de la fossette lunarienne du radius (Rauch et al., 2018). C : Pour la construction du PRSA, deux marqueurs ont été placés sur les bords postérieur et antérieur de la fossette scaphoïdienne du radius, et deux autres marqueurs ont été positionnés au niveau du point le plus dorsal du scaphoïde et sur le bord postérieur de la fossette scaphoïdienne, dans le plan sagittal situé le plus près du centre de la fossette scaphoïdienne du radius (Gondim-Teixeira et al., 2021).

Figure 38. Photographies du système de réglage des amplitudes d'inclinaisons radiales et ulnaires, comprises entre 10° et 30°.

Figure 39. Photographie montrant la compatibilité en termes d'encombrement du dispositif avec la table d'examen du scanner Aquilion One du *service d'imagerie Guilloz*. À noter la simulation hors acquisition scanographique, de l'installation sur le dispositif du membre supérieur droit d'un médecin volontaire.

Figure 40. Acquisition scanographique (scanner Aquilion One du *service d'imagerie Guilloz*) du dispositif, centrée sur la zone d'intérêt à analyser, montrant l'absence d'artéfact induit par le capteur électronique (cercles rouges).

Figure 41. Photographies illustrant l'installation du membre droit d'un volontaire sain sur le dispositif GWMD avec son poignet positionné à 0° puis en inclinaison radiale à 10°, 20°, 30° et en inclinaison ulnaire à 10°, 20°, 30°.

Figure 42. Acquisition en IRM dynamique du poignet droit d'un volontaire sain pendant un mouvement de DRU. Images coronales du poignet dans les positions d'inclinaisons radiale (A), neutre (B) et ulnaire (C) lors de la manœuvre continue de déviation. Il s'agit d'une séquence RF-Spoiled Radial FLASH : voxel size (mm^3) = 0.62x0.62x5, temporal resolution (ms) = 600, TR/TE (ms) = 4.65/2.27.

TABLE DES TABLEAUX

INTRODUCTION GENERALE

Le LIOSL est un ligament intrinsèque essentiel du carpe (Carlsen et Shin, 2008; Kitay et Wolfe, 2012; Kijima et Viegas, 2009; Kamal et al., 2016; Taleisnik, 1985; Short et al., 2002; Short et al., 2005; Short et al., 2007). Selon Ward et al., (2015), sa lésion est la plus fréquemment retrouvée dans le spectre lésionnel des pathologies ligamentaires du poignet.
L'ISL représente la principale instabilité du carpe (Carlsen et Shay, 2008; Kani et al., 2016). Elle touche le plus souvent des patients jeunes ou d'âge moyen en activité professionnelle (Pliefke et al., 2007). Un traumatisme isolé à haute énergie ou des microtraumatismes répétés, dus à l'activité professionnelle, représentent les principaux facteurs en cause (Murphy et al., 2018). Il est acquis que cette pathologie fait suite à une combinaison de lésions ligamentaires dont celle du LIOSL, mais également d'autres stabilisateurs tels que les ligaments extrinsèques palmaires et dorsaux du carpe (Berger, 1997; Viegas et al., 1999; Short et al., 2002; Short et al., 2005; Short et al., 2007). La genèse des différents stades de cette instabilité, et les ligaments progressivement impliqués ne sont actuellement pas établis. Toutefois, Watson et Ballet précisaient en 1984, l'évolution naturelle de cette pathologie vers le développement d'une arthrose de poignet dite « SLAC ».

L'ISL est responsable de douleurs chroniques invalidantes de poignet avec diminution progressive de la force de poigne et des mobilités articulaires entrainant un retentissement sur les activités quotidiennes et professionnelles. Ainsi, elle constitue un réel enjeu socio-économique. L'ISL pose des difficultés tant diagnostiques que thérapeutiques (Crawford et al., 2016). Sur le plan diagnostique, les outils d'imagerie conventionnels présentent des insuffisances majeures conduisant de multiples auteurs à réaliser une étape chirurgicale pré-thérapeutique à visée purement diagnostique : l'arthroscopie exploratrice (Dautel et al., 1993; Geissler, 1996; Messina et al.,2013; Löw et al., 2017). Sur le plan thérapeutique, au stade pré-arthrosique, de multiples techniques de ligamentoplastie sont décrites dans la littérature pour traiter l'ISL (Crawford et al., 2016). Leur objectif commun est de reconstruire les stabilisateurs ligamentaires lésés afin de réduire la dissociation et ainsi prévenir le risque à long terme du collapsus arthrosique. Ces diverses procédures chirurgicales ont servi de base à plusieurs études cliniques. Même si ces dernières partagent de bons résultats cliniques similaires, l'aspect radiographique reste très variable. En effet, la récidive à court et moyen terme des anomalies radiologiques est fréquemment observée.

L'objectif initial principal de cette thèse est d'évaluer l'intérêt de l'imagerie dynamique quatre dimensions dans la prise en charge chirurgicale des ISL. Ce manuscrit est composé de quatre chapitres incluant l'ensemble des articles publiés ou en cours d'évaluation pour publication. Il est composé d'études anatomiques cadavériques, d'études cliniques prospectives et d'une étude portant sur la conception d'un dispositif de recherche.

Tout d'abord, le premier chapitre abordera l'état des connaissances en termes d'ISL, et introduira les différentes problématiques actuelles permettant de définir nos axes de recherche qui serviront à émettre nos hypothèses. Dans ce premier chapitre, nous traiterons des concepts actuels sur la physiopathologie de l'ISL, sa problématique diagnostique et ses enjeux thérapeutiques.

Le deuxième chapitre sera consacré à l'apport du 4DCT dans le bilan diagnostic et pronostic des ISL. Grâce à ce nouvel outil d'imagerie, nous évaluerons, par des études cliniques prospectives, les différentes caractéristiques anatomiques de l'ISL.

Le troisième chapitre s'intéressera au traitement chirurgical conservateur de ces ISL. Après une revue de la littérature sur les différentes options de reconstruction existantes, nous proposerons la description d'une nouvelle technique chirurgicale qui fera l'objet d'évaluations cliniques prospectives et anatomiques cadavériques avec l'utilisation des outils d'imagerie conventionnels ainsi que du 4DCT.

Enfin, le dernier chapitre sera destiné à la conception et au cahier des charges d'un dispositif de recherche destiné à guider et enregistrer les mouvements du poignet pour les acquisitions en imagerie dynamique.

LISTE DES PUBLICATIONS ET COMMUNICATIONS

- **Articles publiés :**

Athlani L, Pauchard N, Dautel G. Radiological evaluation of scapholunate intercarpal ligamentoplasty for chronic scapholunate dissociation in cadavers. *J Hand Surg Eur Vol*. 2018, 43:387-393.

Athlani L, Pauchard N, Detammaecker R, Huguet S, Lombard J, Dap F, Dautel G. Treatment of chronic scapholunate dissociation with tenodesis: A systematic review. *Hand Surg Rehabil*. 2018, 37:65-76.

Athlani L, Pauchard N, Dautel G. Outcomes of scapholunate intercarpal ligamentoplasty for chronic scapholunate dissociation. A prospective study in 26 patients. *J Hand Surg Eur Vol*. 2018, 43:700-707.

Athlani L, Pauchard N, Dautel G. Treatment of chronic scapholunate instability: results with three-ligament tenodesis versus scapholunate and intercarpal ligamentoplasty. *Hand Surg Rehabil.* 2019, 38:157-164.

Athlani L, Rouizi K, Granero J, Gabriela H, Blum A, Dautel G, Teixeira P.A.G. Assessment of scapholunate instability with dynamic computed tomography. *J Hand Surg Eur Vol.* 2020, 45:375-382.

Athlani L, Pauchard N, Dautel G. Intercarpal ligamentoplasty for scapholunate dissociation: comparison of two techniques. *J Hand Surg Eur Vol.* 2020, 19:1753193420940498.

Athlani L, Granero J, Rouizi K, Hossu G, Blum A, Dautel G, Gondim Teixeira PA. Evaluation of dorsal scaphoid displacement using posterior radioscaphoid angle in patients with suspected scapholunate instability : a preliminary study. *J Hand Surg Am*. 2021, 46:10-16.

Athlani L, Granero J, Rouizi K, Hossu G, Blum A, Dautel G, Gondim Teixeira PA. Four-dimensional CT analysis of Dorsal Intercalated Segment Instability in patients with suspected scapholunate instability. *J Wrist Surg*. 2021, 1:1-7.

Athlani L, Rauch A, Weber N, Blum A, Dautel G, Gondim Teixeira PA. Quantitative Four-dimensional CT evaluation of scapholunate intercarpal ligamentoplasty for scapholunate dissociation: a cadaveric study. *Journal Hand Surgery Eur Vol*. 2020, 26:1753193420973883.

Athlani L, Sapa MC, De Almeida YK, Braun M, Dautel G. A new capsulotomy-based dorsal approach to the wrist: a cadaver study**.** *Hand Surg Rehabil*. 2020, 10:S2468-1229(20)30233-4.

- **Article soumis :**

Granero J, Orkut S, Rauch A, Blum A, Dautel G, Gondim Teixeira PA, Athlani L. Dynamic 4D computed tomography data corresponds well to dynamic arthroscopic testing of scapholunate instability: a preliminary study. *J Hand Surg Am.* 2021.

- **Communications orales :**

Athlani L, Pauchard N, Dautel G. Résultats préliminaires de la ligamentoplastie « SLIC » dans le traitement de la dissociation scapho-lunaire. *50° Congrès de la société Française de chirurgie de la Main (SFCM)*, Paris, Décembre 2014.

Athlani L, Pauchard N, Dautel G. Résultats préliminaires de la ligamentoplastie « SLIC » dans le traitement de la dissociation scapho-lunaire. *90° Congrés de la société Francaise de Chirurgie Orthopédique et Traumatologique (SOFCOT)*, Paris, Novembre 2015.

Athlani L, Pauchard N, Dap F, Dautel G. Étude biomécanique cadavérique de la ligamentoplastie « SLIC » dans le traitement de la dissociation scapho-lunaire. *52° Congrès de la société Française de chirurgie de la Main (SFCM)*, Paris, Décembre 2016.

Athlani L, Pauchard N, Dap F, Dautel G. La ligamentoplastie SLIC dans le traitement de la dissociation scapho-lunaire : étude biomécanique cadavérique. *92° Congrés de la société Francaise de Chirurgie Orthopédique et Traumatologique (SOFCOT),* Paris, Novembre 2017.

Athlani L, Pauchard N, Dap F, Dautel G. La ligamentoplastie SLIC dans le traitement de la dissociation scapho-lunaire : résultats cliniques au recul minimum de 12 mois. *92° Congrés de la société Francaise de Chirurgie Orthopédique et Traumatologique (SOFCOT),* Paris, Novembre 2017.

Athlani L, Pauchard N, Dap F, Dautel G. La ligamentoplastie ScaphoLunaire et InterCarpienne « SLIC » dans le traitement de la dissociation scapho-lunaire. A propos d'une modification de la technique opératoire. *53° Congrès de la société Française de chirurgie de la Main (SFCM),* Paris, Décembre 2017.

Athlani L, Dautel G. Arthrex Symposium : Des solutions innovantes pour vos chirurgies de la main et du poignet : Ligamentoplastie ScaphoLunaire InterCarpien (SLIC), nouvelle version. Ligamentoplastie du pouce. *53° Congrès de la société Française de chirurgie de la Main (SFCM),* Paris, Décembre 2017.

Athlani L, Pauchard N, Dautel G. SLIC Reconstruction as an alternative to the triple tenodeis for scapholunate dissociation. *Congrés annuel de la Société Belge de Chirurgie de la main (BHG)*, Tournai, May 2018.

Athlani L, Dautel G. SLIC reconstruction : Further technical refinements. *Congrés annuel de la Société Belge de Chirurgie de la main (BHG),* Tournai, May 2018.

Athlani L, Pauchard N, DAP F, Dautel G. Traitement de l'instabilité scapho-lunaire chronique : résultats avec la triple ténodèse versus la ligamentoplastie ScaphoLunaire et InterCarpienne. *93° Congrés de la société Francaise de Chirurgie Orthopédique et Traumatologique (SOFCOT),* Paris, Novembre 2018.

Athlani L, Pauchard N, DAP F, Dautel G. Traitement de l'instabilité scapho-lunaire chronique : résultats avec la triple ténodèse versus la ligamentoplastie ScaphoLunaire et InterCarpienne. *54° Congrès de la société Française de chirurgie de la Main (SFCM),* Paris, Décembre 2018.

Athlani L, Granero J, Rouizi K, Blum A, Dautel G, Gondim Teixeira PA. Apport du TDM dynamique 4D au bilan d'évaluation en imagerie des instabilités scapho-lunaires du poignet. *55° Congrès de la société Française de chirurgie de la Main (SFCM),* Paris, Décembre 2019.

Athlani L. Arthrex Symposium : instabilité scapho-lunaire en 2019, what's hot what's not. Traitements et techniques de réparation du ligament scapho-lunaire. Diagnostic en Scanner 4D et SLIC ligamentoplastie. *55° Congrès de la société Française de chirurgie de la Main (SFCM)*, Paris, Décembre 2019.

- **Communications affichées :**

Athlani L, Pauchard N, Dautel G. Radiological evaluation of the ScaphoLunate InterCarpal Ligamentoplasty for chronic scapholunate dissociation in cadavers. *Congrés de la Federation of European Societies for Surgery of the Hand (FESSH),* Copenhagen, Juin 2018.

Athlani L, Pauchard N, Dautel G. Preliminary results of the ScaphoLunate InterCarpal Ligamentoplasty for chronic scapholunate dissociation in a prospective study. *Congrés de la Federation of European Societies for Surgery of the Hand (FESSH),* Copenhagen, Juin 2018.

Athlani L, Pauchard N, Dautel G. Preliminary results of the scapholunate intercarpal ligamentoplasty in a prospective study. *73RD Annual Meeting of the ASSH*, Boston, Septembre 2018.

Athlani L, Pauchard N, Dautel G. Radiological evaluation of the scapholunate intercarpal ligamentoplasty in cadavers. *73RD Annual Meeting of the ASSH,* Boston, Septembre 2018.

Athlani L, Pauchard N, Dautel G. Results with a three-ligament tenodesis versus a scapholunate and intercarpal ligamentoplasty. *73RD Annual Meeting of the ASSH*, Boston, Septembre 2018.

CHAPITRE 1.
CONTEXTE ET PROBLÉMATIQUES

Le complexe scapho-lunaire : une entité ligamentaire unique

Ce complexe représente une réelle entité ligamentaire influençant la cinétique du carpe (Salva-coll et al., 2013; Kamal et al., 2016; Kani et al., 2016; Kijima et al., 2009; Kitay et Wolfe, 2012; Rajan et Day, 2015; Short et al., 2002; Short et al., 2005; Short et al., 2007; Taleisnik, 1985). Au sein de celui-ci, le LIOSL représente la clé de voute. Il s'agit d'un ligament intrinsèque, intra-articulaire, reliant le scaphoïde et le lunatum (Figure 1). En forme de « C » ou « U inversé », il s'insère sur les berges dorsales, proximales et palmaires du scaphoïde et du lunatum, laissant entre ces deux os un espace ouvert en distal. Il est formé de trois portions qui ont une structure et des propriétés distinctes : les portions dorsales et palmaires sont de vraies structures ligamentaires, constituées de fibres de collagène et d'un tissu de soutien contenant des pédicules vasculo-nerveux, alors que la portion intermédiaire est un fibrocartilage fin et avasculaire. La portion dorsale, constituée de fibres transversales, est la partie la plus épaisse (3 mm) et offre le plus de stabilité de l'articulation scapho-lunaire (Ranjan et Day, 2015; Berger et al., 1999; Kitay et Wolfe, 2012). Le LIOSL n'est pas suffisant pour assurer à lui seul, l'ensemble de la stabilité du couple scapho-lunaire.

***Figure 1**. Représentations schématiques et anatomiques (flèche rouge) du LIOSL avec ses trois portions. La portion palmaire (P) en vert ; la portion centrale (I) en jaune ; la portion dorsale (D) en bleu.*

Pour Viegas et al., (1999) et Short et al., (2002; 2005; 2007), même si le LIOSL est le stabilisateur principal de l'articulation scapho-lunaire, d'autres ligaments stabilisateurs du complexe sont tout aussi importants. Parmi eux, sont classiquement cités des ligaments extrinsèques dorsaux tels que le DRC, le DIC et le DCISS (Van de Overstraeten et al., 2013) ; mais aussi des ligaments extrinsèques palmaires tels que le RSC, le RLL et enfin le complexe ligamentaire STT (Figures 2 et 3). De Roo et al., (2019) ont montré par une modélisation 3D

des mouvements du scaphoïde et du lunatum, que l'axe de rotation du couple scapho-lunaire passait par la portion dorsale du pôle proximal du scaphoïde et par l'arête dorsale du lunatum. Le scaphoïde avait une flexion moyenne de 38° par rapport au lunatum lors d'un mouvement de flexion-extension du poignet.

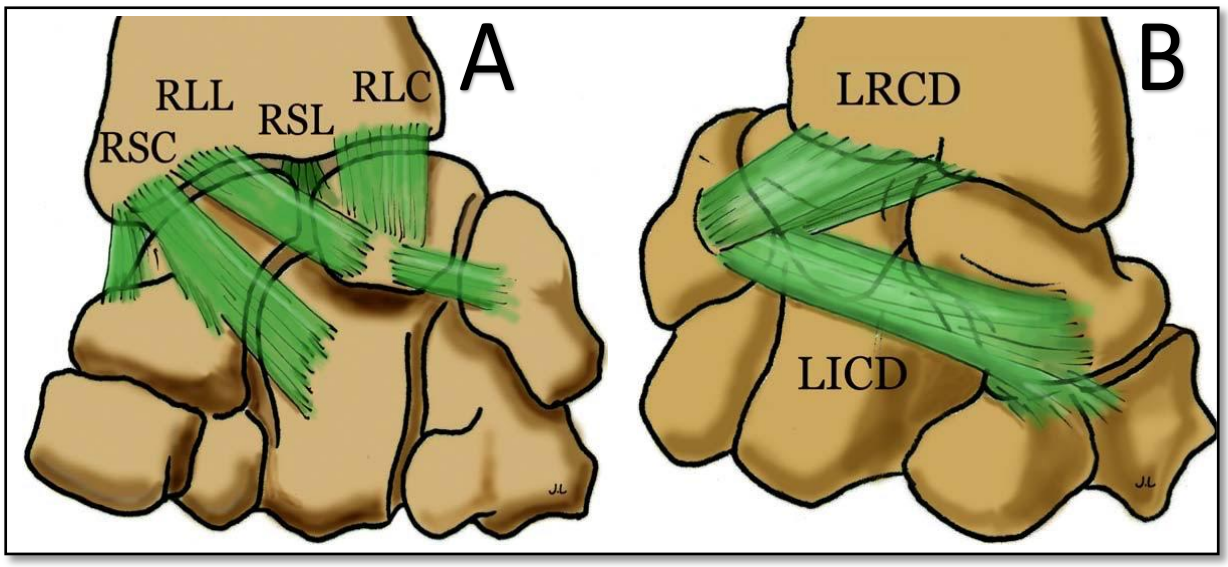

Figure 2. *Schéma représentant les ligaments extrinsèques palmaires (A) et dorsaux (B) (d'après Laulan, 2009).* ***A*** *: RSC : radio-scapho-capital ; RLL : long radio-lunaire ; RLC : court radio-lunaire ; RSL : radio-scapho-lunaire.* ***B*** *: LRCD : ligament radio-carpien dorsal ; LICD : ligament inter-carpien dorsal.*

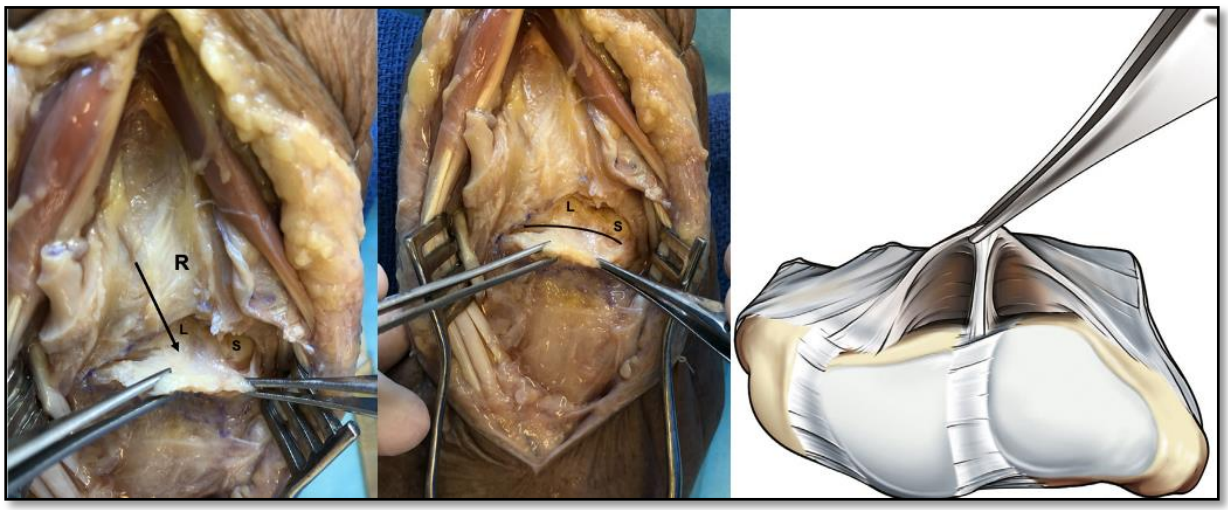

Figure 3*. Représentations anatomiques (flèche et ligne noires) et schématiques du* DCSS (Van Overstraeten et al., 2013). Il s'agit d'une structure fibreuse, étendue depuis la face profonde de *la capsule articulaire (notamment le ligament DIC) vers la portion dorsale du LIOSL. R : radius, S : scaphoïde, L : lunatum.*

L'instabilité dissociative scapho-lunaire : définition et concepts actuels

Linscheid et al., (1972) ont décrit le concept d'instabilité du carpe par une modification des rapports normaux entre les os du carpe. Cette instabilité est dite « dissociative » lorsqu'elle concerne deux os d'une même rangée carpienne et « non dissociative » lorsqu'il s'agit d'os des deux rangées carpiennes. L'ISL est donc une instabilité dissociative du carpe.

Larsen et al., (1995) ont proposé une classification en fonction du délai du traumatisme, supposé responsable de l'instabilité : à moins d'une semaine, il s'agit d'une instabilité aigüe pour laquelle la cicatrisation ligamentaire primaire est envisageable ; entre 2 et 6 semaines, la lésion est classée comme subaigüe et il existe encore des possibilités de cicatrisation primaire mais dans des conditions plus difficiles ; au-delà de 6 semaines, on parle de lésion chronique avec de très faibles possibilités de cicatrisation primaire. Taleisnik entre 1985 et 1990 a introduit les notions d'instabilités dynamique et statique ; il s'agit d'une définition radiologique. L'instabilité dynamique est visible sur des clichés dynamiques ou en stress (poing serré), alors que l'instabilité statique est mise en évidence sur des radiographies standards de face et de profil strict.

Watson et al., (1993) ajoutaient la notion d'instabilité pré-dynamique ou occulte qui représente une instabilité sans anomalie radiologique rendant l'arthroscopie exploratrice indispensable au diagnostic. Sous sa forme statique, l'ISL se caractérise anatomiquement par un écart scapho-lunaire pathologique ou diastasis, par une instabilité en extension du lunatum ou Dorsal Intercaled Segment Instability – DISI – et par un déplacement dorsal du scaphoïde ou subluxation postéro-latérale du scaphoïde – SPS – (Laulan et al., 2009) (Figure 4).

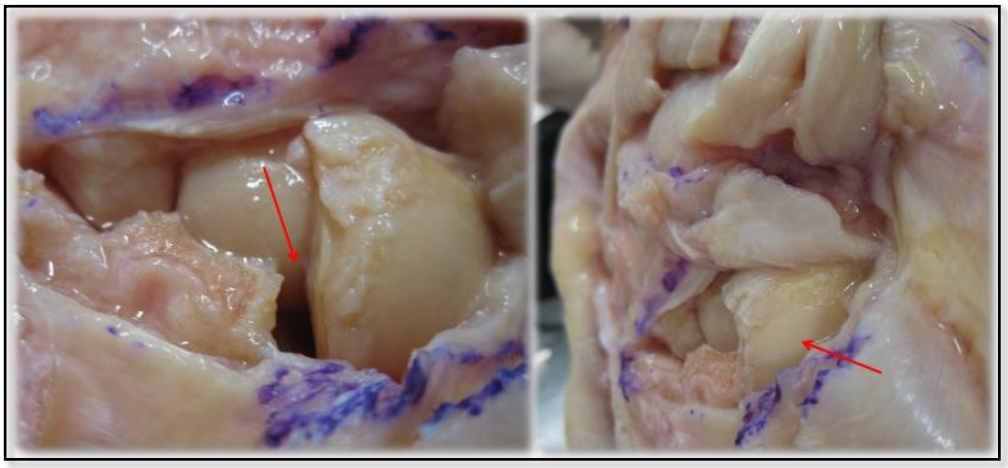

Figure 4. *Vues anatomiques d'une ISL. Les flèches rouges indiquent le diastasis scapho-lunaire (photographie de gauche) et la SPS (photographie de droite).*

Une lésion complète du LIOSL n'est pas forcément synonyme d'ISL statique (Taleisnik, 1985; Kani et al., 2016; Kijima et al., 2009; Kitay et Wolfe, 2012; Rajan et Day, 2015). C'est l'atteinte associée du LIOSL et d'autres structures stabilisatrices, notamment les ligaments DRC, DIC, et DCSS, qui entrainerait le passage du stade dynamique à statique (Viegas et al., 1999; Short et al., 2002; Short et al., 2005; Short et al., 2007; Van Overstraeten et al., 2013). Aucune certitude n'existe en ce qui concerne l'aggravation des ISL occultes vers le stade dynamique (Kitay and Wolfe, 2012). En revanche le passage d'une instabilité dynamique en statique est largement admis, même si selon Taleisnik (1988), il difficile de prédire que toutes instabilités dynamiques évolueraient vers un stade statique. Selon Watson et Ballet (1984), la survenue d'une arthrose SLAC n'est certaine qu'au stade d'ISL statique. La SPS est responsable d'un contact entre la berge dorsale du radius et le pôle proximal du scaphoïde aboutissant à l'arthrose radio-scaphoïdienne. La déformation en DISI est responsable d'un décentrage médio-carpien, source de l'arthrose capito-lunaire (Figure 5).

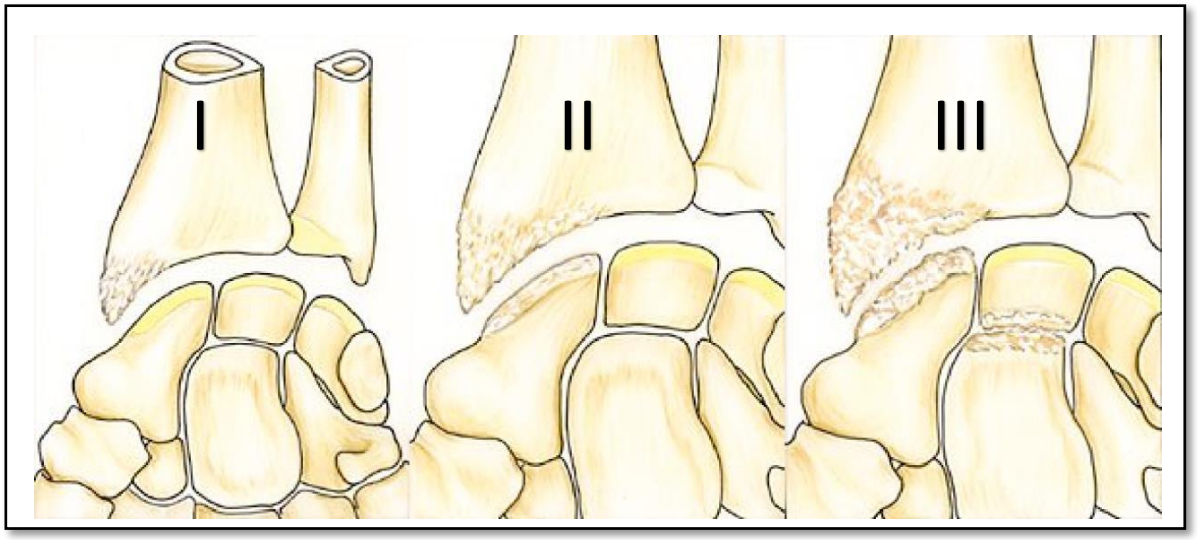

***Figure 5**. Classification de l'arthrose « SLAC wrist » selon Watson et al., (1993). Stade I : arthrose stylo-scaphoïdienne. Stade II : arthrose radio-scaphoïdienne. Stade III : arthrose capito-lunaire.*

Tant sur le plan clinique que sur le plan de l'imagerie conventionnelle, leurs insuffisances respectives font que le diagnostic de l'ISL reste à ce jour un véritable challenge. En effet, aucun signe clinique ne semble pathognomonique d'une ISL. La principale plainte est une douleur chronique à la face dorsale du poignet en regard de l'articulation scapho-lunaire, majorée à la dorsiflexion. La perte de force et la raideur articulaire du poignet sont également classiques (Kitay et Wolfe, 2012; Guss et al., 2015) mais non systématiques. Certaines manœuvres dynamiques existent : le test décrit par Watson et al., (1988) a pour objectif de détecter une douleur déclenchée par une pression exercée sur le tubercule scaphoïde lors du passage du poignet d'une position d'inclinaison ulnaire en inclinaison radiale. Il est classique d'observer en cas de dissociation scapho-lunaire, la présence d'un ressaut associé à la douleur.

En cas de suspicion clinique d'ISL, le bilan d'imagerie initial associe le plus souvent, en France, des radiographies et un arthroscanner. Les radiographies doivent être bilatérales, standards de face et de profil strict, mais également dynamiques de face poings serrés (Gilula, 1978; Megerle et al., 2011; Lawland et Foulkes, 2003; Pliefke et al., 2008). L'objectif est l'identification de signes indirects d'ISL (Figures 6 et 7). Cependant, la présence d'un critère radiographique avec une valeur supérieure à la normale, n'est pas nécessairement synonyme de pathologique. Picha et al., (2012) rapportaient une majorité d'anomalies radiologiques (52% de SLG pathologiques, 70% de SLA anormaux) bilatérales chez des patients asymptomatiques.

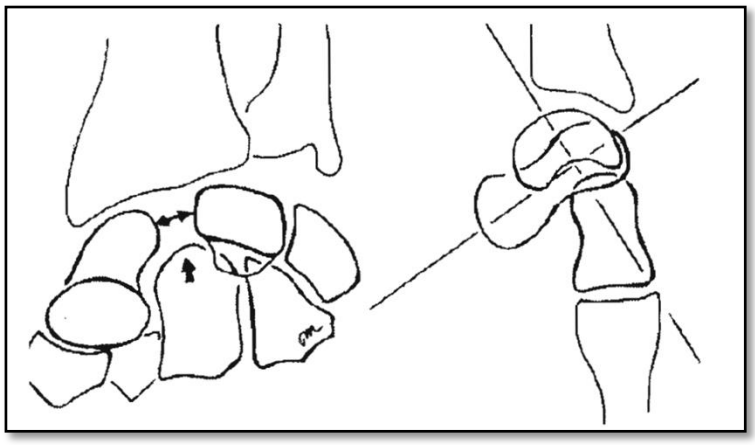

Figure 6. *Schéma représentant les signes radiographiques retrouvés dans l'ISL statique. On note le diastasis scapho-lunaire, la déformation en DISI et la SPS.*

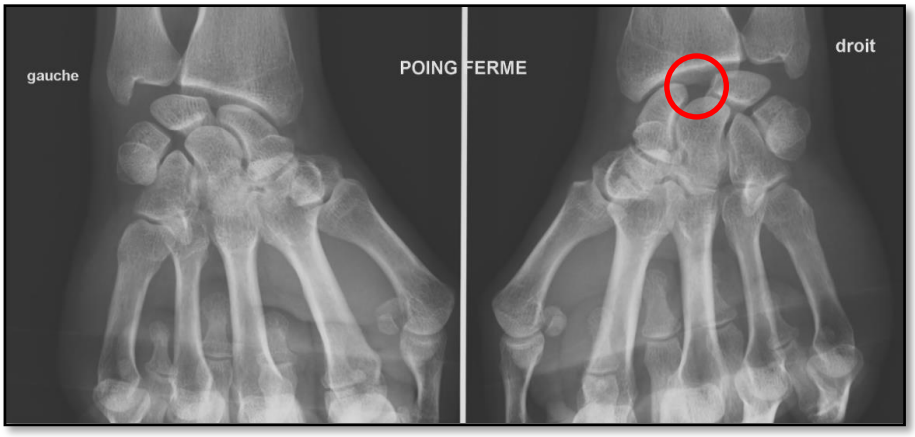

Figure 7. *Exemple radiographique d'une ISL dynamique avec apparition d'un diastasis scapho-lunaire sur le cliché de face poing serré, poignet droit.*

Depuis plusieurs années, l'arthroscanner est un outil d'imagerie fréquemment utilisé pour le diagnostic de rupture du LIOSL (Shahabpour et al., 2015; Bille et al., 2007; Cognet et al., 2008). Par l'injection d'un produit de contraste, il permet d'identifier des lésions ligamentaires intrinsèques du carpe de façon indirecte en testant la perméabilité de chaque ligament (Figure 8).

Figure 8. *Arthroscanner d'un poignet droit en coupe coronale montrant des signes de rupture du LIOSL : Passage du produit de contraste depuis l'articulation médio-carpienne vers l'articulation radio-carpienne. À noter le reliquat ligamentaire (flèche rouge).*

Différentes études ont montré la bonne performance diagnostique de l'arthroscanner pour mettre en évidence une rupture partielle ou totale du LIOSL. Pour Schmid et al., (2005), sa sensibilité atteignait 100% et sa spécificité 77%. Pour Kitay et Wolfe, (2012), la première était de 95% et la seconde de 86%. Toutefois, la positivité de l'examen pour une lésion ligamentaire ne signifie pas l'existence d'une ISL (Kitay et Wolfe, 2012; Rajan et Day, 2015), car il s'agit le plus souvent d'un état pathologique dynamique, à l'exception des stades statiques plus avancés, pour lesquels la dissociation intra-carpienne ne fait aucun doute sur des radiographies standards. La SPS semble représenter un élément essentiel dans le diagnostic d'une ISL, quel que soit son stade. Sa mise en évidence sur des clichés radiographiques de profil ou des incidences scanographiques sagittales est possible ; le repère étant la tangente à la corne postérieure du lunatum et la position du pôle proximal du scaphoïde par rapport à celle-ci (Athlani et al., 2018-3) (Figure 9). Toutefois, la mise en évidence de ce signe lors de stade précoce de SPS est fortement influencée par la grande variabilité des incidences d'imagerie statique, rendant cette analyse parfois difficile. Ainsi, Gondim Teixeira et al., (2016) préfèrent mesurer le PRSA sur des incidences sagittales scanographiques (Figure 10). Ils le considèrent comme un facteur pronostic d'évolution arthrosique. Une valeur supérieure à 114° semblerait associée à la présence de signes d'arthrose SLAC dans 80% des cas, avec une sensibilité et une spécificité respectivement de 80% et 90%.

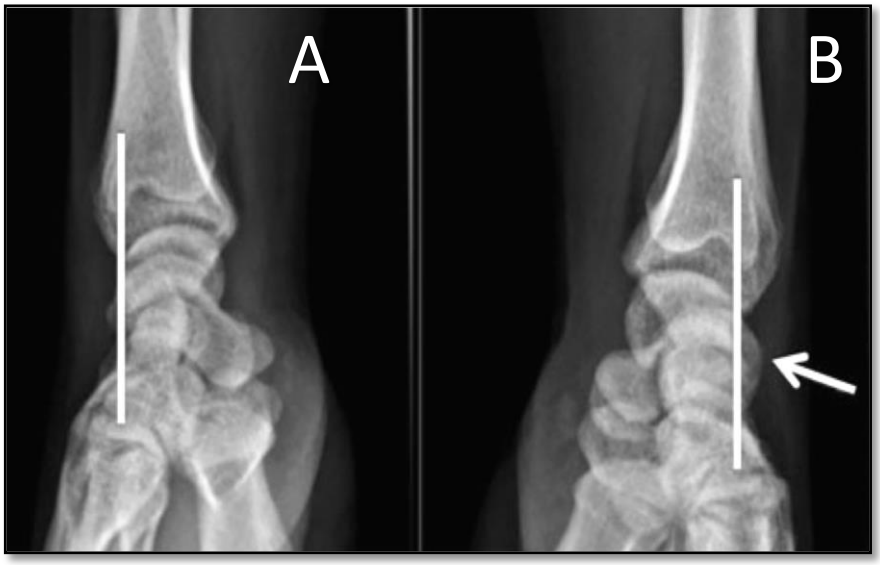

Figure 9. *Radiographies de poignet de profil strict. Évaluation radiographique de la SPS selon Athlani et al., (2018-3).* ***A :*** *Aucun déplacement postérieur du pôle proximal n'apparaît en l'absence d'ISL, avec un scaphoïde parfaitement centré sous sa fossette radiale.*
B : *En cas d'ISL, on visualise le déplacement dorsal du pôle proximal du scaphoïde par rapport à la tangente à la corne postérieure du lunatum.*

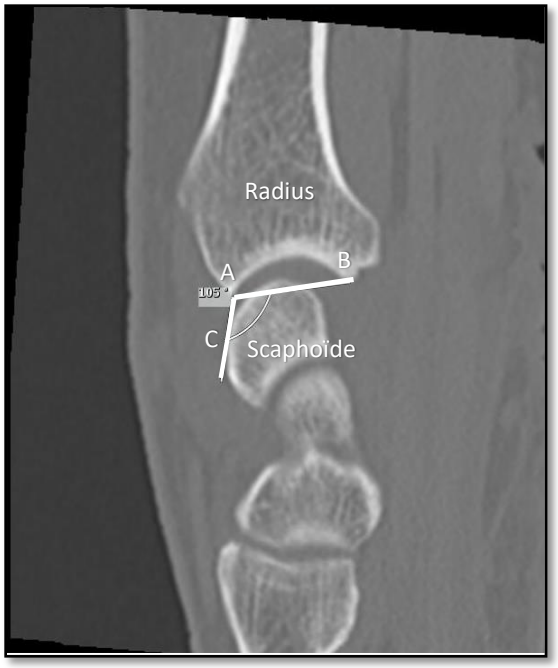

Figure 10. *Méthode de mesure radiographique du PRSA (Gondim Teixeira et al., 2016). Le point le plus postérieur du scaphoïde (C) est sélectionné. Puis, les bords postérieur (A) et antérieur (B) de la fossette scaphoïdienne du radius sont identifiés. Deux lignes sont ensuite tracées, l'une du point A au point C et l'autre du point A au point B. L'angle formé par ces deux lignes correspond au PRSA (ici valeur de 105°).*

Alternative non invasive, l'IRM a fait l'objet de beaucoup d'articles (Johnstone et al., 1997; Scheck et al., 1997; Schädel-Höpfner et al., 2001; Mahmood et al., 2012; Morley et al., 2001; Hazefi-Nejad et al., 2016). Par son analyse morphologique, elle permet de visualiser directement les lésions ligamentaires et cartilagineuses. Il est cependant nécessaire d'utiliser des machines performantes de type 3,0T et des protocoles précis, utilisant notamment des séquences 3D en écho de gradient, afin d'objectiver les lésions des ligaments intrinsèques. Plusieurs études récentes ont comparé les mêmes séquences à 1,5T et 3,0T (Saupe et al., 2005; Anderson et al., 2015). La qualité subjective et le rapport signal sur bruit des images étaient significativement plus élevés en 3,0T. Magee (2009), avec une IRM 3,0T, retrouvait une spécificité de 100% avec une sensibilité de 89% pour le diagnostic d'une lésion du LIOSL. L'injection de gadolinium accentue ces zones déjà hyper-intenses en pondération T2. De plus, les structures ligamentaires extrinsèques peuvent être visualisées (Özkan et al., 2019). L'inconvénient reste toujours sa disponibilité limitée (notamment pour les IRM 3T) et son coût (Figure 11). En outre, comme pour l'arthroscanner, il s'agit d'un examen statique tout aussi inadapté pour les stades dynamiques de la pathologie.

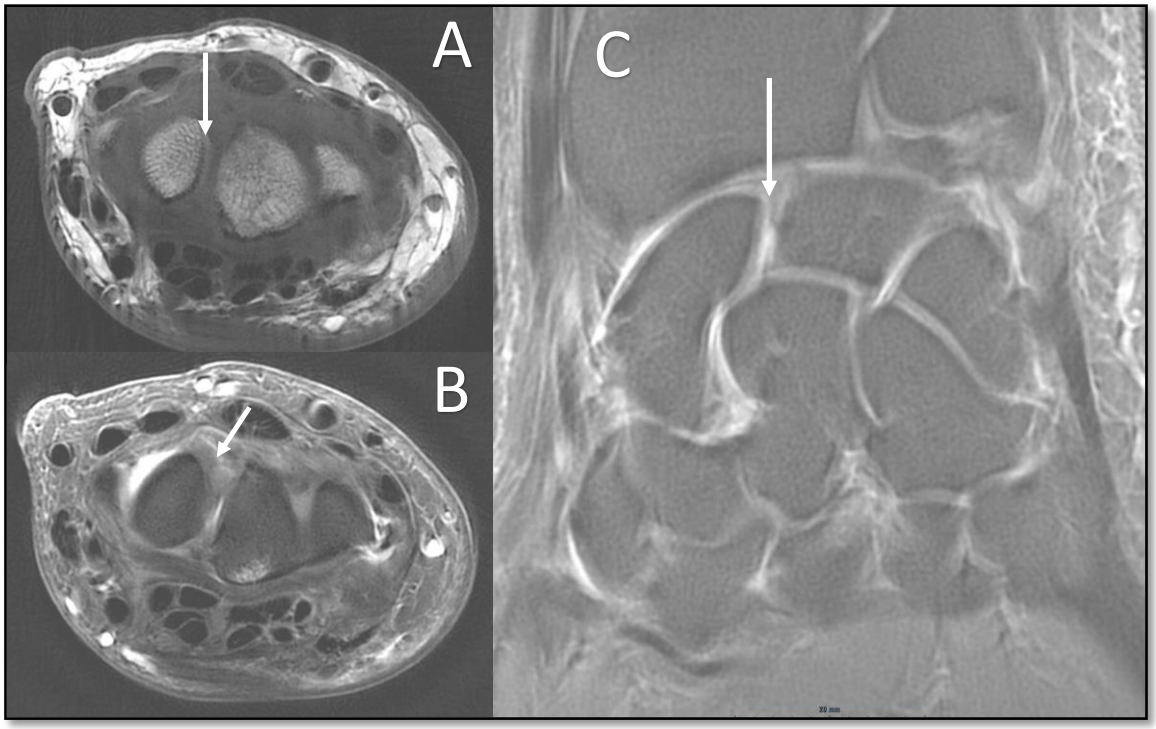

***Figure 11**. IRM de poignet droit objectivant une lésion du LIOSL.*
***A** : Incidence axiale en pondération T1 mettant en évidence un hyper-signal dans la portion dorsale du LIOSL (flèche indiquant la localisation de la rupture LIOSL).*
***B** : Incidence axiale en pondération T2 fat-sat mettant en évidence un hypo-signal de cette même lésion LIOSL (flèche indiquant la localisation de la rupture LIOSL).*
***C** : Incidence coronale en pondération T2 révélant par hypo-signal une rupture du LIOSL (indiquée par la pointe de la flèche).*

Au final, les examens complémentaires en imagerie conventionnelle sont des examens statiques visant à confirmer le diagnostic de lésion du LIOSL (plus ou moins les ligaments extrinsèques du carpe), sans pourvoir affirmer celui d'ISL notamment à des stades précoces. En effet, le comportement dynamique du couple scapho-lunaire est impossible à analyser par ces examens d'imagerie. Seuls des signes indirects d'ISL sont visualisables. Au stade statique, même si les signes radiologiques sont évidents, il est également difficile d'évaluer la mobilité du scaphoïde et donc la réductibilité de cet état de dissociation.

Devant cette insuffisance de performance diagnostique, une majorité d'auteurs recommande l'utilisation première pré-thérapeutique de l'arthroscopie exploratrice (Dautel et al., 1993; Bille et al.,2007; Johnstone et al., 1997; Morley et al., 2001). Cette intervention chirurgicale permet d'établir le diagnostic certain d'une atteinte ligamentaire intrinsèque, mais aussi une gradation de la sévérité lésionnelle. Elle rend précis l'évaluation des surfaces articulaires avec des lésions décelables dès le stade de chondrite.

Par la réalisation de divers tests dynamiques, l'arthroscopie évalue le comportement du scaphoïde et de l'articulation scapho-lunaire. Ceci permet de confirmer le diagnostic d'ISL à des stades précoces non visibles en imagerie conventionnelle.

L'articulation scapho-lunaire doit être normalement serrée et congruente, sans aucune « ouverture » possible lors des tests dynamiques. Parmi ces derniers, un état d'ISL peut être mis en évidence par l'introduction du crochet d'un palpeur arthroscopique dans l'articulation scapho-lunaire, et par la possibilité de dissocier le scaphoïde du lunatum par un mouvement de « twist » (Figure 12). Dautel et Merle (1993), puis plus récemment Corella et al., (2013), décrivaient un autre test dynamique complémentaire (Figure 13). Par une pression manuelle externe sur le tubercule du scaphoïde en direction dorsale, ce test cherche à identifier en cas d'état d'ISL, un déplacement non harmonieux du scaphoïde par rapport au lunatum.

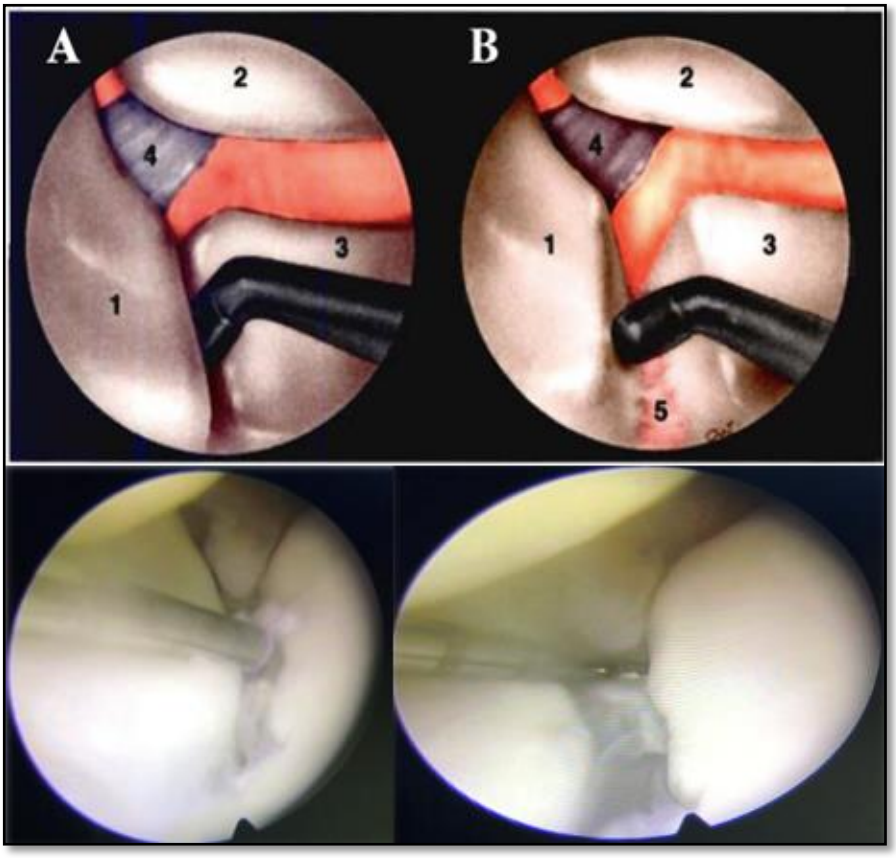

Figure 12. *Schémas et vues arthroscopiques d'un poignet au niveau de l'articulation médio-carpienne. Le testing de la congruence articulaire scapho-lunaire est réalisé par le crochet du palpeur.*
A : *Le crochet est introduit dans l'espace entre le scaphoïde (1) et le lunatum (3). La tête du capitatum est visible en haut (2), de même que le ligament RSC (4).*
B : *Sous l'effet du mouvement de torsion appliqué au crochet, un diastasis se démasque entre le scaphoïde (1) et le lunatum (3). L'articulation scapho-lunaire s'ouvre et les reliquats ligamentaires (5) deviennent visibles au niveau de l'articulation radio-carpienne.*

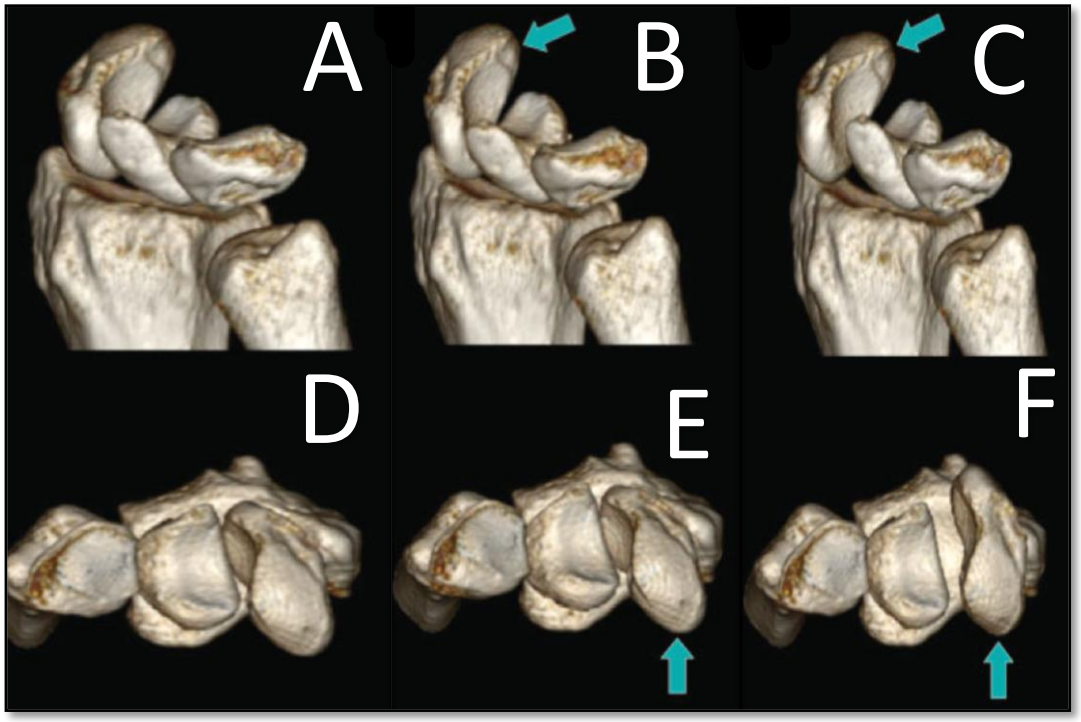

Figure 13. *Représentation graphique tridimensionnelle d'un poignet droit, au niveau de la première rangée du carpe, expliquant la positivité du test arthroscopique de Corella et al., (2013) en cas d'ISL.*
A-B-C : *En vue latérale, la pression externe sur le tubercule du scaphoïde (flèches vertes) entraine la SPS (**C**).*
D-E-F *: Vues axiales de la même manœuvre (flèches vertes) entrainant un déplacement dorsal du pôle proximal du scaphoïde.*
La manœuvre se révèle positive lorsqu'elle entraine un déplacement scaphoïdien de proximal en distal (aspect de marche d'escalier au niveau de l'interligne scapho-lunaire), une translation radiale du scaphoïde par rapport au lunatum (diastasis scapho-lunaire) ainsi qu'une bascule dorsale du pôle proximal du scaphoïde.

Dans un objectif de quantification de l'ISL, de nombreuses classifications arthroscopiques ont été développées afin de graduer l'ISL. Ces classifications associent le plus souvent une analyse morphologique de l'état du ligament, à un testing dynamique de l'articulation scapho-lunaire par le crochet palpeur (Dréant et Dautel, 2003; Dréant et al., 2009; Geissler et al., 1996; Messina et al., 2013). Dans tous les cas, le stade 0 (absence d'ISL) correspond à l'impossibilité de faire pénétrer le crochet au sein de l'espace scapho-lunaire. Malgré tout, Löw et al., (2017) rapportaient le fait que même en l'absence d'ISL, l'introduction du crochet dans l'interligne scapho-lunaire (stade 1) était possible chez des patients présentant une laxité physiologique. Ils confirmaient cependant, l'impossibilité de réaliser un mouvement de « twist » ouvrant l'espace.

De plus, l'arthroscopie reste une intervention chirurgicale avec de potentiels risques interventionnels. Leclerc et Mathoulin (2016), dans leur étude portant sur plus de 10.000 arthroscopies de poignet, retrouvaient un taux de complication de 6%. Ils notaient l'échec de réalisation de la procédure chirurgicale comme l'une des complications les plus fréquentes. Les risques de lésions nerveuses, ainsi que les lésions cartilagineuses étaient également mis en avant. Obdeijn et al., (2013) mettaient en évidence la variabilité inter et intra-observateur de l'arthroscopie de poignet, due notamment à une longue courbe d'apprentissage. Ces variabilités auraient tendance à freiner la reproductibilité des tests et donc la performance diagnostique de l'arthroscopie exploratrice.

La reconstruction chirurgicale du complexe scapho-lunaire pour traiter l'instabilité chronique avant l'arthrose : un véritable challenge.

Depuis la fin des années 1970, plusieurs techniques de reconstruction du complexe scapho-lunaire, ou ligamentoplasties, ont été décrites (Almquist et al., 1991; Bain et al., 2013; Brunelli and Brunelli, 1995; De Carli et al., 2011; Garcia-Elias et al., 2006; Linscheid et Dobyns, 1992; Ross et al., 2013; Van Den Abbeele et al., 1998). Ces techniques sont proposées dans les ISL chroniques, réductibles, sans moignon ligamentaire réparable, sans lésion chondrale. Elles ont pour objectif de corriger le diastasis, la DISI et la SPS, en utilisant un transplant tendineux libre ou pédiculé, dans le but d'améliorer la symptomatologie et de préserver à long terme du collapsus arthrosique (Laulan, 2001; Garcia-Elias et Geissler, 2005). Le caractère réductible de l'ISL est difficilement évaluable. Sur le cliché radiographique de face en inclinaison ulnaire, on cherche à observer une reverticalisation du scaphoïde montrant toute sa longueur. Lors de l'arthroscopie, il est également possible de juger de la mobilité préservée du scaphoïde, et donc de la correction plausible de l'ISL. La réductibilité complète est définitivement confirmée en début de chirurgie. À l'issue de l'arthrotomie, et préalablement à la réalisation de la ligamentoplastie, une étape initiale de réduction de l'ISL par manœuvres externes permettra de poser définitivement l'indication (Figure 14).

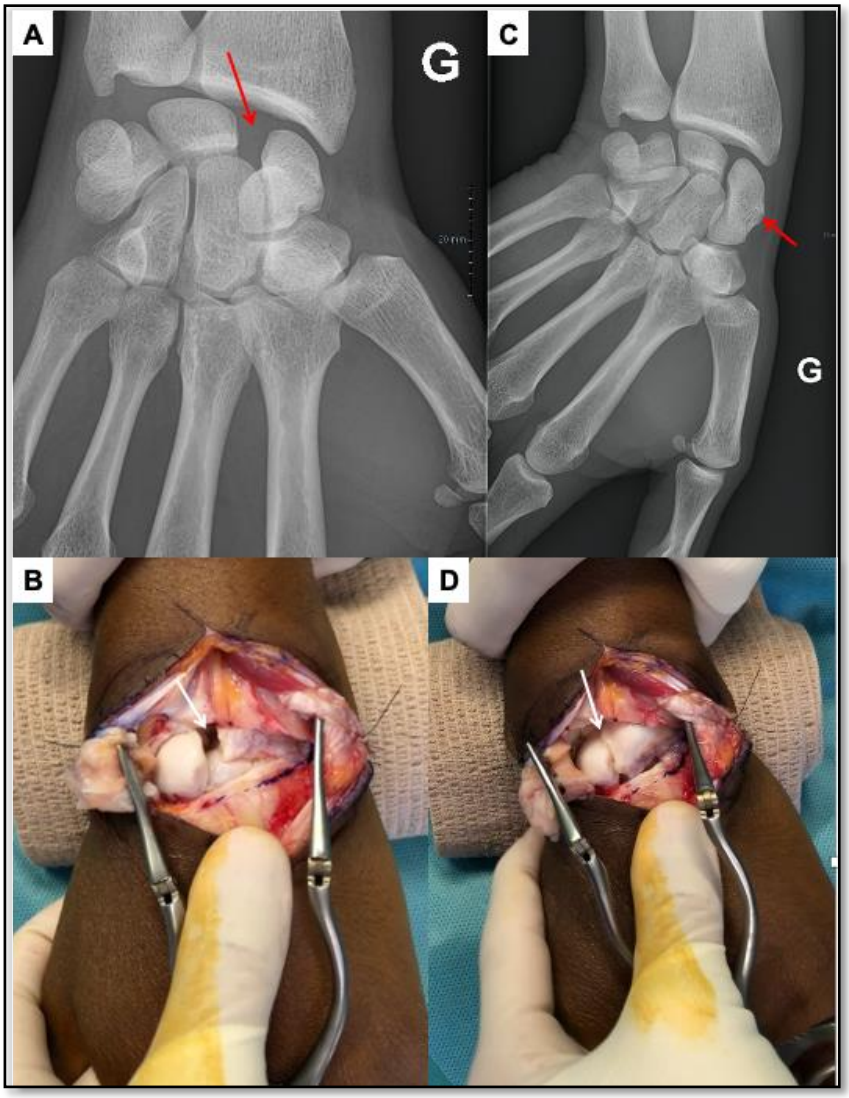

Figure 14. *Radiographies de face en position neutre (A) puis en inclinaison ulnaire (B) d'un poignet gauche. Vues per-opératoires (B et C) après arthrotomie dorsale du poignet de type Berger et al., (1995). L'ISL suspectée en radiographie standard (A – flèche rouge) s'est confirmée en per-opératoire (B – flèche blanche). On note la bonne mobilité du scaphoïde avec sa reverticalisation lors du cliché radiographique en inclinaison ulnaire (C – flèche rouge), et la confirmation de la réductibilité de l'ISL en per-opératoire (D – flèche blanche).*

Parmi les différentes options chirurgicales, les techniques de Brunelli modifiée par Van Den Abbeele (Van Den Abbeele et al., 1998) et de Garcia-Elias (Garcia-Elias et al., 2006) utilisent une bandelette de Flexor Carpi Radialis laissée pédiculée en distal, afin de reconstruire la portion dorsale du LIOSL et de reverticaliser le scaphoïde (Figure 15). Elles sont considérées comme des « gold standards », et ont fait l'objet de nombreuses études cliniques (Brunelli et Brunelli, 1995; Chabas et al., 2008; Elgammal et Lukas, 2016; Ellanti et al., 2014; Garcia-Elias et al., 2006; De Smet et Van Hoonacker, 2007; Links et al., 2008; Moran et al., 2006; Nienstedt, 2013; Talwalkar et al., 2006; Van Den Abbeele et al., 1998) (Tableau 1).

Si la grande majorité des auteurs partage de bons résultats cliniques avec une amélioration constante des douleurs au repos et à l'effort, ces derniers divergent cependant sur les résultats radiologiques, avec une grande variabilité d'une étude à l'autre. En effet, à court et moyen terme, une récidive des anomalies radiologiques pré-existantes est fréquemment observée. Les auteurs incrimineraient la détente ligamentaire, la présence d'un point d'ancrage triquétral capsulaire de faible solidité, mais aussi l'importance des contraintes exercées lors de l'utilisation du poignet. De plus, la réalisation d'un tunnel trans-scaphoïdien pour le passage du transplant est à l'origine de complications iatrogènes, à type de nécrose du pôle proximal du scaphoïde par dévascularisation et d'arthrose STT par effraction de cette articulation (Pauchard et al., 2013).

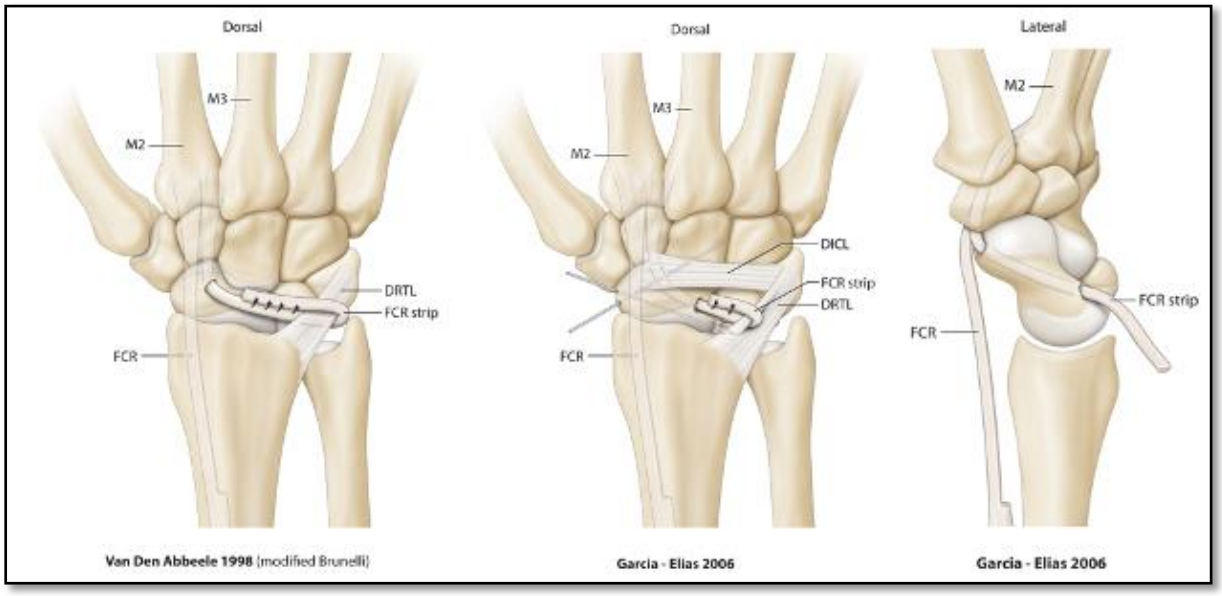

Figure 15. *Schémas représentant les techniques de Brunelli modifiée par Van Den Abbeele (Van Den Abbeele et al., 1998) et de Garcia-Elias (Garcia-Elias et al., 2006) qui utilisent une bandelette de Flexor Carpi Radialis laissée pédiculée en distal.*

Généralement, dans ces études, seule une évaluation radiographique est réalisée pour confirmer l'efficacité de leurs techniques respectives en termes de correction de l'alignement intra-carpien. Cette évaluation purement statique, rend limitée l'interprétation des résultats en ce qui concerne la correction du caractère dissociatif du couple scapho-lunaire.

Tableau 1. Résultats cliniques et radiographiques des principales séries publiées pour les ligamentoplasties de Brunelli modifiée par Van Den Abbeele et de Garcia-Elias.

Auteurs	Technique	P/D/S	N	FU	Douleur (0-10)	Flexion	Extension	Inclinaison radiale	Inclinaison ulnaire	Force /controlatéral	SLA		SLG		Arthrose SLAC
											Pré-op	Post-op	Pré-op	Post-op	
Van Den Abbeele et al. (1998)	MB	P/D/S	22	9	3 /10	42°	49°	19°	30°	58%	50°	50°	/	/	/
Talwalkar et al. (2006)	MB	D/S	55	48	3.7/10 0-3 = 62%	46.5°	55.7°	17.5°	29°	80%	Résultats cliniques seulement				/
Moran et al. (2006)	MB	D/S	15	36	0-3 = 27%	40°	43°	16°	26°	87%	63°	54°	3mm	2.6mm	13%
Garcia-Elias al. (2006)	3LT	D/S	38	46	0-3 = 95%	51°	52°	15°	29°	65%	Résultats cliniques seulement				23%
De Smet and Van Hoonacker (2007)	MB	D/S	10	29	0-3 = 90%	49°	48°	17°	34°	77%	Résultats cliniques seulement				/
Chabas et al. (2008)	MB	D/S	19	37	3/10 0-3 = 79%	41°	50°	24°	29°	78%	61°	62°	2.8mm	2.4mm	5%
Links et al. (2008)	MB	D/S	21	30	2 /10	45°	55°	13°	21°	98%	61°	46°	3.9mm	2.2mm	/
Pauchard et al. (2013)	3LT	D/S	20	25	1.6/10	39°	43°	14°	24°	76%	72°	75°	3.9mm	3.7mm	10.5%
Nienstedt et al. (2013)	MB	S	8	164	0-3 = 88%	37°	63°	21°	32°	85%	72°	63°	5.1mm	2.8mm	12.5%
Ellanti et al. (2014)	MB	D/S	13	12	1.5/10	38°	56°	20°	20°	75%	61°	63°	2.8mm	2.8mm	/
Elgamma and Lukas (2016)	MB	D/S	20	24	3/10 0-3 = 80%	41°	54°	19°	31°	81%	82°	77°	4mm	3mm	15%
Moyenne			22	41	2.6/10 0-3 = 73.5%	42.7°	51.7°	17.8°	27.7°	78%	65°	61°	3.6mm	2.8mm	13%

P/D/S : Instabilité Pré-dynamique / Dynamique / Statique ; N : nombre de cas ; FU : recul en mois ; SLA : angle scapho-lunaire ; SLG : espace scapho-lunaire ; MB : Brunelli modifiée par Van Den Abbeele (Van Den Abbeele et al., 1998) ; 3LT : Triple ténodèse de Garcia-Elias (Garcia-Elias et al., 2006) ; SLAC : Scapholunate advanced collapse.

Il est important de rappeler que d'autres gestes thérapeutiques sur les parties molles ont été mis au point à la même période. Ils cherchent à s'opposer à la bascule du scaphoïde et au diastasis scapho-lunaire. La capsulodèse dorsale décrite par Blatt (1987) utilise le ligament DRC laissé pédiculé en proximal sur le radius et fixé en distal sur le scaphoïde. Son objectif est de créer un « frein proximal et dorsal sur le pôle proximal du scaphoïde ». Elle corrige la flexion du scaphoïde mais pas le diastasis scapho-lunaire et est responsable d'une perte importante de flexion du poignet.

Pour ne pas ponter l'articulation radio-carpienne et ainsi tenter de limiter cette perte de de mobilité en flexion, des capsulodèses intra-carpiennes ont été développées par la suite (Baxamusa et Williams, 2005; Cueno, 1999; Gajendran et al., 2007; Moran et al., 2005; Salter et al., 1999; Schweizer et Steiger, 2002; Szabo et al., 2002). La plupart utilisent une partie (proximale ou distale) du ligament DIC. Ce dernier peut être pédiculé sur une charnière médiale et fixé sur le scaphoïde, comme décrit par Slater et al., (1999). Il peut aussi être prélevé en conservant une charnière latérale et fixé sur le lunatum selon la technique de Moran et al., (2005) ou celle de Cueno (1999). Selon ces auteurs, l'utilisation du ligament DIC contrôlerait mieux le diastasis que la capsulodèse de Blatt.

Plusieurs séries de capsulodèses sont présentes dans la littérature (Pomerance, 2006). À court terme, les patients sont généralement améliorés mais rarement asymptomatiques. Les paramètres radiographiques ne sont pas significativement améliorés et peuvent même être aggravés, sans qu'il n'y ait de relation entre le résultat radiologique et le résultat clinique. Les résultats se dégradent en moyenne après deux à trois ans, surtout si la demande fonctionnelle est importante. Ainsi, les techniques de capsulodèse ne semblent pas prévenir de la dégradation articulaire et de l'évolution vers l'arthrose (Gajendran et al., 2007; Moran et al., 2005). Les publications récentes rapportant des résultats de capsulodèses intracarpiennes à moyen terme, montrent une prévalence inquiétante de l'arthrose qui est présente dans plus de 25% des cas à cinq ans (Schweizer et Steiger, 2002) et dans 50% des cas à sept ans (Gajendran et al., 2007). Pour finir, il est important de souligner que ces procédures utilisent un ligament extrinsèque dorsal du carpe, notamment le ligament DIC, dont la lésion est fréquemment rencontrée en cas d'ISL.

Conclusion

L'analyse de la littérature rend compte des difficultés tant diagnostiques que thérapeutiques que posent l'ISL chronique, pré-arthrosique.

Lorsque cette instabilité est dynamique, le diagnostic est souvent difficile à établir sur la base unique des données en imagerie conventionnelle, rendant l'arthroscopie exploratrice comme étape chirurgicale intermédiaire. Malgré sa performance diagnostique, l'arthroscopie reste limitée par son manque de reproductibilité, par son défaut de quantification et par son caractère invasif non dénué de risque.

Lorsque cette instabilité est statique, le diagnostic semble évident sous réserve d'une analyse radiographique et arthroscanographique rigoureuse ; mais c'est à ce stade où les choix thérapeutiques sont les plus difficiles, notamment pour évaluer la « réductibilité » du scaphoïde rendant faisable la reconstruction ligamentaire.

Quel que soit son stade, la stratégie chirurgicale de l'ISL avant l'arthrose reste à ce jour mal codifiée, avec de multiples techniques notamment en ce qui concerne les ligamentoplasties. L'évaluation de leur efficacité sur la restitution de la synergie du couple scapho-lunaire fait souvent défaut dans les différentes séries publiées.

Environnement de travail

Notre travail de thèse est le fruit d'une collaboration avec plusieurs services et laboratoires, détaillée dans le tableau 2.

Tableau 2. Environnement de travail de thèse.

Outils	Superviseurs et collaborateurs	Service / Laboratoire
Études cliniques prospectives		
Patients inclus	Gilles DAUTEL Jonathan GRANERO Alain BLUM Pedro TEIXEIRA Kamel ROUIZI Gabriela HOSSU	*Service de chirurgie de la main* *Service d'imagerie Guilloz* *IADI, INSERM U1254, CIC-IT*
Études anatomiques cadavériques		
Sujets anatomiques	Romain DETAMMAECKER Marc BRAUN Marine KREBS Pedro TEIXEIRA Aymeric RAUCH Gabriela HOSSU Nicolas WEBER Frédérique GROUBATCH-JOINEAU Marion LUCAS	*Laboratoire Anatomie Nancy* *Service d'imagerie Guilloz* *IADI, INSERM U1254, CIC-IT* *École de Chirurgie Nancy*
Dispositif de recherche		
Verre PMMA (polyméthacrylate de méthyle) ABS (acrylonitrile butadiène styrène) Imprimante 3D FDM (Fused Deposition Modeling)	Nicolas WEBER Jacques FELBLINGER	*IADI, INSERM U1254, CIC-IT*

L'ensemble des patients inclus dans ce travail ont été vus en consultation chirurgicale par l'équipe du *service de chirurgie de la main, chirurgie plastique et reconstructrice de l'appareil locomoteur* du Centre Chirurgical Émile Gallé (CHRU de Nancy), dirigée par le Professeur Gilles Dautel. Les évaluations cliniques et radiographiques ont été effectuées lors de ces consultations. De même, les patients ayant bénéficié d'une chirurgie de reconstruction ligamentaire ont tous été opérés par cette même équipe chirurgicale.

Dans le *service d'imagerie Guilloz* (CHRU de Nancy), dirigé par le Professeur Alain Blum, nous avons travaillé avec le scanner à 320 détecteurs (Aquilion ONE, Canon Medical Systems, Otawara, Japan). Ce scanner représentait, lors de son installation, une véritable avancée scientifique car était le premier scanner à large système de détection installé en France. Grâce à sa rangée de 320 détecteurs de 0,5 mm, ce scanner permet l'acquisition de 16 cm de données dans l'axe z en une seule rotation du tube. L'analyse des images en 4DCT a été réalisée avec une station de travail de post-traitement indépendante, à l'aide de l'application 4D Ortho (Vitrea, version 7.0; Canon Medical Systems).

Les pièces anatomiques provenaient du *Laboratoire d'Anatomie de Nancy* (Faculté de médecine de Nancy, Université de Lorraine), dirigé par le Professeur Marc Braun, où nous avons pu notamment réaliser la préparation des spécimens et la plus grande partie des dissections.

Le travail de mise au point de la technique de ligamentoplastie ScaphoLunaire et InterCarpienne « SLIC » a été mené au sein de l'École de Chirurgie de Nancy-Lorraine (Faculté de médecine de Nancy, Université de Lorraine), co-dirigée par le Professeur François Sirveaux et par le Docteur Nguyen Tran.

Les travaux d'élaboration des protocoles d'études, de réalisation des supports méthodologiques, d'analyse des résultats ainsi que de développement des dispositifs de recherche, ont été réalisés au sein du *Laboratoire IADI* (Imagerie Adaptative Diagnostique et Interventionnelle) *INSERM U1254 - Université de Lorraine*, dirigé par le Professeur Jacques Felblinger. Le laboratoire est spécialisé dans les techniques et méthodes pour améliorer l'imagerie des organes en mouvement, le traitement de l'image, la méthodologie et les validations cliniques.
Basée au sein du CHRU de Nancy-Brabois, l'unité *U1254* bénéficie du support du *CIC-IT Nancy* (Centre d'Investigation Clinique – Innovation Technologique) et entretient des liens privilégiés avec les différents services des pôles d'imagerie et de l'appareil locomoteur du CHRU de Nancy. Le *service d'imagerie Guilloz* dispose de temps recherche sur TDM et IRM permettant ainsi une mise en œuvre et une validation rapide des méthodes de recherche développées.

CHAPITRE 2.
APPORT DU SCANNER DYNAMIQUE 4-DIMENSIONS DANS LE BILAN DIAGNOSTIC ET PRONOSTIC DES INSTABILITÉS SCAPHO-LUNAIRES

Ce chapitre sera illustré par quatre articles :

- **Athlani L, Rouizi K, Granero J, Gabriela H, Blum A, Dautel G, Teixeira P.A.G.** Assessment of scapholunate instability with dynamic computed tomography. *J Hand Surg Eur Vol.* 2020, 45:375-382.
- **Athlani L, Granero J, Rouizi K, Hossu G, Blum A, Dautel G, Gondim Teixeira PA.** Evaluation of dorsal scaphoid displacement using posterior radioscaphoid angle in patients with suspected scapholunate instability : a preliminary study. *J Hand Surg Am*. 2021, 46:10-16.
- **Athlani L, Granero J, Rouizi K, Hossu G, Blum A, Dautel G, Gondim Teixeira PA.** Four-dimensional CT analysis of Dorsal Intercalated Segment Instability in patients with suspected scapholunate instability. *J Wrist Surg*. 2021, 1:1-7.
- **Granero J, Orkut S, Rauch A, Blum A, Dautel G, Gondim Teixeira PA, Athlani L.** Dynamic 4D computed tomography data corresponds well to dynamic arthroscopic testing of scapholunate instability: a preliminary study. *J Hand Surg Am.* 2021.

Cette étude prospective s'intègre dans le cadre d'un protocole de recherche clinique approuvé par le Comité de Protection des Personnes Est-III et intitulé : **Analyse couplée des anomalies morphologiques et biomécaniques des ligaments carpiens « Étude EDLIS ».** Le consentement écrit de tous les participants a été obtenu. Ce protocole est enregistré auprès du registre des essais cliniques sous le numéro NCT02401568.
Canon Medical Systems France est le fournisseur du logiciel de post-traitement. Les auteurs avaient le plein contrôle des données et des informations soumises.

De janvier 2015 à décembre 2018, 43 patients (24 hommes et 19 femmes) consécutifs âgés de plus de 18 ans et présentant une douleur chronique (au-delà de 6 semaines) (spontanée et / ou induite à la palpation) du poignet en regard de l'articulation scapho-lunaire ont été vus en consultation par des chirurgiens seniors du *service de chirurgie de la main, chirurgie plastique et reconstructrice de l'appareil locomoteur* du Centre Chirurgical Émile Gallé (CHRU de Nancy) puis adressés au *service d'imagerie Guilloz* (CHRU de Nancy) pour un bilan d'imagerie complet devant la suspicion d'une ISL chronique. Tous ces patients présentaient un contexte de traumatisme de poignet. Les participants présentant une raideur articulaire majeure, des antécédents de chirurgie du poignet, du matériel d'ostéosynthèse ou prothétique au niveau du poignet, ou la notion de malformation congénitale de poignet n'ont pas été inclus.

Un examinateur indépendant (chirurgien spécialiste, 10 ans d'expérience clinique) a dans un premier temps revu l'ensemble des dossiers médicaux afin de confirmer l'inclusion. Trois patients ont ainsi été exclus car présentaient des antécédents de chirurgie du poignet. Notre population d'étude finale était composée de 40 participants (22 hommes et 18 femmes). Chaque patient a bénéficié d'une évaluation en imagerie qui associait des radiographies standards et dynamiques, un arthroscanner et un 4DCT du poignet douloureux.

Dans un premier temps, il convenait de réaliser une revue de la littérature sur le 4DCT dans l'analyse cinématique du complexe scapho-lunaire.

Le scanner dynamique 4-Dimensions : un nouvel outil d'imagerie

Le 4DCT fait l'objet de nombreux travaux récents (Abou Arab et al., 2018; De Roo et al., 2019; Garcia-Elias et al., 2014; Gondim-Teixeira et al., 2017; Kakar et al., 2016; Leng et al., 2011; Mat Jais et al., 2017; Rauch et al., 2018; Zhao et al., 2015). Il s'agit d'un examen d'imagerie permettant une analyse dynamique d'une région anatomique donnée, lors d'un mouvement articulaire défini. Cette évaluation cinématique en tomodensitométrie permet l'analyse directe des changements de position d'un os dans les trois plans de l'espace pendant le mouvement. Divers auteurs ont montré le rôle potentiel de cet outil pour l'évaluation de l'ISL, même en cas de doute à l'issue du bilan en imagerie conventionnelle (Figures 16 et 17).

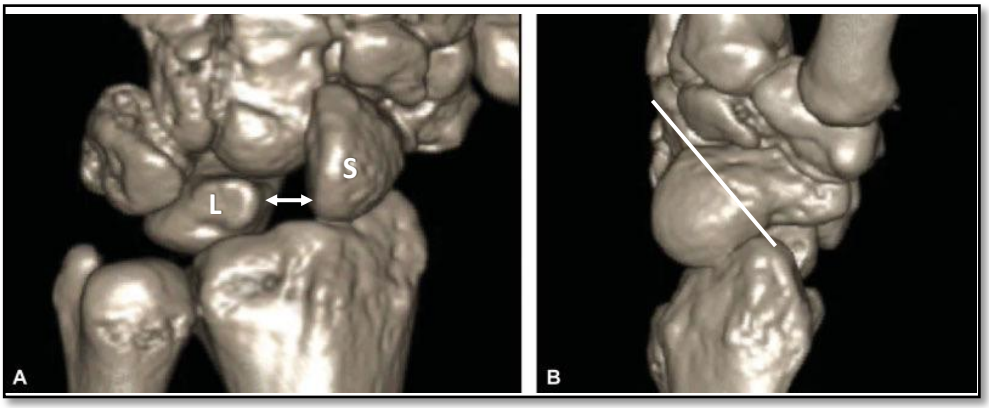

Figure 16. *Reconstructions 3D à partir d'acquisitions en 4DCT mettant en évidence une ISL. A : Vue dorsale du carpe avec présence d'un diastasis scapho-lunaire (flèche), et d'une projection dorsale du pôle proximal du scaphoïde (S). Le lunatum (L) présente un aspect de bascule dorsale ou DISI. B : Vue latérale du carpe avec présence d'une SPS responsable d'un contact entre le pôle proximal du scaphoïde et la berge dorsale du radius (Carr et al., 2018).*

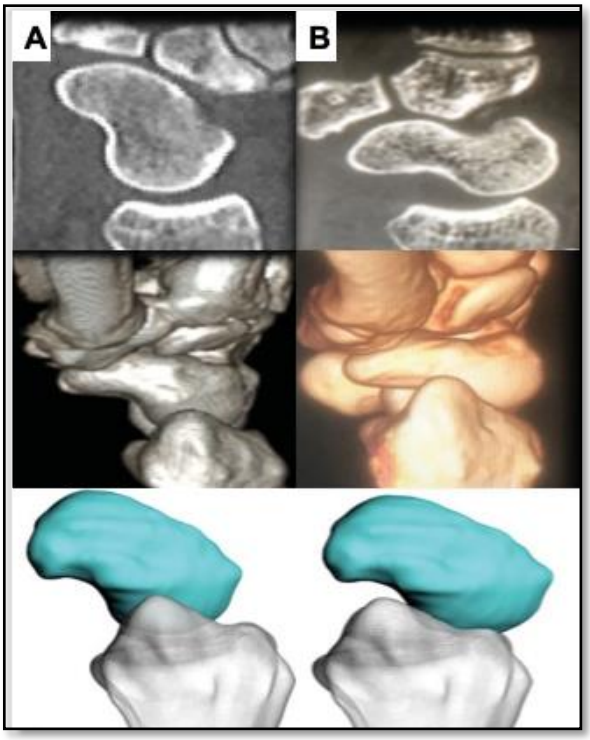

Figure 17. *Coupes scanographiques sagittales et reconstruction 3D à partir d'acquisitions en 4DCT d'un poignet en position neutre (A) puis en inclinaison radiale maximale (B). A : En position neutre, on note un scaphoïde centré par rapport à la glène radiale. B : En inclinaison radiale maximale, apparaît une SPS responsable d'un contact entre le pôle proximal du scaphoïde et la berge dorsale du radius (Kakar et al., 2016).*

Gondim-Teixeira et al., (2016) ont établi les recommandations concernant les paramètres d'acquisition en 4DCT pour les analyses musculo-squelettiques (Tableau 3). Les auteurs recommandent une vitesse de rotation élevée du tube et une semi-reconstruction des images. L'axe du mouvement influence de manière significative les artefacts de l'image et doit être pris en compte dans la formation du patient et l'évaluation adéquate du protocole d'acquisition.

Tableau 3. Paramètres d'acquisition en 4DCT selon Gondim-Teixeira et al., (2016)

Mode acquisition	**Séquence TDM dynamique 4D**
Field of view (cm)	8 à 10
z-axis coverage (cm)	8
Section thickness (mm)	0,5
Tube rotation (sec)	0,35
Tube voltage (kVp)	100
Milliamperage (mAs)	35
Reconstruction matrix	512 X 512
Image reconstruction	Soft-tissue kernel

Leng et al., (2011) ainsi que Mat Jais et al., (2017) ont permis de mettre en évidence la capacité du 4DCT à évaluer les déplacements du scaphoïde dans tous les plans de l'espace. Après section des principaux éléments stabilisateurs du complexe scapho-lunaire, en inclinaison radiale de poignet, Mat Jais et al., (2017) observaient une augmentation significative du déplacement dorsal du scaphoïde responsable d'un subluxation postéro-latérale. Cette dernière pouvait être quantifiée (Figure 18).

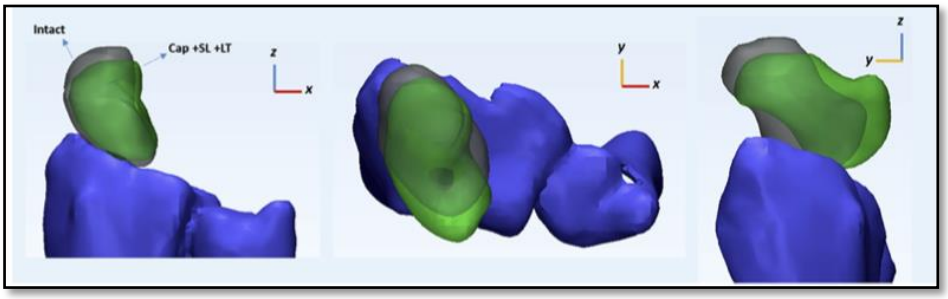

Figure 18. *Évaluation tridimensionnelle du déplacement du scaphoïde après section des stabilisateurs ligamentaires du complexe scapho-lunaire (Mat Jais et al., 2017).*

Dans l'étude de Carr et al., (2018), l'évaluation en 4DCT avait modifié le diagnostic radiographique initial chez 69% des patients. Dans 53% des cas, le 4DCT avait permis d'affiner le diagnostic initial. Dans 16% des cas, le diagnostic était complètement différent. L'analyse en 4DCT avait entrainé une modification de prise en charge thérapeutique dans 58% des cas.

Récemment, Abou Arab et al., (2018), Rauch et al., (2018) et Gondim-Teixeira et al., (2021), ont décrit le protocole permettant l'utilisation du 4DCT pour l'analyse du carpe dans les mouvements de DRU et de poing serré (Figure 19). Leurs premiers résultats étaient très encourageants en termes de précision diagnostic. Selon les auteurs, trois paramètres quantifiables, avec leurs variations au cours du mouvement, étaient mesurables et présentaient un réel intérêt dans le diagnostic de rupture du LIOSL : le SLG, le LCA et le PRSA (Figure 20). L'analyse dynamique de ces paramètres montrait des différences de valeurs significatives chez les patients porteurs d'une rupture totale du LIOSL, avec une bonne performance diagnostique. Pour ces auteurs, le mouvement de DRU offrait de meilleures performances et une reproductibilité supérieure à celle de la manœuvre du poing serré.

Pour finir, il est important de préciser que malgré son caractère irradiant, le 4DCT reste un examen faiblement irradiant puisque l'index de dose CT volumique, le produit dose-longueur et la dose efficace, varient respectivement de 16.60 mGy, 133.2 mGy.cm, et 0.013 mSv pour une acquisition de huit volumes, à 22.3 mGy, 222.8 mGy.cm, et 0.022 mSv pour une acquisition de dix-neuf volumes (Rauch et al., 2018).

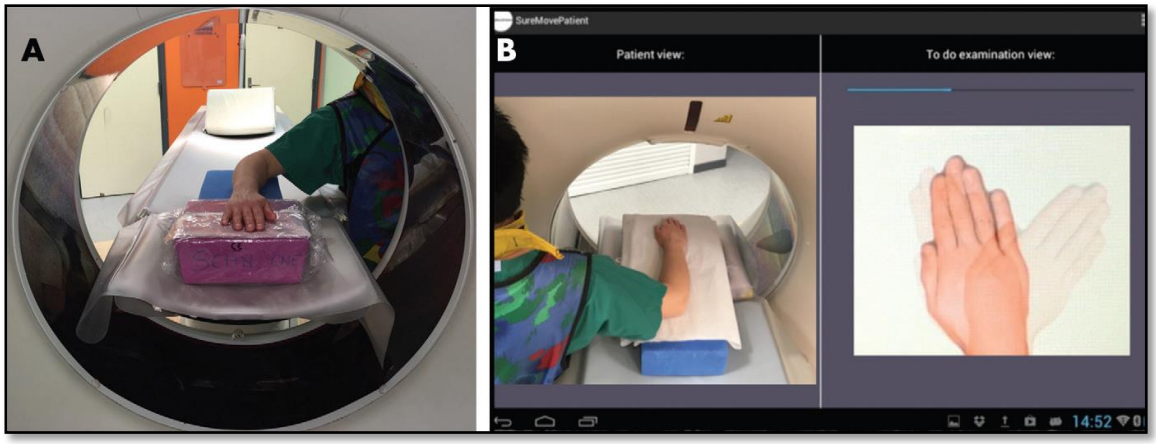

Figure 19. *Photographies illustrant la procédure d'acquisitions en 4DCT. A. Le patient, protégé par un tablier de plomb, est assis à côté du scanner, son poignet est en position neutre, placé sur la table du scanner et reposant sur des coussinets en mousse. B. La capture d'écran d'une tablette montre l'amplitude et la vitesse de déplacement en DRU du poignet (à droite), et la vision directe de l'installation du patient (à gauche) (Rauch et al., 2018).*

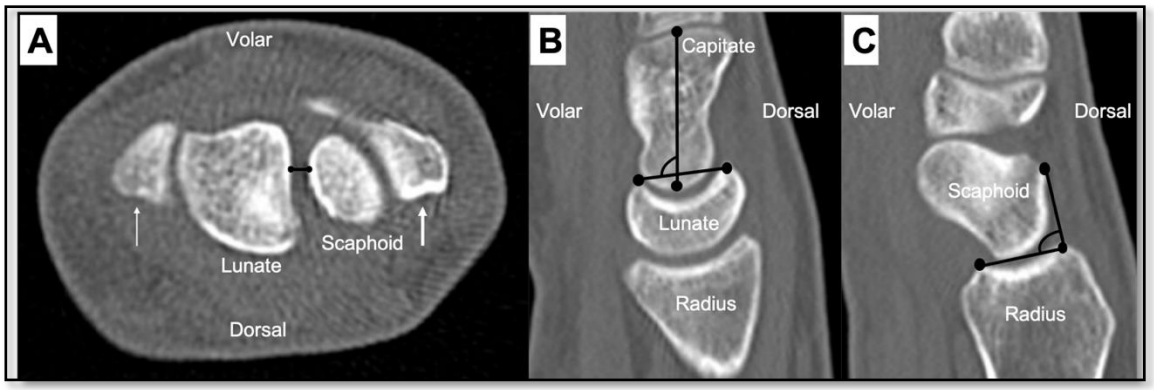

Figure 20. *Plans de référence et position des points repères utilisés pour effectuer les mesures des SLG (A), LCA (B) et PRSA (C), sur des images scanographiques multiplanaires.*
A : Pour la construction du SLG, deux marqueurs ont été placés sur le scaphoïde et le lunatum, à hauteur de la distance la plus courte entre ces deux os, dans le plan axial passant par la styloïde radiale (flèche fine) et la styloïde ulnaire (flèche épaisse) (Abou Arab et al., 2018).
B : Pour la construction du LCA, deux marqueurs ont été placés sur les cornes palmaire et dorsale du lunatum, et deux autres marqueurs ont été positionnés le long du grand axe du capitatum, dans le plan sagittal situé le plus près du centre de la fossette lunarienne du radius (Rauch et al., 2018).
C- Pour la construction du PRSA, deux marqueurs ont été placés sur les bords postérieur et antérieur de la fossette scaphoïdienne du radius, et deux autres marqueurs ont été positionnés au niveau du point le plus dorsal du scaphoïde et sur bord postérieur de la fossette scaphoïdienne, dans le plan sagittal situé le plus près du centre de la fossette scaphoïdienne du radius (Gondim-Teixeira et al., 2021).

À l'issue de cette revue de la littérature, nous évoquons l'hypothèse que le 4DCT pourrait être un complément d'imagerie performant pour l'analyse des patients suspects d'ISL, quel qu'en soit son stade, et notamment en cas de doute persistant après réalisation du bilan d'imagerie conventionnel. La suite de ce chapitre sera donc consacrée à l'apport du 4DCT dans le bilan diagnostic et pronostic chez nos 40 patients suspects cliniquement d'ISL.

Full Length Article

JHS(E)

Journal of Hand Surgery
(European Volume)
0(0) 1–8

DOI: 10.1177/1753193419893890
journals.sagepub.com/home/jhs
SAGE

Assessment of scapholunate instability with dynamic computed tomography

Lionel Athlani[1], Kamel Rouizi[2], Jonathan Granero[1], Gabriela Hossu[2], Alain Blum[3], Gilles Dautel[1] and Pedro Augusto Gondim Teixeira[3]

Abstract

We performed a prospective study to evaluate the values of dynamic four-dimensional computed tomography in assessing suspected chronic scapholunate instability. Forty patients were evaluated with radiographs, arthrography, and four-dimensional computed tomography. On plain radiographs and computed tomography, we found 16 patients with definite scapholunate instability, five with questionable scapholunate instability, and 19 with absence of scapholunate instability. We used four-dimensional computed tomography to evaluate the size of the scapholunate gap during radioulnar deviation. The mean and maximal values of the gap size were lowest in the patients with absence of scapholunate instability and highest in those with definite scapholunate instability. When comparing the scapholunate gap sizes of the patients with absent and questionable scapholunate instability, the range of the gap sizes was significantly higher in the patients with questionable scapholunate instability. We conclude that four-dimensional computed tomography aids assessment of chronic scapholunate instability, which allows the differentiation between patients without and those with definite or questionable scapholunate instability.

Level of evidence: II

Keywords

Four-dimensional computed tomography, scapholunate instability, wrist injury

Date received: 21st October 2019; revised: 11th November 2019; accepted: 19th November 2019

Introduction

Scapholunate (SL) ligament tears are challenging to diagnose and treat (Athlani et al., 2018; Crawford et al., 2016). In static SL instability, the diagnosis is obvious when a careful radiographic analysis is performed. However, the choice of the surgical treatment is not as straightforward at this stage, especially when evaluating the scaphoid's reducibility when ligament reconstruction is an option. In the predynamic and dynamic SL instability stages, the diagnosis is harder to make on static imaging methods, such as radiographs or computed tomography (CT). Consequently, exploratory arthroscopy may be required (Kitay and Wolfe, 2012; Linscheid et al., 2002; Watson et al., 1993). The static imaging methods provide information about carpal anatomy and alignment. Dynamic imaging can analyse changes in the carpus and joint spaces during movements (Zhao et al., 2015).

Abou Arab et al. (2018) and Rauch et al. (2018) described the use of dynamic four-dimensional computed tomography (4-DCT) to analyse the carpus during radioulnar deviation (RUD) and clenched fist movements. 4-DCT allows a dynamic and quantitative analysis of the SL gap. 4-DCT provides a more accurate evaluation of the scaphoid's reducibility in patients with static SL instability and better identifies predynamic and dynamic SL instability. The purpose

[1]Department of Hand Surgery, Plastic and Reconstructive Surgery, Nancy University Hospital, Nancy, France
[2]Inserm, Université de Lorraine, Nancy, France
[3]Guilloz Imaging Department, Nancy University Hospital, Nancy, France

Corresponding Author:
Lionel Athlani, Department of Hand Surgery, Plastic and Reconstructive Surgery, Centre Chirurgical Emile Gallé, Nancy University Hospital, 49 rue Hermite, 54000 Nancy, France.
Email: lionel.athlani@gmail.com

of this study was to assess the values of 4-DCT in 40 patients with chronic, post-traumatic wrist pain suspected to have chronic SL instability and various findings on plain radiographs and CT.

Methods

Study population

This prospective study was approved by our institutional review board. All patients provided their written informed consent. Between January 2015 and December 2018, 40 consecutive patients older than 18 years with more than a 6-week history of post-traumatic wrist pain (spontaneous and/or induced by palpation) over the SL joint were referred by the same surgical team for a complete imaging work-up because of suspected SL instability. Patients with major joint stiffness, history of wrist fractures, surgery, or congenital deformity were excluded. An independent examiner (senior surgeon, with 9 years of clinical experience), reviewed all the medical records to confirm the patients met the inclusion criteria. Each patient underwent radiographs and 4-DCT, followed by CT arthrography.

Radiographic evaluation

All patients underwent standard anterioposterior (AP) and lateral radiographs along with dynamic AP views in clenched fist. The images were analysed on an OsiriX© workstation (Pixmeo® 2016, Geneva, Switzerland). Measurements were performed by two readers independently (R1 – senior surgeon with 5 years of clinical experience and R2 – radiologist with 5 years of clinical experience). Static and dynamic SL gap (SLG) (in mm) and SL angle (SLA) (in degrees) were calculated (0.1 mm and 1° accuracy). SLGs greater than 3 mm and SLAs greater than 70° were considered pathological (Larsen et al., 1995).

4-DCT acquisition

Images were acquired with a 320-detector row CT scanner (Aquilion ONE™, Canon Medical Systems, Otawara, Japan). The acquisition parameters were the same as those used by Gondim Teixeira et al. (2017). All acquisitions were performed using continuous volumic mode (no table feed), 8–10 cm field of view (FOV), 512 × 512 matrix and 0.5 mm slice thickness. Tube rotation time and inter-volume interval were 0.35 seconds. Tube output was 100 kVp and 100 mAs (35 mAs effective). Images were reconstructed with half reconstruction and soft-tissue kernels. The *z*-axis coverage was 8 cm in the RUD manoeuvre. Before the acquisition, the patients were instructed on how to perform the RUD manoeuvre. The patient's position in the CT scanner is shown in Figure 1. To perform the RUD manoeuvre, patients were asked to

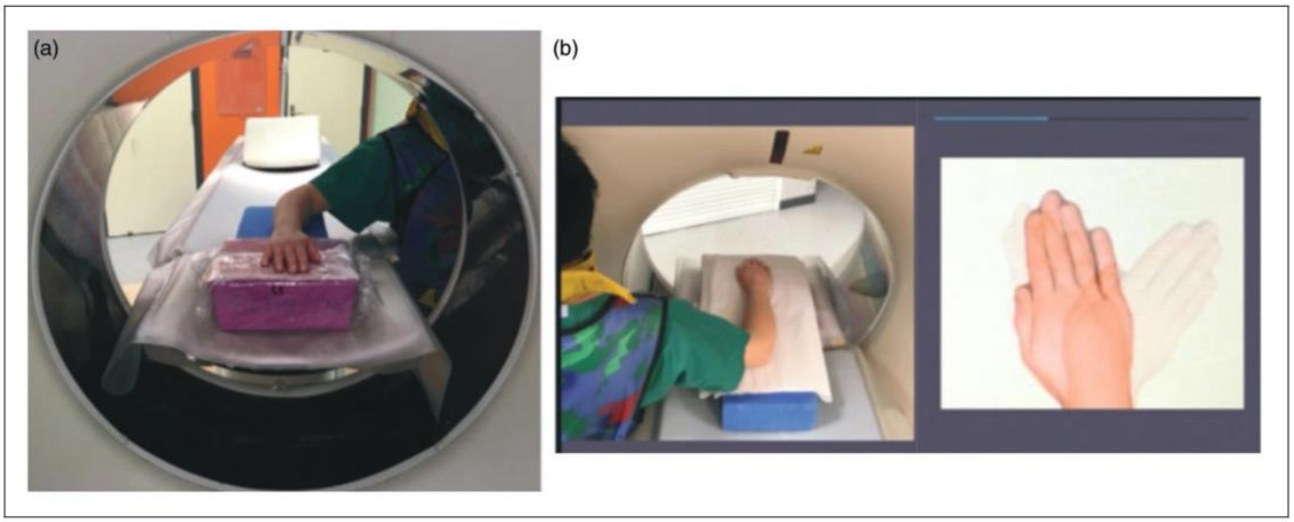

Figure 1. Photographs of the acquisition protocol for 4-DCT images. (a) Wearing lead protection, the participant is standing beside the CT scanner table. Their wrist is in neutral and is placed on the table on foam cushions. (b) Screen capture from a tablet showing the amplitude and displacement speed during radioulnar deviation (right side) and direct view from the video camera (left side) visible to the participant and technician performing the examination.

move their wrist in a continuous and homogenous manner, from maximum radial deviation to maximum ulnar deviation and then to return to the starting point (RUD cycle). Several RUD cycles (each about 8 seconds long) were performed. The examination lasted about 5 minutes (positioning and acquisition). Since RUD amplitude can affect carpus displacement, it was measured in all patients on coronal slices. A line passing through the long axis of the radius and another through the third metacarpal was drawn in the volumes acquired in maximum radial deviation and maximum ulnar deviation. The sum of these two angles was considered as the RUD amplitude.

Data analysis of 4-DCT images

The 4-DCT images were analysed on a post-processing workstation (Vitrea, version 7.0; Canon Medical Systems) using the 4-D Ortho application. Two independent readers (R1 and R2), blinded to clinical and CT arthrogram findings performed all measurements. Once all the 4-DCT volumes were loaded, multiplanar and three-dimensional images were displayed. On a multiplanar image of one of the acquisition volumes, the readers manually selected the distal radius by placing a point in its medullary canal. The software then registered this bone in all acquisition volumes making it a static reference point, which served as the basis for the manual selection of the measurement reference planes. Next, two markers were placed manually on an axial multiplanar image at the central portion of the SL joint to measure the shortest distance between these bones, which defines the SLG (Figure 2). The software automatically tracked the selected markers on all the remaining acquired volumes, which allowed SLG calculation on each acquired volume.

Four variables were calculated based on these data: mean (SLG_{mean}, in millimetres), maximum (SLG_{max}, in millimetres), coefficient of variation (SLG_{cv}, standard deviation/mean, in percentage), range (SLG_{range}, maximum–minimum SLG value, in millimetres). Because the CT scans had 0.5 mm slice thickness, the precision of the distances shown in CT images could not be smaller than 0.5 mm, though measurements in CT images could read to 0.1 mm in the study.

CT arthrogram

All patients underwent a CT arthrogram less than 1 hour after the 4-DCT using the same CT scanner.

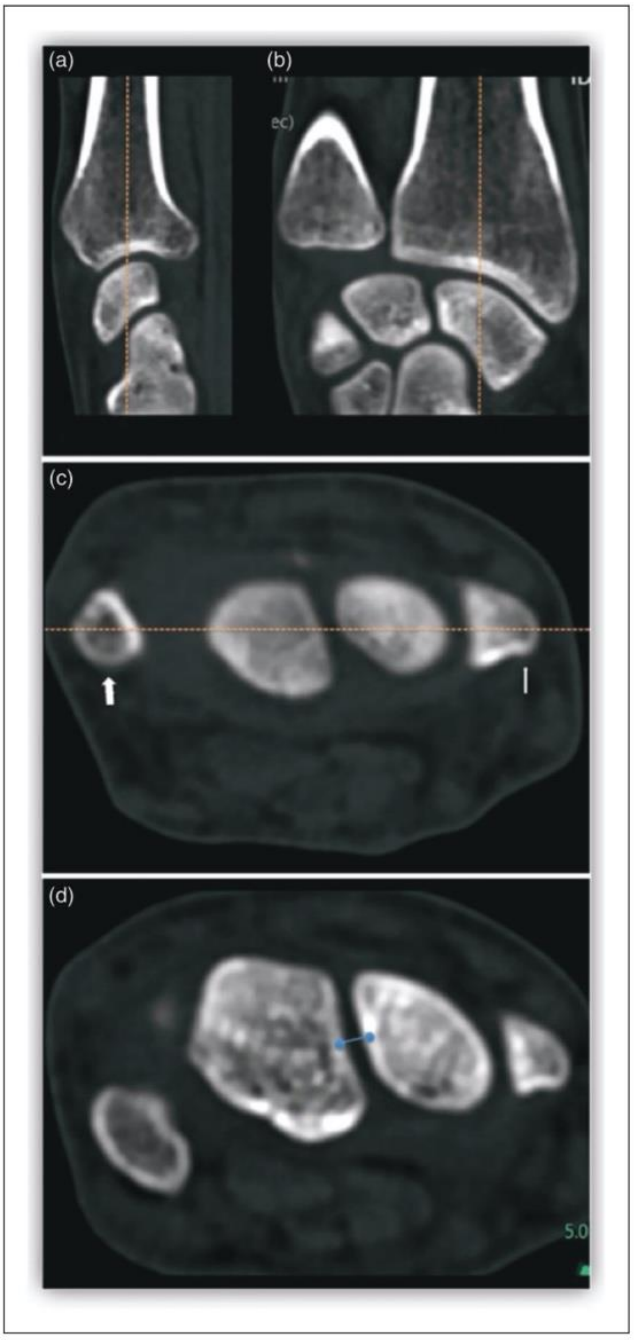

Figure 2. Reference planes and marker position used to measure the SLG in the CT multiplanar images. The sagittal (a) and coronal (b) planes were defined by the parallel orientation of the long axis of the radius in neutral position. The axial plane (c) passes through the radial styloid (thin arrow) and ulnar styloid (thick arrow). Two markers (d) were placed on the axial plane that was previously defined on the scaphoid and lunate as the shortest distance between these two bones (blue points).

The contrast agent was injected into the joint in aseptic conditions under fluoroscopic control by a musculoskeletal radiologist to obtain opacification of the midcarpal and radiocarpal compartments. The contrast agent was specific to arthrography (non-diluted Iodixanol). The three portions of the SL interosseous ligament (dorsal, volar, and proximal) were analysed by an independent examiner (senior radiologist with 12 years of experience with musculoskeletal imaging). Based on the ligament's appearance, two groups were created: no tear or isolated tear of proximal portion only (normal SL ligament) and partial or full tear of dorsal and/or volar portions (ruptured SL ligament). The SL ligament ruptures were further split into partial tears (partial or total loss of continuity in the dorsal or volar segment) and full tears (total loss of continuity in the dorsal and volar segments).

Patient groups

Using the radiographic and CT arthrogram data, three groups of patients were defined: '*definite SL instability*' consisting of patients with at least one pathological radiographic finding and a ruptured SL ligament; '*absent SL instability*' consisting of patients with normal radiographs and CT arthrograms; and '*questionable SL instability*' consisting of patients with either at least one pathological radiographic finding or a ruptured SL ligament.

Study of diagnostic performance of 4-DCT images

We studied sensitivity and specificity of 4-DCT images in two groups of patients with largest sample numbers through receiver operating characteristics (ROC) of the data collected. ROC analysis uses a graphical plot that illustrates the diagnostic ability of a binary classifier system as its discrimination threshold is varied (Hajian-Tilaki, 2013; Hanley and McNeil, 1982). ROC analysis is a tool to select possibly optimal thresholds and to discard suboptimal ones independently from the cost context or the class distribution. ROC analysis is related in a direct and natural way to cost/benefit analysis of diagnostic decision making.

In this study, ROC curves were calculated to evaluate the diagnostic performance of each 4-DCT-derived parameter describing the distribution of SLG values during wrist RUD by plotting the true positive incidence (sensitivity) against the false positive rate (1 – specificity) at various threshold settings (Figure 3). By the analysis of ROC-derived data, the threshold yielding the best sensitivity and specificity values for each parameter were selected. The optimal cutoff values were assessed by the difference between the true positive rate and the false positive rate, namely the Youden index.

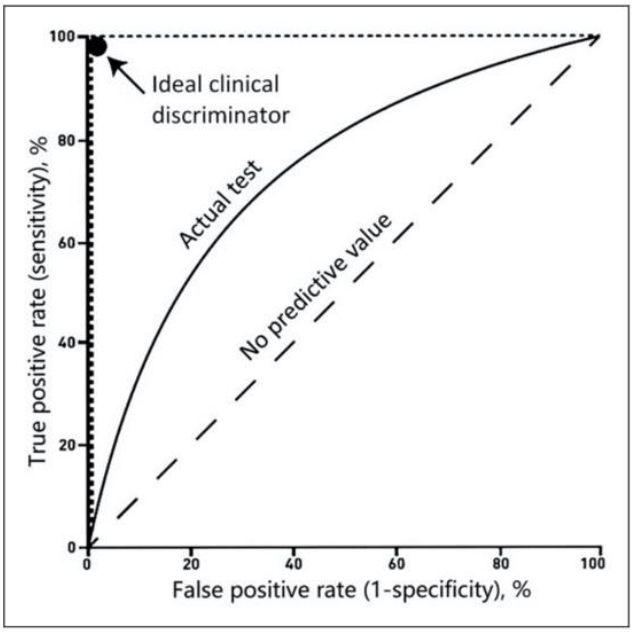

Figure 3. The ROC curve is a plot of the true positive rate (vertical axis) against the false positive rate (horizontal axis) for the different possible thresholds of a diagnostic test. The various thresholds for each studied 4-DCT parameter (SLG_{mean}, SLG_{max}, SLG_{cv}, SLG_{range}) will give points represented by their coordinates in the plot creating a curve for each parameter. The closer the curve comes to the 45° diagonal of the ROC space, the lower the sensitivity and specificity of the parameter. The data obtained in our 4-DCT study that give curves closer to the top-left corner indicate a better sensitivity and specificity for the differentiation between definite and absent SL instability.

Statistical analysis

Quantitative variables were described by their mean (standard deviation, SD) or by their median and interquartile range. Qualitative variables were described by their counts and percentages. Interobserver variability was measured with the intraclass correlation coefficient and its 95% confidence interval. Quantitative radiological and 4-DCT data were compared between groups using the Wilcoxon test with Holm–Bonferroni correction for multiple comparisons. This comparison was performed for the two readers (R1 and R2). The between-group characteristics were compared using the Fisher test or the X^2 depending on the nature of the data. The significant threshold was set at 5%.

Results

The mean age of the 40 patients was 47 years (SD13). There were 18 women and 22 men. Sixteen patients had definite SL instability, five had questionable SL instability, and 19 had no SL instability. The interobserver variability for each radiographic and 4-DCT variable was excellent (intraclass correlation coefficient (ICC): 0.79 to 0.96).

Radiographic evaluation

For the two readers, all the radiographic variables were significantly higher in the patients with positive SL instability than those with negative SL instability ($p < 0.01$). The static and dynamic SLGs were significantly higher in the patients with definite SL instability than in those with questionable SL instability ($p = 0.02$, $p = 0.03$, or $p = 0.04$). There was no significant difference in any of the parameters between the patients with absent SL instability and questionable SL instability, although the values were generally higher in the patients with questionable SL instability (Table 1).

CT arthrogram evaluation

On the CT arthrogram, three wrists had a full tear of the SL ligament, 17 had a partial tear, and 20 wrists had a normal SL ligament. In the 16 wrists with definite SL instability, a full tear of the SL ligament was found in three wrists and a partial tear in 13 wrists. In the five wrists with questionable SL instability, a partial tear was found in four wrists; the other wrist appeared normal. There were no full tears in this group.

4-DCT evaluation

The SLG_{mean} and SLG_{max} values were lowest in the patients with absent SL instability and highest in the patients with definite SL instability. The patients with definite SL instability had significantly higher SLG_{mean}, SLG_{max}, SLG_{cv}, and SLG_{range} values than those with absent SL instability ($p < 0.05$ or $p < 0.01$). The difference in all the SLG parameters between the patients with definite SL instability and those with questionable SL instability was not statistically significant. However, there was a trend towards higher values in the patients with definite SL instability compared with those with questionable SL instability.

When comparing the patients with absent SL instability and questionable SL instability, only the SLG_{range} was significantly different ($p < 0.05$). However, the values were higher in the patients with questionable SL instability (Table 2).

Diagnostic performance for chronic SL instability

Given the similar sample size in the definite SL instability ($n = 16$) and absent SL instability ($n = 19$) groups and the small size of the questionable SL instability ($n = 5$) group, only the patients with definite and absent SL instability were included in the ROC analysis. Thus, for the two readers, the best differentiation of patients with and without SL instability was achieved with the SLG_{cv} (AUC: 0.80 and 0.87) and the SLG_{range} (AUC: 0.78 and 0.85) parameters. The specificity and sensitivity of each SLG parameter ranged between 79% and 89% and between 69% and 81%, respectively (Table 3).

Table 1. The gap sizes and SLA measured on radiographs by two evaluators and their respective statistical significance in comparisons.

Measurements	Group 1: Definite SL instability* ($n = 16$)	Group 2: Absent SL instability** ($n = 19$)	Group 3: Questionable SL instability*** ($n = 5$)
SL gaps (mm)			
Static	2.5 (1.3); 2.7 (0.7)	1.5 (0.6); 1.4 (0.6)	1.3 (0.7); 1.5 (0.7)
	$p < 0.01$; $p < 0.01$	NS	$p = 0.02$; $p = 0.03$
Dynamic	3.9 (1.8); 3.6 (1.9)	2.2 (0.5); 2 (0.8)	2.1 (0.8); 2.2 (1)
	$p < 0.01$; $p < 0.01$	NS	$p = 0.03$; $p = 0.04$
SLA (°)	82 (15); 82 (17)	57 (9); 56 (14)	61 (7); 64 (14)
	$p < 0.01$; $p < 0.01$	NS	NS

The data shown are median (interquartile range).
SL: scapholunate; SLA: scapholunate angle; NS: no significant difference.
*p values shown in this column are results compared with Group 2. **p values are results compared with Group 3. ***p values are results compared with Group 1.

Table 2. The gap sizes measured on 4-DCT by two evaluators and their respective statistical significance in comparisons.

Measurements of SL gaps	Group 1: Definite SL instability* ($n=16$)	Group 2: Absent SL instability** ($n=19$)	Group 3: Questionable SL instability*** ($n=5$)
Mean (mm)	3.3 (1.6); 3.5 (2.4)	2.3 (0.9); 2.7 (0.7)	2.4 (1.8); 2.9 (2.5)
	$p=0.03$; $p=0.01$	NS	NS
Max (mm)	4.2 (2.3); 4.2 (2.5)	2.7 (1.1); 3 (0.9)	3.3 (2.7); 3.9 (3.6)
	$p=0.015$; $p=0.028$	NS	NS
Cv (%)	15 (7); 13 (9)	9 (3); 7 (4)	20 (10); 22 (10)
	$p=0.014$; $p<0.01$	NS	NS
Range (mm)	1.8 (1.4); 1.4 (1.1)	0.7 (0.3); 0.5 (0.4)	1.5 (1.8); 2 (2.6)
	$p<0.01$; $p<0.01$	$p=0.039$; $p=0.046$	NS

The data shown are median (interquartile range).
SL: scapholunate; NS: no significant difference.
*p values shown in this column are results compared with Group 2. **p values are results compared with Group 3. ***p values are results compared with Group 1.

Table 3. Threshold values and their sensitivity and specificity of 4-DCT for two evaluators in differentiation between the patients with definite and absent scapholunate (SL) instability.

SL gaps	Threshold	Sensitivity (%)	Specificity (%)	Area under curve (AUC)
Mean	3 mm	69; 56	84; 79	0.76; 0.70
Maximum	3.5 mm	56; 56	84; 89	0.78; 0.76
Cv	11%	81; 69	79; 84	0.80; 0.87
Range	1.1 mm	69; 69	89; 79	0.78; 0.85

SL: scapholunate.

Discussion

Our study's findings confirm the benefits of using 4-DCT with RUD movements in assessing suspected chronic SL instability. We defined our patients' diagnosis using combined radiographic and CT arthrogram data, which better reflect current practice. With a RUD manoeuvre, 4-DCT allowed to differentiate these groups and confirm the SL instability status with an excellent interobserver reproducibility. Using the threshold values identified in the ROC analysis, the diagnostic performance of SLG measurements was confirmed with a specificity of 79% to 89%. The best performance was achieved with the SLG_{cv} and SLG_{range}. Even with the physiological variation in SLG due to ligament laxity, the median values were significantly higher in the definite SL instability patients. Thus, 4-DCT data may be beneficial, since arthroscopy scores for SL instability diagnosis are known to have inter- and intraobserver errors (Dreant and Dautel, 2003; Geissler, 2006), making them less reproducible than 4-DCT.

Despite the small sample size of the questionable SL instability group ($n=5$), when it was compared with the absent SL instability group, the SLG_{cv} and SLG_{range} values were higher in the questionable SL instability group. Given the significant difference found, the SLG_{range} appears to be the only relevant determination for differentiating between these two groups. Based on SLG_{range} analysis, two patients in the questionable group could be reclassified as absent SL instability. Also, the SLG_{cv} and SLG_{range} values were similar between the patients with definite and questionable SL instability. The SLG_{mean} and SLG_{max} values were higher in the patients with definite SL instability than those with questionable SL instability. This non-significant but non-trivial difference can be explained by the various stages of SL instability encountered in practice. Static SL instability patients are not difficult to diagnose with radiographs and CT arthrogram. However, a portion of patients with dynamic or predynamic SL instability will present with SL diastasis on clenched fist views only, placing these patients in the questionable instability group. This underscores the importance of sub classifying patients with questionable SL instability and the potential role of 4-DCT is to identify this group.

The SLG_{mean} and SLG_{max} values were higher in the 4-DCT analysis than those in the radiographic analysis. These differences can be explained by the measurement methods, given that SL diastasis and rotation differences contribute to the SLG measurements during 4-DCT. Since the rotational difference is an important element of the pathogenesis of SL instability, it likely contributes to the diagnostic performance of the SLG analysis. Also, one of the advantages of 4-DCT is that it avoids a superimposition phenomenon and errors related to the patient's wrist position during standard radiographs.

Kakar et al. (2016) and Abou Arab et al. (2018) stated that the RUD movement was better at detecting SL ligament lesions than clenched fist movements. These authors also emphasized the advantages of 4-D analysis for the SLG because its dynamic changes can be influenced not only by full SL ligament tears but also dorsal or ventral tears separately. Thus, it may be possible to identify patients with mechanically important partial SL ligament tears, which could be treated by partial ligament reconstruction.

The primary limitation of our study is the small number of patients in each group, especially the questionable SL instability group ($n = 5$). We did not perform a power analysis, and it is possible some of the comparisons with no significant differences represent a type II error. However, in clinical practice, these questionable cases based on radiography and CT arthrogram analysis are rare, and further studies are necessary to explore this group of patients. Second, the SL ligament ruptures and SL instability were not confirmed by arthroscopy. However, CT arthrogram is highly successful for diagnosing SL ligament tears and arthroscopy is an invasive procedure that places the patient at risk of an infection, nerve lesion, pain, and stiffness. Third, the amplitude of the RUD movement was not standardized, and it varied from one patient to another. In our study, the mean RUD amplitude was similar between the three groups, and this parameter did not influence the diagnostic performance of 4-DCT in prior studies (Abou Arab et al., 2018; Rauch et al., 2018). Fourth, implementation of this new imaging modality requires training of the medical staff and also teaching the patient how to perform the movement correctly without moving the forearm. Moving too quickly produces movement artefacts, while moving too slowly results in images not being recorded at the end of the acquisition sequence (Gondim Teixeira et al., 2017). Finally, because the slice distance for CT scan is 0.5 mm, any measurement below 0.5 mm exceeds the precision of the measurement system. The data reported in this article therefore have a possible error range of 0.5 mm.

Acknowledgements We thank Dr Joanne Archambault for English language support.

Declaration of conflicting interests The authors declared the following potential conflicts of interest with respect to the research, authorship, and/or publication of this article: Pedro Augusto Gondim Teixeira and Alain Blum, who participated in this study, had a non-remunerated research contract with Toshiba Medical Systems for the development and clinical testing of post-processing tools for musculoskeletal CT. The authors declared no potential conflicts of interest with respect to the research, authorship, and/or publication of this article. None of the authors received payments or services, either directly or indirectly (i.e. via his or her institution), from a third party in support of any aspect of this work. None of the authors have had any other relationships, or have engaged in any other activities, that could be perceived to influence or have the potential to influence what is written in this work.

Funding The authors received no financial support for the research, authorship, and/or publication of this article.

Ethical approval This study was approved by our institutional review board and by the local ethics committee (Personal Protection Committee EST-III, Vandœuvre-les-Nancy, France). This study was registered with the Clinical Trials Registry (no. NCT02401568).

Informed consent All patients gave their informed consent for this study.

References

Abou Arab W, Rauch A, Chawki MB et al. Scapholunate instability: improved detection with semi-automated kinematic CT analysis during stress maneuvers. Eur Radiol. 2018, 28: 4397–406.

Athlani L, Pauchard N, Detammaecker R et al. Treatment of chronic scapholunate dissociation with tenodesis: a systematic review. Hand Surg Rehabil. 2018, 37: 65–76.

Crawford K, Owusu-Sarpong N, Day C, Iorio M. Scapholunate ligament reconstruction: a critical analysis review. JBJS Rev. 2016, 4: 41–8.

Dreant N, Dautel G. Development of an arthroscopic severity score for scapholunate instability. Chir Main. 2003, 22: 90–4.

Geissler WB. Arthroscopic management of scapholunate instability. Chir Main. 2006, 25: 187–96.

Gondim Teixeira PA, Formery AS, Hossu G et al. Evidence-based recommendations for musculoskeletal kinematic 4D-CT studies using wide area-detector scanners: a phantom study with cadaveric correlation. Eur Radiol. 2017, 27: 437–46.

Hajian-Tilaki K. Receiver operating characteristic (ROC) curve analysis for medical diagnostic test evaluation. Caspian J Intern Med. 2013, 4: 627–35.

Hanley JA, McNeil BJ. The meaning and use of the area under a receiver operating characteristic (ROC) curve. Radiology. 1982, 143: 29–36.

Kakar S, Breighner RE, Leng S et al. The role of dynamic (4D) CT in the detection of scapholunate ligament injury. J Wrist Surg. 2016, 5: 306–10.

Kitay A, Wolfe SW. Scapholunate instability: current concepts in diagnosis and management. J Hand Surg Am. 2012, 37: 2175–96.

Larsen CF, Amadio PC, Gilula LA, Hodge JC. Analysis of carpal instability: I. Description of the scheme. J Hand Surg Am. 1995, 20: 757–64.

Linscheid RL, Dobyns JH, Beabout JW, Bryan RS. Traumatic carpal instability of the wrist. Diagnosis, classification and pathomechanics. J Bone Joint Surg Am. 2002, 84: 142.

Rauch A, Arab WA, Dap F, Dautel G, Blum A, Gondim Teixeira PA. Four-dimensional CT analysis of wrist kinematics during radioulnar deviation. Radiology. 2018, 289: 750–8.

Watson H, Ottoni L, Pitts EC, Handal AG. Rotary subluxation of the scaphoid: a spectrum of instability. J Hand Surg Br. 1993, 18: 62–4.

Zhao K, Breighner R, Holmes D III, Leng S, McCollough C, An KN. A technique for quantifying wrist motion using four-dimensional computed tomography: approach and validation. J Biomech Eng. 2015, 137: epub.

Évaluation de la subluxation postérieure du scaphoïde par l'analyse du PRSA

EDITOR'S CHOICE

Evaluation of Dorsal Scaphoid Displacement Using Posterior Radioscaphoid Angle in Patients With Suspected Scapholunate Instability: A Preliminary Study

Lionel Athlani, MD,*† Jonathan Granero, MD,* Kamel Rouizi, MD,‡ Gabriela Hossu, PhD,† Alain Blum, MD, PhD,‡ Gilles Dautel, MD, PhD,* Pedro Augusto Gondim Teixeira, MD, PhD†‡

Purpose To assess the validity and reliability of the posterior radioscaphoid angle (PRSA), an indicator of dorsal displacement of the scaphoid, in distinguishing wrists with and without chronic scapholunate instability (SLI).

Methods We prospectively evaluated 40 patients (22 men and 18 women; mean age, 46 ± 13 years) with suspected SLI with radiographs and computed tomography arthrography. Based on these data, 3 groups were defined: positive SLI (n = 16), negative SLI (n = 19), and questionable SLI (n = 5). An independent reader measured the PRSA on sagittal computed tomography images using the same procedure.

Results The PRSA median values were significantly lower in the negative SLI group (98°) compared with the positive SLI (110°) and questionable SLI (111°) groups. The difference between the positive SLI and questionable SLI groups was not significant. The best differentiation between patients with and without SLI was obtained with a PRSA threshold value of 103° (specificity of 86% and sensitivity of 79%).

Conclusions In this preliminary study, PRSA analysis offers a quantitative tool for the evaluation of dorsal scaphoid displacement in cases of SLI, including for patients presenting with questionable initial radiography findings. *(J Hand Surg Am. 2020;■(■):■−■.*

Type of study/level of evidence Diagnostic II.

Key words Carpal instability, computed tomography arthrogram, scaphoid dorsal displacement, scapholunate ligament, wrist injury.

*From the Department of Hand Surgery, Plastic and Reconstructive Surgery, Centre Chirurgical Emile Gallé, Nancy University Hospital; and the †IADI Laboratory, INSERM U1254, University of Lorraine; and the ‡Guilloz Imaging Department, Central Hospital, Nancy University Hospital, Nancy, France.

Received for publication November 28, 2019; accepted in revised form September 16, 2020.

No benefits in any form have been received or will be received related directly or indirectly to the subject of this article.

Corresponding author: Lionel Athlani, MD, Department of Hand Surgery, Plastic and Reconstructive Surgery, Centre Chirurgical Emile Gallé, Nancy University Hospital, Lorraine 54000, France; e-mail: lionel.athlani@gmail.com.

0363-5023/20/■ ■-0001$36.00/0
https://doi.org/10.1016/j.jhsa.2020.09.016

SCAPHOLUNATE INSTABILITY (SLI) is the most common dissociative carpal instability.[1,2] It is the most frequent cause of scapholunate advanced collapse (SLAC) wrist.[3] Damage to the scapholunate interosseous ligament (SLL) is the main factor in the development of SLI; however, the extrinsic, palmar, and dorsal ligaments of the carpus are also important. Indeed, static SLI can appear only in the event of an associated injury of the SLL and extrinsic ligaments.[4,5]

Scapholunate instability may be challenging to diagnose. In static SLI, the diagnosis is obvious when a careful radiographic analysis is performed showing a fixed pattern of carpal collapse. In the predynamic and dynamic SLI stages, the diagnosis is harder to make based solely on standard radiographs. Dorsal displacement of the scaphoid is an important diagnostic factor, but its assessment is difficult on plain radiographs.[6] Bone superimposition and patient positioning issues can influence the relative projection of the scaphoid and the radius on a lateral view.[7] In addition to radiographs, computed tomography (CT) arthrogram or magnetic resonance (MR) arthrogram studies are frequently used to evaluate SLL tears and associated osteoarthritis.[1,2] Meister et al[8] evaluated the diagnostic utility of scaphoid dorsal subluxation on MR imaging as a predictor of SLL tears. With a sensitivity of 72% and a specificity of 100%, the authors concluded that the presence of as little as 10% dorsal subluxation of scaphoid predicts SLL tear.

Recently, Gondim Teixeira et al[9] described the posterior radioscaphoid angle (PRSA) on sagittal CT images. They concluded that this angle is a quantitative and reproducible predictor of SLAC wrist in patients with SLL lesion. We believe it could be also an indicator of the dorsal displacement of the scaphoid in patients with chronic SLI. The aim of this study was to assess the validity and reliability of the PRSA in distinguishing wrists with and without chronic SLI.

MATERIALS AND METHODS

Study sample

This prospective study was approved by our institutional review board. All patients provided written informed consent. Between January 2015 and December 2018, 40 consecutive patients aged greater than 18 years, who presented with chronic, posttraumatic wrist pain (more than 6-week history) and tenderness to palpation over the scapholunate joint, were referred by the same surgical team for complete imaging workup because of suspected SLI. We excluded any patient with major joint stiffness, history of wrist surgery, fracture fixation, or arthroplasty implants in the wrist, or congenital wrist deformity. An independent examiner (a hand surgeon with 9 years' clinical experience) reviewed all medical records to confirm that patients met inclusion criteria. Each patient underwent an imaging evaluation consisting of radiographs and CT arthrogram of the painful wrist.

Radiographic evaluation

All patients underwent standard posteroanterior (PA) and lateral radiographs along with dynamic posteroanterior views in a clenched fist position. The images were analyzed on an OsiriX workstation (Pixmeo 2016, Geneva, Switzerland). Measurements were performed independently by 2 readers (reader 1 was a surgeon with 5 years' clinical experience and reader 2 was a radiologist with 5 years' musculoskeletal imaging experience). Static and dynamic scapholunate gap (SLG) (in millimeters) and scapholunate angle (SLA) (in degrees) were calculated (with 0.1 mm accuracy for gaps and 1° for angles), in which SLGs greater than 3 mm and SLAs greater than 70° were considered pathological.[10]

Computed tomography arthrogram

All patients underwent a CT arthrogram using the same protocol. Images were acquired with a 320-detector row CT scanner (Aquilion ONE, Canon Medical Systems, Otawara, Japan).

All acquisitions were performed using the continuous volumetric mode (no table feed) with an 8 to 10 cm field of view, a 512 × 512 matrix, and a 0.5-mm slice thickness. The tube rotation time and intervolume interval were 0.5 seconds. The tube output was 100 kVp and 50 mAs. Images were reconstructed with bone kernel. The z axis coverage was 8 cm.

The contrast agent was injected into the joint under strict aseptic conditions using fluoroscopy control by a musculoskeletal radiologist, with opacification of the midcarpal and radiocarpal compartments. The contrast agent was specific to arthrography (nondiluted iodixanol). An independent examiner who was a radiologist with 12 years' experience in musculoskeletal imaging analyzed the 3 portions of the SLL (dorsal, volar, and proximal) on axial, sagittal, and coronal reformatted images. The SLL ruptures were characterized by a clear loss in continuity of the dorsal or ventral portion of the ligament. Based on the ligament's appearance, patients were divided into 2 groups: no tear or isolated tear of proximal portion only (normal SLL), and partial tear (PT) or full tear (FT) of the dorsal and/or volar portions (ruptured SLL). The SLL ruptures were further stratified into 2 groups: PT (partial or total loss of continuity in the dorsal or volar segment) and FT (total loss of continuity in the dorsal and volar segments).

Posterior radioscaphoid angle measurement

The same examiner and an orthopedic surgeon with 10 years of clinical experience measured the PRSA

(in degrees, with an accuracy of 0.5°) on sagittal images using the same procedure as described by Gondim Teixeira et al.[9] First, we identified the image with the dorsal-most point of the scaphoid. If this point was similar in 2 or more images, the one located closest to the center of the scaphoid fossa of the radius was selected for analysis. Then, a line passing through the dorsal and volar rims of the scaphoid fossa of the radius was drawn on this image. A second line was drawn, passing through the dorsal rim of the radius and the dorsal-most point of the scaphoid. The angle between these lines was designated the PRSA (Fig. 1).

Group definition

Radiographic and CT arthrogram data were used as the reference standard. Using those data, 3 groups were defined. The positive SLI groups consisted of patients who had at least one pathological radiographic variable and PT or FT on the CT arthrogram. The negative SLI group consisted of patients who had normal radiographs and CT arthrogram. The questionable SLI groups consisted of patients who had either at least one pathological radiographic variable or PT or FT on the CT arthrogram.

Statistical analysis

Quantitative variables are described as mean ± SD or median and interquartile range. Qualitative variables are described as numbers and percentages. Interobserver variability was measured with the intraclass correlation coefficient and its 95% confidence interval. Quantitative radiological and CT data were compared between groups using the Wilcoxon test with Holm-Bonferroni correction for multiple comparisons. This comparison was performed for readers 1 and 2). Between-group characteristics were compared using Fisher test or chi-square test, depending on the nature of the data.

The sensitivity, specificity, cutoff value, and area under the curve (AUC) value for the PRSA were determined using receiver operating characteristic (ROC) curve analysis. We performed ROC analysis to predict positive or negative SLI. For this purpose, the cutoff value was chosen to maximize the specificity and sensitivity of r. The significance threshold was set at .05 (2-tailed tests).

RESULTS

Mean age of the 40 patients enrolled in the study was 46 ± 13 years. There were 18 women and 22 men. Sixteen patients were in the positive SLI group (40%), 5 were in the questionable SLI group (12%), and 19 patients in the negative SLI group (47%). Interobserver variability for each radiographic variable was deemed excellent (SLG static: 0.79; SLG dynamic: 0.81; and SLA: 0.91). Table 1 summarizes data for each group.

FIGURE 1: Posterior radioscaphoid angle measurement. The dorsal-most point of scaphoid (A) is identified. Then, dorsal (B) and volar (C) rims of scaphoid fossa of radius are selected. Two lines are drawn: one from dorsal rim of scaphoid fossa to the dorsal-most point of scaphoid (A to B) and another between dorsal and ventral rims of radial scaphoid fossa (B to C). The angle formed by these 2 lines is the posterior radioscaphoid angle.

Radiographic evaluation

For the 2 readers, all radiographic variables were significantly higher in the positive SLI group than the negative SLI group ($P < .05$). When the positive SLI and questionable SLI groups were compared, only the SLG static and SLG dynamic variables were significantly higher in the positive SLI group ($P < .05$). There was no identifiable difference in any parameters ($P > .05$) between the negative SLI and questionable SLI groups, although the values were generally higher in the questionable SLI group.

Computed tomography arthrogram evaluation

Upon the CT arthrogram, 3 wrists had an FT of the SLL, 17 had a PT, and 20 had normal SLL. In the positive SLI group (n = 16), an FT of the SLL was found in 3 wrists and a PT in 13. In the questionable

TABLE 1. Radiography and CT Arthrogram Findings in Each Group

Parameter		Positive SLI (n = 16)	Negative SLI (n = 19)	Questionable SLI (n = 5)
Age, y (mean ± SD)		54 ± 11	39 ± 12	53 ± 6
Sex (% women / men)		6% / 94%	68% / 32%	60% 40%
Radiographs (median [interquartile range])				
SLG static, mm	R1	2.5 (2.2–3.5)	1.5 (1.3–1.9)	1.3 (1–1.7)
	R2	2.7 (2.2–2.9)	1.4 (1.3–1.9)	1.5 (1–1.7)
SLG dynamic, mm	R1	3.9 (3–4.8)	2.2 (1.9–2.4)	2.1 (1.9–2.7)
	R2	3.6 (2.8–4.7)	2 (1.8–2.6)	2.2 (1.7–2.7)
SLA (degrees)	R1	82 (68–83)	57 (55–64)	61 (53–70)
	R2	82 (68–85)	56 (49–63)	64 (50–64)
CT arthrogram, n		3 FT 13 PT	19 normal	0 FT 4 PT 1 normal

SLI group (n = 5), a PT was found in 4 wrists; in the other wrist, the SLL appeared normal. There was no FT in this group.

Posterior radioscaphoid angle assessment

The PRSA median values were lowest in the negative SLI group and similar in the positive SLI and questionable SLI groups. The positive SLI group and questionable SLI groups had significantly higher PRSA value than the negative SLI group ($P < .05$). The difference in PRSA values between the positive SLI and questionable SLI groups was not significant ($P = .84$) (Table 2, Figs. 2, 3A).

Diagnostic performance for chronic SLI with PRSA

Because of the similar sample size in the positive SLI (n = 16) and negative SLI (n = 19) groups and the small size of the questionable SLI group (n = 5), only the positive and negative groups were included in the ROC analysis. Thus, PRSA (area under the curve, 0.73) with a threshold of 103° was the best parameter for differentiating patients with and without SLI, with a specificity of 86% and sensitivity of 79% (Fig. 3B).

DISCUSSION

The current study showed that PRSA values were significantly different between patients with and without SLI. The threshold value of 103° was the best cutoff for differentiating patients in those 2 groups, with a specificity and sensitivity of 86% and 79%, respectively.

Despite the small sample size of the questionable SLI group (n = 5), compared with the negative SLI groups, the PRSA value was higher. Also, the positive SLI and questionable SLI groups had similar median values (110° and 111°, respectively). Therefore, PRSA may be relevant for differentiating between the questionable SLI and negative SLI groups.

Without SLI, the scaphoid exhibits both flexion-extension and radioulnar deviation motion during radioulnar deviation motion of the wrist. The dorsal extrinsic ligaments (dorsal radiocarpal and dorsal intercarpal) and dorsal component of the SLL provide dorsal stability, preventing the tendency toward dorsal displacement of the scaphoid, yet allow relative free motion of the scaphoid.[6]

Dorsal displacement of the scaphoid is an important element of the pathogenesis of SLI.

These positional abnormalities of the scaphoid contribute to the development of SLAC wrist. Classically described as a rotatory subluxation of the scaphoid with dorsal intercalated segment instability deformity, static SLI manifests as a complex deformity with dorsal subluxation of the unit formed by the scaphoid and the capitate. This deformity explains the dorsal radioscaphoid contact and lunocapitate decentering with lunate instability in extension that is the origin of the radioscaphoid and midcarpal osteoarthritis that appears later.[11]

Gondim Teixeira et al[9] showed that in patients with SLL tears, high PRSA values were correlated with the presence of SLAC wrist. The threshold value of 114° was deemed optimal for identifying SLAC wrist.

To date, the evaluation of dorsal scaphoid displacement has been subjective, which has hampered its usefulness for the diagnosis of SLI. Athlani et al[12] used a radiographic evaluation of

TABLE 2. Findings for PRSA in Each Group

Parameter	Positive SLI (n = 16)	Negative SLI (n = 19)	Questionable SLI (n = 5)
PRSA (degrees) (median [interquartile range])	110 (104–116)	98 (97–102)	111 (110–114)
P value	Positive vs negative <.01*	Negative vs questionable <.01*	Questionable vs positive .84

*Statistically significant ($P < .05$).

FIGURE 2: Example of chronic SLI in a 30-year-old man with a long history of chronic right wrist pain. **A** Standard anteroposterior radiograph showing SLG static position, which was measured at 2.7 mm. **B** Dynamic anteroposterior view in clenched fist showing SLG dynamic position, which was measured at 4.7 mm. **C** Standard lateral radiograph showing SLA, which was measured at 63°. **D** Frontal CT arthrogram slice showing tear of scapholunate ligament (arrow). **E** Axial CT arthrogram slice showing full tear of scapholunate ligament (arrow). **F** Sagittal CT arthrogram slice showing PRSA, which was measured at 110°.

dorsal scaphoid subluxation. On a lateral view, dorsal displacement of the proximal pole of the scaphoid with respect to its radial fossa and the posterior horn of the lunate is seen in the case of SLI. Using this method, quantification is not possible; however, the PRSA is a quantifiable measurement. Although the PRSA is not measurable on plain radiographs, it can be measured on sagittal CT and MR images. Thus, PRSA evaluation is interesting because it is quantitative and reproducible.

Meister et al[8] evaluated the presence of a dorsal subluxation of the proximal pole of the scaphoid on sagittal MR images when the SLL was torn. They found a high positive predictive value with a

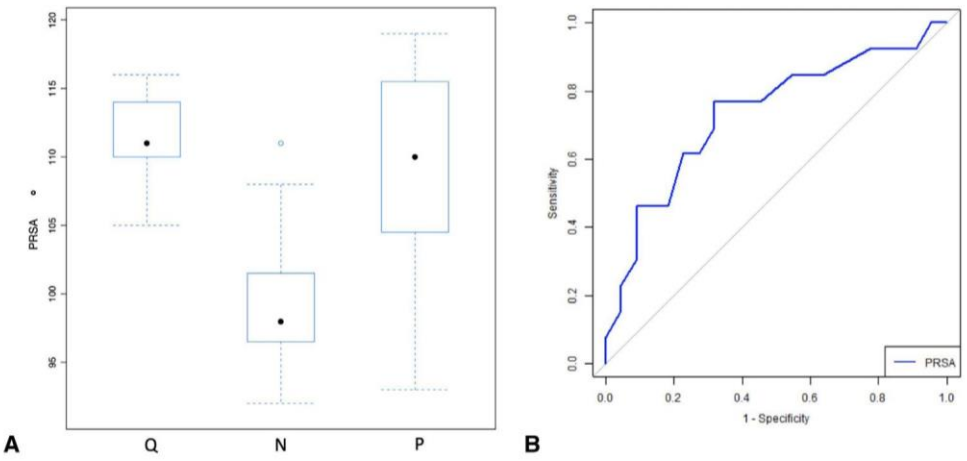

FIGURE 3: **A** Box plot graph showing distribution of the PRSA in groups. **B** Receiver operating characteristic curve for the diagnosis of SLI using the PRSA.

specificity of 100%, whereas it was 86% in our study. Their sensitivity was similar to ours (72% vs 79%).

The presence of dorsal scaphoid displacement (PRSA $>$ 103°) and its quantification could be used as an imaging marker of injury of the scapholunate complex (SLL and extrinsic ligaments) and the severity of SLI. Thus, it might be possible to identify and treat patients with early-stage SLI.[13–15]

Abou Arab et al[16] and Rauch et al[17] described a protocol in which dynamic 4-dimensional CT was used to analyze the carpus during radioulnar deviation and clenched fist movements. Their initial findings were encouraging in terms of the diagnostic accuracy. A dynamic analysis of the SLG found significant differences in patients with and without SLI. A dynamic analysis of PRSA using 4-dimensional CT could also be interesting, especially during radioulnar deviation movements.

The primary limitation of this study lay in the choice of the sample. We included patients with a painful wrist with tenderness to palpation over the scapholunate joint. We suspected these patients had SLI. Thus, it may have been a high-prevalence sample in which a much higher proportion of patients were likely to have SLI than in a more general wrist pain population. This may have spuriously inflated the sensitivity and specificity of the test.

Second, there was a small number of patients in each group, especially the questionable SLI group (n = 5). Third, the SLL ruptures and SLI were not confirmed by arthroscopy, which is generally considered the true reference standard for the diagnosis. However, CT arthrogram has a high sensitivity and specificity for the diagnosis of SLL tears (95% to 100% and 86% to 100%, respectively),[18] and arthroscopy is an invasive procedure that places the patient at risk for an infection, nerve lesion, pain, or stiffness.[19] Obdeijn et al[20] reported large interobserver and intra-observer variability of wrist arthroscopy. Magnetic resonance arthrogram can be also performed to assess SLL tears with good sensitivity and specificity (65% to 89% and 90% to 100%, respectively).[19] Lee et al[21] compared axial and oblique axial planes on multidetector CT arthrogram and MR arthrogram to evaluate the dorsal and volar parts of SLL. The accuracy of both examinations in revealing SLL tear was higher using the oblique axial plane. The overall accuracy for detecting SLL tear on CT arthrogram improved from 94% to 100% and from 89% to 94% on MR arthrogram. According to that study, the accuracy of reformatted oblique axial imaging on CT arthrogram performed better than direct oblique axial imaging with MR arthrogram, most likely because of the improved spatial resolution and interactive nature of CT reformation.

Finally, the degree of scaphoid flexion may have influenced the PRSA values, especially in cases of static SLI with a large scapholunate diastasis. Indeed, the dorsal-most point of the scaphoid is radially displaced, near the radial styloid, and there is dorsal angulation of the radial articular surface plane, leading to underestimation of PRSA.

Posterior radioscaphoid angle analysis offers a quantitative tool for the evaluation of dorsal scaphoid displacement in suspected cases of SLI. Values over 103° are associated with SLI, including for patients presenting with questionable initial radiography findings. Abnormal PRSA values could indicate notable biomechanical changes in the wrist.

ACKNOWLEDGMENTS

Two authors involved in this work (P.A.G. and A.B.) participate on a nonremunerated research contract with Toshiba Medical Systems for the development and clinical testing of postprocessing tools for musculoskeletal CT.

The authors wish to thank Dr Joanne Archambault for English language support.

REFERENCES

1. Athlani L, Pauchard N, Detammaecker R, et al. Treatment of chronic scapholunate dissociation with tenodesis: a systematic review. *Hand Surg Rehabil*. 2018;37(2):65–76.
2. Crawford K, Owusu-Sarpong N, Day C, Iorio M. Scapholunate ligament reconstruction: a critical analysis review. *JBJS Rev*. 2016;4(4):41–48.
3. Watson HK, Ballet FL. The SLAC wrist: scapholunate advanced collapse pattern of degenerative arthritis. *J Hand Surg Am*. 1984;9(3):358–365.
4. Linscheid RL, Dobyns JH, Beabout JW, Bryan RS. Traumatic carpal instability of the wrist: diagnosis, classification and pathomechanics. *J Bone Joint Surg Am*. 2002;84(1):142.
5. Viegas SF, Yamaguchi S, Boyd NL, Patterson RM. The dorsal ligaments of the wrist: anatomy, mechanical properties, and function. *J Hand Surg Am*. 1999;24(3):456–468.
6. Watson H, Ottoni L, Pitts EC, Handal AG. Rotary subluxation of the scaphoid: a spectrum of instability. *J Hand Surg Br*. 1993;18(1):62–64.
7. Kitay A, Wolfe SW. Scapholunate instability: current concepts in diagnosis and management. *J Hand Surg Am*. 2012;37(10):2175–2196.
8. Meister DW, Hearns KA, Carlson MG. Dorsal scaphoid subluxation on sagittal magnetic resonance imaging as a marker for scapholunate ligament tear. *J Hand Surg Am*. 2017;42(9):717–721.
9. Gondim Teixeira PA, De Verbizier J, Aptel S, et al. Posterior radioscaphoid angle as a predictor of wrist degenerative joint disease in patients with scapholunate ligament tears. *Am J Roentgenol*. 2016;206(1):144–150.
10. Larsen CF, Amadio PC, Gilula LA, Hodge JC. Analysis of carpal instability: I. Description of the scheme. *J Hand Surg Am*. 1995;20(5):757–764.
11. Laulan J. Rotatory subluxation of the scaphoid: pathology and surgical management. *Chir Main*. 2009;28(4):192–206.
12. Athlani L, Pauchard N, Dautel G. Radiological evaluation of scapholunate intercarpal ligamentoplasty for chronic scapholunate dissociation in cadavers. *J Hand Surg Eur Vol*. 2018;43(4):387–393.
13. Mathoulin CL. Indications, techniques, and outcomes of arthroscopic repair of scapholunate ligament and triangular fibrocartilage complex. *J Hand Surg Eur Vol*. 2017;42(6):551–566.
14. Degeorge B, Coulomb R, Kouyoumdjian P, Mares O. Arthroscopic dorsal capsuloplasty in scapholunate tears EWAS 3: preliminary results after a minimum follow-up of 1 year. *J Wrist Surg*. 2018;7(4):324–330.
15. Ho PC, Wong CW, Tse WL. Arthroscopic-assisted combined dorsal and volar scapholunate ligament reconstruction with tendon graft for chronic SL instability. *J Wrist Surg*. 2015;4(4):252–263.
16. Abou Arab W, Rauch A, Chawki MB, et al. Scapholunate instability: improved detection with semi-automated kinematic CT analysis during stress maneuvers. *Eur Radiol*. 2018;28(10):4397–4406.
17. Rauch A, Arab WA, Dap F, et al. Four-dimensional CT analysis of wrist kinematics during radioulnar deviation. *Radiology*. 2018;289(3):750–758.
18. Bille B, Harley B, Cohen H. A comparison of CT arthrography of the wrist to findings during wrist arthroscopy. *J Hand Surg Am*. 2007;32(6):834–841.
19. Lee YH, Choi YR, Kim S, Song HT, Suh JS. Intrinsic ligament and triangular fibrocartilage complex (TFCC) tears of the wrist: comparison of isovolumetric 3D-THRIVE sequence MR arthrography and conventional MR image at 3 T. *Magn Reson Imaging*. 2013;31(2):221–226.
20. Obdeijn MC, Tuijthof GJ, van der Horst CM, Mathoulin C, Liverneaux P. Trends in wrist arthroscopy. *J Wrist Surg*. 2010;2(3):239–246.
21. Lee RK, Griffith JF, Ng AW, et al. Intrinsic carpal ligaments on MR and multidetector CT arthrography: comparison of axial and axial oblique planes. *Eur Radiol*. 2017;27(3):1277–1285.

Évaluation de la bascule dorsale du lunatum ou DISI par l'analyse du LCA

Scientific Article

Four-Dimensional CT Analysis of Dorsal Intercalated Segment Instability in patients with Suspected Scapholunate Instability

Lionel Athlani, MD[1,3] Jonathan Granero, MD[1] Kamel Rouizi, MD[2] Gabriela Hossu, PhD[3] Alain Blum, MD, PhD[2,3] Gilles Dautel, MD, PhD[1] Pedro Augusto Gondim Teixeira, MD, PhD[2]

[1] Department of Hand Surgery, Plastic and Reconstructive Surgery, Centre Chirurgical Emile Gallé, Nancy University Hospital, Nancy, France
[2] Guilloz Imaging Department, Central Hospital, Nancy University Hospital, Nancy, France
[3] IADI Laboratory, INSERM U1254, Université de Lorraine, Nancy, France

Address for correspondence Lionel Athlani, MD, Department of Hand Surgery, Plastic and Reconstructive Surgery, Centre Chirurgical Emile Gallé, Nancy University Hospital, 49 rue Hermite, Nancy, 54000, France (e-mail: lionel.athlani@gmail.com).

J Wrist Surg

Abstract

Background In this study we sought to evaluate the contribution of dynamic four-dimensional computed tomography (4DCT) relative to the standard imaging work-up for the identification of the dorsal intercalated segment instability (DISI) in patients with suspected chronic scapholunate instability (SLI).

Methods Forty patients (22 men, 18 women; mean age 46.5 ± 13.1 years) with suspected SLI were evaluated prospectively with radiographs, arthrography, and 4DCT. Based on radiographs and CT arthrography, three groups were defined: positive SLI ($n = 16$), negative SLI ($n = 19$), and questionable SLI ($n = 5$). Two independent readers used 4DCT to evaluate the lunocapitate angle (LCA) (mean, max, coefficient of variation [CV], and range values) during radioulnar deviation.

Results The interobserver variability of the 4DCT variables was deemed excellent (intraclass correlation coefficient = 0.79 to 0.96). Between the three groups, there was no identifiable difference for the LCA_{mean}. The LCA_{max} values were lower in the positive SLI group (88 degrees) than the negative SLI group (102 degrees). The positive SLI group had significantly lower LCA_{cv} (7% vs. 12%, $p = 0.02$) and LCA_{range} (18 vs. 27 degrees, $p = 0.01$) values than the negative SLI group. The difference in all the LCA parameters between the positive SLI group and the questionable SLI group was not statistically significant. When comparing the negative SLI and questionable SLI groups, the LCA_{cv} ($p = 0.03$) and LCA_{range} ($p = 0.02$) values were also significantly different. The best differentiation between patients with and without SLI was obtained with a LCA_{cv} and LCA_{range} threshold values of 9% (specificity of 63% and sensitivity of 62%) and 20 degrees (specificity of 71% and sensitivity of 63%), respectively.

Conclusion In this study, 4DCT appeared as a quantitative and reproducible relevant tool for the evaluation of DISI deformity in cases of SLI, including for patients presenting with questionable initial radiography findings.

Level of evidence This is a Level III study.

Keywords
- carpal instability
- dorsal intercalated segment instability
- four-dimensional computed tomography
- kinematics
- scapholunate ligament

received
September 14, 2020
accepted
November 27, 2020

Thieme Medical Publishers, Inc.,
333 Seventh Avenue, 18th Floor,
New York, NY 10001, USA

DOI https://doi.org/10.1055/s-0040-1722571.
ISSN 2163-3916.

Scapholunate instability (SLI) may be challenging to diagnose.[1,2] It is the most frequent cause of wrist osteoarthritis, defined as scapholunate advanced collapse or SLAC wrist.[3] In static stage, the diagnosis is obvious when a careful radiographic analysis is performed. However, in the predynamic and dynamic SLI stages, the diagnosis is harder to make solely based on static imaging methods (radiographs, computed tomography [CT] arthrogram), which means exploratory arthroscopy may be required prior to surgical treatment. SLI is visible on lateral radiograph or sagittal CT scan as lunate instability in extension or dorsal intercalated segment instability (DISI), along with dorsal displacement of the scaphoid.[4–9] With the wrist in a neutral position, DISI typically demonstrates dorsal tilt of the lunate with an increase of scapholunate (SLA) and lunocapitate (LCA) angles.[10] DISI deformity is an important diagnostic factor and its assessment is difficult on static view. Bone superimposition and patient positioning issues can influence the relative projection of the lunate with the scaphoid and capitate on radiographs.[6] Dynamic imaging can provide information about carpal anatomy and alignment by analyzing the carpus and its joint spaces during various wrist movements.[11] Abou Arab et al[12] and Rauch et al[13] described the use of dynamic four-dimensional CT (4DCT) to analyze the carpus during radioulnar deviation (RUD). 4DCT allowed a dynamic and quantitative analysis of the LCA with a correlation to scapholunate ligament (SLL) status on CT arthrogram.[13] 4DCT could improve SLI imaging assessment by providing a more accurate evaluation of the DISI deformity in static SLI cases and by improving the identification of predynamic and dynamic SLI. We hypothesize quantitative evaluation of lunate displacement with the 4DCT can provide means to distinguish wrists with and without chronic SLI. In this study, we sought to evaluate the contribution of 4DCT relative to the standard imaging work-up for the identification of the DISI.

Materials and Methods

Study Population

This was a prospective study approved by our institutional review board. This study was registered with the Clinical Trials Registry (no. NCT02401568). Between January 2015 and December 2018, we included 40 consecutive patients older than 18 years who presented with chronic, posttraumatic wrist pain (more than 6-week history) (spontaneous and/or induced by palpation) over the scapholunate joint. They were referred by the same surgical team for complete imaging work-up because of suspected SLI. Patients with major joint stiffness, history of wrist surgery, fracture fixation, or arthroplasty implants in the wrist or congenital wrist deformity were excluded. All patients provided a written informed consent. An independent examiner (hand surgeon with 9 years of clinical experience) reviewed all the medical records to confirm the patients met the inclusion criteria. Each patient underwent an imaging evaluation consisting of radiographs and CT arthrogram of the painful wrist.

Radiographic Evaluation

All patients underwent standard anteroposterior (AP) and lateral radiographs along with dynamic AP views with a clenched fist. The images were analyzed on an OsiriX workstation (Pixmeo 2016, Geneva, Switzerland). Measurements were performed by two readers independently (R1–hand surgeon with 5 years of clinical experience and R2–radiologist with 5 years of experience with musculoskeletal imaging). Static and dynamic scapholunate gaps (SLGs) (in mm), SLA, and LCA (in degrees) were calculated (0.1 mm accuracy for gaps and 1 degree for angles). SLGs greater than 3 mm, SLAs greater than 70 degrees, and capitolunate angles greater than 15 degrees were considered pathological.[10]

4DCT Acquisition and Postprocessing of Images

Images were acquired with a 320-detector row CT scanner (Aquilion ONE, Canon Medical Systems, Otawara, Japan). We used acquisition parameters as described by Gondim Teixeira et al.[14] All acquisitions were performed using continuous volumetric mode (no table feed), 8 to 10 cm field-of-view, 512×512 matrix, and 0.5 mm slice thickness. Tube rotation time and intervolume interval were 0.5 second. Tube output was 100 kVp and 50 mAs. Images were reconstructed with bone kernel. The *z*-axis coverage was 8 cm.

Before the acquisition, the patients were instructed on how to perform the RUD manoeuver. Patients were asked to move their wrist in a continuous and homogenous manner, from maximum radial deviation to maximum ulnar deviation, and then to return to the starting point (RUD cycle). Several RUD cycles (each ~8 seconds long) were performed. Once patient motion was adequate, one RUD cycle was imaged. The examination lasted approximately 5 minutes (positioning + acquisition). The patient's position in the CT scanner is shown in ►**Fig. 1**. RUD amplitude was measured in all patients on coronal slices. A line passing through the long axis of the radius and another through the third metacarpal were drawn in the volumes acquired in maximum radial deviation and maximum ulnar deviation. The sum of these two angles was considered as the RUD amplitude. The 4DCT images were analyzed on a postprocessing workstation (Vitrea, version 7.0; Canon Medical Systems) using the 4D Ortho application. Two independent readers (R1 and R2), blinded to clinical and CT arthrogram findings performed all measurements. Once all the 4DCT volumes were loaded, multiplanar and three-dimensional images were displayed. On a multiplanar image of one of the acquisition volumes, the readers manually selected the distal radius by placing a point in its medullary canal. The software then, registered this bone in all acquisition volumes making it a static referential, which served as the basis for the manual selection of the measurement reference planes. The LCA was measured by manually placing four markers on a sagittal plane located closest to the center of the lunate fossa of the radius (►**Fig. 1**). Then, the software automatically tracked the selected markers on all the remaining volumes allowing the calculation of the LCA in degrees on each acquired volume. Four variables were calculated based these data: mean (LCA_{mean}), maximum (LCA_{max}), coefficient of variation (LCA_{cv}, standard

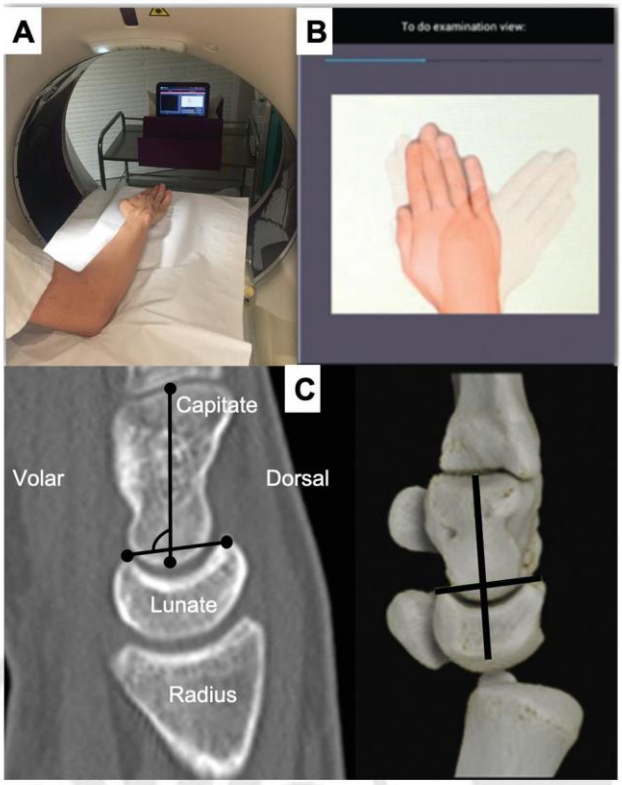

Fig. 1 Photographs of the acquisition protocol for four-dimensional computed tomography (4DCT) images: (**A**) Participant is standing beside the CT scanner table, with their wrist in neutral, placed on the table on foam cushions while wearing the lead apron and thyroid protector. (**B**) Screen capture from a tablet showing the amplitude and displacement speed during radioulnar deviation (right side). (**C**) Reference planes and marker position used for performing the lunocapitate angle (LCA) measurements in the CT multiplanar images. For construction of LCA, two markers were placed in volar and dorsal horns of lunate bone and two other markers were positioned over capitate bone long axis, in sagittal plane located closest to the center of the lunate fossa of the radius.

deviation/mean in %), and range (LCA_{range}, maximum – minimum LCA value). The estimated measurement accuracy was 1 degree.

CT Arthrogram

All patients underwent a CT arthrogram less than 1 hour after the 4DCT using the same CT scanner. The contrast agent was injected into the joint in strict aseptic conditions under fluoroscopy control by a musculoskeletal radiologist with opacification of the midcarpal and radiocarpal compartments. Nondiluted iodixanol was used as a contrast agent. The three portions of the SLL (dorsal, volar, proximal) were analyzed by an independent examiner (radiologist, 12 years' experience in musculoskeletal imaging). Based on the ligament's appearance, the patients were split into two groups: no tear or isolated tear of proximal portion only (normal SLL) and partial or full tear of dorsal and/or volar portions (ruptured SLL). The SLL ruptures were further split into two groups: partial tears (PT) (partial or total loss of continuity in the dorsal or volar segment) and full tear (FT) (total loss of continuity in the dorsal and volar segments).

Group Definition

Using the radiographic and CT arthrogram data, three groups were defined. The positive SLI groups consisted of patients who had at least one pathological radiographic variable and a ruptured SLL on the CT arthrogram (►**Fig. 2**). The negative SLI group consisted of patients who had normal radiographs and CT arthrogram. The questionable SLI groups consisted of patients who had either at least one pathological radiographic variable or a ruptured SLL on the CT arthrogram.

Statistical Analysis

Quantitative variables were described by their mean ± standard deviation, or by their median and interquartile range. Qualitative variables were described by their counts and percentages. Interobserver variability was measured with the intraclass correlation coefficient (ICC). Quantitative radiological and 4DCT data were compared between subgroups using the Wilcoxon test with Holm–Bonferroni correction for multiple comparisons. This comparison was performed for the two readers (R1 and R2). The between-group characteristics were compared using the Fisher's test or the chi-square test depending on the nature of the data.

The sensitivity, specificity, cutoff value, and area under the curve (AUC) value for each parameter calculated from 4DCT (mean, maximum, CV, and range), were determined using the receiver operating characteristic (ROC) curve analysis. The ROC analysis was performed to predict positive or negative SLI. The significant threshold was set at 5% (two-tailed tests).

Results

The mean age of the 40 patients was 47 ± 13 years. There were 18 women and 22 men. Sixteen patients were in the positive SLI group, 5 in the questionable SLI group, and 19 in the negative SLI group. The interobserver variability for each radiographic and 4DCT variable was excellent (ICC: 0.79 to 0.96). ►**Table 1** summarizes the data for each group.

Radiographic Evaluation

For the two readers, all the radiographic variables, except the LCA, were significantly higher in the positive SLI group than the negative SLI group ($p < 0.01$). When comparing the positive SLI and questionable SLI groups, the SLG static ($p = 0.02$) and SLG dynamic ($p = 0.03$) were found to be significantly higher in the positive SLI group. There was no significant difference in any of the parameters ($p > 0.05$) between the negative SLI and questionable SLI groups, although the SLA and LCA values were generally higher in the questionable SLI group.

CT Arthrogram Evaluation

In the positive SLI group ($n = 16$), a FT of the SLL was found in 3 wrists and a PT in 13 wrists. In the questionable SLI group ($n = 5$), a PT was found in 4 wrists and the other wrist had a normal SLL on CT arthrogram. There were no FTs in this group.

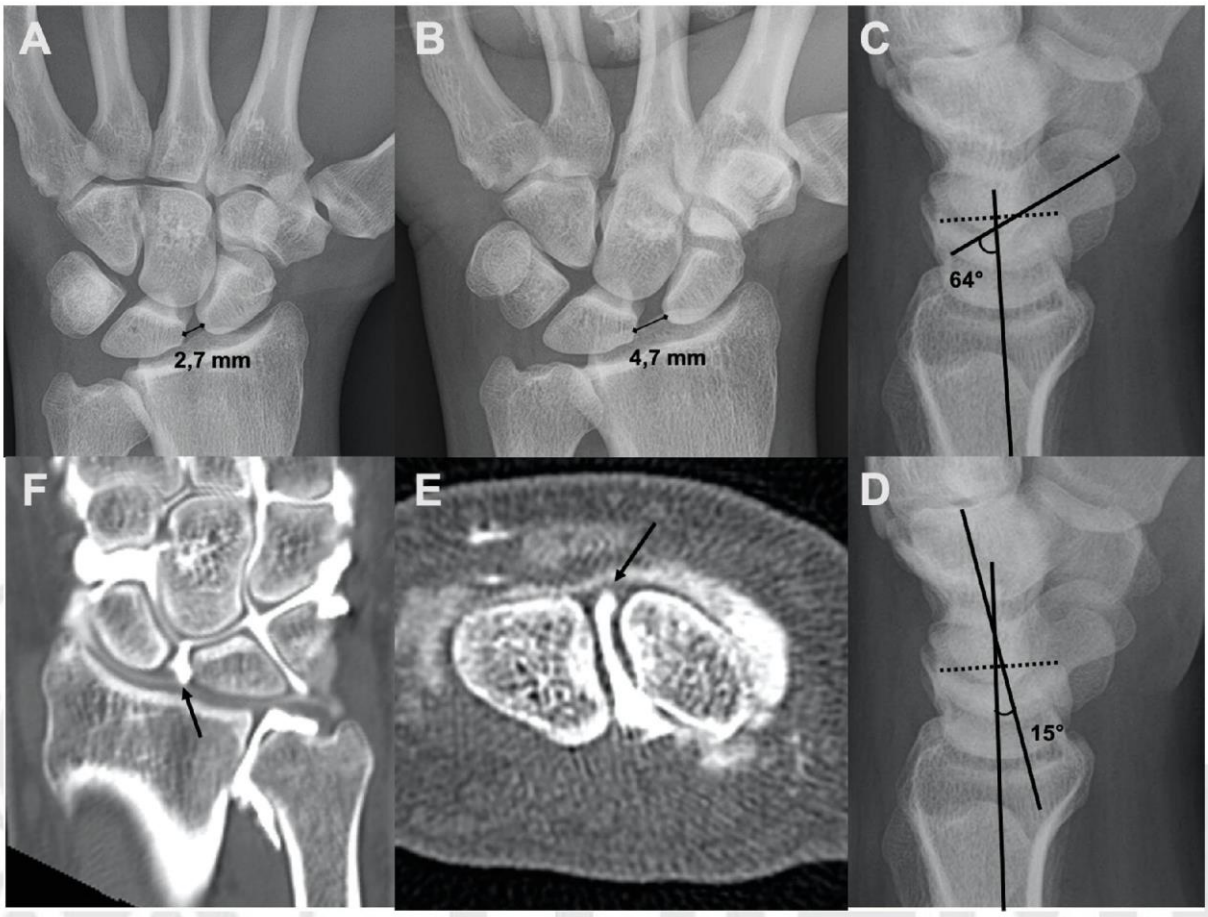

Fig. 2 Example of chronic scapholunate instability (SLI) in a 33-year-old man with a history of chronic right wrist pain for many years. (**A**) Standard anteroposterior (AP) radiograph showing scapholunate gap (SLG) static, which was measured at 2.7 mm. (**B**) Dynamic AP view in clenched fist showing SLG dynamic, which was measured at 4.7 mm. (**C**, **D**) Standard lateral radiographs showing scapholunate angle (SLA) and capitolunate angle (CLA), which was measured at 64 and 15 degrees, respectively. (**E**) Frontal computed tomography (CT) arthrogram slice showing tear of scapholunate ligament (arrow). (**F**) Axial CT arthrogram slice showing full tear of scapholunate ligament (arrow).

Table 1 Radiography and CT arthrogram findings in each group

Parameters		Group positive SLI ($n=16$)	Group negative SLI ($n=19$)	Group questionable SLI ($n=5$)
Age in years (mean ± SD)		54 ± 11	39 ± 12	53 ± 6
Sex (% women / men)		6% W; 94% M	68% W; 32% M	60% W; 40% M
Radiographs, median (IQR)	SLG static (mm)	2.7 (2.2–2.9)	1.4 (1.3–1.9)	1.5 (1–1.7)
	SLG dynamic (mm)	3.6 (2.8–4.7)	2 (1.8–2.6)	2.2 (1.7–2.7)
	SLA (degrees)	82 (68–85)	56 (49–63)	64 (50–64)
	LCA (degrees)	12 (9–23)	10 (4–12)	12 (9–15)
CT arthrogram (*n*)		3 FT; 13 PT	19 N	0 FT; 4 PT; 1 N

Abbreviations: CLA, capitolunate angle; CT, computed tomography; FT, full tear; IQR, interquartile range; LCA, lunocapitate angle; N, normal; PT, partial tear; SD, standard deviation; SLA, scapholunate angle; SLG, scapholunate gap; SLI, scapholunate instability.

4DCT Evaluation

The RUD movement amplitude was similar between subgroups: 27 ± 19 degrees for positive SLI, 30 ± 21 degrees for negative SLI, and 29 ± 20 degrees for questionable SLI.

Between the three groups, there was no significant ($p > 0.05$) difference for the LCA_{mean} and LCA_{max}. However, the LCA_{max} values were lower in the positive SLI group than the negative SLI group. There was a trend toward lower values in the positive SLI group compared with the negative SLI group of 14% for the LCA_{max}.

The positive SLI group had significantly lower LCA_{cv} ($p = 0.02$) and LCA_{range} ($p = 0.01$) values than the negative SLI group. For both readers, the values were 41% lower for the LCA_{cv} and 40% lower for the LCA_{range}.

Table 2 The LCA measured on 4DCT and their respective statistical significance in comparisons

Measurements of LCA	Group positive SLI[a] ($n=16$)	Group negative SLI[b] ($n=19$)	Group 3: questionable SLI[c] ($n=5$)
Mean (degrees)	76 (66–88)	83 (78–93)	81 (77–88)
	NS	NS	NS
Max (degrees)	88 (77–106)	102 (89–108)	97 (85–100)
	NS	NS	NS
CV (%)	7 (5–12)	12 (6–16)	8 (6–10)
	$p=0.02$	$p=0.03$	NS
Range (degrees)	18 (11–23)	27 (15–41)	18 (15–24)
	$p=0.01$	$p=0.02$	NS

Abbreviations: 4DCT, four-dimensional computed tomography; CV, coefficient of variation; LCA, lunocapitate angle; NS, no significant difference; SLI, scapholunate instability.
Note: The data shown are median (interquartile range).
[a]*p*-Values in this column are results compared with group negative SLI.
[b]*p*-Values in this column are results compared with group questionable SLI.
[c]*p*-Values in this column are results compared with group positive SLI.

The difference in all the LCA parameters between the positive SLI group and the questionable SLI group was not statistically significant ($p>0.05$).

When comparing the negative SLI and questionable SLI groups, the LCA_{cv} ($p=0.03$) and LCA_{range} ($p=0.02$) values were also significantly different (►**Table 2**).

Diagnostic Performance for Chronic SLI

Given the similar sample size in the positive SLI ($n=16$) and negative SLI ($n=19$) subgroups, and the small size of the questionable SLI ($n=5$) subgroup, only the positive and negative subgroups were included in the ROC analysis. Thus, for the two readers (►**Fig. 3**), the best overall performance for differentiation between patients with and without SLI was reached with the LCA_{cv} and LCA_{range} parameters. LCA_{cv} yielded a specificity and sensitivity of 63 and 62% by using a threshold of 9%, whereas LCA_{range} yielded a specificity and sensitivity of 71 and 63% with a threshold of 20 degrees for both readers. For $LCAc_v$ and LCA_{range}, the respective AUC were 0.62 and 0.67 (►**Table 3**).

Discussion

The current study is consistent with that of Rauch et al[13] and confirm the benefits of using 4DCT with RUD movements during the imaging work-up of patients with suspected chronic SLI.

LCA_{cv} and LCA_{range} values were significantly different between patients with and without SLI. In the studied population, low values were correlated with the presence of SLI. The threshold values of 9% and 20 degrees were the best parameters for differentiation of these patients. Moreover, despite the absence of a significant difference,

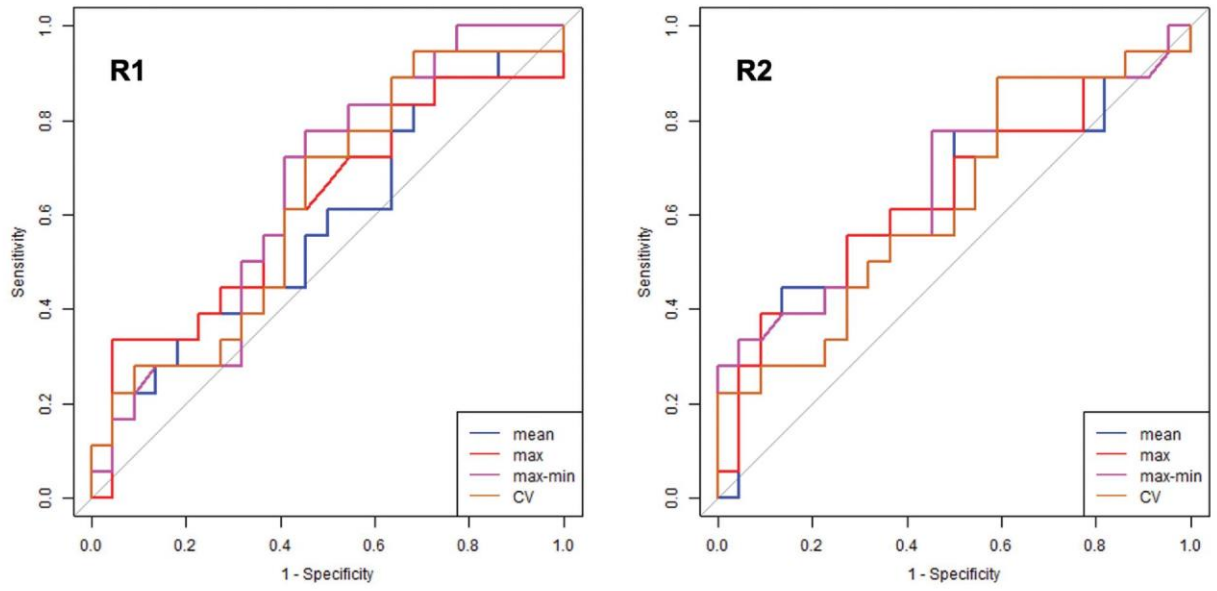

Fig. 3 Receiver operating characteristic (ROC) curves for the lunocapitate angle (LCA) parameters during four-dimensional computed tomography (4DCT) for the diagnosis of scapholunate instability (SLI) for the two readers (R1 and R2).

Table 3 Threshold values used for LCA_{cv} and LCA_{range} of 4DCT with their sensitivity, specificity, PPV, NPV, and AUC in differentiation between the patients with positive and negative SLI

LCA	Threshold	Sensitivity (%)	Specificity (%)	PPV (%)	NPV (%)	AUC
CV	9%	62	63	60	65	0.62
Range	20 degrees	63	71	67	65	0.67

Abbreviations: 4DCT, four-dimensional computed tomography; AUC, area under curve; CV, coefficient of variation; LCA, lunocapitate angle; NPV, negative predictive value; PPV, positive predictive value; SLI, scapholunate instability.

there was a trend toward lower LCA_{max} values in patients with SLI. With a RUD manoeuver, 4DCT allowed to identify and quantify the lunate instability in extension or DISI and confirmed the SLI status with an excellent interobserver reproducibility.

Contrary to Rauch et al.,[13] our groups were defined using combined radiographic and CT arthrogram data, which better reflects our current practice when making a diagnosis. However, according to those authors, the best differentiation of patients with and without SLL tears was achieved with the LCA_{cv}, LCA_{range}, and LCA_{max}.

Despite the small sample size of the questionable SLI group ($n = 5$), when it was compared with the negative SLI groups, the LCA_{cv} and LCA_{range} values were clearly lower in the questionable SLI group. Given the significant difference found, those two parameters appear to be the most relevant for differentiating between these two groups. Also, the LCA_{cv} and LCA_{range} values were fairly similar between the positive SLI patients and questionable SLI patients.

DISI deformity is an important element of the pathogenesis of SLI. Classically described as a lunate dorsiflexion with a rotatory subluxation of the scaphoid, static SLI manifests itself as a complex deformity with posterior subluxation of the unit formed by the scaphoid and the capitate.[5,6] Omori et al,[15] in a three-dimensional analysis of the DISI deformity in the scapholunate dissociated wrists confirmed the lunate is extended and supinated secondarily to SLI. Thus, these positional abnormalities of the scaphoid and lunate contribute in the development of SLAC wrist. The posterior radioscaphoid contact and the lunocapitate decentering are the origin of the radioscaphoid and midcarpal osteoarthritis that later appears.[16]

Up to now, evaluation of DISI deformity was made using static imaging methods, without assessing carpal bone position during motion, which may be of interest for the diagnostic SLI. On lateral radiographic view or sagittal CT images, DISI typically demonstrates dorsal tilt of the lunate with an increase of SLA and LCA.[10] In our study, for the both readers, on the radiographic analysis, SLA and LCA values were not systematically correlated. Koh et al[17] suggested with their study that even minimal degrees of wrist flexion-extension (from 20 degrees of flexion to 20 degrees of extension) can affect the measurements of carpal measurements on lateral radiographs, such as the SLA and the LCA. Also, one of the advantages of 4DCT is that it gets around superimposition phenomenon and errors related to the patient's wrist position during standard radiographs or CT scan. Thus, LCA on 4DCT is interesting because it is quantitative and reproducible. LCA could be used as a single parameter for the DISI deformity and lunate motion amplitude assessment with potential surgical implications. The presence of a lunate dorsiflexion and its quantification could be used as a marker of the biomechanical importance of the scapholunate complex (SLL and extrinsic ligaments) injury and the severity of SLI. Pérez et al, in a cadaveric study, evaluated the role of the scaphotrapeziotrapezoid, and dorsal intercarpal (DIC) ligaments in preventing DISI.[18] To produce that deformity, SLL injuries require the associated disruption of at least one extrinsic ligament, stabilizer of the scaphoid or lunate. Mitsuyasu et al had already highlighted the essential role of the DIC in stabilizing the scaphoid and lunate and preventing DISI deformity in cases of SLI.[19] Thus, it might be possible to identify and treat patients with an early stage of SLI characterized by a partial SLL tears associated with an extrinsic ligament injury.[20–22]

As for the type of movement used during 4DCT, Abou Arab et al[12] and Rauch et al[13] stated that the RUD movement was better at detecting SLL lesions than clenched fist movements. According to these authors, analyzing the carpus during RUD movements has better diagnostic performance and superior reproducibility than during clenched fist movements.

The primary limitation of our study is the small number of patients in each group, especially the questionable SLI group ($n = 5$). Thereby, further studies are necessary to explore this group of patients. Second, the SLL ruptures and SLI were not confirmed by arthroscopy, which is generally considered the true reference standard for the diagnosis. However, CT arthrogram has a high performance for the diagnosis of SLL tears (95% sensitivity and 86% specificity)[23] and arthroscopy is an invasive procedure that places the patient at risk of an infection, nerve lesion, pain, or stiffness.[24] Also, it is currently impossible to quantify the DISI deformity during arthroscopy. 4DCT data could be beneficial since arthroscopy scores[7,8] for SLI diagnosis are known to have inter- and intraobserver errors,[25] making them less reproducible than 4DCT. Third, the amplitude of the RUD movement was not standardized, thus varied from one patient to another. In our study, the mean RUD amplitude was fairly similar between the three groups. This parameter did not seem to have influence the diagnostic performance of 4DCT.

Lastly, implementation of this new imaging modality requires training of the medical staff and also teaching the patient beforehand how to perform the movement correctly without moving the forearm.

Conclusion

Given our study's findings, 4DCT appeared as a quantitative relevant tool for the evaluation of DISI deformity in cases of

SLI, including for patients presenting with questionable initial radiography findings. LCA analysis was invariably measurable and reproducible. LCA_{cv} and LCA_{range} were the best parameters to identify patients with and without SLI. Values under 9% and 20 degrees were strongly associated with SLI. Abnormal LCA values, especially CV and range, seem to be indicative of significant biomechanical changes in the dissociated wrists with potential implications for patient treatment. The continuation of our prospective study is necessary to fully appreciate the prognostic value of LCA.

Note

All patients gave their informed consent for this study.

Ethical Approval

This study was approved by our institutional review board and by the local ethics committee (PERSONAL PROTECTION COMMITTEE EST-III, VANDŒUVRE-LES-NANCY, France). This study was registered with the Clinical Trials Registry (no. NCT02401568).

Funding

None.

Conflict of Interest

Two authors involved in this work (Pedro Augusto Gondim Teixeira and Alain Blum) participate on a non-remunerated research contract with TOSHIBA Medical Systems for the development and clinical testing of postprocessing tools for musculoskeletal CT. The authors declare no potential conflicts of interest with respect to the research, authorship, and/or publication of this article.

References

1 Athlani L, Pauchard N, Detammaecker R, et al. Treatment of chronic scapholunate dissociation with tenodesis: a systematic review. Hand Surg Rehabil 2018;37(02):65–76
2 Crawford K, Owusu-Sarpong N, Day C, Iorio M. Scapholunate ligament reconstruction: a critical analysis review. JBJS Rev 2016;4(04):e41–e48
3 Watson HK, Ballet FL. The SLAC wrist: scapholunate advanced collapse pattern of degenerative arthritis. J Hand Surg Am 1984;9 (03):358–365
4 Linscheid RL, Dobyns JH, Beabout JW, Bryan RS. Traumatic instability of the wrist: diagnosis, classification, and pathomechanics. J Bone Joint Surg Am 2002;84(01):142
5 Watson H, Ottoni L, Pitts EC, Handal AG. Rotary subluxation of the scaphoid: a spectrum of instability. J Hand Surg [Br] 1993;18(01): 62–64
6 Kitay A, Wolfe SW. Scapholunate instability: current concepts in diagnosis and management. J Hand Surg Am 2012;37(10): 2175–2196
7 Dreant N, Dautel G. Development of a arthroscopic severity score for scapholunate instability [in French]. Chir Main 2003;22(02):90–94
8 Geissler WB. Arthroscopic management of scapholunate instability [in French]. Chir Main 2006;25(Suppl 1):S187–S196
9 Taleisnik J. Current concepts review. Carpal instability. J Bone Joint Surg Am 1988;70(08):1262–1268
10 Larsen CF, Amadio PC, Gilula LA, Hodge JC. Analysis of carpal instability: I. Description of the scheme. J Hand Surg Am 1995;20 (05):757–764
11 Zhao K, Breighner R, Holmes D III, Leng S, McCollough C, An KN. A technique for quantifying wrist motion using four-dimensional computed tomography: approach and validation. J Biomech Eng 2015;137(07):
12 Abou Arab W, Rauch A, Chawki MB, et al. Scapholunate instability: improved detection with semi-automated kinematic CT analysis during stress maneuvers. Eur Radiol 2018;28(10):4397–4406
13 Rauch A, Arab WA, Dap F, Dautel G, Blum A, Gondim Teixeira PA. Four-dimensional CT analysis of wrist kinematics during radioulnar deviation. Radiology 2018;289(03):750–758
14 Gondim Teixeira PA, Formery AS, Hossu G, et al. Evidence-based recommendations for musculoskeletal kinematic 4D-CT studies using wide area-detector scanners: a phantom study with cadaveric correlation. Eur Radiol 2017;27(02):437–446
15 Omori S, Moritomo H, Omokawa S, Murase T, Sugamoto K, Yoshikawa H. In vivo 3-dimensional analysis of dorsal intercalated segment instability deformity secondary to scapholunate dissociation: a preliminary report. J Hand Surg Am 2013;38(07): 1346–1355
16 Laulan J. Rotatory subluxation of the scaphoid: pathology and surgical management [in French]. Chir Main 2009;28(04): 192–206
17 Koh KH, Lee HI, Lim KS, Seo JS, Park MJ. Effect of wrist position on the measurement of carpal indices on the lateral radiograph. J Hand Surg Eur Vol 2013;38(05):530–541
18 Pérez AJ, Jethanandani RG, Vutescu ES, Meyers KN, Lee SK, Wolfe SW. Role of ligament stabilizers of the proximal carpal row in preventing dorsal intercalated segment instability: a cadaveric study. J Bone Joint Surg Am 2019;101(15):1388–1396
19 Mitsuyasu H, Patterson RM, Shah MA, Buford WL, Iwamoto Y, Viegas SF. The role of the dorsal intercarpal ligament in dynamic and static scapholunate instability. J Hand Surg Am 2004;29(02): 279–288
20 Mathoulin CL. Indications, techniques, and outcomes of arthroscopic repair of scapholunate ligament and triangular fibrocartilage complex. J Hand Surg Eur Vol 2017;42(06):551–566
21 Degeorge B, Coulomb R, Kouyoumdjian P, Mares O. Arthroscopic dorsal capsuloplasty in scapholunate tears EWAS 3: preliminary results after a minimum follow-up of 1 year. J Wrist Surg 2018;7 (04):324–330
22 Ho PC, Wong CW, Tse WL. Arthroscopic-assisted combined dorsal and volar scapholunate ligament reconstruction with tendon graft for chronic SL instability. J Wrist Surg 2015;4(04):252–263
23 Bille B, Harley B, Cohen H. A comparison of CT arthrography of the wrist to findings during wrist arthroscopy. J Hand Surg Am 2007; 32(06):834–841
24 Lee YH, Choi YR, Kim S, Song HT, Suh JS. Intrinsic ligament and triangular fibrocartilage complex (TFCC) tears of the wrist: comparison of isovolumetric 3D-THRIVE sequence MR arthrography and conventional MR image at 3 T. Magn Reson Imaging 2013;31 (02):221–226
25 Obdeijn MC, Tuijthof GJ, van der Horst CM, Mathoulin C, Liverneaux P. Trends in wrist arthroscopy. J Wrist Surg 2013;2(03): 239–246

Corrélation des données scanographiques dynamiques 4-Dimensions avec celles de l'analyse arthroscopique.

Dynamic 4D computed tomography data corresponds well to dynamic arthroscopic testing of scapholunate instability: a preliminary study.

Jonathan Granero[(1)], Sinan Orkut[(2)], Aymeric Rauch[(2)], Alain Blum[(2,3)], Gilles Dautel[(1)], Pedro Augusto Gondim Teixeira[(2,3)], Lionel Athlani[(1,3)*]

[1] Department of Hand Surgery, Plastic and Reconstructive Surgery, Centre Chirurgical Emile Gallé, Nancy University Hospital, 49 rue Hermite, 54000 Nancy, France.

[2] Guilloz Imaging Department, Central Hospital, Nancy University Hospital, 29 avenue du Maréchal de Lattre de Tassigny, 54035 Nancy, France.

[3] IADI Laboratory, INSERM U1254, Nancy, France.

[*] Corresponding author: Lionel Athlani (lionel.athlani@gmail.com)

ABSTRACT

Purpose - To evaluate the correspondences between the arthroscopic dynamic analysis of the scapholunate (SL) joint and the quantitative multiparametric dynamic four-dimensional computed tomography (4DCT) analysis for the diagnosis of suspected chronic SL instability.

Methods - Thirty-three patients (16 men, 17 women; mean age 48 ± 13 years) with suspected SL instability were evaluated prospectively with 4DCT and wrist arthroscopy. Based on the arthroscopic Dréant and Dautel's score, two groups were defined: Group 1 (n=8) consisted of patients who had no or a slight incongruency of SL alignment in the midcarpal space, Group 2 (n=25) consisted of patients who had a proven or a severe incongruency of SL alignment. Two independent readers used 4DCT to evaluate the scapholunate gap (SLG) (mean, maximum, minimum, and range values), the lunocapitate (LCA), and radioscaphoid (RSA) angles (mean and range values) during radioulnar deviation.

Results - The interobserver variability was deemed good for most of the 4DCT variables.

For both readers, the SLG mean, maximum, minimum values were significantly higher, and the LCA mean significantly lower in the Group 2 than in the Group 1 ($p=0.01$ or <0.01). Only for one reader, the SLG range was significantly higher, and the LCA range significantly lower in the Group 2 than in the other group ($p=0.01$ and 0.02). For both readers, in the Group 2, the RSA range values were lower, and the RSA mean values were slightly higher than the Group 1.

Conclusion - quantitative 4DCT data corresponded well with the arthroscopic dynamic analysis of the SL joint in patients with suspected chronic SL instability.

Key words: Arthroscopy; Four-dimensional computed tomography; Joint instability; Kinematics; Wrist injury

Type of study / Level of evidence: Diagnostic IV

INTRODUCTION

Scapholunate (SL) instability may be challenging to diagnose[1,2]. In the static stage, the diagnosis is usually obvious when careful radiographic analysis is performed. However, the surgical treatment choice is not as straightforward at this stage, especially when it comes to evaluating the scaphoid's reducibility. Indeed, a mobile, reducible scaphoid is a known requirement for SL ligament reconstruction, and in its absence, partial intracarpal arthrodesis may be required[2]. The diagnosis of predynamic and dynamic SL instability is harder to make solely based on conventional static imaging methods (radiographs, CT arthrogram), which means exploratory arthroscopy may be required prior to surgical treatment[3-5]. For many surgical teams, wrist arthroscopy is considered the gold standard to directly explore the SL interosseus ligament and the SL joint space[6-8]. Indeed, this surgical procedure allows us to see the lesions, even at an early stage. Moreover, the cartilage surfaces are visible under magnification and bright light, and therefore, it possible to identify focal chondral damages. Dréant and Dautel' s[6] classification is widely accepted in arthroscopic diagnostics of SL instability. Thereby, the degree of probe insertion allowed into the SL joint space from the midcarpal approach indicates the stage of SL instability in wrists with SL ligament tear as seen from the radiocarpal approach. Based on this dynamic testing, the authors report the development of a three-stage arthroscopic severity score for SL instability.

Recently, Abou Arab et al.[9] and Rauch et al.[10] described using Four-dimensional computed tomography (4DCT) to analyze the carpus during radioulnar deviation (RUD). This dynamic imaging can analyze changes in the carpal joint spaces during wrist movements[11]. In these studies, 4DCT allowed a dynamic and quantitative analysis of the scapholunate gap (SLG), lunocapitate angle (LCA), and radioscaphoid angle (RSA) with a correlation to SL ligament status on CT arthrogram. However, the diagnosis of SL instability was not confirmed by arthroscopy. Given the positive correlation between 4DCT data and SL ligament status, we hypothesize there is a correlation between the Dréant and Dautel' s[6] score and the 4DCT evaluation of SL instabilities.

This study aimed to assess the correspondences between arthroscopic dynamic analysis of the SL joint and quantitative multiparametric 4DCT in patients with suspected chronic SL instability. Having an accurate non-invasive method for evaluating SL instability might reduce the need for diagnostic wrist arthroscopy prior to the actual surgical treatment in patients with SL instability.

METHODS

Study population

Between January 2015 and March 2020, a prospective study was carried out with 33 consecutively included patients (16 men, 17 women) older than 18 years, who presented with chronic post-traumatic wrist pain (more than 6-week history) (spontaneous and/or induced by palpation) over the SL joint space. None had major joint stiffness, history of wrist surgery, fracture fixation or arthroplasty implants in the wrist, or congenital wrist deformity.

Each patient underwent an imaging evaluation consisting of standard radiographs (anteroposterior and lateral views, dynamic clenched fist view, anteroposterior views in radial deviation and ulnar deviation), and CT arthrography of the painful wrist. Acquisition parameters are presented in table 1. All patients were diagnosed with suspected chronic reducible SL instability (SLG greater than 3 mm and/or scapholunate angle (SLA) greater than 70°; partial or full tear of dorsal and/or volar portions of SL interosseous ligament), with no chondral damage[12, 13]. Radiographs of the asymptomatic contralateral wrist were used to verify that no congenital scapholunate ligament laxity was present that could lead to scapholunate pseudo-dissociation[14]. 4DCT followed by arthroscopy of the injured wrist were performed in all cases to confirm and stage the SL instability. All patients were operated on the same healthcare facility by the same surgical team. All patients provided written informed consent, and the local ethics committee approved this study.

Evaluation of CT arthrography findings

Two independent examiners (L1 and L2 – radiologists with 13 and 8 years of experience with musculoskeletal imaging) reviewed all CT arthrogram imaging. The three portions of the SL ligament (dorsal, volar, proximal) were analyzed. Based on the ligament's appearance, the patients were divided into two groups: no tear or isolated tear of proximal portion (normal SL ligament) and partial or full tear of dorsal and/or volar portions (ruptured SL ligament). The SL ligament ruptures were further divided into partial tears (PT) (partial or total loss of continuity in the dorsal or volar segment) and full tears (FT) (total loss of continuity in the dorsal and volar segments).

4DCT acquisition and post-processing of images

Images were acquired with a 320-detector row CT scanner (Aquilion ONE™, Canon Medical Systems, Otawara, Japan) with the acquisition protocol proposed by Gondim Teixeira et al.[15] (Table 1).

Before the acquisition, the patients were instructed on how to perform the RUD manoeuver. Patients were asked to move their wrist in a continuous and homogenous manner, from maximum radial deviation to maximum ulnar deviation, and then return to the starting point (RUD cycle). Several RUD cycles (each about 8 seconds long) were performed. Once patient motion was adequate, one RUD cycle was imaged. The examination lasted about 5

minutes (positioning + acquisition). The patient's position in the CT scanner is shown in Figure 1. The 4DCT images were analyzed on a post-processing workstation (Vitrea, version 7.0; Canon Medical Systems) using the 4D Ortho application. Two independent readers (R1 and R2, specialist surgeon and radiologist with 6 and 4 years of experience), blinded to clinical, radiographs, and CT arthrogram findings, performed all measurements. Once all the 4DCT volumes were loaded, multiplanar and three-dimensional images were displayed. On a multiplanar image of one of the acquisition volumes, the readers manually selected the distal radius by placing a point in its medullary canal. The software then registered this bone in all acquisition volumes making it a static referential, which served as the basis for the manual selection of the measurement reference planes. Next, two markers for distance measurements, and four markers for angle measurements were placed manually. The SLG was measured in the axial plane, and the LCA and RSA were measured on the sagittal plane. The marker positioning procedure and anatomic landmarks used for each of these measurements are shown in Figure 2. The software then automatically tracks the selected markers on all the remaining acquired volumes, allowing the SLG, LCA, and RSA calculation on each acquisition volume.

For the SLG, four variables were calculated based on the data: mean (in mm), maximum or max (in mm), minimum or min (in mm), range (max - min, in mm). Two variables were calculated for the angles: mean (in degrees) and range (in degrees). The software measurement accuracy was estimated at 0.1 mm for the gap and 1° for the angles.

Surgical procedure of wrist arthroscopy.

The surgical procedures were performed by senior surgeons (minimum of 10 years' clinical experience) under regional anesthesia and a tourniquet applied on the upper arm.

First, the operated arm was placed in a wrist traction tower, and 5–8 kg of vertical traction force was applied through plastic finger traps to the middle 3 fingers for joint distraction on a hand table. We used a 30° 2.5 mm (Richard Wolf GmbHP, Knittlingen, Germany) video arthroscope, a 2.9 mm shaver (Arthrex®, Naples, Florida, United States), and a hook probe for surgical instruments. We applied continuous irrigation. We made 3-4 and 6R portals for the radiocarpal joint space and midcarpal radial - MCR -, midcarpal ulnar - MCU -, for the midcarpal joint space. The radiocarpal joint space was inspected first. Special attention was placed on the interosseous ligaments' status during this step, especially the three portions of the SL ligament and the articular cartilage. We then transferred the arthroscope to the midcarpal joint space and examined the SL alignment by probing the scapholunate joint using the arthroscopic hook probe. We used the Dréant and Dautel' s[6] classification to assess the severity of the SL instability. We also confirmed that no chondritis was present (Figure 3).

Table 1. Acquisition parameters for wrist 4DCT and CT arthrography.

Acquisition Mode	Sequential CT arthrography	Sequential 4DCT
Field-of-view (cm)	8 to 10	8 to 10
z-axis coverage (cm)	8	8
Section thickness (mm)	0.5	0.5
Tube rotation (sec)	0.5	0.35
Tube voltage (kVp)	100	100
Milliamperage (mAs)	50	35
Reconstruction matrix	512 X 512	512 X 512
Image reconstruction	Bone kernel	Soft-tissue kernel

Adaptive iterative dose reconstruction 3D (AIDR 3D; Canon Medical Systems, Otawara, Japan) was used at the standard level for all acquisitions. Images were obtained without table feed.

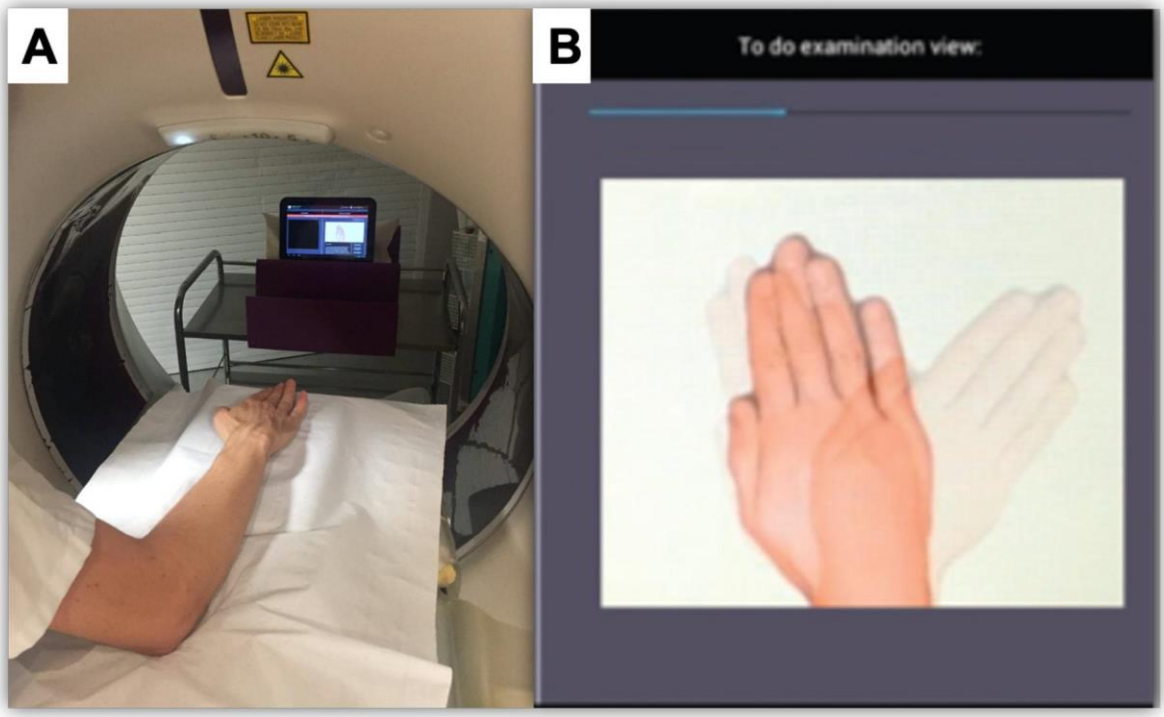

Figure 1. *Photographs of the acquisition protocol for 4DCT images. A- Participant is standing beside the CT scanner table, with their wrist in neutral, placed on the table on foam cushions while wearing the lead apron and thyroid protector. B- Screen capture from a tablet showing the amplitude and displacement speed during radioulnar deviation (right side).*

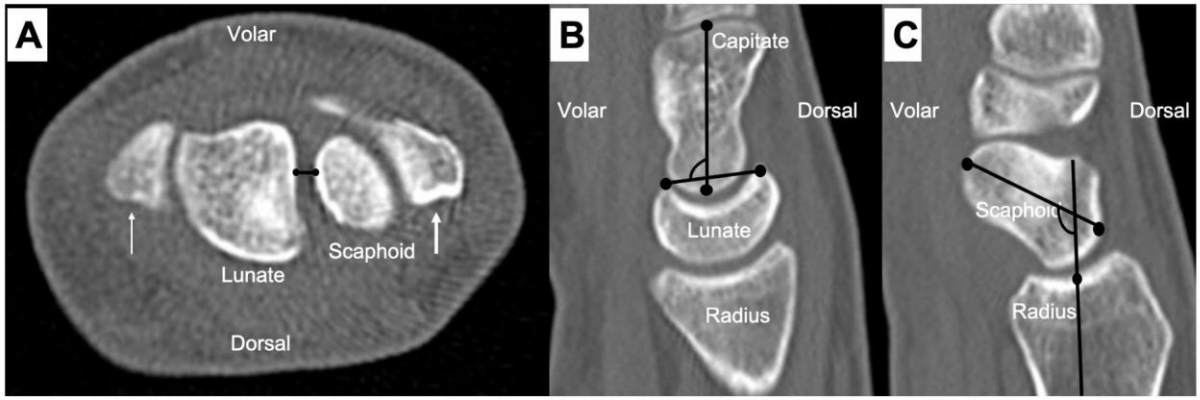

Figure 2*. Reference planes and marker position used for performing the gap and angular measurements in the CT multiplanar images.*
A- For construction of SLG, two markers were placed on the scaphoid and lunate as the shortest distance between these two bones, in axial plane passing through the radial styloid (thin arrow) and ulnar styloid (thick arrow).
B- For construction of LCA, two markers were placed in volar and dorsal horns of lunate bone and two other markers were positioned over capitate bone long axis, in sagittal plane located closest to the center of the lunate fossa of the radius.
C- For construction of RSA, two markers were placed in posterior and anterior-most points of scaphoid and two other markers were positioned in medullary cavity of radius following its long axis, in sagittal plane located closest to the center of the scaphoid fossa of the radius.

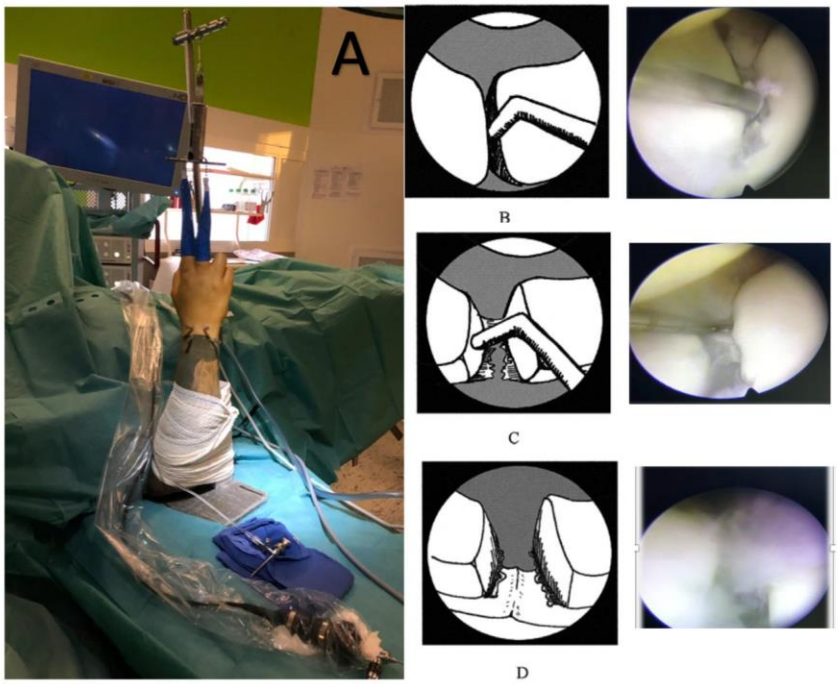

Figure 3. *Photographs and Diagrams illustrating a wrist arthroscopy procedure. A right wrist is suspended in a traction tower (A). In the midcarpal joint space, we used a midcarpal radial portal and a midcarpal ulnar portal to probe the SL joint. According to Dréant and Dautel' s[6] classification, stage 1 (slight SL instability) is the possibility to put the tip of the hook between the bones (A); stage 2 (proven SL instability) is the possibility to create a SL diastasis with the use of a twisting motion applied to the hook (B); stage 3 (severe SL instability) is the possibility to pass the 2.7-mm arthroscope between the scaphoid and lunate from the midcarpal to the radiocarpal joint spaces (C). We also noted the absence (C-) or presence (C+) of chrondal damages.*

Group definition

Using the Dréant and Dautel' s[6] score, two groups were defined: group 1 consisting of patients who had no (stage 0) or a slight incongruency (stage 1) of SL alignment in the midcarpal space and group 2 consisting of patients who had a proven (stage 2) or a severe incongruency (stage 3) of SL alignment in the midcarpal space.

Statistical analysis

Quantitative variables were described by their mean ± standard deviation or by their median and interquartile range. Qualitative variables were described by their counts and percentages. Interobserver variability was measured with the intraclass correlation coefficient - ICC – and its 95% confidence interval. We suggest that ICC values less than 0.5 indicate poor reliability, values between 0.5 and 0.75 indicate moderate reliability, values between 0.75 and 0.9 indicate good reliability, and values greater than 0.90 indicate excellent reliability[16]. Quantitative 4DCT data were compared between groups using the Wilcoxon test with Holm-Bonferroni correction for multiple comparisons. This comparison was performed for the two readers (R1 and R2). The between-group characteristics were compared using the Fisher test or the X^2 depending on the data's nature. The statistical significance threshold was set at 5% (two-tailed tests).

RESULTS

The mean age of the 33 patients included in this study was 48 ± 13 years. There were eight patients in group I and 25 in group II.

Arthroscopic findings

Arthroscopically, there was no wrist with chondral lesions. Based on the radiocarpal joint space analysis, none of the patients had a normal concave appearance of the SL ligament. In the patients of the group 1, we systematically found a SL ligament perforated or partially ruptured with some torn fibers in its dorsal or ventral part. In patients of the group 2, the SL ligament was always totally torn in all included patients.

CT arthrogram assessment

The interobserver variability for evaluating the SL ligament was deemed poor for the proximal and ventral portions and good for the dorsal portion. Global ligament analysis presented a moderate interobserver variability (Table 2).

On the CT arthrogram, in the Group 1, 5 wrists had normal SL ligament and 3 wrists a PT, for both readers. In the Group 2, 2 wrists had normal SL ligament, 13 (L1) - 11 (L2) wrists a PT, and 10 (L1) – 12 (L2) wrists a FT.

4DCT assessment

The interobserver variability was deemed good or excellent for the SLG mean, SLG max, SLG min, LCA mean, RSA mean and RSA range. It was deemed moderate for the LCA range, and poor for the SLG range (Table 2).

For both readers, the SLG mean, max, and min values were significantly higher in the Group 2 than in the Group 1 ($p=0.01$ or <0.01). The SLG range values were also significantly higher in the Group 2 than in the other group, but only for R1 ($p=0.01$). For R2, the values were similar in the two groups.

For both readers, the LCA mean values were significantly lower in the Group 2 than in the Group 1 ($p<0.01$). The LCA range values were significantly lower in the Group 2 than in the other group, but only for R1 ($p=0.02$). For R2, despite the absence of significant values, they were also lower in the Group 2.

For both readers, in the Group 2, the RSA range values were lower, and the RSA mean values were slightly higher than the Group 1, but these differences were not statistically significant ($P = 0.07$-0.61) (Table 3).

Table 2. Interobserver variability in the CT arthrogram (L1 / L2) and 4DCT parameters measured (R1 / R2).

Inter-observer variability	CT Arthogram				SLG				LCA		RSA	
	Dorsal Portion Analysis	Proximal Portion Analysis	Ventral Portion Analysis	Final Analysis	Mean	Max	Min	Range	Mean	Range	Mean	Range
ICC (95% CI)	**0.77** (0.56 – 0.97)	**0.03** (0.10 – 0.03)	**0.16** (0.03 – 0.29)	**0.71** (0.50 – 0.92)	**0.89** (0.80 – 0.94)	**0.76** (0.57 – 0.87)	**0.77** (0.59 – 0.88)	**0.30** (0.03 – 0.58)	**0.75** (0.54 – 0.86)	**0.64** (0.38 – 0.80)	**0.93** (0.86 – 0.96)	**0.91** (0,84 – 0.85)

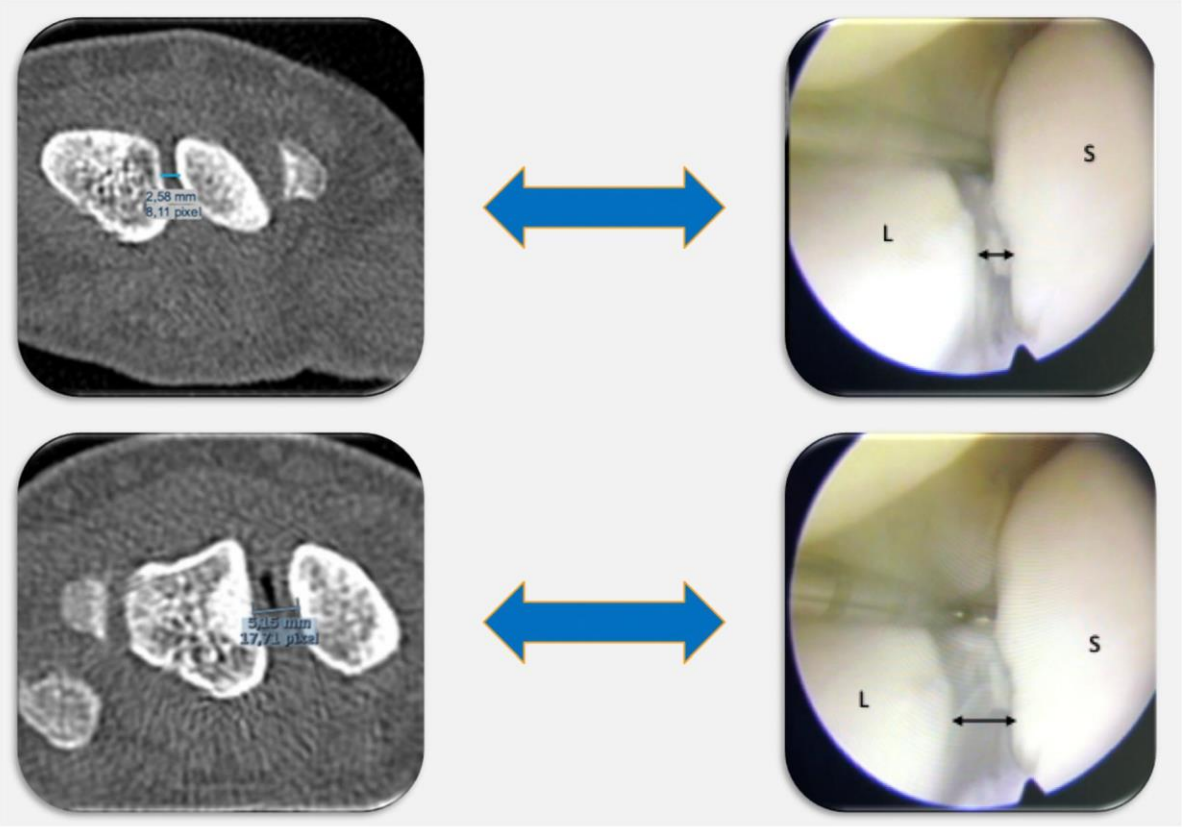

Figure 4. *Example of chronic SL instability in a 25-year-old man with a history of chronic right wrist pain. In neutral position, the SLG measured 2.6 mm on the axial CT slice in the reference plane. In ulnar deviation, the SLG measured 5.1 mm on the axial CT slice in the reference plane. By probing the SL joint arthroscopically through the midcarpal joint, we noted a correspondence with a proven SL instability.*

Table 3. 4DCT findings in each group

			Group 1 (n=8)	Group 2 (n=25)	p value
4DCT (Median (Q1-Q3))	**SLG Mean (mm)**	**R1**	2.2 (1.8 - 2 .8)	3.9 (3.1 - 5.5)	<0.01
		R2	2.5 (2.1- 2.6)	3.9 (3.0 - 5.0)	<0.01
	SLG Max (mm)	**R1**	2.5 (2.1- 3.3)	5 (3.4 - 6)	<0.01
		R2	2.5 (2.4 - 3.2)	3.9 (3.1 - 4.5)	0.01
	SLG Min (mm)	**R1**	2 (1.7 - 2.5)	2.9 (2.5 – 3.7)	<0.01
		R2	2.1 (1.8 – 2.3))	2.8 (2.6 – 3.5)	<0.01
	SLG Range (mm)	**R1**	0.75 (0.7 - 1.1)	1.4 (1 - 2.2)	0.01
		R2	0.7 (0.4 - 0.9)	0.5 (0.3 - 1.3)	0.98
	LCA Mean (°)	**R1**	92 (86 - 100)	77 (71 - 86)	<0.01
		R2	89 (82 - 95)	75 (69 - 83)	<0.01
	LCA Range (°)	**R1**	28 (18 - 33)	14 (12 - 19)	0.02
		R2	21 (11 - 31)	16 (12 - 22)	0.49
	RSA Mean (°)	**R1**	100 (97 - 102)	103 (97 - 106)	0.61
		R2	100 (99 - 104)	104 (100 - 106)	0.44
	RSA Range (°)	**R1**	34 (24 - 38)	24 (14 - 29)	0.07
		R2	33 (23 - 40)	21 (13 - 28)	0.07

DISCUSSION

Our study's findings confirm a correspondence between the arthroscopic dynamic analysis of the SL joint using the Dréant and Dautel' s[6] classification and the quantitative multiparametric 4DCT analysis for the diagnosis of suspected chronic SL instability. Among the evaluated parameters, the SLG appears to be the most relevant for differentiating between patients with no or slight and proven or severe SL incongruence. Indeed, median SLG values were significantly higher in the Group 2, with a 67%, 78%, 39% and 47% increase for mean, maximal, minimal, and range values, respectively compared to group I. Moreover, the interobserver reproducibility of SLG derived parameters except for the range was deemed good. Our results add to those of Abou Arab et al.[9] confirming not only the association between SL ligament morphology and quantitative 4DCT kinematic analysis but also the correspondence of 4DCT parameters (particularly SLG) and arthroscopic findings.

Many authors currently consider wrist arthroscopy as the "gold standard" for the diagnosis of SL instability[5]; however, its role is mainly diagnostic[17,18]. Using arthroscopy findings as a reference, Bille et al.[19] reported the inferiority of CT arthrogram for the analysis of cartilage surfaces (sensitivity of 45%) as well as for the assessment of SL ligament tears (sensitivity of 85%). The main drawbacks of arthroscopy are the technical complexity and invasiveness of the technique with potential complications such as infection, nerve lesion, pain, or stiffness[18]. Leclercq and Mathoulin[17] noted a significant relationship between the complication rate and the individual surgeon's experience, the threshold for a lower complication rate being approximately 25 arthroscopies a year and/or greater than 5 years of experience. Also, Obdeijn et al.[18] underlined the inter- and intra-observer variability of wrist arthroscopy. Moreover, arthroscopic scores[6-8] to assess SL instability are based on subjective SL joint dynamic tests, as quantification is currently possible during arthroscopy. Thus, 4DCT data could be beneficial due to the quantitative approach and its reproducibility.

Rauch et al.[10] demonstrated that lunate instability in extension or dorsal intercalated segment instability, along with scaphoid flexion deformity, could be assessed by measuring the LCA and RSA. The authors found low LCA Range and RSA Range values correlated with SL ligament tears on the CT arthrogram. In our study, median values were significantly lower in the Group 2, corresponding to 37% for the LCA Range and 33% for the RSA Range, respectively. Abnormal LCA and RSA values could be indicative of significant biomechanical changes in the wrist. With arthroscopic scores[6-8], only SL alignment's congruency is evaluated, but scaphoid or lunate bone positional anomalies are not accessible. Corella et al.[20] described a test to explore the proximal to distal displacement of the scaphoid (the step-off) in case of SL instability. According to these authors, this test can add information to the SL instability's arthroscopic classifications, but it is not quantifiable. Thus, the quantitative analysis

of scaphoid motion amplitude with LCA and RSA measurements with the 4DCT could be used as an imaging marker of the SL instability's severity with a potential prognostic role. A more accurate evaluation of SL dissociation reducibility in patients with SL instability could potentially optimize indications for ligament reconstructions. The reducible nature of the dissociation is the basic criterion that must be met for those surgical procedures.

For several authors, CT arthrogram has a high performance for the diagnosis of SL ligament tears. For Schmid et al.[21], the sensitivity reached 100%, with a specificity of 77%. In our study, we found a poor interobserver reproducibility for the analysis of the SL ligament ventral portion, and the differentiation between PT and FT was based on the analysis of the dorsal and ventral portions. Furthermore, in patients with severe SL incongruence, the SL ligament morphology was heterogeneous with 8% normal appearance of the SL ligament, 44% - 52% of PT, and 40% - 48% of FT, suggesting ligament morphology is not always correlated to ligament sufficiency. With the CT arthrogram, false negatives could be explained, in part, by the presence of residual scar fibrous tissue in the SL joint, thus masking an authentic rupture of the SL ligament. Hence, the diagnosis of SL ligament tear on CT arthrogram doesn't necessarily indicate the presence of an SL instability, and dynamic assessment is required to confirm instability[5].

Our study has its limitations. The primary limitation is the small number of patients in each group, especially the Group 1 (n=8). However, in current practice, it is unusual to diagnose arthroscopic stage 0 or 1 SL incongruence in patients with chronic post-traumatic wrist pain since arthroscopy is recommended for patients with abnormal radiographic and CT arthrography findings. Nevertheless, further complementary clinical studies with a kinematic 4DCT assessment are required to confirm our results. Secondly, the RUD movement's amplitude was not standardized, and motion variations from one patient to another might have occurred. However, prior studies indicated that RUD motion amplitude did not significantly influence the diagnostic performance of 4DCT [9,10]. Lastly, implementing this new imaging modality requires wide-area detector CT scanner models, training the medical staff and patients to perform the movement correctly without parasite motion, which might restrict its availability.

In conclusion, 4DCT analysis demonstrated a correspondence with the SL joint's arthroscopic dynamic analysis for the diagnosis of suspected chronic SL instability, especially for the assessment of SL joint space congruency (SLG analysis). This may represent a potential advantage with respect to arthroscopic scores for SL instability, as 4DCT is a quantitative and reproducible technique providing a multiparametric approach to SL instability. Furthermore, lunate and scaphoid bone motion can be evaluated by measuring the LCA and RSA, indicating that 4DCT could have a prognostic value in assessing SL instability severity. These findings serve as bases for further studies.

Disclosures of Potential Conflicts of Interest: Two authors involved in this work (Pedro Augusto Gondim Teixeira and Alain Blum) participate on a non-remunerated research contract with TOSHIBA Medical Systems for the development and clinical testing of post-processing tools for musculoskeletal CT. The authors declare no potential conflicts of interest with respect to the research, authorship, and/or publication of this article.

Funding: The authors state that this work has not received any funding.

Acknowledgements: The authors wish to thank Dr. Gabriela Hossu for her support for the statistical analysis.

Informed consent: All patients gave their informed consent for this study.

Ethical approval : This study was approved by our institutional review board and by the local ethics committee (PERSONAL PROTECTION COMMITTEE EST-III, VANDŒUVRE-LES-NANCY, France). This study was registered with the Clinical Trials Registry (no. NCT02401568).

REFERENCES

1. Athlani L, Pauchard N, Detammaecker R, Huguet S, Lombard J, Dap F, Dautel G. Treatment of chronic scapholunate dissociation with tenodesis: A systematic review. *Hand Surg Rehabil. 2018;* 37:65-76.
2. Crawford K, Owusu-Sarpong N, Day C, Iorio M. Scapholunate Ligament Reconstruction: A Critical Analysis Review. *JBJS Rev*. 2016; 4:41-8.
3. Linscheid RL, Dobyns JH, Beabout JW, Bryan RS. Traumatic carpal instability of the wrist. Diagnosis, classification and pathomechanics. *J Bone Joint Surg Am*. 2002; 84:142.
4. Watson H, Ottoni L, Pitts EC, Handal AG. Rotary subluxation of the scaphoid: a spectrum of instability. *J Hand Surg Br*. 1993; 18:62-4.
5. Kitay A, Wolfe SW. Scapholunate instability: current concepts in diagnosis and management. *J Hand Surg Am*. 2012; 37:2175-96.
6. Dreant N, Dautel G. Development of an arthroscopic severity score for scapholunate instability. *Chir Main*. 2003; 22:90-4.
7. Geissler WB. Arthroscopic management of scapholunate instability. *Chir Main.* 2006; 25 Suppl 1:S187-96.
8. Messina JC, Van Overstraeten L, Luchetti R, Fairplay T, Mathoulin CL. The EWAS Classification of Scapholunate Tears: An Anatomical Arthroscopic Study. *J Wrist Surg*. 2013; 2:105-9.
9. Abou Arab W, Rauch A, Chawki MB, Dap F, Dautel G, Blum A, Gondim Teixeira PA. Scapholunate instability: improved detection with semi-automated kinematic CT analysis during stress maneuvers. *Eur Radiol*. 2018; 28:4397-4406.

10. Rauch A, Arab WA, Dap F, Dautel G, Blum A, Gondim Teixeira PA. Four-dimensional CT Analysis of Wrist Kinematics during Radioulnar Deviation. *Radiology*. 2018; 289:750-758.
11. Zhao K, Breighner R, Holmes D III, Leng S, McCollough C, An KN. A technique for quantifying wrist motion using four-dimensional computed tomography: approach and validation. *J Biomech Eng.* 2015; 137.
12. Watson HK, Ballet FL. The SLAC wrist: scapholunate advanced collapse pattern of degenerative arthritis. *J Hand Surg Am.* 1984; 9:358-65.
13. Larsen CF, Amadio PC, Gilula LA, Hodge JC. Analysis of carpal instability: I. Description of the scheme. *J Hand Surg Am*. 1995; 20:757-64.
14. Picha BM, Konstantkos EK, Gondon DA. Incidence of bilateral scapholunate dissociation in symptomatic and asymptomatic wrists. *J Hand Surg Am.* 2012; 37:1130-1135.
15. Gondim Teixeira PA, Formery AS, Hossu G, Winninger D, Batch T, Gervaise A, Blum A. Evidence-based recommendations for musculoskeletal kinematic 4D-CT studies using wide area-detector scanners: a phantom study with cadaveric correlation. *Eur Radiol*. 2017; 27:437-446.
16. Terry K. Koo, Mae Y. Li. A Guideline of Selecting and Reporting Intraclass Correlation Coefficients for Reliability Research. *J Chiropr Med.* 2016; 15:155–163.
17. Leclercq C, Mathoulin C. Complications of Wrist Arthroscopy: A Multicenter Study Based on 10,107 Arthroscopies. *J Wrist Surg*. 2016; 5:320–326.
18. Obdeijn MC, Tuijthof G JM, van der Horst C, Mathoulin C, Liverneaux P. Trends in Wrist Arthroscopy. *J Wrist Surg*. 2013; 2:239–24.
19. Bille B, Harley B, Cohen H. A comparison of CT arthrography of the wrist to findings during wrist arthroscopy. *J Hand Surg Am.* 2007; 32:834 – 841.
20. Corella F, Del Cerro M, Ocampos M, Larrainzar-Garijo R. Arthroscopic ligamentoplasty of the dorsal and volar portions of the scapholunate ligament. *J Hand Surg Am*. 2013; 38:2466–2477.
21. Schmid MR, Schertler T, Pfirrmann CW, Saupe N, Manestar M, Wildermuth S, Weishaupt D. Interosseous ligament tears of the wrist : a comparaison of mulit-detector row CT arthrograpgy and MR imaging. *Radiology*. 2005; 237:1008-1013.

Discussion et Conclusion

Nos résultats confirment l'intérêt du 4DCT dans le bilan d'imagerie des patients suspects d'ISL chronique. Par son analyse dynamique, quantitative multiparamétrique et reproductible, le 4DCT s'est avéré pertinent pour confirmer de façon significative l'état d'ISL, y compris chez les patients présentant une évaluation radiographique et/ou arthroscanographique initiale douteuse.

Avec des valeurs seuil caractérisées par l'analyse ROC, le 4DCT a permis d'identifier et de quantifier l'ISL avec une excellente reproductibilité, ainsi qu'une très bonne Sp et Se. Le SLG s'est révélé comme un paramètre à prédominance diagnostic de l'ISL, tandis que le PRSA et le LCA sont apparus comme des paramètres à prédominance pronostic.

L'analyse en 4DCT du SLG prend en compte à la fois le diastasis scapho-lunare, mais aussi la différence de rotation entre les deux os. Puisque cette différence de rotation est un élément important de la pathogénèse de l'ISL, elle contribuerait aux performances diagnostiques de l'évaluation du SLG.

Le déplacement dorsal du scaphoïde et la dorsiflexion du lunatum sont également deux composants majeurs de la pathogenèse de l'ISL. Ces anomalies de position du scaphoïde et du lunatum expliquent le contact radio-scaphoïdien dorsal et le décentrage capito-lunaire, qui sont à l'origine du développement progressif de l'arthrose SLAC. Sur la base des radiographies standards, en raison des problèmes de superposition, l'évaluation de ces déformations reste subjective, entravant leur utilité pour le diagnostic d'ISL. L'analyse sur des images tomodensitométriques sagittales du PRSA rend l'évaluation du déplacement dorsal du scaphoïde objective, reproductible et quantifiable. Le PRSA peut être ainsi utilisé comme marqueur d'imagerie de l'ISL, et sa quantification pourrait renseigner sur la sévérité de la dissociation. De même, des valeurs anormales du LCA semblent indiquer une déformation en DISI ainsi qu'une réduction de l'amplitude de mouvement du lunatum. La quantification du LCA pourrait être utilisée comme marqueur de l'importance biomécanique de la lésion du complexe scapho-lunaire, et donc de la gravité de l'ISL.

L'un des avantages du 4DCT est de pouvoir s'affranchir des phénomènes de superposition et des erreurs de mesure liées à la position du poignet lors des radiographies standards. Koh et al. (2013) ont suggéré avec leur étude, que des degrés de flexion-extension du poignet même minimes (de 20 ° de flexion à 20 ° d'extension), peuvent affecter les mesures des paramètres radiographiques.

Nous avons également pu confirmer la correspondance entre le testing dynamique arthroscopique de l'articulation scapho-lunaire et l'analyse quantitative multiparamétrique en 4DCT pour le diagnostic d'ISL. En comparaison avec la classification arthroscopique de Dréant et Dautel (2003), parmi les trois paramètres 4DCT, le SLG est apparu comme le plus pertinent pour différencier les patients avec ou sans incongruence articulaire scapho-lunaire. Ces résultats nous paraissent essentiels car de nombreux auteurs considèrent actuellement l'arthroscopie du poignet comme le "gold standard" pour confirmer l'état d'ISL. Cependant, l'arthroscopie exploratrice a un rôle principalement diagnostic. L'impossibilité de quantifier le diastasis scapho-lunaire mais également les difficultés d'évaluation des anomalies de position du scaphoïde et du lunatum, rendent compte des limites de cette analyse sur le versant pronostic. De plus, les principaux inconvénients de l'arthroscopie sont la complexité technique et le caractère invasif de la procédure, avec des complications potentielles non négligeables. Contrairement au 4DCT, l'arthroscopie présente une étroite relation entre l'expérience individuelle du chirurgien et sa reproductibilité dans l'analyse. Tout ceci représente un avantage potentiel du 4DCT par rapport aux scores arthroscopiques pour l'ISL.

Au vu des différents résultats de ce chapitre, des valeurs anormales des paramètres étudiés en 4DCT semblent indiquer des changements biomécaniques significatifs dans les poignets dissociés, y compris pour des stades précoces d'ISL. Ainsi, il pourrait être possible d'identifier et de traiter des patients présentant un stade débutant d'ISL, caractérisé par exemple, par une déchirure partielle du LIOSL associée à une lésion ligamentaire extrinsèque. De même, il semblerait faisable d'évaluer la réductibilité de la dissociation statique avec des implications potentielles dans le choix de la stratégie chirurgicale, notamment lorsque la reconstruction ligamentaire est envisageable.

Les limites de nos études sont connues. La principale est le nombre limité de patients, notamment ceux avec un diagnostic douteux en imagerie conventionnelle. Cependant, en pratique clinique, ces cas douteux basés sur l'analyse radiographique et arthroscanographique, restent moins fréquemment rencontrés. Deuxièmement, le critère principal d'inclusion de notre cohorte était la présence d'une douleur systématisée à l'interligne scapho-lunaire. Ainsi, il pourrait s'agir d'un échantillon dans lequel une proportion plus élevée de patients serait susceptible d'avoir une ISL, que dans une population générale avec des douleurs du poignet non systématisées. Par ailleurs, l'amplitude de mouvement de la manœuvre DRU n'était pas standardisée et donc variable d'un patient à l'autre.

Cependant, les valeurs moyennes d'amplitude DRU étaient assez similaires, considérant que ce paramètre ne semblait pas avoir entraîné de modification des performances diagnostiques. Enfin, la mise en place de ce nouvel outil d'imagerie nécessite la formation du personnel soignant, mais également une éducation préalable du patient à l'exécution correcte des manœuvres du poignet sans mouvement de l'avant-bras, ce qui pourrait limiter sa disponibilité.

Des études complémentaires, avec un effectif plus important, sont nécessaires pour assoir nos résultats et apprécier pleinement la valeur diagnostic et pronostic du 4DCT.

CHAPITRE 3.
LA LIGAMENTOPLASTIE SCAPHO-LUNAIRE ET INTER-CARPIENNE DANS LE TRAITEMENT DES INSTABILITÉS SCAPHO-LUNAIRES

Ce chapitre est composé de sept articles publiés :

- **Athlani L, Pauchard N, Detammaecker R, Huguet S, Lombard J, Dap F, Dautel G.** Treatment of chronic scapholunate dissociation with tenodesis: A systematic review. *Hand Surg Rehabil*. 2018, 37:65-76.
- **Athlani L, Pauchard N, Dautel G.** Radiological evaluation of scapholunate intercarpal ligamentoplasty for chronic scapholunate dissociation in cadavers. *J Hand Surg Eur Vol*. 2018, 43:387-393.
- **Athlani L, Pauchard N, Dautel G.** Outcomes of scapholunate intercarpal ligamentoplasty for chronic scapholunate dissociation. A prospective study in 26 patients. *J Hand Surg Eur Vol*. 2018, 43:700-707.
- **Athlani L, Pauchard N, Dautel G.** Treatment of chronic scapholunate instability: results with three-ligament tenodesis versus scapholunate and intercarpal ligamentoplasty. *Hand Surg Rehabil.* 2019, 38:157-164.
- **Athlani L, Rauch A, Weber N, Blum A, Dautel G, Gondim Teixeira PA.** Quantitative Four-dimensional CT evaluation of scapholunate intercarpal ligamentoplasty for scapholunate dissociation: a cadaveric study. *Journal Hand Surgery Eur Vol*. 2020, 26:1753193420973883.
- **Athlani L, Pauchard N, Dautel G.** Intercarpal ligamentoplasty for scapholunate dissociation: comparison of two techniques. *J Hand Surg Eur Vol.* 2020, 19:1753193420940498.
- **Athlani L, Sapa MC, De Almeida YK, Braun M, Dautel G.** A new capsulotomy-based dorsal approach to the wrist: a cadaver study**.** *Hand Surg Rehabil*. 2020, 10:S2468-1229(20)30233-4.

Ce chapitre s'intéresse au traitement chirurgical des ISL chroniques avant l'apparition d'arthrose. Devant les multiples techniques de ligamentoplasties proposées pour lutter contre cette instabilité dissociative, il convenait dans un premier temps, de réaliser une revue systématique des différentes options existantes dans la littérature. Par la suite, nous décrirons notre nouvelle technique chirurgicale intitulée « ligamentoplastie ScaphoLunaire et InterCarpienne – SLIC », ses objectifs et ses étapes chirurgicales. Cette procédure fera l'objet d'évaluations anatomiques puis cliniques prospectives. Les résultats de ces études nous amènerons à proposer une modification récente de la technique, ainsi que son évaluation cadavérique en 4DCT, puis clinique comparative. Ces études prospectives s'intègrent dans le cadre d'un protocole de recherche clinique approuvé par le Comité de Protection des Personnes Est-III et intitulé : **Chirurgie de reconstruction ligamentaire du complexe scapho-lunaire « Étude SLIC ».** Le consentement écrit a été obtenu de tous les participants. Ce protocole est enregistré auprès du registre des essais cliniques.

Pour finir ce chapitre, nous proposerons, dans une étude anatomique, la description et les avantages d'une nouvelle capsulotomie permettant d'aborder le poignet par voie dorsale, et ainsi réaliser les ligamentoplasties scapho-lunaires.

Revue de la littérature sur les ligamentoplasties scapho-lunaires

Hand Surgery and Rehabilitation 37 (2018) 65–76

Available online at ScienceDirect www.sciencedirect.com

Elsevier Masson France EM|consulte www.em-consulte.com

Literature review

Treatment of chronic scapholunate dissociation with tenodesis: A systematic review

Les ligamentoplasties dans le traitement de l'instabilité scapho-lunaire dissociative chronique : revue de la littérature

L. Athlani *, N. Pauchard, R. Detammaecker, S. Huguet, J. Lombard, F. Dap, G. Dautel

Service de chirurgie de la main, chirurgie plastique et reconstructrice de l'appareil locomoteur, centre chirurgical Emile-Gall, CHU de Nancy, 49, rue Hermitte, 54000 Nancy, France

ARTICLE INFO

Article history:
Received 24 June 2017
Received in revised form 11 December 2017
Accepted 12 December 2017
Available online 29 December 2017

Keywords:
Wrist instability
Scapholunate instability
Scapholunate dissociation
Scapholunate ligament
Tenodesis

ABSTRACT

Scapholunate (SL) instability is the most common dissociative carpal instability condition. It is the most frequent cause of wrist osteoarthritis, defined as scapholunate advanced collapse or SLAC wrist. Familiarity with the SL ligament complex is required to understand the various features of SL instability. Damage to the SL interosseous ligament is the main prerequisite for SL instability; however the extrinsic, palmar and dorsal ligaments of the carpus also come into play. When more than 6 weeks has passed since the initial injury event, SL instability is considered chronic because ligament healing is no longer possible. Before osteoarthritis sets in and when the SL instability is still reducible (scaphoid can be reverticalized), ligament reconstruction surgery is indicated. Since the end of the 1970s, various ligament reconstruction or tenodesis techniques have been described. These techniques are used in cases of chronic, dynamic or static reducible SL instability, when no repairable ligament stump and no chondral lesions are present. The aim is to correct the SL instability using a free or pedicled tendon graft to reduce pain while limiting the loss of mobility and protecting against osteoarthritis-related collapse in the long-term. We will perform a systematic review of the various tenodesis techniques available in the literature.

Mots clés :
Instabilité du carpe
Instabilité scapho-lunaire
Dissociation scapho-lunaire
Ligament scapho-lunaire
Ligamentoplastie

RÉSUMÉ

L'instabilité scapho-lunaire (ISL) est l'instabilité dissociative du carpe la plus courante. Elle est la cause la plus fréquente d'arthrose du poignet définie sous le terme de SLAC ou scapholunate advanced collapse wrist. Pour comprendre les différents aspects de l'ISL, il faut raisonner en utilisant la notion de complexe ligamentaire scapho-lunaire, dont la lésion du ligament scapho-lunaire interosseux représente le prérequis essentiel, et mettant en jeu aussi les ligaments extrinsèques, palmaires et dorsaux, du carpe. Lorsque le délai par rapport au traumatisme initial est supérieur à six semaines, l'ISL est considérée comme chronique et il n'existe plus de possibilité de cicatrisation ligamentaire. Avant l'apparition d'arthrose et lorsque l'ISL est réductible (reverticalisation possible du scaphoïde), la chirurgie de reconstruction ligamentaire semble tout indiquée. Depuis la fin des années 1970, plusieurs techniques de ligamentoplasties ou ténodèses ont été décrites. Ces techniques sont proposées dans les ISL chroniques, dynamiques ou statiques réductibles, sans moignon ligamentaire réparable, sans lésion chondrale. Elles ont pour objectif de corriger l'ISL en utilisant un transplant tendineux libre ou pédiculé, dans le but de diminuer les douleurs tout en limitant la perte de mobilité et de préserver à long terme du collapsus arthrosique. Nous proposons une revue systématique des différentes techniques de ligamentoplasties présentes dans la littérature.

* Corresponding author.
E-mail addresses: lionel.athlani@gmail.com (L. Athlani), pauchard.nicolas@neuf.fr (N. Pauchard), romain.detammaecker@hotmail.fr (R. Detammaecker), huguet.sa@gmail.com (S. Huguet), j.lombardihn@gmail.com (J. Lombard), dapfrancois@gmail.com (F. Dap), gillesdautel@me.com (G. Dautel).

https://doi.org/10.1016/j.hansur.2017.12.001
2468-1229/

1. Introduction

The concept of carpal instability was first described by Linscheid et al. in 1972 [1]. It is defined as an alteration in the normal relationship between carpal bones [1,2]. Dissociative instability is the result of damage to the intrinsic ligaments [3]. Scapholunate (SL) instability is the most common dissociative carpal instability condition [1,4–8]. It is the most frequent cause of wrist osteoarthritis, defined as scapholunate advanced collapse or SLAC wrist [7]. Familiarity with the SL ligament complex is required to understand the various features of SL instability. Damage to the scapholunate interosseous ligament (SLIL) is the main prerequisite for SL instability; however the extrinsic ligaments of the carpus also come into play. [8–11]. While the SLIL is known to be the primary stabilizer of the SL joint, the extrinsic, palmar and dorsal ligaments also play an important role in stabilizing it [1,12–17]. Recently, Viegas et al. [15] and then Mitsuyasu et al. [18] showed that the dorsal intercarpal ligament (DICL) is an important stabilizer, especially during the progression from dynamic to static SL instability. This means that both the SLIL and the extrinsic ligaments must be damaged for static SL instability to develop [1,14,16–20].

When more than 6 weeks has passed since the initial injury event, SL instability is considered chronic because ligament healing is no longer possible [21]. Taleisnik [5,13] introduced the concepts of dynamic and static instability in the late 1980s; however this was purely a radiographic definition. Dynamic instability is visible on dynamic or stress X-rays, while static instability can be seen on standard A/P and lateral X-ray views [13,21]. Static SL instability is visible on radiographs as lunate instability in extension or dorsal intercalated segment instability (DISI) [1], along with flexion and pronation of the scaphoid with posterior, rotary subluxation (SRS) [22–24]. Its proximal pole gets closer to the posterior margin of the carpal articular surface of the radius, which increases radioscaphoid pressure and contributes to secondary radioscaphoid osteoarthritis [19,24,25]. This subluxation causes midcarpal decentering which leads to secondary capitolunate osteoarthritis [26]. In addition to scaphoid flexion and lunate extension, the scaphoid and lunate move away from each other (SL diastasis). Lastly, there is a tendency for ulnar translation and reduction in the proximal carpal row's height [14] (Fig. 1).

A few years later, Watson et al. [22] added the concept of predynamic or occult instability [22,23,26,27], which corresponds to SL instability with no abnormal radiographic findings [28] that does not always deteriorate [8]. SL instability is both difficult to diagnose and treat, particularly at the static SL instability stage when true intracarpal misalignment is present [9]. Before osteoarthritis sets in and when the SL instability is still reducible, ligament reconstruction surgery is indicated [21].

2. Indications for ligament reconstruction or tenodesis

Since the late 1970s, several tenodesis techniques have been described. These techniques are used in cases of chronic, dynamic or static reducible SL instability, when no repairable ligament stump and no chondral lesions are present, which corresponds to stage 3 and 4 in the Garcia-Elias classification [29]. The aim is to correct the SRS, DISI and SL diastasis using a free or pedicled tendon graft to reduce pain, while preserving as much mobility as possible and preventing osteoarthritis-related collapse in the long-term [13,26,30–32].

The reducible nature of the static SL instability is evaluated on an A/P view in ulnar deviation with scaphoid reverticalization visible over its entire length. During arthroscopy, it is also possible to assess the scaphoid mobility and how well the instability can be corrected. Performing a dynamic maneuver, similar to Watson et al.'s test [33], after having released wrist traction [34] helps to objectively assess the reducibility of the scaphoid horizontalization.

Complete reduction is confirmed during the first phase of surgery, after the arthrotomy and before the ligament reconstruction is performed. This preliminary step is used to confirm the indication.

3. Techniques and results

3.1. Tenodesis using the extensor carpi radialis brevis (ECRB)

Almquist et al. [35] described the four-bone ligament reconstruction (FBLR) procedure in 1991 that uses a slip of the ECRB pedicled distally. The aim is to reconstruct the dorsal portion of the SLIL. This slip is passed through anteroposterior tunnels in the

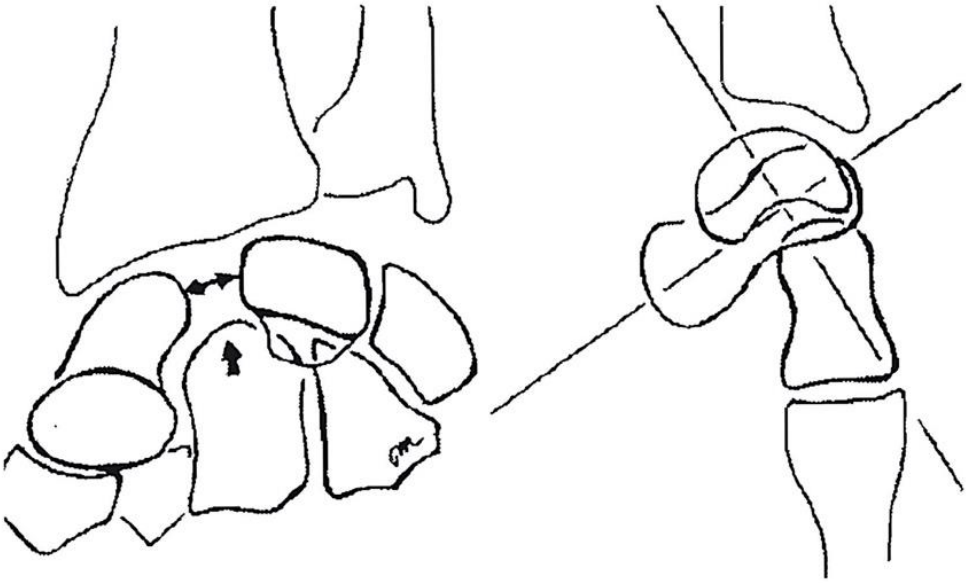

Fig. 1. Drawing of the radiographic signs found in cases of static SL instability. On A/P view (left panel), SL diastasis (two-headed arrow) and tendency for elevation of the capitate head between the scaphoid and lunate (single-headed arrow). On lateral view (right panel), scaphoid flexion, lunate extension (DISI) and midcarpal decentering.

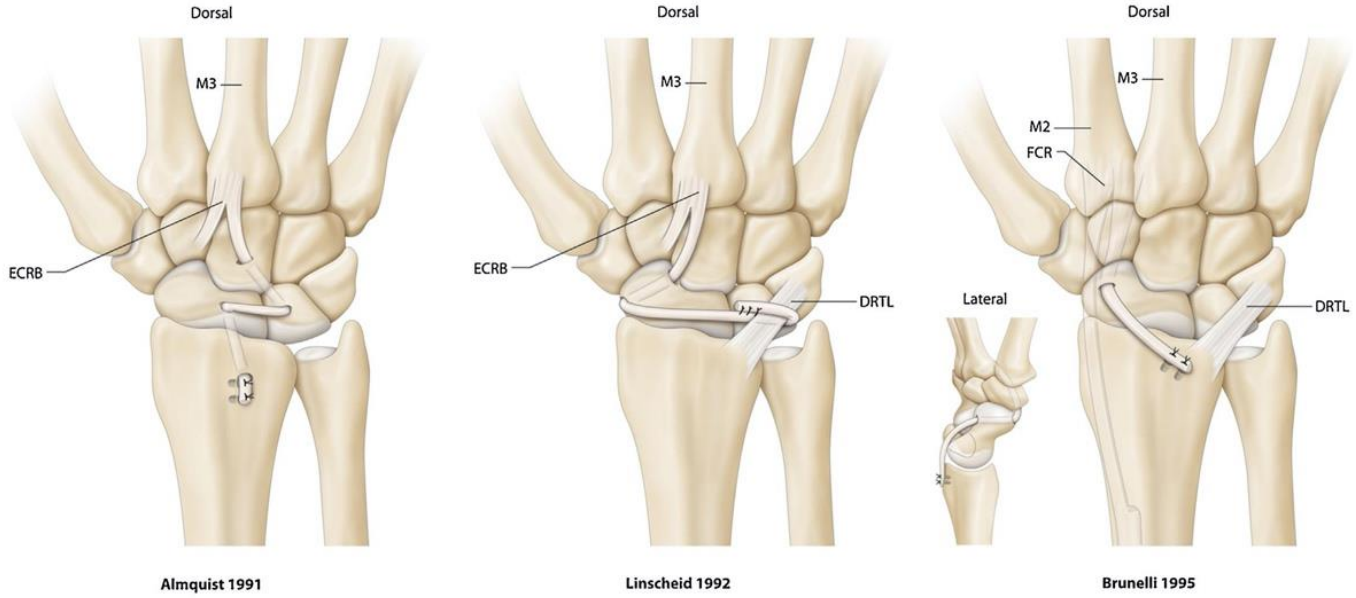

Fig. 2. SL tenodesis procedures described by Almquist [35] (ECRB), Linscheid [36] (ECRB) and Brunelli [42] (FCR). DRTL: dorsal radiotriquetral ligament; ECRB: extensor carpi radialis brevis; FCR: flexor carpi radialis; M3: third metacarpal.

capitate, the proximal pole of the scaphoid, the radial side of the lunate and then bridges the radiocarpal joint before being inserted on the dorsal side of the radius. Thirty-six patients operated with this technique were evaluated after an average of 56 months' follow-up (Fig. 2).

In 1992, Linscheid et Dobyns [36] passed a distally pedicled ECRB slip through bone in the distal pole of the scaphoid, and then under the dorsal radiocarpal ligament (DRCL) without bridging the radiocarpal joint. The tendon was then secured to itself. This technique aims to recreate the SLIL and the DRCL (Fig. 2).

Other authors have described tenodesis with the ECRB. Brunelli et al. [37] in 2004 described a case of post-traumatic static SL instability at 6 months in a 22-year-old male treated by active muscle transfer of the ECRB tendon. The latter was transected at the base of the 3rd metacarpal, then reattached on the distal portion of the scaphoid using two suture anchors after being shortened 1 cm. To ensure it was in the scaphoid axis, a pulley was created at Lister's tubercle for the tendon to pass over (Fig. 3). Radiological follow-up at 8 months postoperative showed good reduction and the patient's wrist was pain-free.

More recently, Papadogeorgou and Mathoulin [38] reported the results of 32 patients with reducible static SL instability after an average follow-up of 50 months. The surgical technique consisted of a distally pedicled ECRB slip passed around the DRCL superficial to deep, then fixed with a suture anchor on the dorsal side of the distal pole of the scaphoid. The procedure was supplemented by temporary SL screw fixation. They found a significant reduction in pain and an increase in grip strength. While the range of motion in flexion was reduced (46° vs. 42°), 23 patients had a SL angle (SLA) of less than 60°.

3.2. Tenodesis using the extensor carpi radialis longus (ECRL)

In 2008, Bleuler et al. [39] described a dynamic ECRL tenodesis technique. It consisted of ECRL tendon fixation on the dorsal side of the scaphoid using a cancellous bone screw, once the scaphoid flexion had been corrected. The aim was to reset the scaphoid vertical position by increasing the extension loads on it (Fig. 4). Twenty patients with static SL instability underwent this procedure. The authors reported that pain levels were reduced but did not disclose other outcomes. Peterson and Freeland [40] modified this technique in 2010 by performing direct transfer of the ECRL insertion to the distal pole of the scaphoid through a blind tunnel. Fixation involved transosseous sutures in the scaphoid tubercle (Fig. 4).

In 2011, De Carlis et al. [41] described a technique in which a distally pedicled ECRL slip is secured with three suture anchors: on the dorsal side of the distal pole of the scaphoid (to correct scaphoid flexion), at the proximal pole of the scaphoid, and on the dorsal side of the lunate (reconstruction of dorsal portion of SLIL). The tendon end was ultimately sutured to the distal portion of the DRCL to correct the ulnar translation of the carpus and lunate extension (Fig. 5). Eight patients were reviewed after a minimum follow-up of 1 year. The SL gap (SLG) was reduced (2.6 mm vs. 4.6 mm), as was the SLA (60° vs. 82°).

3.3. Tenodesis using the flexor carpi radialis (FCR)

3.3.1. Brunelli tenodesis and its modifications

In 1995, GA Brunelli and GR Brunelli [42] described a ligament reconstruction procedure using a distally pedicled FCR slip. Their aim was to reconstruct the ligament complex on the distal pole of the scaphoid, in particular the scaphotrapeziotrapezoid ligament (deep side of the FCR sheath). In their opinion, this ligament is the main element of scaphoid stability. This technique requires two incisions:

- anterior;
- posterior.

The tendon slip is passed through an anteroposterior transosseous tunnel in the distal pole of the scaphoid. The tendon is retrieved on the dorsal side, fixed to the remains of the dorsal portion of the SLIL and then on the dorsoulnar margin of the radius after having bridged the radiocarpal joint. There is no lunate fixation to avoid altering the scaphoid motion relative to the lunate. This technique does not require a transosseous tunnel in the proximal pole of the scaphoid, which is the source of fractures, osteonecrosis and poor bone integration of the transplanted tendon (Fig. 2). In a cohort of 13 patients with 0.5 to 2 years' follow-up, they found that pain was reduced significantly and that 85% of patients had little to no pain. Grip strength was 25% less than the

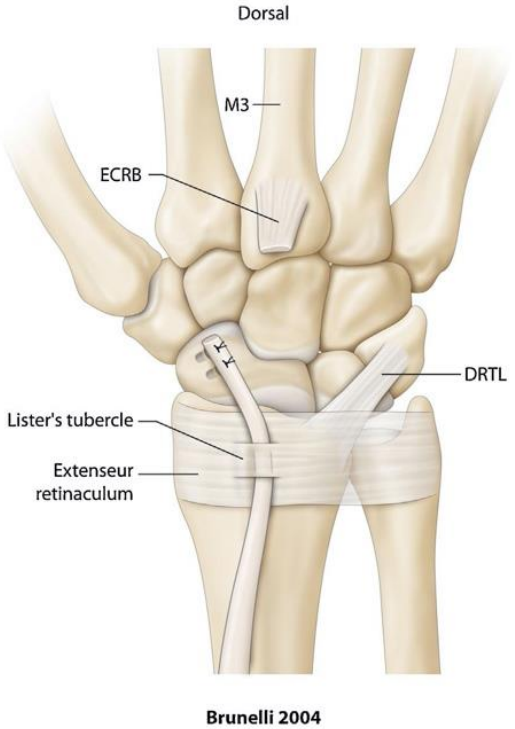

Fig. 3. Active transfer of the ECRB tendon according to Brunelli [37] for cases of reducible static SL instability. DRTL: dorsal radiotriquetral ligament; ECRB: extensor carpi radialis brevis; M3: third metacarpal.

opposite side, but was 50% higher than preoperative levels. Wrist flexion was reduced by 30 to 60%. On radiographs, the authors noted the SL instability had not recurred but gave no information on the SLG or SLA.

Because of the significant loss of wrist flexion, the Brunelli technique [42] was modified in 1998 by Van Den Abbeele et al. [43] to not cross the radiocarpal joint. In this modification, the tendon graft is passed around the DRCL and then sutured to itself. The first steps of the technique remain the same (Fig. 6). They reported on a 22-patient cohort with an average follow-up of 9 months. Fifteen of these patients had predynamic SL instability, 4 had dynamic instability and 3 had static instability. For this reason, the average SLA was 50° preoperatively and at the last follow-up. Since the instability had not caused SL dissociation in most patients, it is logical that no recurrences were found in the short term. Nevertheless, wrist flexion ability was not diminished as much as in the Brunelli [42] study.

There are many published reports on the outcomes of the Brunelli technique [42] as modified by Van Den Abbeele et al. [43] (Modified Brunelli: MB). In 2006, Talwalkar et al. [44] published the results of a cohort of 55 patients with a mean follow-up of 4 years. Dynamic instability was present in 32 of these patients and static instability in the other 23. Little to no pain was found in 62% of patients. The mean loss of wrist flexion was 31%, with a 20% loss of wrist extension and 20% loss of grip strength. They found no significant differences in the outcomes between cases of static and dynamic instability. Unfortunately, the authors did not perform a radiographic assessment of the angles (maintenance of reduction) or the osteoarthritis progression in the medium-term (prevention of arthritic collapse).

Moran et al. [45] published a comparative study in which 14 patients underwent dorsal capsulodesis (with a DICL) and 15 underwent the MB technique. At 38 months' follow-up, they found no significant differences between the two groups in terms of wrist mobility (64% in the capsulodesis group versus 63% in the MB group) or the grip strength (91% versus 87% of the opposite side). There were also no differences between the subgroup of patients with static instability (6 patients) and dynamic instability (9 patients). However, the MB procedure appears to better correct and maintain the SLA than the capsulodesis (54° vs. 65°). Both groups had a similar number of cases with arthritic progression (13%).

In 2007, De Smet and Van Hoonacker [46] reported the results of 10 patients at 29 months' follow-up and in 2008, Chabas et al.

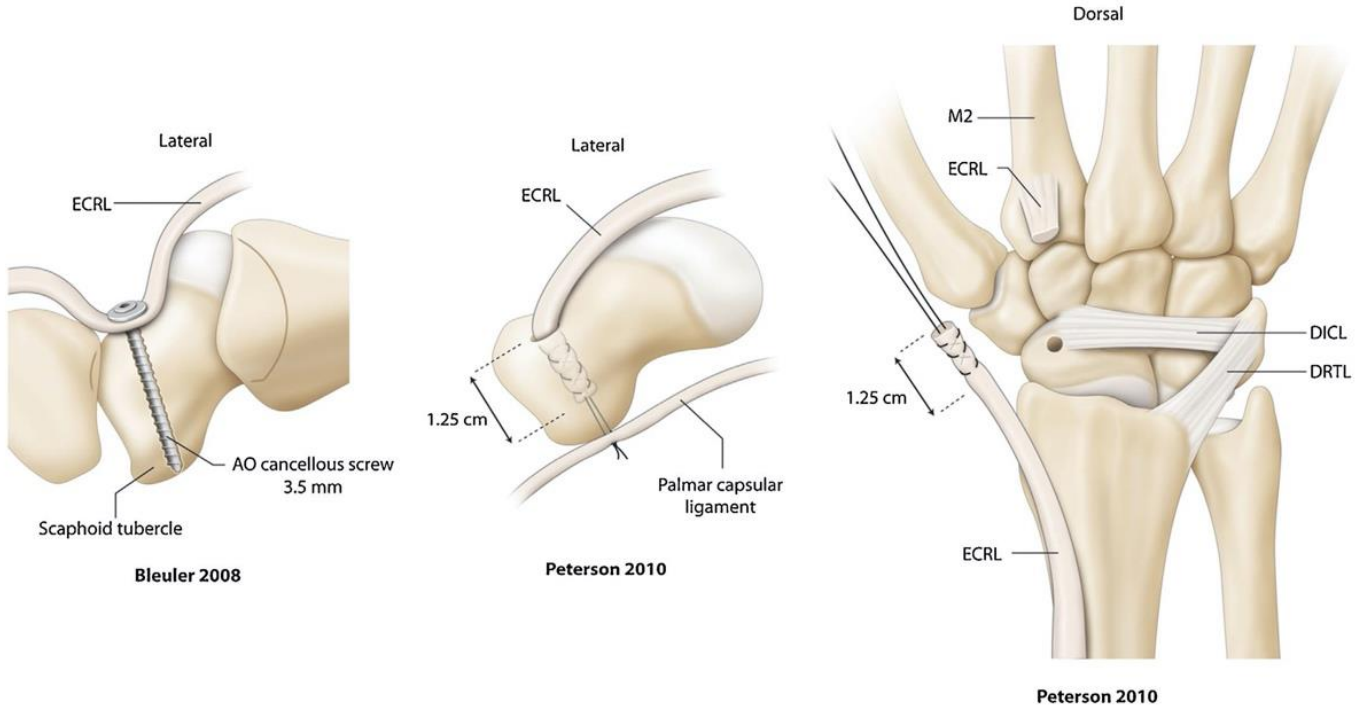

Fig. 4. Dynamic ECRL tenodesis as described by Bleuler [39] (A) and Peterson [40] (B, C). DICL: dorsal intercarpal ligament; DRTL: dorsal radiotriquetral ligament; ECRL: extensor carpi radialis longus; M2: second metacarpal.

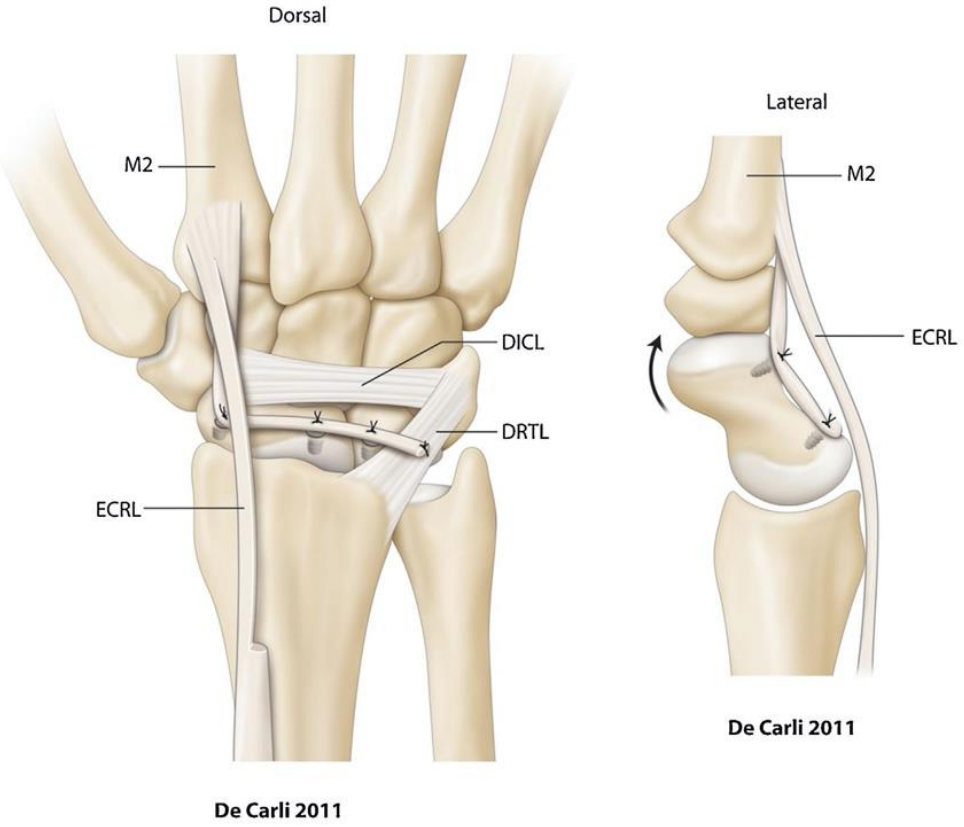

Fig. 5. SL reconstruction using the ECRL as described by De Carlis [41]. DICL: dorsal intercarpal ligament; DRTL: dorsal radiotriquetral ligament; ECRL: extensor carpi radialis longus; M2: second metacarpal.

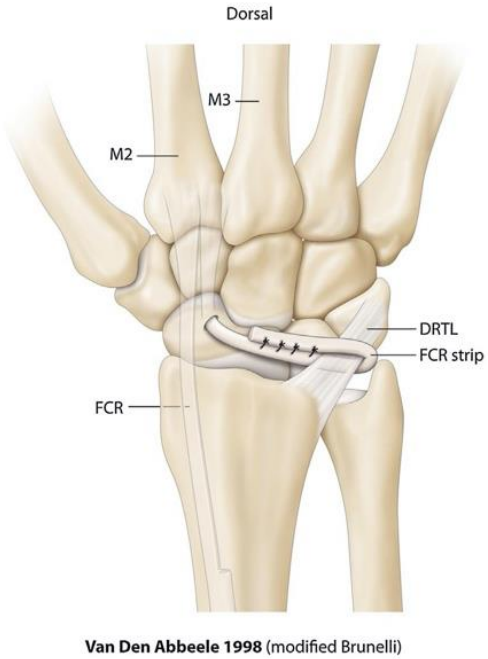

Fig. 6. The Brunelli tenodesis modified by Van Den Abbeele [43]. DRTL: dorsal radiotriquetral ligament; FCR: flexor carpi radialis; M2: second metacarpal; M3: third metacarpal.

[47] reported the results of 19 patients at 37 months' follow-up who were treated with a MB procedure for static and dynamic SL instability. Their findings were similar to those of prior studies.

Links et al. [48] compared the MB and FBLR techniques in 2008. The two patient groups were similar in terms of size (21 in MB group and 23 in FBLR group) and the distribution of static and dynamic instability cases. At 30 months' follow-up, the MB group had significantly better clinical and radiological outcomes. Pain had decreased by 4.8 points versus 3.2 points and the grip strength had increased 37% versus 13%. Reduction in range of motion was less in the MB group than the FBLR group (−14% vs. −40%) especially for wrist flexion (−24% vs. −55%) and extension (−10% vs. −41%). On radiographs, the SLG had decreased by an average of 1.6 mm in the MB group versus 0.7 mm in the FBLR group. The SLA decreased an average of 15° versus 10°.

Howlett et al. [49] explored the relationship between the position of the scaphoid tunnel (distal vs. proximal) and its effectiveness for correcting the flexion deformity. Based on this cadaver study, a distal transosseous tunnel provides better control over scaphoid flexion, thus the SLA, while preserving a normal SLG.

Nienstedt [50] reported the results of 8 patients with static instability treated with the MB technique, in 2013. These were long-term results with more than 10 years' follow-up (average of 13.8 years). Six patients had no pain and one patient occasionally had slight pain. Range of motion and grip strength were 85% of the healthy contralateral side. On radiographs, the SL instability was still reduced and there was only one case of osteoarthritic progression. However, these results must be interpreted carefully given the small sample size.

In a 2014 study of 13 patients with a mean follow-up of 12 months, Ellanti et al. [51] found a loss of 38° flexion, 20° extension, 4° radial deviation and 14° ulnar deviation. Sousa et al. [52] reported that in 22 patients after a mean follow-up of 61 months, there was a loss of 23° flexion, 22° extension, 6° radial deviation and 3° ulnar deviation. Both studies found a significant decrease in pain and a significant increase in grip strength.

Elgammal and Lukas [53] reported on 20 patients operated because of dynamic or static instability with the MB technique in

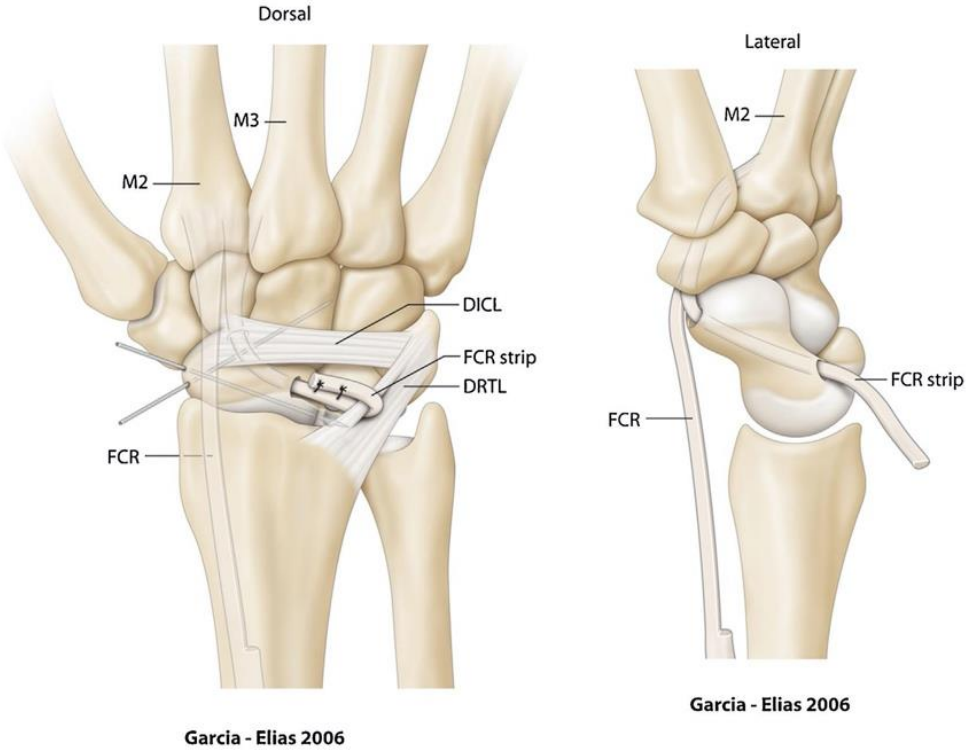

Fig. 7. FCR tenodesis as described by Garcia-Elias [29]. DICL: dorsal intercarpal ligament; DRTL: dorsal radiotriquetral ligament; FCR: flexor carpi radialis; M1: first metacarpal; M2: second metacarpal.

2015. Wrist mobility was reduced by 19° in flexion, 14° in extension, 6° in radial deviation and 9° in ulnar deviation; 80% had little to no pain at the final follow-up visit. They found no significant difference between the subgroups of static and dynamic instability based on the clinical outcomes (pain, grip strength, mobility). However, there were significant differences between groups on the radiographs. In the dynamic SL instability patients, the SLG and SLA were better reduced immediately postoperatively and this reduction was more stable at the last follow-up. Moreover, there were 3 cases of osteoarthritis progression.

3.3.2. Three-ligament tenodesis by Garcia-Elias

In 2006, Garcia-Elias et al. [29] described a technique with the FCR called the three-ligament tenodesis (3LT) which was derived from the MB technique. Two changes were made. First, the trajectory of the trans-scaphoid tunnel was more oblique, which provided an exit over the previous insertion of the dorsal portion of the SLIL. Second, after the FCR slip crossed the scaphoid, it was secured with a suture anchor in a trench made on the dorsal side of the lunate. The final step was unchanged, with passage through the DRCL and suturing of the FCR transplant to itself (Fig. 7). Fixation to the lunate aimed to reduce the ulnar translation and better maintain the SLG. The authors reported the outcomes of 38 patients after 46 months' follow-up. The mobility was good when compared to the contralateral side:

- 74% flexion;
- 77% extension;
- 78% radial deviation;
- 92% ulnar deviation.

Nearly all the patients (95%) were pain-free or had only occasional mild pain. There were no cases of scaphoid necrosis. Conversely, there were 7 cases of styloscaphoid osteoarthritis that did not require surgical revision. Two patients developed a SLAC 3 wrist.

In 2013, De Smet et al. [54] verified whether 3LT reduces the static SL instability on radiographs. In 12 patients after 39 months' follow-up, the SLG was significantly reduced (4.25 mm vs. 3.29 mm) as was the SLA (77° vs. 68°). However, the SLG was normal (≤ 3 mm) in only 4 patients and the SLA was normal (≤ 60°) in only 3 patients. In 2011, the same authors [55] had compared these two parameters in two homogeneous groups: the first group (13 patients) was pain-free and considered "successful" and the second group (12 patients) still had pain and was considered as "failure" The SLG in the successful group was 2.94 mm versus 5.32 mm in the failure group. Similarly, the SLA was 66° in the successful group versus 81° in the failure group.

In 2013, Pauchard et al. [56] described the outcomes of a cohort of 20 patients (8 cases of dynamic instability and 12 cases of static instability) after 25 months' follow-up. They found a significant 50% reduction in pain levels relative to the preoperative condition. Grip strength was 76% of the contralateral side. The wrist's mobility was good with a 25% reduction in flexion, 14% in extension, and 20% in radial and ulnar deviation. Conversely, there was no difference between groups in terms of the SLA (72° vs. 75°) and SLG (3.9 mm vs. 3.7 mm). There were 4 cases of osteoarthritis (10.5%): 2 in the STT joint and 2 of SLAC 2.

3.3.3. The Ross scapholunotriquetral tenodesis

In 2013, Ross et al. [57] proposed a different approach for complex SL reconstruction with scapholunotriquetral tenodesis (SLT). A distally pedicled FCR slip is passed through transosseous tunnels in the scaphoid (proximal anteroposterior tunnel) and then the lunate and triquetral (sagittal tunnel). The graft is then secured to the triquetral using a PEEK (polyetheretherketone) screw, after having set the tension to allow reduction of the scaphoid subluxation and the SL diastasis. To reconstruct the DICL, a third step consists of passing the remaining graft over the dorsal side of the midcarpal joint (capitate) and then securing it at the scaphoid waist (isthmus) using an absorbable suture anchor. The authors reported on an 11-patient cohort after 14 months' follow-up. They found a significant reduction in pain and a significant improvement in grip strength. There was a 27° loss in flexion-extension amplitude

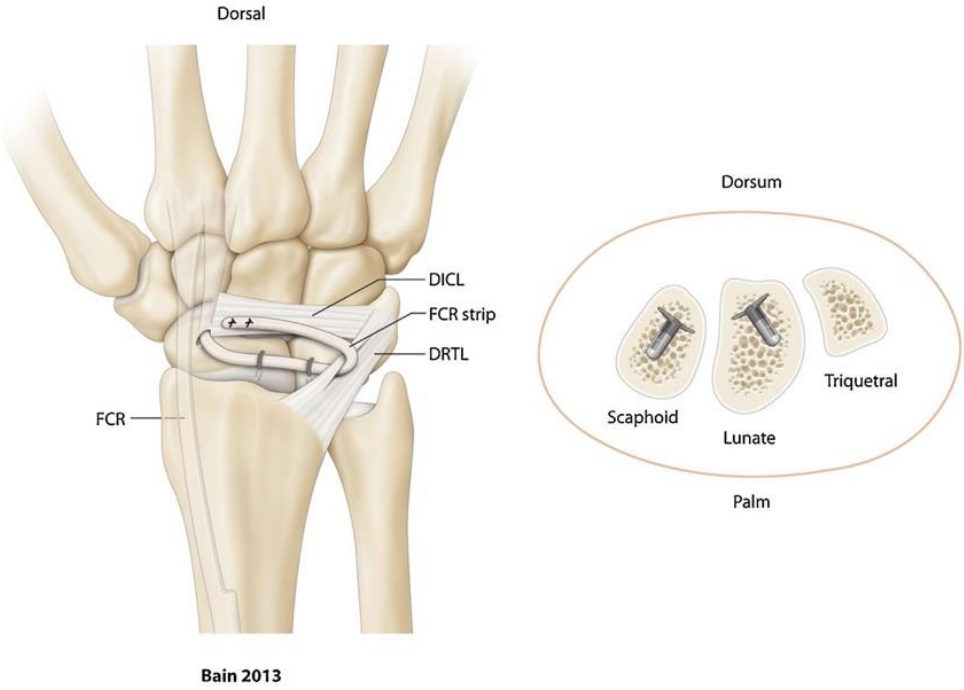

Fig. 8. FCR tenodesis as described by Bain [59]. DICL: dorsal intercarpal ligament; DRTL: dorsal radiotriquetral ligament; FCR: flexor carpi radialis.

(130° vs. 103°). On radiographs, there was a significant reduction in the SLG (4.1 mm vs. 1.6 mm) and the SLA (80° vs. 56°).

Hsu et al. [58] compared the SLT technique to the MB technique in a cadaver study in 2014. The study had two important findings: the SLT technique reduced the static SL instability and held it after 100 flexion-extension cycles; there were no significant differences between the two techniques on the radiological measurements.

3.3.4. Bain's quad ligament tenodesis

In 2013, Bain et al. [59] described a technique with the FCR that uses a suture tensioning bone anchor (Opus Labrafix MiniMagnum® knotless fixation device). Two of these anchors are placed at the former attachments of the SLIL's dorsal portion on the scaphoid and lunate. A FCR slip (distally pedicled) is passed through a distal scaphoid transosseous tunnel and then sutured under tension (made possible by this type of anchor) at both anchors to reduce the SL diastasis and reconstruct the dorsal portion of the SLIL. The tendon graft is then passed through the DRCL at its triquetral insertion, then over the dorsal side of the midcarpal joint (capitate) to the distal pole of the scaphoid (soft tissue fixation) to reconstruct the DICL (Fig. 8). Eight patients who underwent this surgical procedure were reviewed after 2 years. The clinical outcomes were good with a significant reduction in pain and improvement in grip strength with range of motion relative to the contralateral side of 91% in extension and 70% in flexion. However, the radiological outcomes were not as good: 7 of the 8 patients had pathological radiologic variables (SLA, SLG) at 6 months postoperative. This suggests this type of suture anchor provides good initial stability but does not provide sufficient long-term strength when subjected to cyclic loading.

3.3.5. Henry's palmar and dorsal SLIL reconstruction

In 2013, Henry [60] described a procedure in which the FCR is used to reconstruct the palmar and dorsal portions of the SLIL. A FCR slip is passed through transosseous tunnels in the scaphoid (palmar to dorsal) then the lunate (dorsal to palmar) to reconstruct the dorsal portion of the ligament. The oblique scaphoid tunnel goes from the distal pole to the proximal pole, near the former SLIL insertion. The lunate tunnel goes from the ulnar dorsal rim, under the articular surface, to the radial palmar rim, near the SLG. Once the tendon graft is retrieved at the exit of the lunate palmar tunnel, it is sutured to the remaining FCR tendon to reconstruct the palmar portion of the SLIL (Fig. 9). The author described the outcomes of a single patient after 8 years. Along with being pain-free, this patient also had nearly equal grip strength and flexion-extension range to that of the healthy contralateral side. The instability had been reduced and was maintained at the final review; the values of the SLG (2.5 mm vs. 6 mm) and SLA (46° vs. 80°) were normal.

3.3.6. Corella's arthroscopic SL tenodesis

Recently, Corella et al. [61,62] proposed performing FCR tenodesis arthroscopically to better preserve the soft tissue, particularly the extrinsic carpal ligaments. The indications are limited to predynamic and dynamic SL instability. The aim of this technique is to reconstruct the palmar and dorsal portions of the SLIL. Along with standard radiocarpal and midcarpal portals for arthroscopy, three additional incisions are made:

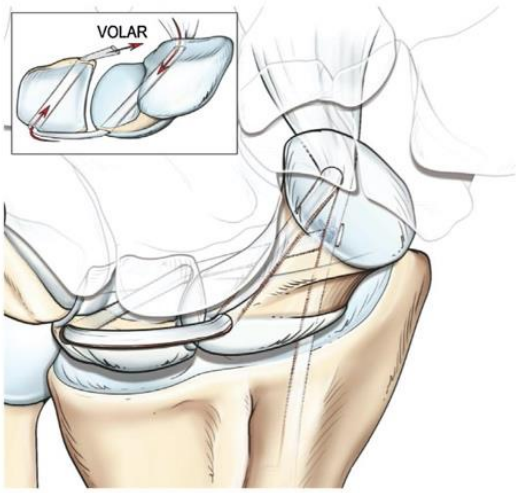

Fig. 9. FCR tenodesis as described by Henry [60].

- a dorsal one over the lunate;
- a palmar one over the lunate;
- another palmar one over the scaphoid tubercle and the FCR.

First, standard wrist arthroscopy is done to confirm the diagnosis, determine its stage and evaluate the articular surfaces and any associated lesions. Second, with arthroscopy guidance, two transosseous tunnels are made: one in the scaphoid (oblique from the tubercle to the former insertion of the dorsal portion of the SLIL) and one in the lunate (middle of lunate and parallel to articular surface). Third, a suture passer (Arthrex® SutureLasso™ is used to pass a FCR slip (distally pedicled) through the transosseous tunnels, which is then fixed under tension to reduce the SL diastasis using absorbable interference screws in the scaphoid (at palmar entrance of tunnel) and the lunate (at dorsal entrance of tunnel). The final step consists in reconstructing the palmar portion of the SLIL. The remaining graft, once it exits the lunate palmar tunnel is attached to the palmar capsule using outside-to-inside arthroscopic suturing technique [63] with 2-0 Arthrex® FiberStick™ suture (Fig. 10). The theoretical advantage of this technique is that the wrist's flexion and extension amplitude are maintained postoperatively; however there is no published data to support this.

3.4. Tenodesis using the palmaris longus (PL)

Elsaftawy et al. [64] performed a cadaver study using a free PL graft for ligament reconstruction in 2014. The aims were to reconstruct the palmar and dorsal portions of the SLIL. Two perpendicular anteroposterior transosseous tunnels were made at the proximal pole of the scaphoid and the lunate. The free graft was inserted in these tunnels; once the SL instability was reduced, it was interlaced and sutured to itself. The free end was attached with a suture anchor to the dorsal side of the distal pole of the scaphoid to prevent subluxation. However, the authors do not address the extrinsic ligaments (particularly the DICL) in this technique.

In 2017, Nicolas Pauchard and Gilles Dautel [65] proposed the scapholunate and intercarpal ligamentoplasty procedure. It uses a free PL graft to reconstruct the dorsal portion of the SLIL and the DICL. The aim was to validate the current biomechanical notion that the DICL acts as a stabilizer, while preserving the FCR, which is considered a secondary stabilizer for the SL complex [8–11]. This technique has two portions: the scapholunotriquetral one aims to correct the SL diastasis and the triquetrolunoscaphoid one aims to correct the DISI and SRS. By using a free PL graft, the tendon can be pre-loaded to prevent loss of ligament tension. A dorsal surgical approach is used to avoid damaging the STT joint. The blind nature of these tunnels prevents the iatrogenic of a complete scaphoid tunnel, which may cause devascularization, particularly in the proximal pole. The scaphoid and triquetral bone anchors use an interference fixation device such as the 2.5 mm mini BioPushlock™ by Arthrex®. There are no fixation points in the capsule (Fig. 11).

Table 1 summarizes the results of the tenodesis studies described in this review.

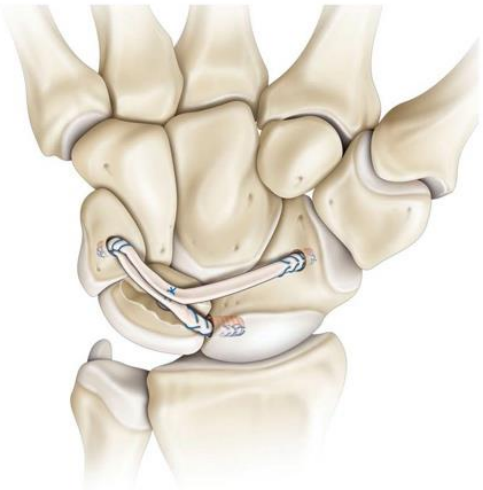

Fig. 11. The scapholunate and intercarpal ligamentoplasty procedure [65].

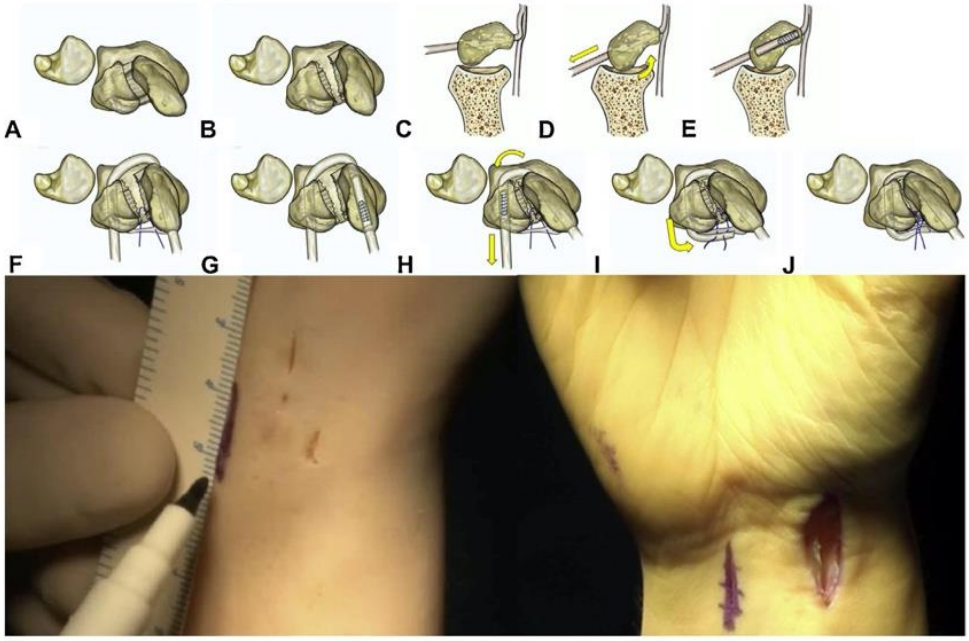

Fig. 10. Arthroscopic FCR tenodesis as described by Corella et al. [61,62]. Dorsal and ventral skin incisions are used to move the tendon graft. A, B. With a SLIL tear, the scaphoid flexes and pronates. C, D, E. When the graft is passed through the scaphoid tunnel and tensioned, the scaphoid extends. F, G, H. When the graft is passed through the lunate tunnel, the scaphoid supinates, avoiding impaction at the dorsal margin of the radius. I, J. Volar fixation prevents volar opening and movement in a sagittal plane.

Table 1
Published SL tenodesis studies.

Authors	Technique	P/D/S	*n*	Follow-up	VAS (pain)	Flex	Ext	RD	UD	Strength	SLA	SLG	Outcome scores/ Satisfaction	RTW
Almquist et al. (91)	FBLR (ECRB)	S	36	56	0-3 35%	37°	52°	//	//	73% CL	//	3.3 (>4 Pre)	//	92%
Brunelli et Brunelli (95) [42]	Brunelli (FCR)	S	13	M6 à A2	0-3 85%	25°	//	//	//	65% CL +50% Pre	Maintains scaphoid reduction	100% satisfaction	100%	
Van Den Abbeele et al. (98) [43]	BM (FCR)	P (15)/D (4)/S (3)	22	9	3 (7 Pre)	42° (51 Pre)	49° (61°Pre)	19° (20° Pre)	30° (26° Pre)	58% CL	50° (50° Pre)	//	15 WWFS (15 Pre)	64%
Brunelli et al. (04) [37]	ECRB	S	1	8	0	45° (40° Pre)	85° (55° Pre)	//	//	30 kg (18 kg Pre)	50° (120° Pre)	2 (9 Pre)	//	100%
Talwalkar et al. (06) [44]	BM (FCR)	D (32)/ S (23)	55	48	0-3 62% 3.7	46.5°	55.7°	17.5°	29°	80% CL	//	//	79% satisfaction	77%
Moran et al. (06) [45]	BM (FCR)	D/S	15	36	0-3 27%	40° (54° Pre)	43° (56° Pre)	16° (18° Pre)	26° (32° Pre)	87% CL	54° (63° Pre)	2.6 (3 Pre)	74 MWS	//
Garcia Elias et al. (06) [29]	3LT (FCR)	D/S	38	46	0-3 95%	51°	52°	15°	29°	65% CL	//	//	//	95%
De Smet and Van Hoonacker (07) [46]	BM (FCR)	D/S	10	29	0-3 90%	49°	48°	17°	34°	77% CL	//	//	12 QD 26 PRWE	90%
Chabas et al. (08) [47]	BM (FCR)	D (12)/ S (7)	19	37	0-3 79% 3 (7.5 Pre)	41°	50°	24°	29°	78% CL	62° (61° Pre)	2.4 (2.8 Pre)	80% satisfaction 30 QD	84%
Links et al. (08) [48]	BM (FCR)	D/S	21	30	2 (6.9 Pre)	45° (59°Pre)	55° (61° Pre)	13° (18° Pre)	21° 26° Pre)	98% CL	46° (61° Pre)	2.2 (3.9 Pre)	25.1 QD (77.9 Pre)	//
Links et al. (08) [48]	FBLR (ECRB)	D/S	23	30	3.4 (6.7 Pre)	27° (60° Pre)	36° (61° Pre)	14° (18° Pre)	21° (25° Pre)	84%CL	53° (61°Pre)	3.0 (3.7 Pre)	45.1 QD (67.5 Pre)	//
Bleuler et al. (08) [39]	ECRL	S	20	12	0-3 50%	//	//	//	//	//	//	//	//	100%
Klab K (09) [66]	3LT (FCR)	D/S	14	10.5	2.8	35°	53°	//	//	80% CL	64° (73° Pre)	3.3 (3.6 Pre)	25 QD 80 MWS	//
Papadogeorgou and Mathoulin (10) [38]	ECRB	S	32	50	0-3 75%	42° (46° Pre)	70° (58° Pre)	22° (15° Pre)	32° (27° Pre)	86% CL	<60° 23 cases	//	22 QD ≥ 80 MWS in 24 cases	100%
Peterson and Freeland (10) [40]	ECRL	S	1	6	0	//	//	//	//	80% CL	//	//	//	100%
De Carli et al. (11) [41]	ECRL	S	8	23	3	//	//	//	//	//	60° (82° Pre)	2.6 (4.6PO)	13 QD 73 MWS	//
De Smet et al. (13) [54]	3LT (FCR)	S	12	39	//	//	//	//	//	//	68° (77° Pre)	3.2 (4.2 Pre)	//	//
Pauchard et al. (13) [56]	3LT (FCR)	D (8)/ S (12)	20	25	1.6 (3.2 Pre)	39° (52° Pre)	43° (50° Pre)	14° (17° Pre)	24° (30° Pre)	76% CL	75° (72° Pre)	3.7 (3.9 Pre)	31.3QD (48.9 Pre) PRWE (55.5 Pre)	100%
Ross et al. (13) [57]	SLT tenodesis (FCR)	D/S	11	14	1.35	AmpFE = 103° (130° Pre)			44 kg (37 kg Pre)	56° (80° Pre)	1.6 (4.1 Pre)	21.2 QD (50 Pre) PRWE (43.1 Pre)	//	
Bain et al. (13) [59]	Quad Ligament tenodesis (FCR)	S	8	24	2.1 (5.8 Pre)	44° (48°Pre)	56° (51° Pre)	//	//	95% CL	71°	3	75% satisfaction	//
Nienstedt (13) [50]	BM (FCR)	S	8	164	0-3 88%	37°	63°	21°	32°	85% CL	63° (72° Pre)	2.8 (5.1 Pre)	9 QD 83 MWS 88% satisfaction	88%
Henry (13) [60]	SLIL palmar & dorsal reconstruction (FCR)	S	1	96	0 (8 Pre)	55° (50° Pre)	75° (50° Pre)	//	//	96%CL	46° (80° Pre)	2.5 (6 Pre)	7 QD (50 Pre)	100%
Corella et al. (13) [62]	Arthroscopic SLIL reconstruction (FCR)	D	1	6	1.2 (8 Pre)	85° (80° Pre)	80° (70° Pre)	//	//	100% CL	//	//	10 QD (51.8 Pre)	100%
Ellanti et al. (14) [51]	BM (FCR)	D/S	13	12	1.5 (8 Pre)	38° (76°Pre)	56° (76° Pre)	20° (24° Pre)	20° (34° Pre)	75% CL	63° (61° Pre)	2.8 (2.8 Pre)	34.9 QD (55.6 Pre)	100%

Table 1 (*Continued*)

Authors	Technique	P/D/S	*n*	Follow-up	VAS (pain)	Flex	Ext	RD	UD	Strength	SLA	SLG	Outcome scores/ Satisfaction	RTW
Sousa et al. (14) [52]	BM (FCR)	D/S	22	61	0-3 68% 2	23° less than CL	22° less than CL	6° less than CL	3° less than CL	67% CL	57°	3.1	16 QD	91%
Rohman (14) [67]	BM (FCR)	D/S	22	6	//	38°	43°	//	//	//	57°	2.3	31.82 QD	//
Elgammal and Lukas (15) [53]	BM (FCR)	D/S	20	24	0-3 80% 3 (6 Pre)	41° (60° Pre)	54° (68° Pre)	19° (25° Pre)	31° (40° Pre)	81% CL	77° (82° Pre)	3 (4 Pre)	20 QD (37 Pre) ≥ 80 MWS in 45%	75%

3LT: three-ligament tenodesis by Garcia Elias; AmpFE: amplitude of flexion-extension in degrees; BM: Brunelli as modified by Van Den Abbeele; CL: contralateral; ECRB: extensor carpi radialis brevis; ECRL: extensor carpi radialis longus; Ext: extension in degrees; FBLR: four-bone ligament reconstruction; FCR: flexor carpi radialis; Flex: flexion in degrees; Follow-up: in months; MWS: Mayo Wrist Score (/100); *n*: number of cases; P/D/S: predynamic/dynamic/static; Pre: preoperative; PRWE: patient rated wrist evaluation (/100); QD: Quick Dash (/100); RD: radial deviation in degrees; RTW: return to work; SLA: scapholunate angle in degrees; SLG: scapholunate gap in mm; SLT: scapholunotriquetral; SLIL: scapholunate interosseous ligament; Strength: in KgF; UD: ulnar deviation in degrees; VAS: visual analog scale (0 to 10); WWFS: Wrightington Wrist function score (/100).

4. Discussion

Based on this review of literature, tenodesis can be separated into two broad groups (Table 2).

The first group corresponds to procedures using a slip of the ECRB or ECRL tendon. They are either radiocarpal (Bleuler et al. [39], Peterson and Freeland [40]) with the aim of verticalizing the scaphoid without reconstructing the SLIL, or intracarpal (Linscheid and Dobyns [36], Papadogeorgou and Mathoulin [38], De Carlis et al. [41]) in order to reconstruct the dorsal portion of the SLIL. These ligament reconstruction procedures are mainly indicated in patients with static SL instability. There are very few clinical studies reporting the results of these techniques. The radiological parameters (SLA and SLG) are rarely studied, which means there is little evidence in favor of this group of ligament reconstruction procedures.

The second group corresponds to procedures using a slip of the FCR tendon. These are all intracarpal procedures except for the Brunelli procedure [42]. In every case, the aim is to reconstruct the dorsal portion of the SLIL. Only the Henry technique [60] aims to reconstruct both the palmar and dorsal portions of the SLIL. The more recent techniques by Ross et al. [57] and Bain et al. [59] aim to reconstruct the DICL in addition to the dorsal portion of the SLIL. The techniques in this subgroup are indicated for dynamic and static SL instability cases. The Brunelli tenodesis, as modified by Van Den Abbeele et al. [43] and the Garcia-Elias procedure [29] are featured in the largest number of published clinical studies. These studies show that pain is decreased significantly and grip strength is increased significantly after the procedure. These studies all show good radiological outcomes (SLA and SLG) for cases of dynamic SL instability. However, the results vary greatly from one study to another for cases of static SL instability and the outcomes are still abnormal or at the upper end of normal. It is common to find recurrence of the abnormal radiological findings in the medium-term likely due to loss of tension in the ligaments [29,44–48,50–54,66,67]. The long-term aim of these SL reconstruction techniques is to prevent the development of osteoarthritis [13,26,30]. Only static instability is said to always progress to osteoarthritis [31,32]. The SLAC osteoarthritis rate ranges from 5% in the Chabas et al. study [47] to 23% in the Garcia Elias et al. study [29]. This complication is reported in studies with at least 2 years' follow-up. Since most studies include only a small number of patients, and the follow-up is not very long, there is not enough evidence to support osteoarthritis prevention.

When using the FCR tendon, a transosseous tunnel must be made in the scaphoid. This is known to lead to complications such as necrosis of the proximal pole of the scaphoid (devascularisation) [46,54,55] and STT osteoarthritis (joint damage) [56].

Furthermore, since all these are open techniques, the required dorsal arthrotomy is known to cause joint stiffening and to reduce the wrist's flexion and extension mobility. Radiocarpal tenodesis cause more stiffening than intracarpal ones. For this reason, Corella et al. [62] proposed using arthroscopy to reconstruct both portions of the SLIL using a slip of FCR tendon. The aim is to preserve the extrinsic ligament structures and cause the least amount of stiffening possible. This technique is suitable for cases of dynamic instability that do not require important scaphoid reduction maneuvers.

The scapholunate and intercarpal ligamentoplasty procedure proposed by Athlani et al. [65] aims to comply with current biomechanical thinking by reconstructing the DICL along with the dorsal portion of the SLIL. The main advantage of this technique is that it avoids the morbidity and technical difficulties in the scaphoid transosseous tunnel using a free PL tendon graft. Also,

Table 2
Comparison of SL tenodesis.

Tenodesis	Graft type	Approach	Type	Reconstruction of SLIL	Reconstruction of DICL	Type of SL instability targeted	SL stabilization	Published clinical studies	Significant improvement strength/pain	SLG	SLA
Almquist [35]	ECRB	Open	RC	+(Dorsal)	–	S	0	1	+	3.0 (3.7)	53 (61)
Linscheid [36]	ECRB	Open	IC	+(Dorsal)	–	S	0	1	+	/	/
Papadogeorgou [38]	ECRB	Open	IC	+ (Dorsal)	–	S	Interference screw (6 months)	1	+	/	/
Bleuler [39]	ECRL	Open	RC	–	–	S	0	1	+	/	/
Peterson [40]	ECRL	Open	RC	–	–	S	0	1 (1 case)	+	/	/
De Carlis [41]	ECRL	Open	IC	$+_S$(Dorsal)	–	S	K-wires (8 weeks)	1	+	2.6 (4.6)	60 (82)
Brunelli [42]	FCR	Open	RC	+(Dorsal)	–	S	K-wires (8 weeks)	1	+	/	/
Van Den Abbeele [43]	FCR	Open	IC	+(Dorsal)	–	D/S	K-wires (8 weeks)	8	+	2.2 to 3 (2.8 to 5.1)	46 to 77 (50 to 82)
Garcia-Elias [29]	FCR	Open	IC	+(Dorsal)	–	D/S	K-wires (8 weeks)	4	+	3.2 to 3.7 (3.6 to 4.2)	64 to 75 (72 to 77)
Ross [57]	FCR	Open	IC	+(Dorsal)	+	D/S	K-wires (8 weeks)	1	+	1.6 (4.1)	56 (80)
Bain [59]	FCR	Open	IC	+(Dorsal)	+	D/S	K-wires (8 weeks)	1	+	3 (?)	71 (?)
Henry [60]	FCR	Open	IC	+(Palmar/Dorsal)	–	D/S	K-wires (8 weeks)	1 (1 case)	+	2.5 (6)	46 (80)
Corella [62]	FCR	Arthroscopic	IC	+(Palmar/Dorsal)	–	P/D	K-wires (8 weeks)	1 (1 case)	+	/	/

DICL: dorsal intercarpal ligament; RC/IC: radiocarpal/intracarpal; ECRB: extensor carpi radialis brevis; ECRL: extensor carpi radialis longus; FCR: flexor carpi radialis; P/D/S: predynamic/dynamic/static; SL: scapholunate; SLA: postoperative scapholunate angle in degrees (preoperative value); SLG: postoperative scapholunate gap in mm (preoperative value); SLIL: scapholunate interosseous ligament.

preloading this graft prevents secondary loosening and the resulting loss of ligament tension.

SL reconstruction procedures are intended for cases of static SL instability that are "easily" reducible. This concept of reducibility must be assessed preoperatively, especially in cases of instability operated more than 1 year after the initial injury event. Thus, it is essential to perform dynamic maneuvers during the preoperative arthroscopy along with dynamic X-ray views in ulnar and radial deviation. Also, during the surgical procedure, it is essential to confirm right away whether the dissociation can be reduced "easily" as this is a basic criterion to confirm the indication. There is currently no way to quantify the loads needed to reduce the scaphoid and thereby to differentiate between "easily" reducible instability cases and "difficult" cases. Only the former is suitable for tenodesis reconstruction.

Lastly, the preoperative radiographs must be bilateral and comparative while taking into account potential congenital SL pseudo-dissociation responsible for SL diastasis and DISI that are not pathological. If these two abnormal radiological findings are detected on an asymptomatic non-injured wrist, they will not have pathological values. Recent 3D CT [68] and X-ray [69] studies support this concept of the presence of bilateral asymptomatic static abnormalities. Thus, it appears that only SRS is always symptomatic and is pathognomic for static SL instability.

Disclosure of interest

The authors declare that they have no competing interest.

References

[1] Linscheid RL, Dobyns JH, Beabout JW, Bryan RS. Traumatic carpal instability of the wrist. Diagnosis, classification and pathomechanics. J Bone Joint Surg 1972;54:1612–32.
[2] Allieu Y. Démembrement du concept d'instabilité du carpe. Rev Chir Orthop 1993;79:45–7.
[3] Wright TW, Dobyns JH, Linscheid RL, Macksoud W, Siegert J. Carpal instability non-dissociative. J Hand Surg 1994;19:763–73.
[4] Crisco JJ, Pike S, Hulsizer-Galvin DL, Akelman E, Weiss APC, Wolfe SW. Carpal bone postures and motions are abnormal in both wrists of patients with unilateral scapholunate interosseous ligament tears. J Hand Surg Am 2003;28:926–37.
[5] Taleisnik J. Carpal instability. Current concepts review. J Bone Joint Surg Am 1988;70:1262–8.
[6] Gajendran VK, Peterson B, Slater Jr RR, Szabo RM. Long-term outcomes of dorsal intercarpal ligament capsulodesis for chronic scapholunate dissociation. J Hand Surg Am 2007;32:1323–33.
[7] Watson HK, Ballet FL. The SLAC wrist: scapholunate advanced collapse pattern of degenerative arthritis. J Hand Surg Am 1984;9:358–65.
[8] Wolfe SW. Scapholunate instability. J Am Soc Surg Hand 2001;1:45–60.
[9] Walsh JJ, Berger RA, Cooney WP. Current status of scapholunate interosseous ligament injuries. J Am Acad Orthop Surg 2002;10:32–42.
[10] Bellemère P. Traitement des ruptures partielles du ligament scapholunaire. Rev Chir Orthop 2001;87:39–42.
[11] Saffar P, Herzberg G. Instabilités ligamentaires traumatiques du carpe. Rev Chir Orthop 1993;79:27–77.
[12] Mayfield JK, Johnson RP, Kilcoyne RK. Carpal dislocations: pathomechanics and progressive perilunar instability. J Hand Surg Am 1980;5:226–41.
[13] Taleisnik J. The wrist. Edinburgh: Churchill Livingstone; 1985.
[14] Short WH, Werner FW, Green JK, Sutton LG, Brutus JP. Biomechanical evaluation of ligamentous stabilizers of the scaphoid and lunate: part III. J Hand Surg Am 2007;32:297–309.
[15] Viegas SF, Yamaguchi S, Boyd NL, Patterson RM. The dorsal ligaments of the wrist: anatomy, mechanical properties and function. J Hand Surg Am 1999;24:456–68.
[16] Meade TD, Schneider LH, Cherry K. Radiographic analysis of selective ligament sectioning at the carpal scaphoid: a cadaver study. J Hand Surg Am 1990;15:855–62.
[17] Blatt G. Capsulodesis in reconstructive hand surgery. Dorsal wrist capsulodesis for the unstable scaphoid and volar capsulodesis following excision of the distal ulna. Hand Clin 1987;3:81–102.
[18] Mitsuyasu H, Patterson RM, Shah MA, Buford WL, Iwamoto Y, Viegas SF. The role of the dorsal intercarpal ligament in dynamic and static scapholunate instability. J Hand Surg Am 2004;29:279–88.
[19] Blevens AD, Light TR, Jablonsky WS, Smith DG, Patwardhan AG, Guay ME, et al. Radiocarpal articular contact characteristics with scaphoid instability. J Hand Surg Am 1989;14:781–90.
[20] Elsaidi GA, Ruch DS, Kuzma GR, Smith BP. Dorsal wrist ligament insertions stabilize the scapholunate interval: cadaver study. Clin Orthop Relat Res 2004;425:152–7.
[21] Larsen CF, Amadio PC, Gilula LA, Hodge JC. Analysis of carpal instability: I. Description of the scheme. J Hand Surg Am 1995;20:757–64.
[22] Watson H, Ottoni L, Pitts EC, Handal AG. Rotary subluxation of the scaphoid: a spectrum of instability. J Hand Surg Br 1993;18:62–4.
[23] Nathan R, Blatt G. Rotary subluxation of the scaphoid revisited. Hand Clin 2000;16:417–31.
[24] Burgess RC. The effect of rotatory subluxation of the scaphoid on radioscaphoid contact. J Hand Surg Am 1987;12:771–4.
[25] Viegas SF, Ballantyne G. Attritional lesions of the wrist joint. J Hand Surg Am 1987;12:1025–9.
[26] Laulan J. Le poignet traumatique. In: Le Nen D, Laulan J, editors. Sémiologie de la main et du poignet. Montpellier: Sauramps Médical; 2001. p. 247–67.
[27] McAuliffe JA, Dell PC, Jaffe R. Complications of intercarpal arthrodesis. J Hand Surg Am 1993;18:1121–8.
[28] Dautel G, Goudot B, Merle M. Arthroscopic diagnosis of scapholunate instability in the absence of X-ray abnormalities. J Hand Surg Br 1993;18:213–8.
[29] Garcia-Elias M, Lluch AL, Stanley JK. Three-ligament tenodesis for the treatment of scapholunate dissociation: indications and surgical technique. J Hand Surg Am 2006;31:125–34.

[30] Palmer AK, Dobyns JH, Linscheid RL. Management of posttraumatic instability of the wrist secondary to ligament rupture. J Hand Surg Am 1978;3:507–32.
[31] Saffar P. Traitement des ruptures totales sans arthrose. Rev Chir Orthop 2001;87:43–5.
[32] Garcia-Elias M, Geissler WB. Carpal instability., In: Green, Hotchkiss, Pederson, Wolfe, editors. Fifth edition, Green's operative hand surgery, 1, Fifth edition Elsevier Churchill Livingstone; 2005. p. 535–604.
[33] Watson HK, Ashmead IV D, Maklhouf MV. Examination of the scaphoid. J Hand Surg Am 1988;13:657–60.
[34] Dautel G. L'arthroscopie du poignet. La main traumatique. Chirurgie secondaire le poignet traumatique, 2. Paris: Masson; 1995. p. 381–97.
[35] Almquist EE, Bach AW, Sack JT, Fuhs SE, Newman DM. Four-bone ligament reconstruction for treatment of chronic complete scapholunate separation. J Hand Surg Am 1991;16:322–7.
[36] Linscheid RL, Dobyns JH. Treatment of scapholunate dissociation. Rotatory subluxation of the scaphoid. Hand Clin 1992;8:645–52.
[37] Brunelli F, Spalvieri C, Bremner-Smith A, Papalia I, Pivato G. Dynamic correction of static scapholunate instability using an active tendon transfer of extensor carpi radialis brevis: preliminary report. Chir Main 2004;23:249–53.
[38] Papadogeorgou E, Mathoulin C. Extensor carpi radialis brevis ligamentoplasty and dorsal capsulodesis for the treatment of chronic post-traumatic scapholunate instability. Chir Main 2010;29:172–9.
[39] Bleuler P, Shafighi M, Donati OF, Gurunluoglu R, Constantinescu MA. Dynamic repair of scapholunate dissociation with dorsal extensor carpi radialis longus tenodesis. J Hand Surg Am 2008;33:281–4.
[40] Peterson SL, Freeland AE. Scapholunate stabilization with dynamic extensor carpi radialis longus tendon transfer. J Hand Surg Am 2010;35:2093–100.
[41] De Carli P, Donndorff AG, Gallucci GL, Boretto JG, Alfie VA. Chronic scapholunate dissociation: ligament reconstruction combining a new extensor carpi radialis longus tenodesis and a dorsal intercarpal ligament capsulodesis. Tech Hand Up Extrem Surg 2011;15:6–11.
[42] Brunelli GA, Brunelli GR. A new technique to correct carpal instability with scaphoid rotary subluxation: a preliminary report. J Hand Surg Am 1995; 20(3 Pt 2):S82–5.
[43] Van Den Abbeele KL, Loh YC, Stanley JK, Trail IA. Early results of a modified Brunelli procedure for scapholunate instability. J Hand Surg Br 1998;23(2): 258–61.
[44] Talwalkar SC, Edwards AT, Hayton MJ, Stilwell JH, Trail IA, Stanley JK. Results of tri-ligament tenodesis: a modified Brunelli procedure in the management of scapholunate instability. J Hand Surg Br 2006;31:110–7.
[45] Moran SL, Ford KS, Wulf CA, Cooney WP. Outcomes of dorsal capsulodesis and tenodesis for treatment of scapholunate instability. J Hand Surg Am 2006;31:1438–46.
[46] De Smet L, Van Hoonacker P. Treatment of chronic static scapholunate dissociation with the modified Brunelli technique: preliminary results. Acta Orthop Belg 2007;73:188–91.
[47] Chabas JF, Gay A, Valenti D, Guinard D, Legré R. Results of the modified Brunelli tenodesis for treatment of scapholunate instability: a retrospective study of 19 patients. J Hand Surg Am 2008;33:1469–77.
[48] Links AC, Chin SH, Waitayawinyu T, Trumble TE. Scapholunate interosseous ligament reconstruction: results with modified Brunelli technique versus four-bone weave. J Hand Surg Am 2008;33:850–6.
[49] Howlett JP, Pfaeffle HJ, Waitayawinyu T, Trumble TE. Distal tunnel placement improves scaphoid flexion with the Brunelli tenodesis procedure for scapholunate dissociation. J Hand Surg Am 2008;33:1756–64.
[50] Nienstedt F. Treatment of static scapholunate instability with modified Brunelli tenodesis: results over 10 years. J Hand Surg Am 2013;38:887–92.
[51] Ellanti P, Sisodia G, Al-Ajami A, Ellanti P, Harrington P. The modified Brunelli procedure for scapholunate instability: a single centre study. Hand Surg 2014;19:39–42.
[52] Sousa M, Aido R, Freitas D, Trigueiros M, Lemos R, Silva C. Scapholunate ligament reconstruction using a flexor carpi radialis tendon graft. J Hand Surg Am 2014;39:1512–6.
[53] Elgammal A, Lukas B. Mid-term results of ligament tenodesis in treatment of scapholunate dissociation: a retrospective study of 20 patients. J Hand Surg Eur 2016;41:56–63.
[54] De Smet L, Goeminne S, Degreef I. Does the "three-ligament tenodesis" procedure restore carpal architecture in static chronic scapholunate dissociation? Acta Orthop Belg 2013;79:271–4.
[55] De Smet L, Goeminne S, Degreef L. Failures of the three-ligament tenodesis for chronic static scapholunate dissociation are due to insufficient reduction. Acta Orthop Belg 2011;77:595–7.
[56] Pauchard N, Dederichs A, Segret J, Barbary S, Dap F, Dautel G. The role of three-ligament tenodesis in the treatment of chronic scapholunate instability. J Hand Surg Eur 2013;38:758–66.
[57] Ross M, Loveridge J, Cutbush K, Couzens G. Scapholunate reconstruction. J Wrist Surg 2013;2:110–5.
[58] Hsu JW, Kollitz KM, Jegapragasan M, Huang JI. Radiographic evaluation of the modified Brunelli technique versus a scapholunotriquetral transosseous tenodesis technique for scapholunate dissociation. J Hand Surg Am 2014;39: 1041–9.
[59] Bain GI, Watts AC, McLean J, Lee YC, Eng K. Cable-augmented, quad ligament tenodesis scapholunate reconstruction: rationale, surgical technique and preliminary results. Tech Hand Up Extrem Surg 2013;17:13–9.
[60] Henry M. Reconstruction of both volar and dorsal limbs of the scapholunate interosseous ligament. J Hand Sur Am 2013;38:1625–34.
[61] Corella F, Del Cerro M, Larrainzar-Garijo R, Vàsquez T. Arthroscopic ligamentoplasty (bone-tendon-tenodesis). A new surgical technique for scapholunate instability: preliminary cadaver study. J Hand Surg Eur 2011;36: 682–9.
[62] Corella F, Del Cerro M, Ocampos M, Larrainzar-Garijo R. Arthroscopic ligamentoplasty of the dorsal and volar portions of the scapholunate ligament. J Hand Surg Am 2013;38:2466–77.
[63] Del Pinal F, Studer A, Thams C, Glasberg A. An all-inside technique for arthroscopic suturing of the volar scapholunate ligament. J Hand Surg Am 2011;36:2044–6.
[64] Elsaftawy A, Jablecki J, Jurek T, Domanasiewicz A, Gworys B. New concept of scapholunate dissociation treatment and novel modification of Brunelli procedure – anatomical study. BMC Musculoskelet Disord 2014;15:172.
[65] Athlani L, Pauchard N, Dautel G. Radiological evaluation of scapholunate intercarpal ligamentoplasty for chronic scapholunate dissociation in cadavers. J Hand Surg Eur 2017;1 [1753193417746055].
[66] Kalb K, Blank S, Van Schoonhoven J, Prommersberger KJ. Stabilization of the scaphoid according to Brunelli as modified by Garcia-Elias. Lluch and Stanley for the treatment of chronic scapholunate dissociation. Oper Orthop Traumatol 2009;21:429–41.
[67] Rohman EM, Agel J, Putnam MD, Adams JE. Scapholunate interosseous ligament injuries: a retrospective review of treatment ant outcomes in 82 wrists. J Hand Surg Am 2014;39:2020–6.
[68] Feipel V, Rooze M. Three-dimensional motion patterns of the carpal bones: an in vivo study using three-dimensional computed tomography and clinical applications. Surg Radiol Anat 1999;21:125–31.
[69] Vitello W, Gordon DA. Obvious radiographic scapholunate dissociation: X-ray of the other wrist. Am J Orthop 2005;34:347–51.

La ligamentoplastie « SLIC » : concept initial et évaluation

Le concept initial de la ligamentoplastie « SLIC » a été développé par le Professeur Gilles Dautel et le Docteur Nicolas Pauchard du *service de chirurgie de la main, chirurgie plastique et reconstructrice de l'appareil locomoteur* du Centre Chirurgical Émile Gallé (CHRU de Nancy). Elle utilise un transplant libre de Palmaris Longus pour reconstruire la portion dorsale du LIOSL et le ligament DIC, permettant ainsi de restaurer la congruence scapho-lunaire. Son objectif premier est de pallier les imperfections des ligamentoplasties uilisant le Flexor Carpi Radialis, notamment la 3LT de Garcia-Elias (Garcia-Elias et al., 2006). En effet, la réalisation d'un tunnel trans-osseux scaphoïdien pour passer le tendon d'une position palmaire à une dorsale, peut être source de complications iatrogènes, de type nécrose vasculaire du pôle proximal du scaphoïde ou collapsus arthrosique STT (Pauchard et al., 2013). Son objectif second est de répondre aux conceptions biomécaniques actuelles, soulignant le rôle important stabilisateur du ligament DIC (Mitsuyasu et al., 2004). De plus, l'utilisation d'un transplant libre de Palmaris Longus respecte ainsi le Flexor Carpi Radialis, considéré comme stabilisateur secondaire du complexe scapho-lunaire (Short et al., 2007). Cela rend également possible la précontrainte tendineuse en prévention de la détente ligamentaire.

Son schéma repose sur deux jambages, Scapho-Luno-Triquétral qui corrige le diastasis scapho-lunaire et Triquétro-Luno-Scaphoïdien corrigeant la DISI et la SPS. La voie d'abord est exclusivement dorsale permettant d'éviter tout abord de l'articulation STT. Le caractère « borgne » des tunnels osseux évite la iatrogénicité d'un tunnel trans-scaphoïdien. Les ancrages osseux scaphoïdien et triquétral sont solides grâce à l'utilisation d'un dispositif de fixation intra-osseux en interférence de type « pushlock » (MiniBioPushlock™ 2,5 mm résorbable Arthrex®) (Figure 21-D).

L'incision cutanée est dorsale dans l'axe du troisième métacarpien et centrée sur l'interligne radio-carpien. Le rétinaculum des extenseurs est abordé entre le troisième et quatrième compartiment. Une capsulotomie dorsale est pratiquée selon la technique de Berger et al., (1995), préservant ainsi les ligaments DRC et DIC. Après confirmation de l'indication, le transplant tendineux est prélevé à la face antérieure du poignet par une courte incision, puis précontraint sur une station de travail dédiée à 3 kg pendant 2 minutes (Arthrex®). Une longueur de transplant de 10 cm est suffisante. Un premier tunnel borgne de 10 mm de profondeur et 2,5 mm de diamètre est réalisé au niveau du pôle proximal du scaphoïde, en regard de l'ancienne insertion de la portion dorsale du LIOSL. Puis, la corne postérieure du lunatum est avivée à la fraise, afin de créer une tranchée lunarienne de quelques millimètres de

profondeur dans l'objectif d'obtenir une interface d'accolement pour le transplant. Un deuxième tunnel borgne de même profondeur et même diamètre est réalisé à la face dorsale du triquétrum, en regard du bord radial de l'insertion du ligament DRC, suivant l'axe de la tranchée lunarienne. Une des deux extrémités du transplant est alors faufilée sur une distance de 10 mm en utilisant un fils boucle résorbable Fiberloop™ 4-0 (Arthrex®) puis, appliquée au fond du premier tunnel scaphoïdien proximal et fixée par l'impaction du système d'ancrage en interférence MiniBioPushlock™ 2,5 mm résorbable (Arthrex®). Au sein de la tranchée lunarienne une ancre titane Micro Corkscrew™ 2,2 mm vissée non résorbable (Arthrex®) est mise en place (Figure 21-A). La dissociation scapho-lunaire est ensuite réduite par manœuvres externes aidées d'un davier à pointe puis stabilisée par un brochage scapho-lunaire et scapho-capitale (broches de Kirschner de 12/10°). La fixation du transplant dans le deuxième tunnel triquétral nécessite la réalisation d'un amincissement et d'une plicature longitudinale de celui-ci. Pour cela, sa moitié centrale va être réséquée sur une distance de 12 à 16 mm depuis le point d'entrée dans le tunnel triquétral. Les deux hémi-bandelettes obtenues sont retournées sur elles-mêmes de manière à obtenir une nouvelle extrémité de transplant de même épaisseur que les deux autres, sur une longueur 6 à 8 mm. Cette extrémité est alors faufilée sur 10 mm puis insérée et fixée au fond du deuxième tunnel borgne par impaction d'un pushlock (Figure 21-B). Le transplant situé entre les deux premiers points de fixation intra-osseux, est appliqué dans la tranchée lunarienne puis fixé par les fils de l'ancre, permettant ainsi l'obtention du premier jambage Scapho-Luno-Triquétral. Un troisième tunnel borgne de même profondeur et diamètre est réalisé au niveau de l'isthme du scaphoïde à la limite de la surface articulaire STT. Afin d'obtenir le deuxième jambage Triquétro-Luno-Scaphoïdien, la partie restante du transplant est à nouveau appliquée dans la tranchée lunarienne, puis fixée par les mêmes fils de l'ancre permettant la superposition des deux jambages au niveau de cette tranchée. L'extrémité restante du transplant va être insérée dans le tunnel scaphoïdien distal, après avoir réséqué le surplus de transplant situé au-delà de 8 mm, depuis le point d'entrée dans le tunnel. Cette dernière extrémité est faufilée sur 10 mm puis insérée et fixée au fond du troisième tunnel par impaction d'un pushlock (Figure 21-C). La tension des deux jambages peut être alors testée. La suture capsulaire et rétinaculaire est réalisée par un fils à résorption lente de type PDS™ (Ethicon®, One Johnson & Johnson Plaza, New Brunswick, NJ, USA). La fermeture cutanée vient alors finir l'intervention.

En pratique clinique, un protocole de rééducation précis a été défini. En post-opératoire immédiat, le poignet est immobilisé par une attelle plâtrée palmaire pour une durée de 48 à 72 heures (durée de l'œdème post-opératoire). Puis, l'immobilisation est prolongée pour 2 mois par une résine anté-brachio-palmaire.

À 2 mois post opératoire, les broches sont retirées et le patient débute son auto-rééducation pendant 1 mois. La kinésithérapie activo-passive sera débutée, après contrôle radiographique, au troisième mois post-opératoire. Le port de charge lourde est contre-indiqué avant le sixième mois.

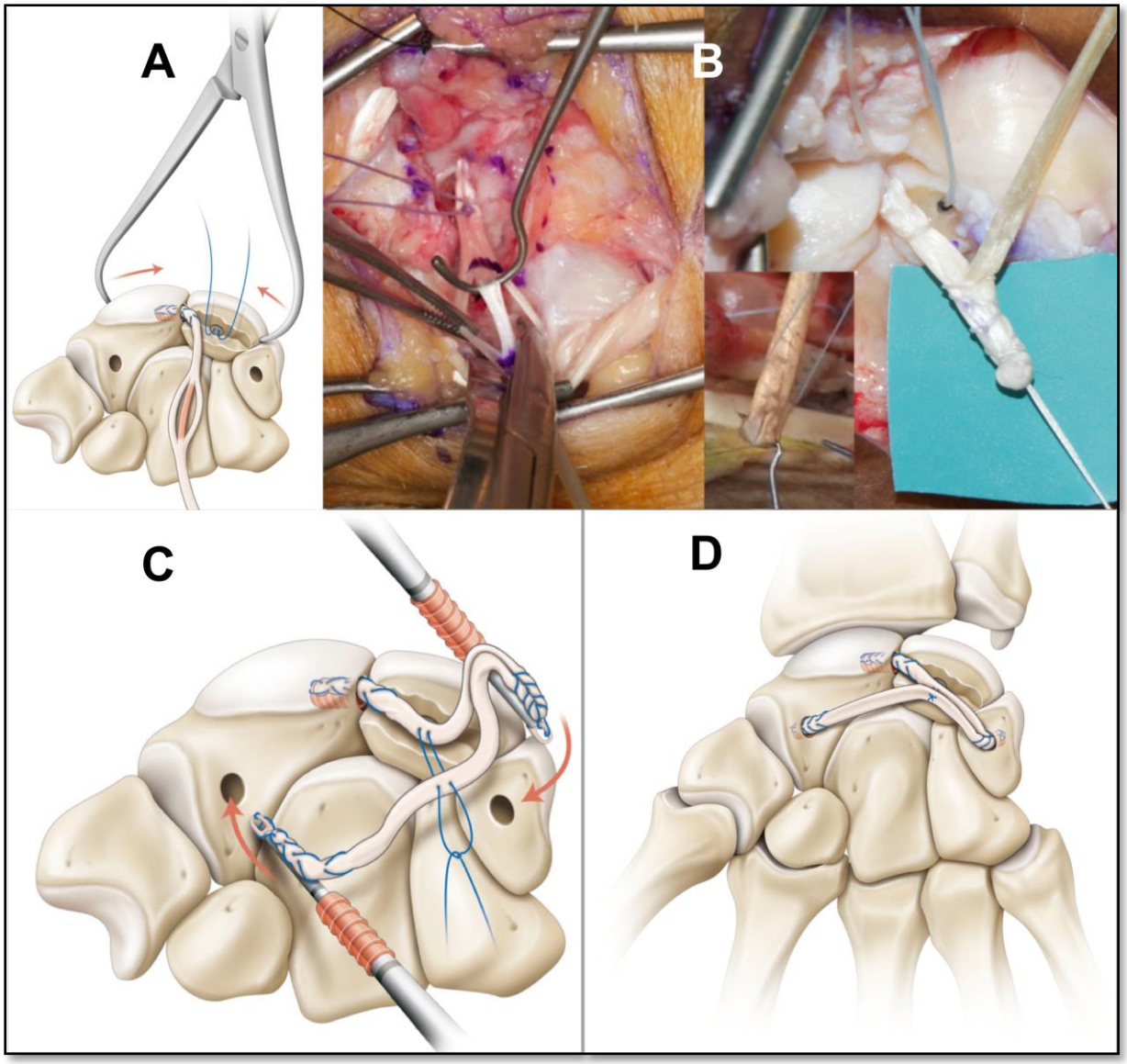

Figure 21. *Schémas et photographies illustrant les différentes étapes de la ligamentoplastie « SLIC » (A, B et C) et son résultat (D) (Athlani et al., 2018-2).*

- *Évaluation radiologique cadavérique*

Full Length Article

Journal of Hand Surgery
(European Volume)
2018, Vol. 43(4) 387–393

DOI: 10.1177/1753193417746055
journals.sagepub.com/home/jhs
SAGE

Radiological evaluation of scapholunate intercarpal ligamentoplasty for chronic scapholunate dissociation in cadavers

Lionel Athlani, Nicolas Pauchard and Gilles Dautel

Abstract
We performed a cadaveric study to evaluate radiological performance of a technique for scapholunate intercarpal ligamentoplasty designed for treating reducible scapholunate dissociation. We created scapholunate instability in 12 fresh adult cadaveric forearms by sectioning the dorsal scapholunate interosseous ligament and the dorsal intercarpal ligament. All wrists showed scapholunate diastasis, dorsal intercalated segmental instability and posterior scaphoid subluxation. We performed scapholunate intercarpal ligamentoplasty in six wrists and Garcia-Elias three-ligament tenodesis in another six. Wrists were examined radiographically both after ligament sectioning and after ligamentoplasty to compare static and dynamic scapholunate gaps and scapholunate and capitolunate angles. Improvement was statistically significant in all measurements, reflecting a return to normal values. Posterior scaphoid subluxation was also corrected. There was no significant difference between the two treatment groups. Our findings suggest that ligamentoplasty can restore scapholunate joint stability and normal carpal anatomy.

Keywords
Wrist instability, scapholunate dissociation, scapholunate ligament, ligamentoplasty

Date received: 27th July 2017; revised: 9th November 2017; accepted: 10th November 2017

Introduction

The Garcia-Elias three-ligament tenodesis (3LT) (Garcia-Elias et al., 2006) is currently widely used to treat chronic reducible scapholunate (SL) dissociation where there is no repairable residual ligament and in the absence of osteoarthritis (Crawford et al., 2016). Its objective is to reduce flexion deformity of the scaphoid, SL gap and dorsal intercalated segmental instability (DISI) deformity using a slip of the flexor carpi radialis (FCR) tendon. Recent studies (Chabas et al., 2008; De Smet and Van Hoonacker, 2007; Elgammal and Lukas, 2016; Ellanti et al., 2014; Links et al., 2008; Moran et al., 2006; Nienstedt, 2013) have shown medium-term recurrence of radiological anomalies (SL gap and DISI deformity) as a result of ligamentous loosening. Moreover, the 3LT, like the other FCR ligamentoplasties (Almquist et al., 1991; Bain et al., 2013; Brunelli and Brunelli, 1995; Linscheid and Dobyns, 1992; Ross et al., 2013; Van Den Abbeele et al., 1998), may result in iatrogenic complications from the transosseous scaphoid tunnel (Pauchard et al., 2013). Recent biomechanical studies have underlined the important stabilizing role of the dorsal intercarpal ligament (DICL), which, when sectioned, seems to cause the evolution from dynamic to static instability (Mitsuyasu et al., 2004).

Scapholunate intercarpal ligamentoplasty is a new technique in the therapeutic arsenal to treat stage 3 (dynamic) and 4 (reducible static) SL instabilities, according to the Garcia-Elias classification (Garcia-Elias et al., 2006). It takes into account recent biomechanical concepts while addressing imperfections in FCR ligamentoplasties, including the 3LT. We report the radiographic evaluation of the new SL ligamentoplasty in a cadaveric study.

Department of Hand Surgery, Plastic and Reconstructive Surgery, Centre Chirurgical Emile Gallé CHU de Nancy, Nancy, France

Corresponding Author:
Lionel Athlani, Department of Hand Surgery, Plastic and Reconstructive Surgery, Centre Chirurgical Emile Gallé CHU de Nancy, 49 rue Hermite, 54000 Nancy, France.
Email: lionel.athlani@gmail.com

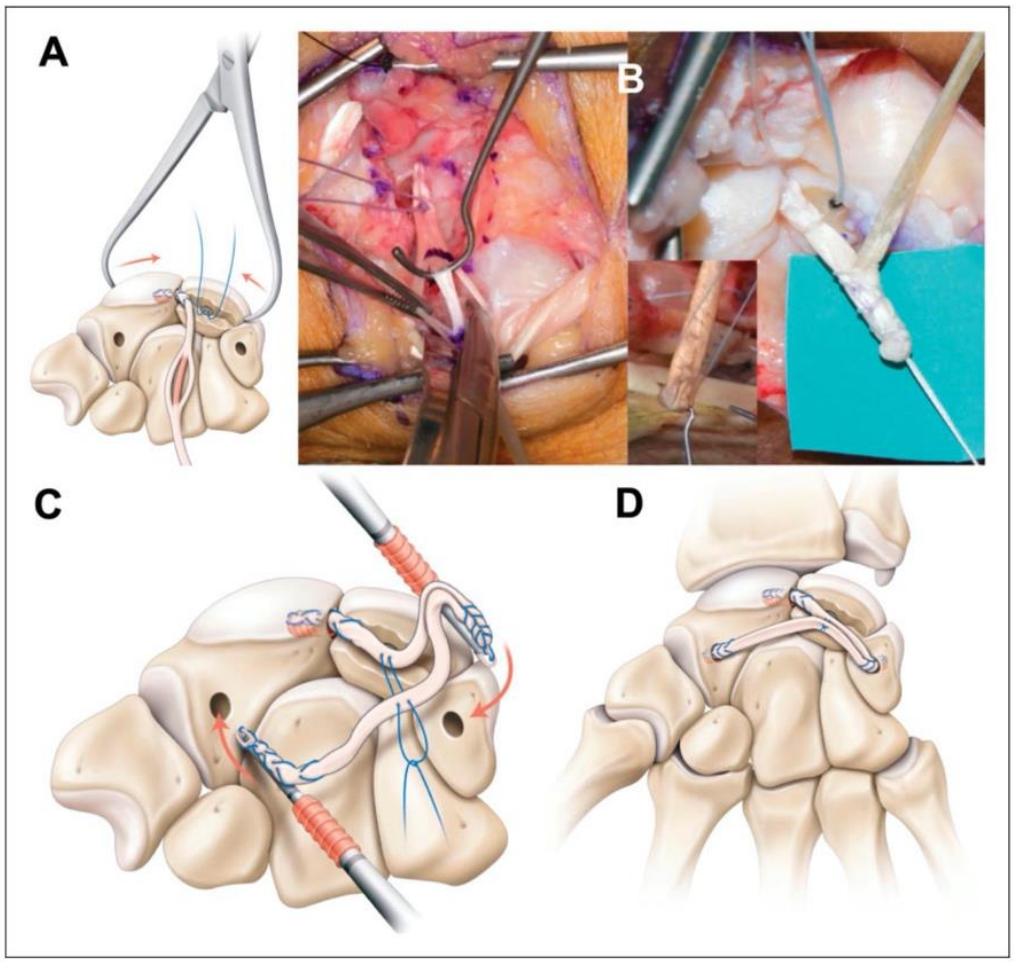

Figure 1. Diagram and photographs showing the scapholunate intercarpal ligamentoplasty. (a) Intraosseous tunnels and the lunate trench tunnels. Manual manoeuvres and pointed reduction forceps used to reduce the SL dissociation. (b) Performing the triquetral extremity of the graft. (c) Anchoring the two segments (scapho–lunate–triquetral and triquetral–lunate–scaphoid). (d) Completion of the entire procedure.

Methods

Scapholunate intercarpal ligamentoplasty

This technique (Figure 1(d)) was developed by two of the authors (NP and GD). It uses a free palmaris longus (PL) graft to reconstruct the dorsal segment of the scapholunate interosseous ligament (SLIL) and the DICL. It creates two segments: a scapho–lunate–triquetral (SLT) segment that corrects the SL gap and a triquetro–lunate–scaphoid (TLS) segment that corrects DISI deformity and scaphoid rotary subluxation. The use of a free PL graft thus respects the FCR, considered to be a secondary stabilizer of the SL complex (Short et al., 2007), and allows for tendinous pretensioning to prevent ligamentous loosening. The approach is dorsal in order to avoid scaphotrapezio-trapezoid (STT) joint segmental collapse. The 'blind' nature of the bone tunnels also prevents the complications associated with a trans-scaphoid tunnel. Moreover, in this technique, both the scaphoid and triquetral bony anchors are resistant, having been solidly wedged into the tunnel with interference (MiniBioPushlock™ 2.5 mm absorbable Arthrex®), leaving no weakness of capsular fixation points.

Surgical technique

Two senior surgeons (LA and NP, Level IV, specialist – highly experienced; Tang and Giddins, 2016) made a dorsal incision along the axis of the third metacarpal, centred on the midline of the radiocarpal joint. The extensor retinaculum was opened between the third and fourth compartments, and a dorsal capsulotomy performed according to Berger et al. (1995), thus preserving the dorsal radiocarpal ligaments and the DICL. We then harvested a 10 cm free PL graft through a short incision on the palmar side of the wrist. The graft was then pretensioned with 3 kg for

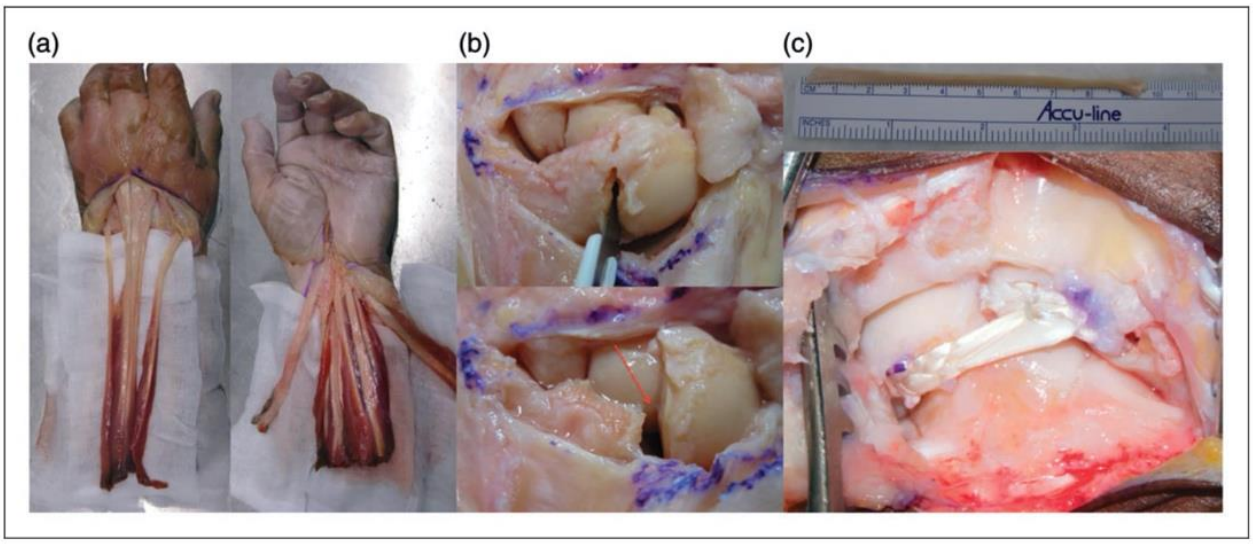

Figure 2. Study protocol: (a) dissection of the wrist creating six tendinous units; (b) sectioning the SLIL and the DICL to obtain SL dissociation; (c) scapholunate intercarpal ligamentoplasty to reduce SL dissociation.

2 min on a dedicated workstation. A first blind tunnel, 10 mm deep and 2.5 mm wide, was drilled at the site of the former scaphoid insertion of the dorsal segment of the SLIL (proximal pole of the scaphoid). The posterior surface of the lunate was then drilled to create a shallow trench to serve as the interface for graft adhesion. A second blind tunnel of the same depth and width was drilled in the dorsal aspect of the triquetrum near the radial side of the dorsal radiocarpal ligaments, following the axis of the lunate trench. One of the two ends of the graft was then whip stitched over a length of 10 mm with a non-absorbable Arthrex® Fiberloop™ 4-0, wedged into the first proximal scaphoid tunnel, and secured in interference by means of an impacted 2.5 absorbable Arthrex® miniBioPushlock™. A 2.2 mm non-absorbable titanium Arthrex® MicroCorkscrew™ anchor was introduced into the lunate trench (Figure 1(a)). The SL dissociation was then reduced by manual manoeuvres (palmarly directed pressure on the capitate and ulnar deviation) and pointed reduction forceps (SL gap). Stabilization was achieved by SL and scaphocapital pinning (1.2 mm K-wires). Fixing the graft in the second triquetral tunnel meant both tapering it and performing a longitudinal plication. The central half was resected over a distance of 12 to 16 mm starting from the entry point in the second tunnel. The two half strips thus obtained were folded back on themselves to create a new intermediary graft end as thick as the other two ends over a length of 6 to 8 mm. This new end was then whip stitched over 10 mm before being inserted and attached to the second blind tunnel by impacting a Pushlock (Figure 1(b)). The graft located between the first two intraosseous fixation points was placed in the lunate trench, and then fixed by the anchor sutures to create the first segment. A third blind tunnel of the same depth and width was drilled at the level of the scaphoid isthmus near the STT joint surface. To create the second segment, the remainder of the graft was again passed through the lunate trench and fixed by the same anchor sutures, to allow for superposition of the two segments in the tunnel. The remaining free end was resected beyond a distance of 8 mm from the entry point in the third blind tunnel and then inserted into the tunnel. To do so, this last end was whip stitched over 10 mm and fixed to the bottom of the third tunnel by impacting a Pushlock (Figure 1(c)). At this point we could test the tension of both segments with a tendon hook. Capsular and retinacular stitching was performed using PDS™ slow-absorbing sutures (Ethicon®).

Study protocol

We carried out a cadaveric study using 12 fresh adult forearms and hands, provided by the anatomy laboratory of the medical faculty (Figure 2). The sample included six right upper extremities and six left. The limbs were disarticulated at the elbow and prepared in a manner similar to that described by Pollock et al. (2010). None showed any pre-existing lesion of the SL ligament or SL instability.

All wrists were prepared according to the same protocol, consisting of longitudinal incisions along the entire palmar and dorsal aspects of the forearm and wrist, to locate tendons and separate them into

three palmar and three dorsal units. The first unit on the palmar side comprised the FCR; the second, the flexor carpi ulnaris; and the third, the finger flexors. On the dorsal side, the first unit corresponded to the two extensor carpi radialis; the second, to the extensor carpi ulnaris; and the third, to the finger extensors. We used a Fiberwire™ 2-0 (Arthrex®) suture to whip stitch each of the units. A static SL instability was then created, following a Berger (Berger et al., 1995) dorsal capsulotomy by sectioning the three segments of the SLIL and the DICL with a scalpel blade.

The forearm was then vertically positioned on a specially designed workstation, as described by Hsu et al. (2014). Metal S-hooks were placed at the end of each whip stitching to bear weights, making it possible to simulate different wrist positions, as described by Slater et al. (1999). A clenched fist was thus simulated with 10 kg pulling on the finger flexors, the wrist extended to a 20° angle with 5 kg distributed between the extensor carpi radialis and extensor carpi ulnaris units.

Before and after sectioning the SLIL and the DICL, standard radiographic views, standard neutral posterior–anterior and lateral views and a clenched fist posterior–anterior view, of all wrists were taken using a digital image intensifier (Siemens AG, ARCADIS® Avantis, Munich, Germany). We then performed a ligament reconstruction on each wrist: scapholunate intercarpal ligamentoplasty in six cases where PL was present and 3LT, as described by Garcia-Elias et al. (2006), in the six remaining cases. Radiographic evaluation was then repeated under the same conditions as described after removing K-wires and having cycled the wrists 100 times through flexion–extension, simulating repetitive loading of the wrist and postoperative ligamentous loosening.

Radiographic evaluation

The digital radiographs were viewed on OsiriX© (Pixmeo® 2016, Geneva, Switzerland). We systematically calculated static and dynamic SL gaps in millimetres and scapholunate angle (SLA) and capitolunate angle (CLA) in degrees (accuracy is 0.1 mm for gaps and 1° for angles). Values greater than 3 mm were considered pathological, as was an SLA greater than 70° and a CLA more than 15° (Larsen et al., 1991, 1995). The existence of a posterior scaphoid subluxation was also verified in the lateral view. Characterized by loss of alignment of the proximal pole of the scaphoid with the radial scaphoid fossa and the posterior horn of the lunate, this misalignment is responsible for dorsal scaphoid displacement resulting in contact with the posterior edge of the radius (Figure 3).

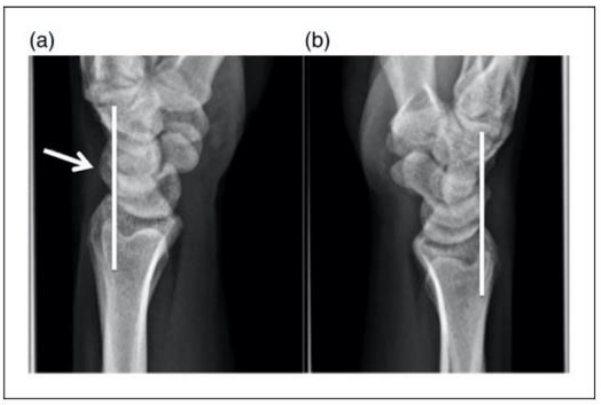

Figure 3. Radiographic evaluation of the posterior scaphoid subluxation: dorsal displacement of the proximal pole of the scaphoid with respect to its radial fossa and the posterior horn of the lunate is seen in static SL instability (a) in the lateral view. This displacement does not appear in the absence of instability (b).

Statistical analysis

Data were compared using the paired Student *t*-test at a significance level of $p < 0.05$.

Results

Before sectioning the SLIL and DICL ligaments, mean static SL gap was 2.0 mm, mean dynamic SL gap was 2.5 mm, mean SLA was 58° and mean CLA was 4°. After sectioning the SLIL and DICL ligaments, the SL complex was unstable with a static SL dissociation, characterized by SL diastasis, DISI deformity and posterior scaphoid subluxation. Radiographic values were pathological in both SL intercarpal ligamentoplasty and 3LT groups, with mean static SL gaps of 3.8 mm and 4.1 mm, dynamic SL gaps of 5.2 mm and 5.6 mm, SLA of 82° and 82°, and CLA of 16° and 17°, respectively. After the respective SL intercarpal ligamentoplasty or 3LT ligamentoplasty, these values returned to normal in both groups, thereby confirming correction of SL dissociation. We noted a significant ($p < 0.05$) improvement of the mean static and dynamic SL gap (respectively, 2.0, 2.1 mm and 2.4, 2.5 mm), as well as SLA (59°, 61°) and CLA (4°, 5°). In all 12 cases, posterior scaphoid subluxation was corrected after ligamentoplasty (Figures 4 and 5). There was no significant difference between the two groups, either in terms of the extent of SL dissociation after ligament sectioning or of its correction following ligamentoplasty. Similarly, mean values of radiographic data from each group did not differ significantly, both before and after SL intercarpal ligamentoplasty or 3LT ligamentoplasty (Table 1).

Figure 4. Example of radiographic SL dissociation after sectioning the ligaments.

Figure 5. Example of radiographs showing reduction of SL dissociation following SL intercarpal ligamentoplasty.

Table 1. Comparative radiographic results (mean and range) for both groups of ligamentoplasties.

	Pre-ligamentoplasty[a]			Post-ligamentoplasty[b]		
Averages	SLIC ($n=6$)	3LT ($n=6$)	p	SLIC ($n=6$)	3LT ($n=6$)	p
Static scapholunate gap	3.8 mm (3.3–5.2)	4.1 mm (3.4–5.2)	0.48	2.0 mm (1.4–2.8)	2.1 mm (1.6–2.9)	0.36
Dynamic scapholunate gap	5.2 mm (4.8–6.1)	5.6 mm (4.7–6.3)	0.53	2.4 mm (1.9–2.9)	2.5 mm (2.0–2.8)	0.49
SL angle	82° (76–90)	82° (77–90)	0.88	59° (54–65)	61° (55–66)	0.20
Capitolunate angle	16° (15–18)	17° (15–18)	0.78	4° (3–5)	5° (4–5)	0.64
Posterior subluxation scaphoid	6	6	—	0	0	—

[a]Pre-ligamentoplasty: after SLIL and DICL sectioning.
[b]Post-ligamentoplasty: after SL intercarpal ligamentoplasty or 3LT ligamentoplasty and flexion–extension cycling.
3LT: three-ligament tenodesis; DICL: dorsal intercarpal ligament; SL: scapholunate; SLIC: scapholunate intercarpal ligamentoplasty; SLIL: scapholunate interosseous ligament.

Discussion

According to this anatomical study, the scapholunate intercarpal ligamentoplasty seems to be able to correct the radiologic features of SL dissociation as well as the Garcia-Elias 3LT reconstruction. Several tenodesis techniques exist to treat chronic, reducible SL dissociation in the absence of osteoarthritis (Almquist et al., 1991; Bain et al., 2013; Brunelli and Brunelli, 1995; Corella et al., 2013; De Carli et al., 2011; Garcia-Elias et al., 2006; Linscheid and Dobyns, 1992; Ross et al., 2013; Van Den Abbeele et al., 1998). Their objective is to correct the radiological anomalies and the functional instability, thereby preventing long-term risk of SL advanced

collapse (Watson and Ballet, 1984). Among these options, the Brunelli technique modified by Van Den Abbeele et al. (1998) and the Garcia-Elias 3LT (Garcia-Elias et al., 2006) use a distally pedicled slip of FCR to reconstruct the dorsal segment of the SLIL and vertically reposition the scaphoid. These techniques are considered benchmarks, and have served as the basis for numerous clinical studies (Brunelli and Brunelli, 1995; Chabas et al., 2008; De Smet and Van Hoonacker, 2007; Elgammal and Lukas, 2016; Ellanti et al., 2014; Garcia-Elias et al., 2006; Links et al., 2008; Moran et al., 2006; Nienstedt, 2013; Talwalkar et al., 2006; Van Den Abbeele et al., 1998) (Supplementary Table S1). While the latter all share similar results in the case of dynamic instabilities, with good clinical and radiological results, they diverge on static instabilities, with widely varying results from one study to the other. Indeed, over the medium term, recurrence of radiological anomalies due to ligamentous loosening is observed, as well as weakness in capsular triquetral anchoring. The creation of a trans-scaphoid tunnel may result in iatrogenic complications, such as necrosis of the proximal pole of the scaphoid from devascularization and scaphotrapeziotrapezoid osteoarthritis from segmental collapse of the joint (Pauchard et al., 2013).

Neither Van Den Abbeele et al. (1998) nor Garcia-Elias et al. (2006) reported on biomechanical performance to confirm the effectiveness of their respective techniques for correcting SL dissociation. Hsu et al. (2014), however, in a cadaveric study, have recently compared six modified Brunelli ligamentoplasties (Van Den Abbeele et al., 1998) with six cases of the recently described Ross (Ross et al., 2013) scapholunotriquetral tenodesis that simultaneously reconstructs both the dorsal segment of the SLIL and the DICL. After sectioning the SLIL and the extrinsic palmar and dorsal ligaments, a static instability was obtained in both groups. After ligament reconstruction, the authors found significant improvement in the two radiographic parameters (SL gaps and SLA) within each group, with no significant difference between the two techniques. Our study is quite similar in its comparison of the SL intercarpal ligamentoplasty with the Garcia-Elias 3LT and our results are similar. According to the radiological criteria of our study, the effectiveness of SL intercarpal ligamentoplasty is confirmed in correcting SL dissociation. A further benefit of the technique is the systematic correction of posterior scaphoid subluxation, the main cause of radioscaphoid osteoarthritis and source of wrist pain from contact of the subluxed scaphoid with the posterior edge of the radius (Watson et al., 1993).

The lack of significant difference between the two types of reconstruction used in our study could be due to small numbers. Another limitation of our study might lie in the way we created SL dissociation, not taking into account the other ligamentous stabilizers of the SL complex – the extrinsic palmar ligaments and the ligamentous complex of the distal pole of the scaphoid (Short et al., 2007). The latter are considered as secondary, but do participate in generating this dissociative instability.

A further limitation is the fact that a cadaveric study, albeit with positive radiographic results, which may not lead to favourable clinical results, particularly in terms of reconstruction stability. Indeed, it is not possible to predict the effects of daily weight-bearing movements of the wrist and thus eventual ligamentous loosening over time. The use of a free graft, however, makes tendinous pretensioning possible, with the aim of preventing the frequently observed postoperative loosening. This fundamental limitation makes a medium- and long-term prospective clinical study, with a sufficiently large sample, indispensable in order to evaluate the clinical effectiveness of this ligamentoplasty.

We believe that the indication for the new ligament reconstruction technique is for 'easily' reducible static SL instabilities. Therefore, it is important, preoperatively and intraoperatively, to assess reducibility, particularly for instabilities dating back to more than a year after trauma.

Acknowledgements The authors wish to thank Dr Gail Taillefer, native speaker and emeritus professor of English, for language support.

Declaration of conflicting interests The authors declared the following potential conflicts of interest with respect to the research, authorship, and/or publication of this article: Gilles Dautel and Nicolas Pauchard declare a conflict of interest with Arthrex®. The other authors declared no potential conflicts of interest with respect to the research, authorship, and/or publication of this article.

Funding The authors received no financial support for the research, authorship, and/or publication of this article.

Informed consent The participants had given informed consent for use of their bodies for medical research.

Supplementary material Supplementary material is available at journals.sagepub.com/doi/suppl/10.1177/1753193417746055.

References

Almquist EE, Bach AW, Sack JT, Fuhs SE, Newman DM. Four-bone ligament reconstruction for treatment of chronic complete scapholunate separation. J Hand Surg Am. 1991, 16: 322–7.

Bain GI, Watts AC, McLean J, Lee YC, Eng K. Cable-augmented, quad ligament tenodesis scapholunate reconstruction: rationale, surgical technique, and preliminary results. Tech Hand Up Extrem Surg. 2013, 17: 13–9.

Berger RA, Bishop AT, Bettinger PC. New dorsal capsulotomy for the surgical exposure of the wrist. Ann Plast Surg. 1995, 35: 54–9.

Brunelli GA, Brunelli GR. A new technique to correct carpal instability with scaphoid rotary subluxation: a preliminary report. J Hand Surg Am. 1995, 20: 82–5.

Chabas JF, Gay A, Valenti D, Guinard D, Legre R. Results of the modified Brunelli tenodesis for treatment of scapholunate instability: a retropective study of 19 patients. J Hand Surg Am. 2008, 33: 1469–77.

Corella F, Del Cerro M, Ocampos M, Larrainzar-Garijo R. Arthroscopic ligamentoplasty of the dorsal and volar portions of the scapholunate ligament. J Hand Surg Am. 2013, 38: 2466–77.

Crawford K, Owusu-Sarpong N, Day C, Iorio M. Scapholunate ligament reconstruction: a critical analysis review. J Bone Joint Surg Am. 2016, 4: 41–8.

De Carli P, Donndorff AG, Gallucci GL, Boretto JG, Alfie VA. Chronic scapholunate dissociation: ligament reconstruction combining a new extensor carpi radialis longus tenodesis and a dorsal intercarpal ligament capsulodésis. Tech Hand Up Extrem Surg. 2011, 15: 6–11.

De Smet L, Van Hoonacker P. Treatment of chronic static scapholunate dissociation with the modifed Brunelli technique: preliminary results. Acta Orthop Belg. 2007, 73: 188–91.

Elgammal A, Lukas B. Mid-term results of ligament tenodesis in treatment of scapholunate dissociation: a retrospective study of 20 patients. J Hand Surg Eur. 2016, 41: 56–63.

Ellanti P, Sisodia G, Al-Ajami A, Ellanti P, Harrington P. The modified Brunelli procedure for scapholunate instablity: a single-centre study. Hand Surg. 2014, 19: 39–42.

Garcia-Elias M, Lluch AL, Stanley JK. Three-ligament tenodesis for the treatment of scapholunate dissociation: indications and surgical technique. J Hand Surg Am. 2006, 31: 125–34.

Hsu JW, Kollitz KM, Jegapragasan M, Huang JI. Radiographic evaluation of the modified Brunelli technique versus a scapholunotriquetral transosseous tenodesis technique for scapholunate dissociation. J Hand Surg Am. 2014, 39: 1041–9.

Larsen CF, Amadio PC, Gilula LA, Hodge JC. Analysis of carpal instability: I. Description of the scheme. J Hand Surg Am. 1995, 20: 757–64.

Larsen CF, Mathiesen FK, Lindequist S. Measurement of carpal bone angles on lateral wrist radiographs. J Hand Surg Am. 1991, 16: 888–93.

Links AC, Chin SH, Waitayawinyu T, Trumble TE. Scapholunate interosseous ligament reconstruction: results with modified Brunelli technique versus four-bone weave. J Hand Surg Am. 2008, 33: 850–6.

Linscheid RL, Dobyns JH. Treatment of scapholunate dissociation. Rotatory subluxation of the scaphoid. Hand Clin. 1992, 8: 645–52.

Mitsuyasu H, Patterson RM, Shah MA, Buford WL, Iwamoto Y, Viegas SF. The role of the dorsal intercarpal ligament in dynamic and static scapholunate instability. J Hand Surg Am. 2004, 29: 279–88.

Moran SL, Ford KS, Wulf CA, Cooney WP. Outcomes of dorsal capsulodesis and tenodesis for treatment of scapholunate instability. J Hand Surg Am. 2006, 31: 1438–46.

Nienstedt F. Treatment of static scapholunate instability with modified Brunelli tenodesis: results over 10 years. J Hand Surg Am. 2013, 38: 887–92.

Pauchard N, Dederichs A, Segret J, Barbary S, Dap F, Dautel G. The role of three-ligament tenodesis in the treatment of chronic scapholunate instability. J Hand Surg Eur. 2013, 38: 758–66.

Pollock PJ, Sieg RN, Baechler MF, Scher D, Zimmerman NB, Dubin NH. Radiographic evaluation of the modified Brunelli technique versus the Blatt capsulodesis for scapholunate dissociation in a cadaver model. J Hand Surg Am. 2010, 35: 1589–98.

Ross M, Loveridge J, Cutbush K, Couzens G. Scapholunate reconstruction. J Wrist Surg. 2013, 2: 110–5.

Short WH, Werner FW, Green JK, Sutton LG, Brutus JP. Biomechanical evaluation of ligamentous stabilizers of the scaphoid and lunate: part III. J Hand Surg Am. 2007, 32: 297–309.

Slater RR Jr, Szabo RM, Bay BK, Laubach J. Dorsal intercarpal ligament capsulodesis for scapholunate dissociation: biomechanical analysis in a cadaver model. J Hand Surg Am. 1999, 24: 232–9.

Talwalkar SC, Edwards AT, Hayton MJ, Stilwell JH, Trail IA, Stanley JK. Results of tri-ligament tenodesis: a modified Brunelli procedure in the management of scapholunate instability. J Hand Surg Br. 2006, 31: 110–7.

Tang JB, Giddins G. Why and how to report surgeons' levels of expertise. J Hand Surg Eur. 2016, 41: 365–6.

Van Den Abbeele KL, Loh YC, Stanley JK, Trail IA. Early results of a modified Brunelli procedure for scapholunate instability. J Hand Surg Br. 1998, 23: 258–61.

Watson HK, Ballet FL. The SLAC wrist: scapholunate advanced collapse pattern of degenerative arthritis. J Hand Surg Am. 1984, 9: 358–65.

Watson H, Ottoni L, Pitts EC et al. Rotary subluxation of the scaphoid: a spectrum of instability. J Hand Surg Br. 1993, 18: 62–4.

- *Évaluation clinique prospective*

Full Length Article

JHS(E)

Journal of Hand Surgery
(European Volume)
0(0) 1–8

DOI: 10.1177/1753193418772801
journals.sagepub.com/home/jhs
SAGE

Outcomes of scapholunate intercarpal ligamentoplasty for chronic scapholunate dissociation: a prospective study in 26 patients

Lionel Athlani, Nicolas Pauchard and Gilles Dautel

Abstract

We report the outcomes of scapholunate intercarpal ligamentoplasty in 26 wrists. For 15 wrists with static instability and 11 with dynamic instability, we used a free palmaris longus graft to reconstruct the dorsal part of the scapholunate interosseous ligament and the dorsal intercarpal ligament. These patients were evaluated for pain and active wrist range of motion, grip strength and radiological appearance after a mean follow-up of 36 months (range 12–54) after surgery. Pain score was improved from 4.5 to 1.4 at rest and 6.7 to 1.9 during hand use. The average wrist flexion was 57°, extension 56°. Grip strength was 89% of the contralateral side. The mean scapholunate angle decreased from 76° to 62°, and static scapholunate gap reduced from 3.2 mm to 2.3 mm and the dynamic gap from 4.6 mm to 3.0 mm. Scaphoid subluxation was corrected. We conclude that this procedure led to satisfactory clinical and radiological results in a short- to mid-term follow-up.

Level of evidence: II

Keywords

Wrist instability, scapholunate dissociation, scapholunate ligament, ligaments

Date received: 6th January 2018; revised: 17th March 2018; accepted: 28th March 2018

Introduction

Athlani et al. (2017) described a scapholunate intercarpal ligamentoplasty for treating symptomatic chronic reducible scapholunate dissociation in the absence of chondral lesions. It uses a free palmaris longus graft to reconstruct the dorsal segment of the scapholunate interosseous ligament (SLIL) and the dorsal intercarpal ligament (DICL). This procedure aims to reduce the scaphoid flexion deformity, the scapholunate gap and the dorsal intercalated segmental instability (DISI) deformity. This procedure does not violate the flexor carpi radialis (FCR), a stabilizer for the scapholunate complex (Short et al., 2007). The 'blind' nature of the bone tunnels also prevents the complications associated with the trans-scaphoid tunnel used in FCR tenodesis procedures. Moreover, recent biomechanical studies have underlined the important stabilizing role of the DICL, which, when transected, seems to trigger the deterioration from dynamic to static instability (Mitsuyasu et al., 2004). This finding corroborates our procedure of reconstructing the DICL.

To assess effectiveness and the functional outcomes of this procedure, we conducted a prospective study in 26 wrists (26 patients). We report the results of this study with follow-up of 12–54 months.

Methods

Patients

Between March 2013 and September 2016, a prospective study was carried out with 26 continuous

Department of Hand Surgery, Plastic and Reconstructive Surgery, Centre Chirurgical Emile Gallé, Nancy, France

Corresponding Author:
Lionel Athlani Department of Hand Surgery, Plastic and Reconstructive Surgery, Centre Chirurgical Emile Gallé, CHU de Nancy, 49 rue Hermite, 54000 Nancy, France.
Email: lionel.athlani@gmail.com

patients (20 men, six women) with a mean age of 40 years (range 22–57).

The 14 right wrists and 12 left wrists were involved. The injury was on the dominant side for 17 patients. Fifteen patients performed manual labour. The injury mechanism was wrist hyperextension and torsion in every patient. The mean time between the injury event and surgery was 12 months (range 3.5–72).

Radiological and arthroscopic findings

These patients were referred to us because of chronic wrist pain for more than 3 months. During the consultation, each patient underwent a full imaging assessment consisting of standard radiographs with anterioposterior and lateral views, dynamic clenched fist views, anterioposterior view of both wrists in radial deviation and ulnar deviation. Computerized tomography arthrography of the painful wrist was also done. All patients were diagnosed with chronic scapholunate instability (Larsen et al., 1995), either dynamic or static reducible (Watson et al., 1997) with no chondral damage (Figure 1). Dynamic instability was present in 11 wrists and static instability in 15 wrists.

Arthroscopy of the injured wrist was first performed in all cases to confirm the scapholunate instability, quantify its magnitude (Dréant and Dautel, 2003), and confirm that no repairable ligament remnant was present. that the scaphoid was easily reducible and that no chondritis was present.

Radiographs of the asymptomatic contralateral wrist were used to verify that no congenital scapholunate ligament laxity was present that could lead to scapholunate pseudo-dissociation (Lindau, 2016). If the radiographic and arthroscopic data confirmed the indication for scapholunate ligament reconstruction, the scapholunate intercarpal ligamentoplasty was proposed.

Surgical techniques

The surgical procedures (Figure 2) were performed by two senior surgeons (NP and GD, Level 4, specialist – highly experienced) according to Tang (2009) and Tang and Giddins (2016). The two senior surgeons made a dorsal incision along the axis of the third metacarpal, centred on the midline of the radiocarpal joint. The extensor retinaculum was opened between the third and fourth compartments, and a dorsal capsulotomy performed according to Berger et al. (1995).

We then harvested a 10 cm free palmaris longus graft through a short incision. The graft was then pretensioned with 3 kg for 2 min on a dedicated workstation. A first blind tunnel, 10 mm deep and 2.5 mm wide, was drilled at the site of the former scaphoid insertion of the dorsal segment of the SLIL (proximal pole of the scaphoid). The posterior surface of the lunate was then drilled to create a shallow trench to serve as the interface for graft adhesion. A second blind tunnel of the same depth and width was drilled in the dorsal aspect of the triquetrum near the radial side of the dorsal radiocarpal ligaments, following the axis of the lunate trench. One of the ends of the graft was then whip stitched over a length of 10 mm with a non-absorbable 4-0 Fiberloop™ (Arthrex®, Naples, FL, USA), wedged into the first proximal scaphoid tunnel and secured in interference by means of an impacted 2.5 absorbable miniBioPushlock™ (Arthrex®, Naples, FL, USA). A 2.2 mm non-absorbable titanium MicroCorkscrew™ anchor (Arthrex®, Naples, FL, USA) was introduced into the lunate trench.

The dissociation was then reduced by manual manoeuvres and pointed reduction forceps (Athlani et al., 2017). Stabilization was achieved by scapholunate and scaphocapitate pinning (1.2 mm K-wires). Fixing the graft in the triquetral tunnel meant both

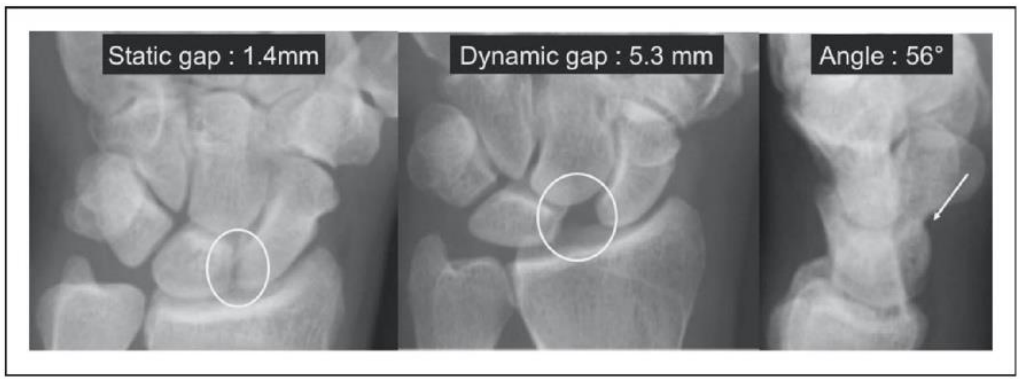

Figure 1. Example of dynamic scapholunate instability detected radiographically.

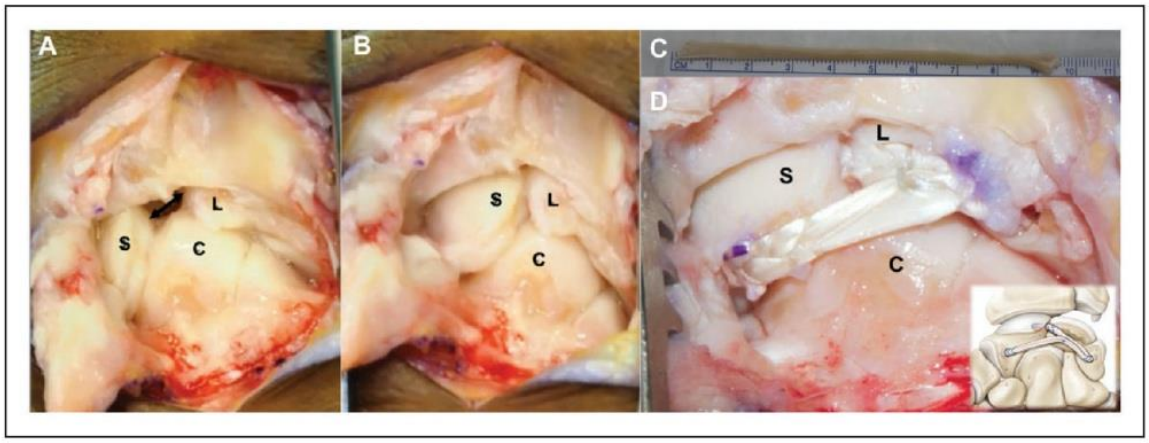

Figure 2. Photographs showing a case of scapholunate dissociation treated with scapholunate intercarpal ligamentoplasty. (a) Static scapholunate instability with scapholunate diastasis (arrow), flexion deformity of the scaphoid (S) and DISI deformity of the lunate (L). (b) Scapholunate dissociation reduced through manipulations: direct pressure on the dorsal side of the capitate (C) and ulnar deviation. (c) Free palmaris longus graft. (d) The dorsal segment of the SLIL and the DICL were reconstructed.

tapering the graft and performing a longitudinal plication. The central half was resected over a distance of 12 mm, starting from the entry point in the second tunnel. The two half strips thus obtained were folded back on themselves to create a new intermediary graft end as thick as the other two ends over a length of 6 mm. This new end was then whip stitched over 10 mm before being inserted and attached to the second blind tunnel by impacting a Pushlock. The graft located between the first two intraosseous fixation points was placed in the lunate trench, and then fixed by the anchor sutures to create the first segment. A third blind tunnel of the same depth and width was drilled at the level of the scaphoid isthmus near the scaphotrapezotrapezoidal joint surface.

To create the second segment, the remainder of the graft was again passed through the lunate trench and fixed by the same anchor sutures to allow for superposition of the two segments in the tunnel. The remaining free end was resected beyond a distance of 8 mm from the entry point in the third blind tunnel and then inserted into the tunnel. To do so, this last end was whip stitched over 10 mm and fixed to the bottom of the third tunnel by impacting a Pushlock. At this point we could test the tension of both segments with a tendon hook. Capsular and retinacular stitching was performed (Figure 2(d)).

Postoperative protocol

Following surgery, the wrist was immobilized in a volar plaster cast for 48 to 72 hours. Immobilization was extended for 2 months with a short-arm fibreglass cast. K-wires were removed 2 months postoperatively, at which point the patients began a month of self-directed rehabilitation. Radiographic were taken at 3 months after surgery, after which physiotherapy sessions were initiated. No heavy loads on the wrist were allowed for the first 6 months. A mean of 30 physiotherapy sessions (range 20–80) were done.

Clinical evaluation

All patients were reviewed in person with a minimum follow-up of 12–54 months. After having collected each patient's consent, an independent examiner performed clinical and radiographic evaluations. Subjective and objective data were collected.

Pain was evaluated using a visual analogue scale (VAS) (out of 10) at rest and during effort. Grip strength in the operated and contralateral side was collected using a Jamar® hydraulic hand dynamometer (Performance Health®, Charleville-Mézières, France). The active joint range of motion (ROM) was measured in degrees during wrist flexion, extension, radial deviation and ulnar deviation. The number of physiotherapy sessions done and the time away from work were also recorded. The functional outcomes were evaluated using standardized questionnaires: Quick Disabilities of the Arm, Shoulder and Hand (QuickDASH) (out of 100) (Hudak et al., 1996), patient-rated wrist evaluation (PRWE) (out of 100) (MacDermid et al., 1998) and Mayo Wrist Score (out of 100) (Amadio et al., 1989).

Radiographic evaluation

At the follow-up visits, standard radiographic neutral posterior-anterior and lateral views and a clenched fist posterior-anterior view were taken in all patients. Immediately post-surgery, only standard radiographic views were taken.

The radiographs were viewed on OsiriX© (Pixmeo® 2016, Geneva, Switzerland). The static and dynamic scapholunate gaps in millimetres along with the scapholunate angle (SLA) and capitolunate angle (CLA) in degrees were measured (0.1 mm accuracy for gaps and 1° for angles). Values greater than 3 mm were considered pathological, as was a SLA greater than 70° and a CLA greater than 15° (Larsen et al., 1991). The presence of posterior scaphoid subluxation was also verified in the lateral view, as described by Athlani et al. (2017). At the time of the in-person review, the patients were assessed for any signs of necrosis of the proximal pole of the scaphoid or posterior horn of the lunate along with the development of scapholunate advanced collapse (SLAC).

Statistical analysis

Wilcoxon signed rank test was used to compare preoperative and postoperative measurements for patients. A significance level was set at $p < 0.05$.

Results

Computerized tomography and arthroscopic findings before the ligamentplasty

In every patient, the computerized tomography arthrography showed a tear of the SLIL with contrast leakage. During the arthroscopic evaluation, we found six wrists had stage 2 instability (scapholunate diastasis with the use of a twisting motion applied to the hook), and 20 wrists had stage 3 instability (2.7 mm arthroscope passes between the scaphoid and lunate from the midcarpal to the radiocarpal space). There were no instances of chondral damage. Central triangular fibrocartilage complex perforations that required shaving were found in three patients (Table 1).

Wrist pain and functional outcomes

At the last follow-up, 23 patients had returned to the original job. Three patients returned to another job.

We found a notable improvement in pain levels at rest with 23 patients having no or only slight pain (VAS of 0 to 3) at rest. Grip strength improved relative to the contralateral side: 59% preoperatively versus 89% at follow-up. There was almost no change in wrist ROM (Table 1).

Table 1. Comparison of clinical and radiographic results (mean and range) for the study population (26 patients) between the preoperative period and last follow-up.

Parameters	Preoperative	Last follow-up	*P* values
Pain at rest (VAS) (/10)	4.5 (2–8)	0.4 (0–3)	<0.001
Pain during effort (VAS) (/10)	6.7 (4–9)	1.9 (0–5)	<0.001
Grip strength (Kg.F)	26 (12–42) 44 contralateral	40 (18–60) 45 contralateral	<0.001
Flexion (°)	59 (40–80)	57 (30–85)	0.663
Extension (°)	56 (35–80)	56 (30–85)	0.885
Ulnar deviation (°)	32 (20–50)	32 (20–45)	0.876
Radial deviation (°)	16 (10–25)	16 (10–25)	0.731
DASH (/100)	57.5 (36.6–79.5)	17.5 (0–59.1)	<0.001
PRWE (/100)	52.6 (21.3–68.7)	13.6 (0–54.5)	0.0004
Mayo Wrist Score (/100)	54 (20–80)	84.8 (65–100)	0.0005
Static scapholunate gap (mm)	3.2 (1.4–5.9)	2.3 (1.3–4.5)	<0.001
Dynamic scapholunate gap (mm)	4.6 (3.1–7.7)	3.0 (1.6–5.3)	<0.001
Scapholunate angle (°)	73 (46–95)	62 (45–88)	<0.001
Capitolunate angle (°)	12.5 (3–20)	5 (1–17)	<0.001
Posterior subluxation scaphoid	22	4	–
SLAC arthritis	0	0	–

VAS: visual analogue scale; DASH: Disabilities of the Arm, Shoulder and Hand; PRWE: patient-rated wrist evaluation; SLAC: scapholunate advanced collapse.

The QuickDASH, PRWE and Mayo Wrist Score were significantly better, with an improvement of 40 points, 39 points and 30 points, respectively ($p < 0.01$, all comparisons) (Table 1).

Radiographic evaluation

We noted improvements of the mean static and dynamic scapholunate gap as well as the SLA and CLA. The static and dynamic scapholunate diastasis and the DISI deformity was corrected. In 22 wrists, the posterior scaphoid subluxation was corrected (Table 1) (Figure 3).

In the subset of 15 wrists with static instability, there was a significant improvement of the static and dynamic scapholunate gap along with the SLA and CLA. Between the immediate postoperative period and the last follow-up, there was a significant increase of 0.5 mm in the static scapholunate gap and 7° SLA. This significant increase in these two radiographic parameters occurred in the subset of 15 wrists with static instability, but not in those 11 wrists with dynamic instability (Table 2).

Complications

There were no intraoperative complications or postoperative infections. In the first postoperative year, three patients had De Quervain's tenosynovitis that resolved with brace and corticosteroid injection treatment. There were no radiographic signs of bone lysis at the proximal pole of the scaphoid and/or the posterior horn of the lunate. In two patients, asymptomatic radiolucent lines appeared around the

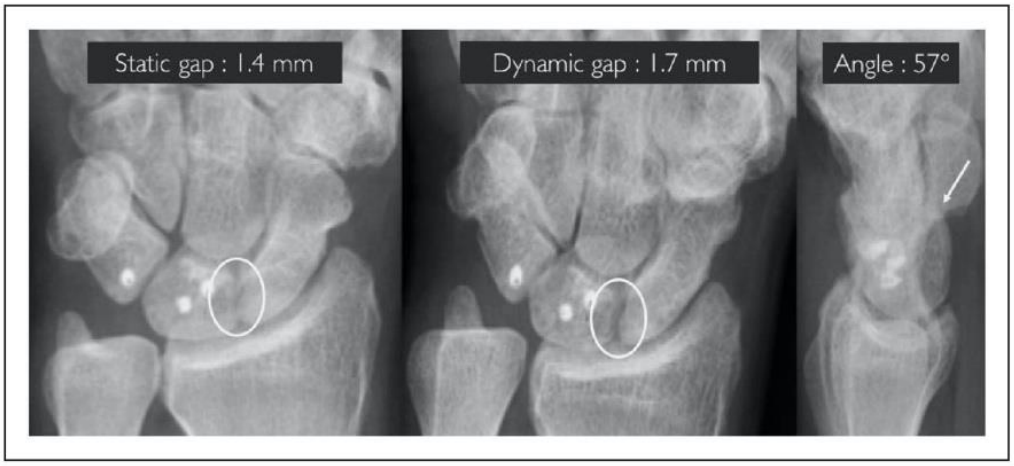

Figure 3. Radiographs showing the reduction of scapholunate dissociation 54 months after scapholunate intercarpal ligamentoplasty.

Table 2. Comparison of the radiographic parameters for the study population (26 patients) between the immediate postoperative period and last follow-up.

	Mean values		
Radiographic parameters	Immediate postoperative	Last follow-up	*P* values
All 26 wrists			
Static scapholunate gap (mm)	1.8	2.3	<0.001
SLA (°)	55	62	<0.001
Dynamic instability (11 wrists)			
Static scapholunate gap (mm)	1.5	1.7	0.569
SLA (°)	53	56	0.582
Static instability (15 wrists)			
Static scapholunate gap (mm)	2.0	2.7	<0.001
SLA (°)	56	65	<0.001

SLA: scapholunate angle.

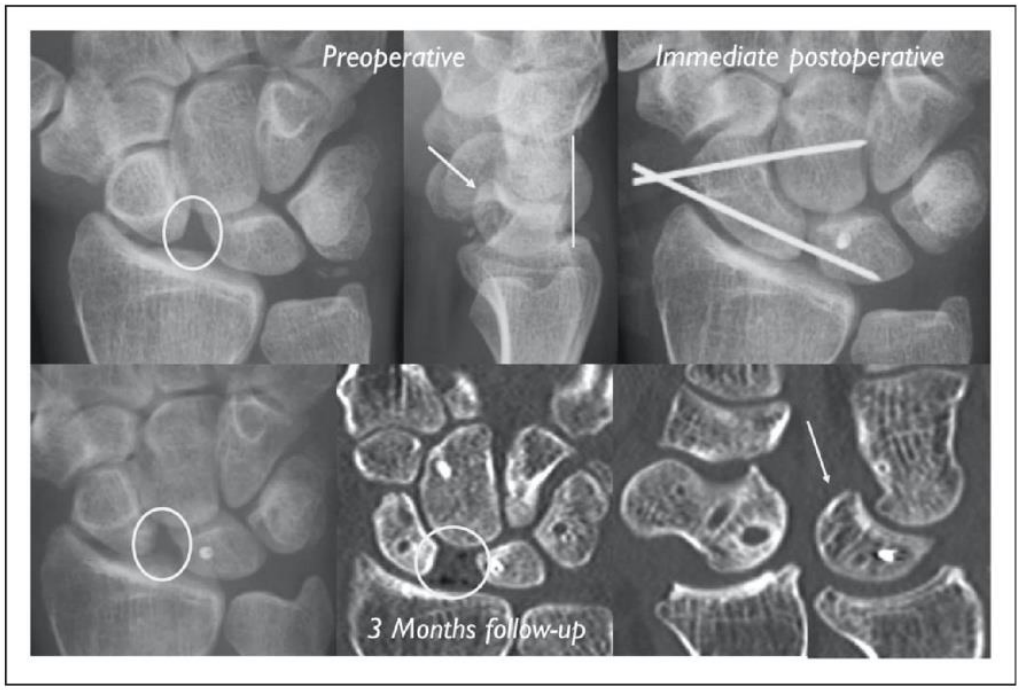

Figure 4. An early recurrence of static scapholunate instability detected on radiographs.

scaphoid and triquetral implants (MiniBioPushlock™ 2.5 mm absorbable, Arthrex®).

In four patients, scapholunate dissociation redeveloped quickly (within 3 to 6 months) with reappearance of the scapholunate diastasis, DISI deformity and posterior scaphoid subluxation. These four patients all had static instability preoperatively that was noted to be difficult to reduce intraoperatively. None of these patients underwent a surgical revision because they had an improvement in pain (Figure 4). At the final follow-up, no patients had signs of osteoarthritis due to SLAC.

Discussion

We found that the scapholunate intercarpal ligamentoplasty reduced pain and increased grip strength in our 26 patients. This procedure corrected the radiologic features of scapholunate dissociation in our short- to mid-term follow-up. The posterior scaphoid subluxation was corrected in 22 of the 26 patients. We believe this is important because subluxation is considered the primary cause of radioscaphoid osteoarthritis and the source of wrist pain due to contact of the scaphoid with the posterior margin of the radius (Athlani et al., 2017).

Several tenodesis techniques exist to treat chronic, reducible scapholunate dissociation in the absence of osteoarthritis (Almquist et al., 1991; Bain et al., 2013; Brunelli and Brunelli, 1995; De Carli et al., 2011; Garcia-Elias et al., 2006; Linscheid and Dobyns, 1992; Ross et al., 2013; Van Den Abbeele et al., 1998). The objective is to correct the radiological anomalies and the functional instability and to prevent SLAC. The Brunelli technique modified by Van Den Abbeele et al. (1998) and the three-ligament tenodesis of Garcia-Elias et al. (2006) use a distally pedicled slip of FCR to reconstruct the dorsal segment of the SLIL and reposition the scaphoid. Each of these reports, generally considered benchmarks, had 22 patients on average (Brunelli and Brunelli, 1995; Chabas et al., 2008; De Smet and Van Hoonacker, 2007; Elgammal and Lukas, 2016; Ellanti et al., 2014; Garcia-Elias et al., 2006; Links et al., 2008; Moran et al., 2006; Nienstedt, 2013; Talwalkar et al., 2006; Van Den Abbeele et al., 1998). The numbers in these reports are comparable with those in our present report (26 wrists). The types of scapholunate instability (static and dynamic) are similar to ours (Appendix S1, available online).

Our patients had reduced pain and improved grip strength, which were the primary reasons for the consultation. Twenty-three out of 26 patients had no or only slight pain (VAS 0–3). The mean grip strength was 89% of the contralateral side. These findings are consistent with those of other studies in which the percentage of patients without pain or only slight pain ranged from 62% for Talwalkar et al. (2006) to 90% for De Smet and Van Hoonacker (2007), and the grip strength ranged from 58% for Van Den Abbele et al. (1998) to 98% for Links et al. (2008). Our patients had no significant differences in the wrist

ROM before and after the surgery. However, there seems to be some joint stiffening, comparable with that reported after FCR tenodesis procedures, except for wrist flexion. The average wrist flexion in the report of Nienstedt (2003) was 37° and of Garcia-Elias et al. (2006) was 51°, while we found an average wrist flexion of 57° in our patients. The relative preservation of wrist flexion in our study can likely be attributed to not using a volar approach or the FCR.

In our patients, the scapholunate diastasis and the DISI deformity were corrected radiographically. The mean scapholunate gap was 2.3 mm and SLA of 62° at the last follow-up. These values are in the range reported by other studies: 2.2 mm gap (Links et al., 2008) or 3.7 mm gap (Pauchard et al., 2013), and a mean of 50° of SLA in the report of Van Den Abbele et al. (1998) and 75° of Pauchard et al. (2013). In the subset of 11 patients with dynamic instability, we found no changes in scapholunate gap and SLA from immediate after surgery to the final follow-up. However, the scaphoulnate gap and SLA changed in the patients with static instability. We speculate that ligament loosening occurred during the graft's healing in patients with static instability, where higher stresses occur.

There were four failures in our patients (rapid recurrence of static scapholunate instability), occurring when the protective K-wires were removed 3 months after surgery. In these patients, the instability had been noted to be difficult to reduce intraoperatively, thus our decision to perform ligament reconstruction may have been incorrect. Since the reducible nature of the scapholunate dissociation was underestimated, we reclassified these four patients as stage 5 in the classification of Garcia-Elias (2006), thus ones who should be treated with partial wrist fusion. None of these patients underwent surgical revision since they had no symptoms. Nevertheless, it is best to have an accurate assessment of the reducible nature of this dissociation. Performing dynamic manoeuvres during the preoperative arthroscopy and taking dynamic views during ulnar and radial deviation is essential. Also, during the surgical procedure, it is essential to confirm right away whether the dissociation can be reduced 'easily' (vertical repositioning of the scaphoid), as this is a basic criterion to confirm the ligament reconstruction indication. Unfortunately, there is no method to quantify the loads needed to reduce the scaphoid.

No bone-related complications were found. Since no anteroposterior scaphoid transosseous tunnel was made, there were no radiological signs of necrosis in the proximal pole of the scaphoid or signs of osteoarthritis in the scaphotrapezotrapezoidal joint. De Smet and Van Hoonacker (2007) reported one case of avascular necrosis of the scaphoid. Pauchard et al. (2013) reported one case of scaphotrapezotrapezoidal osteoarthritis less than 1 year after surgery, which required partial wrist fusion. At a mean follow-up of 36 months, there were no signs of SLAC. The incidence of the latter averages 13% in published studies (5% for Chabas et al. (2008) to 23% for Garcia-Elias et al. (2006)). This complication is reported in studies with at least 2 years' follow-up.

The results of this study support our cadaver study (Athlani et al., 2017), that this procedure restores scapholunate joint stability and normal carpal alignment. This procedure is also effective for reducing pain and increasing grip strength. The future study must extend the follow-up period to ensure the reconstructed ligament is stable and that this procedure prevents the development of osteoarthritis. Based on our findings, this technique is contraindicated when the scapholunate dissociation is difficult to reduce intraoperatively.

Acknowledgement The authors wish to thank Dr Joanne Archambault for English language editing assistance.

Declaration of conflicting interests The authors declared the following potential conflicts of interest with respect to the research, authorship, and/or publication of this article: Gilles Dautel and Nicolas Pauchard declare a conflict of interest with Arthrex®. The other authors declared no potential conflicts of interest.

Funding The authors received no financial support for the research, authorship, and/or publication of this article.

Informed consent All patients gave their informed consent for this study.

Supplementary material Appendix S1: Clinical and radiographic results from the main published studies of FCR tenodesis for scapholunate dissociation.

References

Almquist EE, Bach AW, Sack JT, Fuhs SE, Newman DM. Four-bone ligament reconstruction for treatment of chronic complete scapholunate separation. J Hand Surg Am. 1991, 16: 322–7.

Amadio PC, Berquist TH, Smith DK, Ilstrup DM, Cooney WP 3rd, Linscheid RL. Scaphoid malunion. J Hand Surg Am. 1989, 14: 679–87.

Athlani L, Pauchard N, Dautel G. Radiological evaluation of scapholunate intercarpal ligamentoplasty for chronic scapholunate dissociation in cadavers. J Hand Sur Eur. 2017. DOI: 10.1177/1753193417746055.

Bain GI, Watts AC, McLean J, Lee YC, Eng K. Cable-augmented, quad ligament tenodesis scapholunate reconstruction: rationale, surgical technique, and preliminary results. Tech Hand Up Extrem Surg. 2013, 17: 13–9.

Berger RA, Bishop AT, Bettinger PC. New dorsal capsulotomy for the surgical exposure of the wrist. Ann Plast Surg. 1995, 35: 54–9.

Brunelli GA, Brunelli GR. A new technique to correct carpal instability with scaphoid rotary subluxation: a preliminary report. J Hand Surg Am. 1995, 20: 82–5.

Chabas JF, Gay A, Valenti D, Guinard D, Legre R. Results of the modified Brunelli tenodesis for treatment of scapholunate instability: a retropective study of 19 patients. J Hand Surg Am. 2008, 33: 1469–77.

De Carli P, Donndorff AG, Gallucci GL, Boretto JG, Alfie VA. Chronic scapholunate dissociation: ligament reconstruction combining a new extensor carpi radialis longus tenodesis and a dorsal intercarpal ligament capsulodésis. Tech Hand Up Extrem Surg. 2011, 15: 6–11.

Dréant N, Dautel G. Development of an arthroscopic severity score for scapholunate instability. Chir Main. 2003, 22: 90–4.

De Smet L, Van Hoonacker P. Treatment of chronic static scapholunate dissociation with the modified Brunelli technique: preliminary results. Acta Orthop Belg. 2007, 73: 188–91.

Elgammal A, Lukas B. Mid-term results of ligament tenodesis in treatment of scapholunate dissociation: a retrospective study of 20 patients. J Hand Surg Eur. 2016, 41: 56–63.

Ellanti P, Sisodia G, Al-Ajami A, Ellanti P, Harrington P. The modified Brunelli procedure for scapholunate instablity: a single-centre study. Hand Surg. 2014, 19: 39–42.

Garcia-Elias M, Lluch AL, Stanley JK. Three-ligament tenodesis for the treatment of scapholunate dissociation: indications and surgical technique. J Hand Surg Am. 2006, 31: 125–34.

Hudak PL, Amadio PC, Bombardier C. Development of an upper extremity outcome measure: the DASH (disabilities of the arm, shoulder and hand). The Upper Extremity Collaborative Group (UECG). Am J Ind Med. 1996, 29: 602–8.

Larsen CF, Amadio PC, Gilula LA, Hodge JC. Analysis of carpal instability: I. Description of the scheme. J Hand Surg Am. 1995, 20: 757–64.

Larsen CF, Mathiesen FK, Lindequist S. Measurement of carpal bone angles on lateral wrist radiographs. J Hand Surg Am. 1991, 16: 888–93.

Lindau TR. The role of arthroscopy in carpal instability. J Hand Surg Eur. 2016, 41: 35–47.

Links AC, Chin SH, Waitayawinyu T, Trumble TE. Scapholunate interosseous ligament reconstruction: results with modified Brunelli technique versus four-bone weave. J Hand Surg Am. 2008, 33: 850–6.

Linscheid RL, Dobyns JH. Treatment of scapholunate dissociation. Rotatory subluxation of the scaphoid. Hand Clin. 1992, 8: 645–52.

MacDermid JC, Turgeon T, Richards RS, Beadle M, Roth JH. Patient rating of wrist pain and disability: a reliable and valid measurement tool. J Orthop Trauma. 1998, 12: 77–86.

Mitsuyasu H, Patterson RM, Shah MA, Buford WL, Iwamoto Y, Viegas SF. The role of the dorsal intercarpal ligament in dynamic and static scapholunate instability. J Hand Surg Am. 2004, 29: 279–88.

Moran SL, Ford KS, Wulf CA, Cooney WP. Outcomes of dorsal capsulodesis and tenodesis for treatment of scapholunate instability. J Hand Surg Am. 2006, 31: 1438–46.

Nienstedt F. Treatment of static scapholunate instability with modified Brunelli tenodesis: results over 10 years. J Hand Surg Am. 2013, 38: 887–92.

Pauchard N, Dederichs A, Segret J, Barbary S, Dap F, Dautel G. The role of three-ligament tenodesis in the treatment of chronic scapholunate instability. J Hand Surg Eur. 2013, 38: 758–66.

Ross M, Loveridge J, Cutbush K, Couzens G. Scapholunate reconstruction. J Wrist Surg. 2013, 2: 110–5.

Short WH, Werner FW, Green JK, Sutton LG, Brutus JP. Biomechanical evaluation of ligamentous stabilizers of the scaphoid and lunate: part III. J Hand Surg Am. 2007, 32: 297–309.

Talwalkar SC, Edwards AT, Hayton MJ, Stilwell JH, Trail IA, Stanley JK. Results of tri-ligament tenodesis: a modified Brunelli procedure in the management of scapholunate instability. J Hand Surg Br. 2006, 31: 110–7.

Tang JB. Re: Levels of experience of surgeons in clinical studies. J Hand Surg Eur. 2009, 34: 137–8.

Tang JB, Giddins G. Why and how to report surgeons' levels of expertise. J Hand Surg Eur. 2016, 41: 365–6.

Van Den Abbeele KL, Loh YC, Stanley JK, Trail IA. Early results of a modified Brunelli procedure for scapholunate instability. J Hand Surg Br. 1998, 23: 258–61.

Watson HK, Weinzweig J, Zeppieri J. The natural progression of scaphoid instability. Hand Clin. 1997, 13: 39–49.

- *Comparaison des résultats avec la 3LT de Garcia-Elias*

Hand Surgery and Rehabilitation 38 (2019) 157–164

Available online at ScienceDirect www.sciencedirect.com

Elsevier Masson France EM|consulte www.em-consulte.com

Original article

Treatment of chronic scapholunate instability: Results with three-ligament tenodesis vs. scapholunate and intercarpal ligamentoplasty

Traitement de la dissociation scapho-lunaire chronique : comparaison des résultats de la triple ténodèse versus la ligamentoplastie scapho-lunaire et intercarpienne

L. Athlani *, N. Pauchard, F. Dap, G. Dautel

Service de chirurgie de la main, chirurgie plastique et reconstructrice de l'appareil locomoteur, centre chirurgical Emile-Gallé, CHU de Nancy, France

ARTICLE INFO

Article history:
Received 24 August 2018
Received in revised form 8 March 2019
Accepted 18 March 2019
Available online 20 March 2019

Keywords:
Wrist instability
Scapholunate dissociation
Scapholunate ligament
Three-ligament tenodesis
Scapholunate and intercarpal ligamentoplasty

ABSTRACT

In this retrospective case control/comparison study, we compared the clinical and radiological outcomes in patients with chronic scapholunate dissociation treated with three-ligament tenodesis (3 LT) versus scapholunate and intercarpal ligamentoplasty (SLICL). Twenty patients with a mean age of 43 years were treated with the 3 LT procedure and 26 patients with a mean age of 44 years with the SLICL procedure. All patients had chronic reducible scapholunate dissociation without chondral lesions. The two groups of patients were operated on by senior surgeons, at the same facility, over two different time periods. All patients were evaluated (pain, motion, strength, function, X-rays) with a mean follow-up of 28 months (12–49) in the 3 LT group and 36 months (12–54) in the SLICL group. In the both groups, we found a significant improvement in pain levels, grip strength and functional scores (DASH and PRWE). The SLICL group had significantly less pain and greater grip strength than the 3 LT group. Patients in the SLICL group had a greater improvement in their DASH and PRWE Scores. The mean range of motion in flexion–extension was 82° (102° preoperative) in the 3 LT group and 113° (115° preoperative) in the SLICL group. In the 3 LT, there was no significant improvement in the mean static and dynamic scapholunate gaps (3.6 and 4.8 mm postoperatively versus 3.9 and 4.9 mm preoperatively), or the scapholunate angle (75° versus 72°). In the SLICL group, the mean static and dynamic gaps improved significantly (2.3 and 3.0 mm postoperatively versus 3.2 and 4.6 mm preoperatively), as did the scapholunate angle (62° versus 73°). In the 3 LT group, 4 patients developed osteoarthritis. In conclusion, the SLICL procedure for scapholunate ligament reconstruction led to better clinical and early radiological results than the 3 LT technique.

Mots clés :
Dissociation scapho-lunaire
Instabilité du carpe
Ligament scapho-lunaire
Ténodèse à trois ligaments
Ligamentoplastie scapho-lunaire

RÉSUMÉ

Dans cette étude rétrospective, nous avons comparé les résultats cliniques et radiologiques des patients présentant des dissociations scapho-lunaires chroniques traitées soit par une triple ténodèse selon Garcia-Elias (3 LT) soit par une ligamentoplastie scapho-lunaire et intercarpienne (SLICL). Vingt patients d'âge moyen de 43 ans ont été traités par une 3 LT et 26 patients d'âge moyen de 44 ans avec une SLICL. Tous les patients présentaient une dissociation chronique réductible sans lésions cartilagineuses. Les deux groupes de patients avaient été opérés par des chirurgiens seniors, dans le même établissement, sur deux périodes différentes. Tous les patients ont été évalués (douleur, mobilités, force, scores fonctionnels, radiographies) avec un recul moyen de 28 mois (12–49) dans le groupe 3 LT et de 36 mois (12–54) dans le groupe SLILC. Dans les deux groupes, nous avons constaté une amélioration significative de l'évaluation de la douleur, de la force de préhension et des scores fonctionnels (DASH et PRWE). Le groupe SLICL avait significativement moins de douleur et une plus grande force de préhension

* Corresponding author.
E-mail addresses: lionel.athlani@gmail.com (L. Athlani), pauchard.nicolas@neuf.fr (N. Pauchard), dapfrancois@gmail.com (F. Dap), gillesdautel@me.com (G. Dautel).

https://doi.org/10.1016/j.hansur.2019.03.002
2468-1229/

que le groupe 3 LT. Les patients du groupe SLICL avaient une meilleure amélioration de leurs scores DASH et PRWE par rapport au groupe 3 LT. L'arc de mobilité en flexion-extension était de 82° (102° en préopératoire) dans le groupe 3 LT et de 113° (préopératoire 115°) dans le groupe SLICL. Dans le groupe 3 LT, il n'y a pas eu d'amélioration significative des espaces scapho-lunaires statiques et dynamiques (3,6 et 4,8 mm en postopératoire contre 3,9 et 4,9 mm en préopératoire) ou de l'angle scapho-lunaire (75° versus 72°). Dans le groupe SLICL, les espaces scapho-lunaires statiques et dynamiques s'étaient significativement améliorés (2,3 et 3,0 mm en postopératoire contre 3,2 et 4,6 mm en préopératoire), de même que l'angle scapho-lunaire (62° versus 73°). Dans le groupe 3 LT, 4 patients avaient développé une arthrose. En conclusion, la procédure SLICL pour la reconstruction du complexe scapho-lunaire a conduit à de meilleurs résultats cliniques et radiologiques à court terme que la technique 3 LT.

1. Introduction

Scapholunate (SL) dissociation is the most common cause of intracarpal instability and is often diagnosed at a late stage [1]. Without treatment, scaphoid rotary subluxation and lunate dorsiflexion (dorsal intercalated segment instability, DISI) contribute to the development of SL advanced collapse (SLAC) osteoarthritis [2,3]. Several ligament reconstruction techniques have been described for treating symptomatic chronic reducible SL dissociation when no chondral lesions are present [4]. They all aim to reduce the scaphoid's flexion deformity, SL gap and DISI deformity to prevent SLAC osteoarthritis [5]. Moreover, recent biomechanical studies have highlighted the important stabilizing role of the extrinsic palmar and dorsal ligaments, which are considered secondary stabilizers for the SL complex [6,7].

The three-ligament tenodesis (3 LT) procedure described by Garcia-Elias et al. [8] uses a distally pedicled flexor carpi radialis (FCR) slip to reconstruct the dorsal segment of the SL interosseous ligament and the ligament complex on the distal pole of the scaphoid. In our practice, we initially used the 3 LT procedure and then developed a new SL ligament reconstruction, the scapholunate intercarpal ligamentoplasty (SLICL) [9]. This procedure uses a free palmaris longus (PL) graft to reconstruct the dorsal segment of the SL interosseous ligament and the dorsal intercarpal ligament. Here, we compare the preliminary results of these two procedures with a minimum follow-up of 12 months.

2. Patients and methods

2.1. Patients

This is an institutional review board–approved study reflecting the experience of senior surgeons at the same facility, over two different time periods. From May 2008 to June 2011, twenty patients with chronic SL dissociation were treated with the 3 LT technique as described by Garcia-Elias et al. [8]. From March 2013 to September 2016, twenty-six patients with chronic SL dissociation were treated with the SLICL procedure as described by Athlani et al. [9] (Fig. 1). For the two procedures, stabilization was achieved by scapholunate and scaphocapitate pinning (1.2 mm K-wires) for 2 months.

Both groups were reviewed retrospectively at two different periods by the same independent examiner with the same methodology.

The two groups of patients had comparable characteristics and follow-up time. The mean age in the 3 LT group was 43 years (22–56), and 15 of the patients were men. Eleven were right-handed, and 9 (45%) had their dominant hand injured. Follow-up for the 3 LT group was 28 months (12–49). The SLICL group had an average follow-up time of 36 months (12–54). The mean age in the SLICL group was 44 years (22–57 years), and 20 of the patients were men. Fourteen patients were right-handed, and 17 (65%) was involved of their dominant hand. The time to surgery was similar between the two groups with a mean wait of 13 months (2–79) for the 3 LT group and 14 months (3.5–72) for the SLICL group. Ten (50%) patients performed heavy manual labor in the 3 LT group and 15 patients (58%) in the SLICL group.

2.2. Review

All patients underwent a full imaging assessment consisting of standard radiographs with posterior-anterior (PA) and lateral views, dynamic clenched fist views, PA view in radial deviation and ulnar deviation; CT arthrography was also done. All patients were diagnosed with chronic SL instability [2] – either dynamic or static reducible [11] with no chondral damage – which corresponds to stage 3 or 4 in the Garcia-Elias classification [8] (Figs. 2 and 3). Beforehand, an arthroscopy of the injured wrist was performed in all cases first to confirm the SL instability, quantify its magnitude [12], confirm that no repairable ligament remnant was present, and confirm the scaphoid was easily reducible and that no chondritis was present.

All patients were reviewed in person with a minimum follow-up of 12 months. After having collected each patient's consent, an independent examiner performed a clinical evaluation and requested radiographs.

2.3. Surgical technique of the SLICL procedure

The surgical procedure (Fig. 1B) was performed by two senior surgeons (NP and GD). They made a dorsal incision along the axis of the third metacarpal, centered on the midline of the radiocarpal joint. The extensor retinaculum was opened between the third and fourth compartments, and a dorsal capsulotomy performed according to Berger et al. [13].

They then harvested a 10 cm free PL graft through a short incision on the palmar side of the wrist. The graft was then pretensioned with 3 kg for 2 min on a dedicated workstation (Arthrex®, Naples, Florida, United States). A first blind tunnel, 10 mm deep and 2.5 mm wide, was drilled at the site of the former scaphoid insertion of the dorsal segment of the SL interosseous ligament (proximal pole of the scaphoid). The posterior surface of the lunate was then drilled to create a shallow trench to serve as the interface for graft adhesion. A second blind tunnel of the same depth and width was drilled in the dorsal aspect of the triquetrum near the radial side of the dorsal radiocarpal ligaments (DRCL), following the axis of the lunate trench. One of the two ends of the graft was then whip stitched over a length of 10 mm with a non-absorbable Fiberloop™ 4-0 (Arthrex®, Naples, Florida, United States), wedged into the first proximal scaphoid tunnel, and

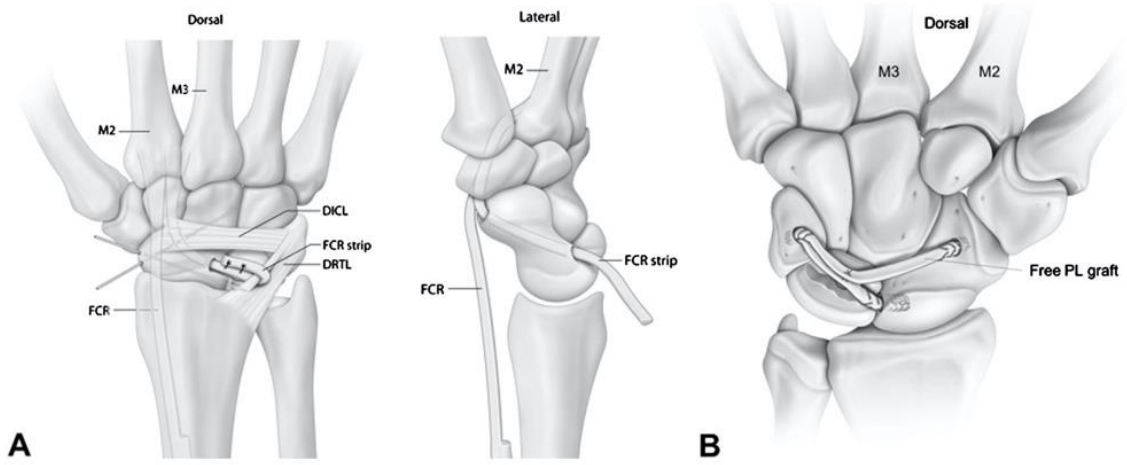

Fig. 1. Diagram illustrating the 3 LT technique as described by Garcia-Elias et al. A. The SLICL technique as described by Athlani et al. B. FCR: flexor carpi radialis; PL: palmaris longus; DICL: dorsal intercarpal ligament; DRTL: dorsal radiotriquetral ligament; M2: second metacarpal; M3: third metacarpal.

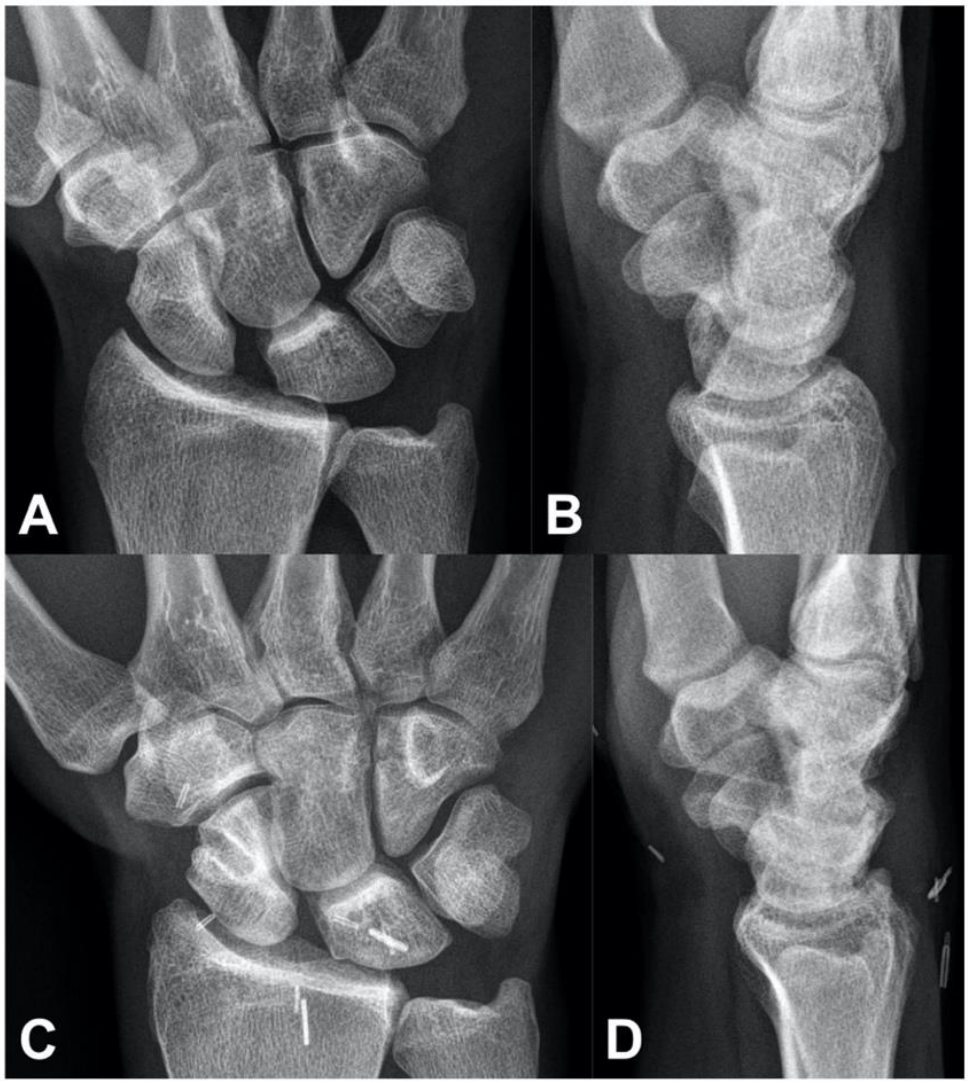

Fig. 2. Example of scapholunate dissociation detected on anteroposterior (A) and lateral (B) radiographs. Postoperative anteroposterior (C) and lateral (D) radiographs at 46 months' follow-up after the 3 LT procedure.

Fig. 3. Example of scapholunate dissociation detected on anteroposterior (A) and lateral (B) radiographs. Postoperative anteroposterior (C) and lateral (D) radiographs at 40 months' follow-up after the SLICL procedure.

secured in interference by means of an impacted 2.5 absorbable miniBioPushlock™ (Arthrex®, Naples, Florida, United States). A 2.2 mm non-absorbable titanium MicroCorkscrew™ anchor (Arthrex®, Naples, Florida, United States) was introduced into the lunate trench.

The dissociation was then reduced by manual maneuvers and pointed reduction forceps [9]. Stabilization was achieved by scapholunate and scaphocapitate pinning (1.2 mm K-wires). Fixing the graft in the second triquetral tunnel meant both tapering it and performing a longitudinal plication. The central half was resected over a distance of 12 mm starting from the entry point in the second tunnel. The two half strips thus obtained were folded back on themselves to create a new intermediary graft end as thick as the other two ends over a length of 6 mm. This new end was then whip stitched over 10 mm before being inserted and attached to the second blind tunnel by impacting a Pushlock. The graft located between the first two intraosseous fixation points was placed in the lunate trench, and then fixed by the anchor sutures to create the first segment. A third blind tunnel of the same depth and width was drilled at the level of the scaphoid isthmus near the scaphotrapeziotrapezoid (STT) joint surface.

To create the second segment the remainder of the graft was again passed through the lunate trench and fixed by the same anchor sutures, to allow for superposition of the two segments in the tunnel. The remaining free end was resected beyond a distance of 8 mm from the entry point in the third blind tunnel and then inserted into the tunnel. To do so, this last end was whip stitched over 10 mm and fixed to the bottom of the third tunnel by impacting a Pushlock. At this point we could test the tension of both segments with a tendon hook. Capsular and retinacular stitching was performed.

2.4. Postoperative protocol

Immediately following surgery, the wrist was immobilized in a volar plaster cast for 48 to 72 hours. Immobilization was extended for 2 months with a short-arm fiberglass splint. K-wires were removed 2 months postoperatively, at which point the patients began 1 month of self-directed rehabilitation. Radiographs were taken at 3 months postoperative, after which physiotherapy sessions were initiated. No heavy loads could be placed on the wrist for the first 6 months postoperative.

2.5. Clinical evaluation

Pain was evaluated using a Visual Analog Scale (VAS) (out of 10) at rest and during effort. Grip strength in the operated and contralateral side in kg/F was collected using a Jamar® hydraulic

hand dynamometer (Performance Health®, Charleville-Mézières, France). The active joint range of motion (ROM) was measured in degrees during wrist flexion, extension, radial deviation and ulnar deviation (accuracy of 1°). The functional outcomes were evaluated using standardized questionnaires: DASH (/100) [14], PRWE (/100) [15]. Postoperative complications were also recorded.

2.6. Radiographic evaluation

At the follow-up visits, standard radiographic views, standard neutral PA and lateral views, and a clenched fist PA view were taken in all patients. The digital radiographs were viewed on OsiriX© (Pixmeo® 2016, Geneva, Switzerland). The static and dynamic SL gaps (SLG) in mm along with the SL angle (SLA) in degrees were calculated (0.1 mm accuracy for gaps and 1° for angles). Values greater than 3 mm were considered pathological, as was an SLA greater than 70° and a capitolunate angle (CLA) more than 15° [16]. At the in-person review, the patients were assessed for any signs of necrosis of the proximal pole of the scaphoid and/or posterior horn of the lunate along with the development of scaphotrapeziotrapezoid (STT) or SLAC osteoarthritis.

2.7. Statistical analysis

The recorded data were summarised using mean values and ranges. The mean values obtained in the preoperative evaluation and at the last follow-up were compared using Student's *t*-test with any differences deemed significant with a type I error risk of 5% ($P < 0.05$).

3. Results

Results for both groups are given in Tables 1 and 2. The 3 LT group had 8 cases of dynamic instability and 12 of static. The SLICL group had 11 cases of dynamic instability and 15 of static. In every patient, the CT arthrography showed a tear of the SL interosseous ligament with contrast product leakage. During the arthroscopy evaluation, stage 2 instability was found in 4 cases and stage 3 in 16 cases in the 3 LT group. In the SLICL group, stage 2 instability was found in 6 cases and stage 3 in 20 cases. There was no chondral damage. All the 3 LT procedures were performed with an FCR and all the SLICL procedures using a free PL graft. The incision was healed within 2 weeks in all patients. The K-wires protecting the SL and scaphocapitate joints were removed at 2 months postoperative in all patients (range 56 – 65 days), and then the rehabilitation protocol initiated. The time away from work averaged 6 months (4–12) in the 3 LT group and 5 months (0–12) in the SLICL group. In the 3 L T group, 90 percent of patients had returned to the original job and in the SLICL group, 88 percent.

3.1. Clinical evaluation

At final follow-up, in the 3 LT and SLICL groups, we found a significant ($P < 0.05$) reduction in pain levels at rest and during effort, a significant improvement in grip strength relative to the preoperative value and the contralateral side, and a significant improvement in the functional scores (DASH and PRWE). The SLICL group reported significantly less pain when compared with the 3 LT group ($P < 0.05$). The SLICL group had significantly higher grip strength at final follow-up. The improvement was greater in the SLICL group than in the 3 LT group (mean 14 kg/F versus 8 kg/F; $P < 0.05$). Also, the grip strength as a percentage of the contralateral side was higher in the SLICL group. Patients in the SLICL group had a larger improvement in their QuickDASH and PRWE scores, with a mean decrease of 40 points and 39 points, respectively, in this group versus a mean decrease of 18 points and 22 points, respectively, in the 3 LT group ($P < 0.05$). The mean ROM in flexion–extension was 82° (102° preoperative) in the 3 LT group and 113° (115° preoperative) in the SLICL group. Thus, the ROM in flexion–extension had significantly decreased ($P < 0.05$) in the 3 LT group (20° reduction) but not significantly ($p > 0.05$) in the SLICL group (2° reduction). Patients treated with the SLICL had better motion in flexion–extension than did the 3 LT group. The differences in radial and ulnar deviation were not statistically significant between groups.

3.2. Radiographic evaluation

At final follow-up, in the 3 L T group, there was no significant ($P < 0.05$) improvement of the mean static and dynamic SLG (3.6 and 4.8 mm postoperatively versus 3.9 and 4.9 mm preoperatively), or the SLA (75° versus 72°) (Fig. 2). In the SLICL group, there was a significant ($P < 0.05$) improvement of the mean static and dynamic SLG (2.3 and 3.0 mm postoperatively versus 3.2 and 4.6 mm preoperatively), as well as the SLA (62° versus 73°) (Fig. 3). The SLICL procedure led significantly greater improvement of the SLG and the SLA when compared with the 3 LT technique ($P < 0.05$).

3.3. Complications

There were no intraoperative complications or local postoperative infections in either group.

Table 1
Clinical and radiographic outcomes (mean) for patients treated with the three-ligament tenodesis (3 LT) and scapholunate intercarpal ligamentoplasty (SLICL) procedures.

Average value	3 LT (n = 20)			SLICL (n = 26)		
	Preoperative	Last follow-up	*P*	Preoperative	Last follow-up	*P*
Pain at rest (VAS) (/10)	3.2	1.6	0.01	4.5	0.4	0.01
Pain during effort (/10)	6.4	4.9	0.01	6.7	1.9	0.01
Grip strength (Kg/F)	24	32	0.01	26	40	0.01
	57% CL	76% CL		59% CL	89% CL	
Flexion (°)	52	39	0.01	59	57	0.663
Extension (°)	50.5	43	0.01	56	56	0.885
Ulnar deviation (°)	30	24	0.01	32	32	0.876
Radial deviation (°)	17	14	0.05	16	16	0.731
DASH (/100)	48.9	31.3	0.01	57.5	17.5	0.01
PRWE (/100)	55.5	33.6	0.01	52.6	13.6	0.01
Static scapholunate gap (mm)	3.9	3.6	0.477	3.2	2.3	0.01
Dynamic scapholunate gap (mm)	4.9	4.8	0.793	4.6	3.0	0.01
Scapholunate angle (°)	72	75	0.356	73	62	0.01
SLAC arthritis	0	2	–	0	0	–

Table 2
Comparison of differences in the clinical and radiographic outcomes between three-ligament tenodesis (3LT) and scapholunate intercarpal ligamentoplasty (SLICL).

Average change	3 LT (n = 20)	SLICL (n = 26)	P
Pain at rest (VAS) (/10)	−1.6	−4.1	0.01
Pain during effort (/10)	−1.5	−4.8	0.01
Grip strength (Kg.F)	+8	+14	0.01
Flexion (°)	−13	−2	0.01
Extension (°)	−7.5	0	0.01
Ulnar deviation (°)	−6	0	0.746
Radial deviation (°)	−3	0	0.896
DASH (/100)	−18	−40	0.01
PRWE (/100)	−22	−39	0.01
Static scapholunate gap (mm)	−0.3	−0.9	0.01

In the SLICL group, 3 patients (11.5%) developed De Quervain's tenosynovitis that resolved with conservative treatment (brace and corticosteroid injection). There were no radiographic signs of bone lysis at the proximal pole of the scaphoid and/or the posterior horn of the lunate. However, we noted 2 cases (7.5%) of asymptomatic loosening around miniBioPushlock™ implants (Fig. 4). The patients no required a new surgery but only radiological monitoring. At final follow-up, none of the patients had signs of SLAC osteoarthritis.

In the 3 LT group, 2 patients (10%) developed type 1 complex regional pain syndrome (CRPS) that resolved with medical treatment. Seven patients (35%) had palmar pain at entry point of the trans-scaphoid tunnel. Four patients (20%) developed osteoarthritis (10% STT osteoarthritis and 10% SLAC). Two patients required a new surgical procedure: one case of early STT osteoarthritis requiring STT arthrodesis at 10 months, and one case of type 2 SLAC osteoarthritis reoperated at 32 months with a four-corner fusion (Fig. 5). Two other patients developed postoperative osteoarthritis (one STT osteoarthritis, one SLAC), but did not require further surgical intervention as of the last follow-up. There was one case (5%) of scaphoid proximal pole radiolucency in the 3 LT group.

Fig. 4. Radiograph showing asymptomatic loosening around absorbable miniBioPushlock™ implants (Arthrex®, Naples, Florida, United States).

4. Discussion

Based on this study's findings, the 3 LT and the SLICL procedures can significantly reduce pain and increase grip strength. The clinical and radiological outcomes were better with the SLICL technique than the 3 LT. The SLICL group reported significantly less pain at rest and during effort than the 3 LT group. Grip strength in the SLICL group had recovered to a mean of 89% when compared with the contralateral side. For the 3 LT group, grip strength was 76%. This difference was also statistically significant. When compared with preoperative values, there was significantly decreased flexion and extension in the 3 LT group only. The preoperative values were similar in the two groups. The mean ROM had decreased by 20° in the 3 LT group while the decrease was 2° in the SLICL group. At final follow-up, the SLICL group had better motion in flexion and extension. Differences between the two procedures in radial and ulnar deviation were not significant.

The 3 LT procedure [8] uses a distally pedicled slip of FCR to reconstruct the dorsal segment of the SL interosseous ligament and vertically reposition the scaphoid. This technique is considered the benchmark and has served as the basis for numerous clinical studies [8,17,18]. Authors of these study described a loss of ROM and grip strength after ligament reconstruction. At 46 months' follow-up, Garcia-Elias et al. [8] reported an average postoperative ROM in flexion-extension of 103° and the grip strength was 65% of the contralateral side. At 10.5 months' follow-up, Kalb et al. [18] reported better recovery of grip strength with an average 80% of the noninvolved side. Average postoperative ROM in flexion–extension was 88°. In the 3 LT group, the average postoperative ROM in flexion was 39° in our study while Garcia-Elias et al. [8] reported 51° and Kalb et al. [18] reported 35°. In the SLICL group, this amplitude was better with a mean 57°. This relative preservation of wrist flexion with the SLICL procedure can be attributed to not using a volar approach or the FCR.

In the SLICL group, we found a significant improvement in SLG and SLA, with a return to normal values [16]. This procedure has corrected the radiologic features of SL dissociation. In the 3 LT group, the SLG and SLA did not decrease significantly. De Smet et al. [17] noted a significant reduction of the SLG (4.25 mm vs. 3.29 mm preoperative) and the SLA (77° vs. 68° preoperative) at 39 months' follow-up. However, the SLG and SLA were considered normal in only 33% and 25% of patients, respectively.

In the 3 LT group, we found seven cases of persistent palmar pain. Talwalker et al. [19] noted four cases, three of which were treated surgically by excising a neuroma of the palmar branch of the median nerve.

We also found two cases (10%) of postoperative STT osteoarthritis. Poor positioning at the entry point of the scaphoid tunnel may have caused joint penetration, or even a modification of articular congruence, owing to pressure exerted by the tenodesis.

In the SLICL group, the rate of SLAC-type osteoarthritis was 0% while it was 10% (2 cases) in the 3 LT group. This rate was similar to that found in the literature: 5% for Chabas et al. [20], 12.5% for Nienstedt et al. [21], 13% for Moran et al. [22], 23% for Garcia Elias et al. [8]. Finally, we also observed a case of scaphoid proximal pole radiolucency six months postoperatively. One case of avascular necrosis of the scaphoid was reported by De Smet and Van Hoonacker [23]. In the SLICL group, no bone-related complications were found. Since no anteroposterior scaphoid transosseous tunnel was made, there were no radiological signs of necrosis in the proximal pole of the scaphoid or signs of osteoarthritis in the STT joint.

Limitations of this comparative study include the relatively short follow-up period and small patient populations in each group. However, the mean sample size and mean follow-up are similar to that found in the literature. Comparisons may be affected

Fig. 5. Radiograph (A) and computed tomography scan (B) showing STT osteoarthritis 10 months after 3 LT. Radiograph (C) and computed tomography scan (D, E) showing SLAC osteoarthritis 30 months after 3 LT.

by the different time periods, as the authors replaced one technique (3 LT) with a new technique (SLICL). Long-term follow-up as well as the inclusion of other chronic SL instability cases will provide greater insight into the optimal management of this difficult problem.

Funding statement

The authors received no financial support for the research, authorship, and/or publication of this article.

Informed consent

All patients gave their informed consent for this study

Disclosure of interest

Gilles Dautel and Nicolas Pauchard declare a conflict of interest with Arthrex®. The authors declare that they have no competing interest.

Acknowledgments

The authors wish to thank Dr. Joanne Archambault for English language editing assistance. The authors wish to thank Mr. Cyrille Martinet for the illustrations.

References

[1] Gelberman RH, Cooney 3rd , Szabo RM. Carpal instability. Instr Course Lect 2001;50:123–34.
[2] Larsen CF, Amadio PC, Gilula LA, Hodge JC. Analysis of carpal instability: I. Description of the scheme. J Hand Surg Am 1995;20:757–64.
[3] Watson HK, Ballet FL. The SLAC wrist: scapholunate advanced collapse pattern of degenerative arthritis. J Hand Surg Am 1984;9:358–65.
[4] Crawford K, Owusu-Sarpong N, Day C, Iorio M. Scapholunate ligament reconstruction: a critical analysis review. J Bone Joint Surg Rev 2016;4:e41–8.
[5] Linscheid RL, Dobyns JH. Treatment of scapholunate dissociation. Rotatory subluxation of the scaphoid. Hand Clin 1992;8:645–52.
[6] Mitsuyasu H, Patterson RM, Shah MA, Buford WL, Iwamoto Y, Viegas SF. The role of the dorsal intercarpal ligament in dynamic and static scapholunate instability. J Hand Surg Am 2004;29:279–88.
[7] Short WH, Werner FW, Green JK, Sutton LG, Brutus JP. Biomechanical evaluation of ligamentous stabilizers of the scaphoid and lunate: part III. J Hand Surg Am 2007;32:297–309.
[8] Garcia-Elias M, Lluch AL, Stanley JK. Three-ligament tenodesis for the treatment of scapholunate dissociation: indications and surgical technique. J Hand Surg Am 2006;31:125–34.
[9] Athlani L, Pauchard N, Dautel G. Radiological evaluation of scapholunate intercarpal ligamentoplasty for chronic scapholunate dissociation in cadavers. J Hand Surg Eur 2018;43:387–93.
[11] Watson HK, Weinzweig J, Zeppieri J. The natural progression of scaphoid instability. Hand Clin 1997;13:39–49.
[12] Dreant N, Dautel G. Development of an arthroscopic severity score for scapholunate instability. Chir Main 2003;22:90–4.
[13] Berger RA, Bishop AT, Bettinger PC. New dorsal capsulotomy for the surgical exposure of the wrist. Ann Plast Surg 1995;35:54–9.
[14] Hudak PL, Amadio PC, Bombardier C. Development of an upper extremity outcome measure: the DASH (disabilities of the arm, shoulder and hand). The Upper Extremity Collaborative Group (UECG). Am J Ind Med 1996;29:602–8.
[15] MacDermid JC, Turgeon T, Richards RS, Beadle M, Roth JH. Patient rating of wrist pain and disability: a reliable and valid measurement tool. J Orthop Trauma 1998;12:577–86.
[16] Larsen CF, Mathiesen FK, Lindequist S. Measurement of carpal bone angles on lateral wrist radiographs. J Hand Surg Am 1991;16:888–93.
[17] De Smet L, Goeminne S, Degreef I. Does the "three-ligament tenodesis" procedure restore carpal architecture in static chronic scapholunate dissociation? Acta Orthop Belg 2013;79:271–4.
[18] Kalb K, Blank S, Van Schoonhoven J, Prommersberger KJ. Stabilization of the scaphoid according to Brunelli as modified by Garcia-Elias, Lluch, and Stanley for the treatment of chronic scapholunate dissociation. Oper Orthop Traumatol 2009;21:429–41.

[19] Talwalkar SC, Edwards AT, Hayton MJ, Stilwell JH, Trail IA, Stanley JK. Results of tri-ligament tenodesis: a modified Brunelli procedure in the management of scapholunate instability. J Hand Surg Br 2006;31:110–7.
[20] Chabas JF, Gay A, Valenti D, Guinard D, Legré R. Results of the modified Brunelli tenodesis for treatment of scapholunate instability: a retrospective study of 19 patients. J Hand Surg Am 2008;33:1469–77.
[21] Nienstedt F. Treatment of static scapholunate instability with modified Brunelli tenodesis: results over 10 years. J Hand Surg Am 2013;38:887–92.
[22] Moran SL, Ford KS, Wulf CA, Cooney WP. Outcomes of dorsal capsulodesis and tenodesis for treatment of scapholunate instability. J Hand Surg Am 2006;31:1438–46.
[23] De Smet L, Van Hoonacker P. Treatment of chronic static scapholunate dissociation with the modified Brunelli technique: preliminary results. Acta Orthop Belg 2007;73:188–91.

La ligamentoplastie « SLIC » : modification technique et évaluation.

Dans notre première étude prospective, nous avons rapporté des résultats cliniques et radiologiques satisfaisants, avec un suivi à court et moyen terme. Cependant, entre la période post-opératoire immédiate et le dernier recul, il y a eu une augmentation significative des paramètres radiographiques (SLG et SLA). Cette augmentation significative concernait le sous-ensemble de poignets présentant une ISL de stade statique (Athlani et al., 2018-3).

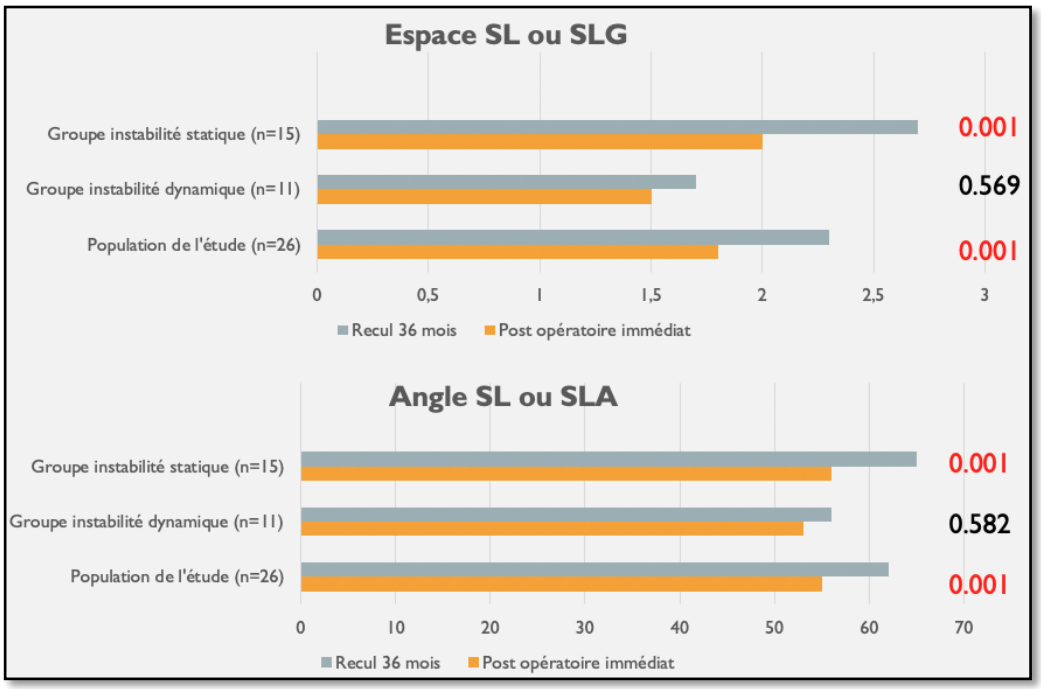

Figure 22. *Diagramme illustrant l'augmentation significative des paramètres radiographiques entre la période post-opératoire immédiate et le dernier recul, pour le groupe des instabilités statiques (Athlani et al., 2018-3).*

Nous avons donc décidé de modifier la procédure originale car nous estimions que l'étape triquétrale contribuait à la fragilité du transplant, et il était de plus, difficile de générer une tension optimale dans la ligamentoplastie. La modification a concerné cette étape intermédiaire et visait à ancrer le transplant au sein d'un tunnel trans-osseux triquétral (Figure 23). Nous avons tout d'abord ajouté une deuxième ancre, similaire à la première, dans la tranchée lunarienne, de manière à avoir une ancre à proximité de l'interligne scapho-lunaire et une autre à proximité de l'interligne luno-triquétral (Figure 24-A). Ensuite, un tunnel trans-osseux triquétral de diamètre 3,0 mm a été foré. Le point d'entrée de ce tunnel était situé directement à l'aplomb de l'interligne luno-triquétral, avec un axe parallèle à l'interligne triquétro-hamatal. Le respect de la corticale dorsale du triquétrum était impératif.

Après cela, nous avons passé le transplant à travers le tunnel à l'aide d'un QuickPass Tendon Shuttle™ (Arthrex®) (Figure 24-B). Le segment scapho-luno-triquétral était placé dans la tranchée lunarienne, et la tension optimale ajustée en tirant sur l'extrémité libre de transplant restante. Dès qu'une tension suffisante était obtenue, nous l'avons verrouillée par l'introduction dans l'orifice ulnaire du tunnel, d'une vis de ténodèse résorbable de 3,0 mm - Tenodesis Screw™ (Arthrex®) (Figure 24-C). Le transplant situé entre les deux premiers points de fixation intra-osseux (pôle proximal du scaphoïde et triquétrum) était solidarisé au sein de la tranchée lunarienne en utilisant les fils des ancres. L'utilisation de deux ancres permettait d'optimiser au mieux la tension à proximité des interlignes scapho-lunaire et luno-triquétral. Les étapes scaphoïdiennes, initiale et finale, sont restées inchangées.

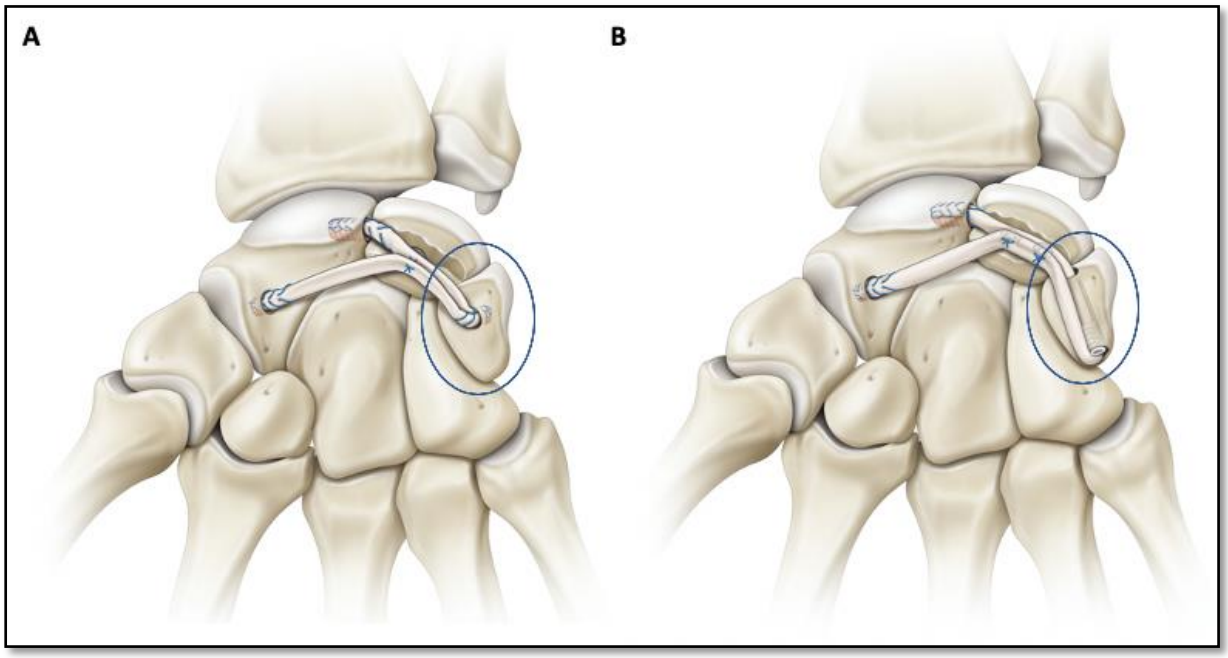

Figure 23. *Schéma montrant la version originale (A) et la version modifiée (B) de la ligamentoplastie « SLIC » (Athlani et al., 2020).*

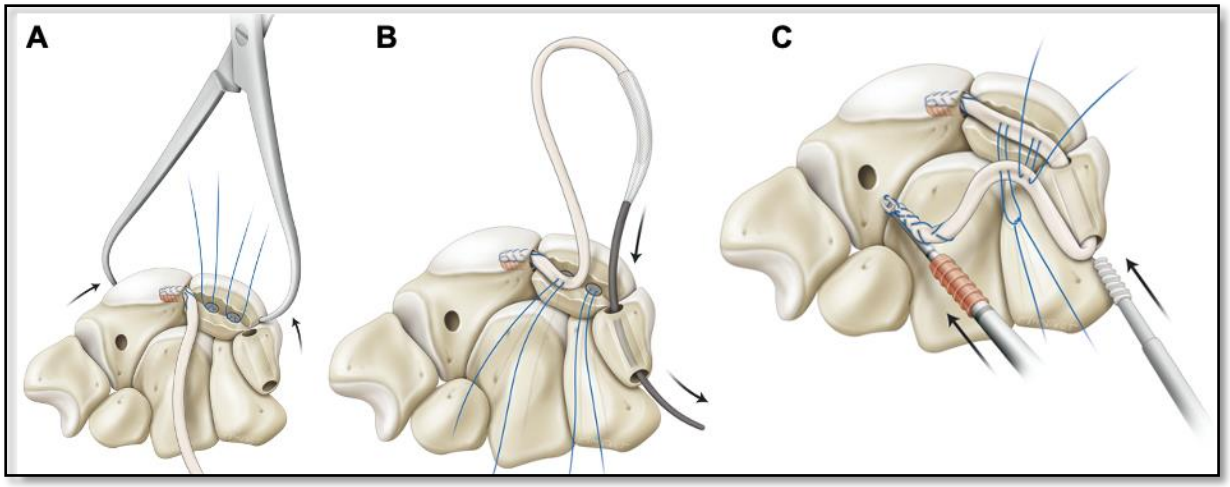

Figure 24. *Schémas illustrant les différentes étapes de la ligamentoplastie « SLIC » dans sa version modifiée (Athlani et al., 2020).*

La ligamentoplastie « SLIC », comme les autres ligamentoplasties scapho-lunaires, nécessite d'aborder l'articulation du poignet. La plupart des auteurs proposent l'utilisation d'une voie d'abord dorsale plutôt que palmaire pour des raisons de facilité d'exposition (Berger et Bishop, 1997). Plusieurs dessins de capsulotomie ont été décrites telles que longitudinale, transversale, oblique, en « L », en « T », etc. (Anakwe et al., 2012). La capsulotomie transligamentaire en « V » à charnière radiale décrite par Berger et al. (1995) reste la technique la plus répandue (Figure 25). Cette dernière a pour avantage d'apporter une bonne exposition des interlignes radio- et médio-carpiens. Toutefois, Hagert et al. (2010) dans leur étude anatomique, notaient l'absence de respect de l'intégrité des fibres longitudinales des ligaments extrinsèques DRC et DIC. De même, l'innervation capsulaire, représentée par le nerf interosseux postérieur, est systématiquement sectionné. Les auteurs soulignaient l'importance du respect de ce nerf par sa fonction proprioceptive du poignet, et notamment lors de la rééducation post-opératoire. Ainsi, une approche dorsale de poignet permettant une exposition de l'ensemble du carpe tout en respectant les structures ligamentaires extrinsèques et vasculo-nerveuses capsulaires, serait d'un grand intérêt.

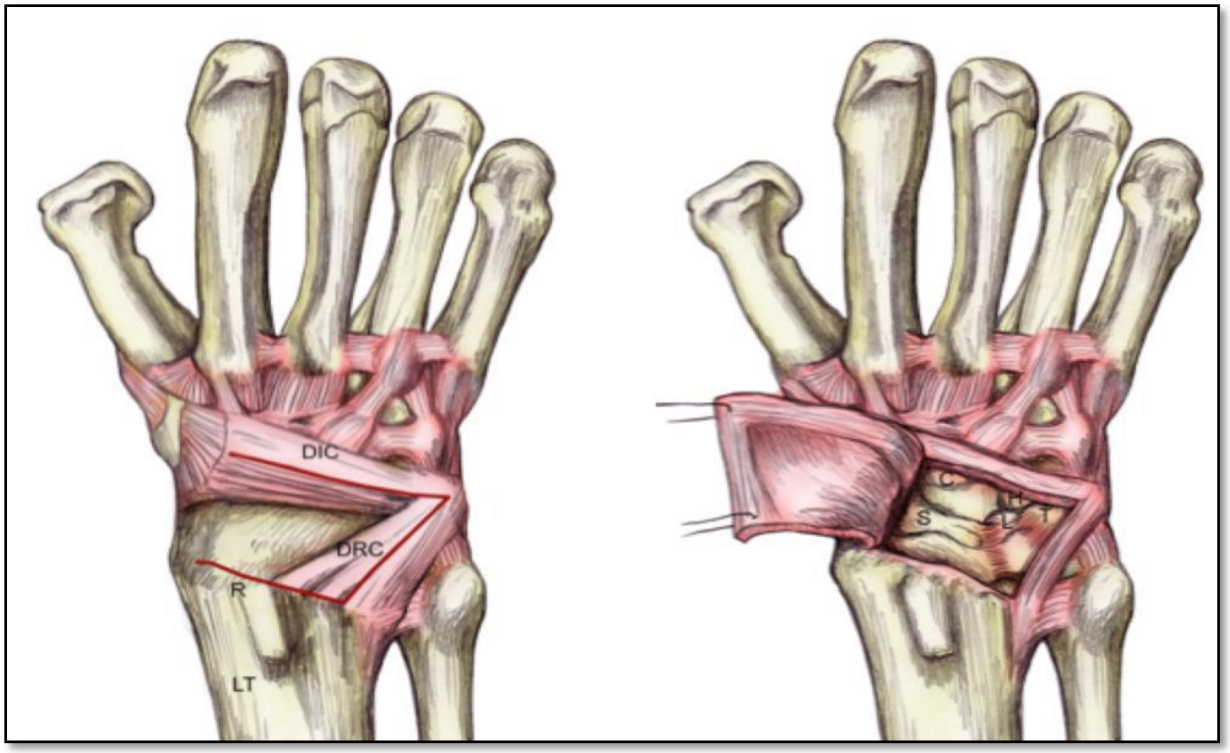

Figure 25. *Schémas illustrant le tracé de la capsulotomie de Berger et al., (1995) et l'exposition du carpe rendue possible. Les ligaments DRC et DIC sont sectionnés longitudinalement, dessinant un triangle à base radial et apex triquétral. Le lambeau capsulaire est soulevé radialement, exposant la partie radiale de l'articulation radio-carpienne et l'ensemble de l'articulation médio-carpienne. À noter que le carpe reste stabilisé par le respect de la moitié de chaque ligament DRC et DIC.*

- *Évaluation cadavérique en scanner dynamique 4-Dimensions*

Short Report Letter

JHS(E)

Journal of Hand Surgery
(European Volume)
0(0) 1–3
journals.sagepub.com/home/jhs
SAGE

Quantitative four-dimensional CT evaluation of scapholunate intercarpal ligamentoplasty for scapholunate dissociation: a cadaveric study

Dear Editor,

In a previous prospective study (Athlani et al., 2020a), we described the scapholunate intercarpal ligamentoplasty (SLICL) to treat symptomatic chronic reducible scapholunate instability, when no chondral lesions are present. The technique involves the use of a free palmaris longus graft to reconstruct the dorsal segment of the scapholunate interosseous ligament and the dorsal intercarpal ligament to reduce the dissociation. Although satisfactory clinical and radiological results with short- to mid-term follow-up was reported, the effectiveness of the procedure was only evaluated from static radiographs, which gives limited information about the dynamic changes in carpal alignment during motion. Consequently, we performed another prospective study (Athlani et al., 2020b) to evaluate the value of dynamic four-dimensional computed tomography (4-DCT) in assessing chronic scapholunate instability. With 4-DCT, we evaluated the sizes of the scapholunate gap (mean, maximal, coefficient of variation and range values) during radioulnar deviation. All values were significantly higher in the patients with definite scapholunate instability than in those

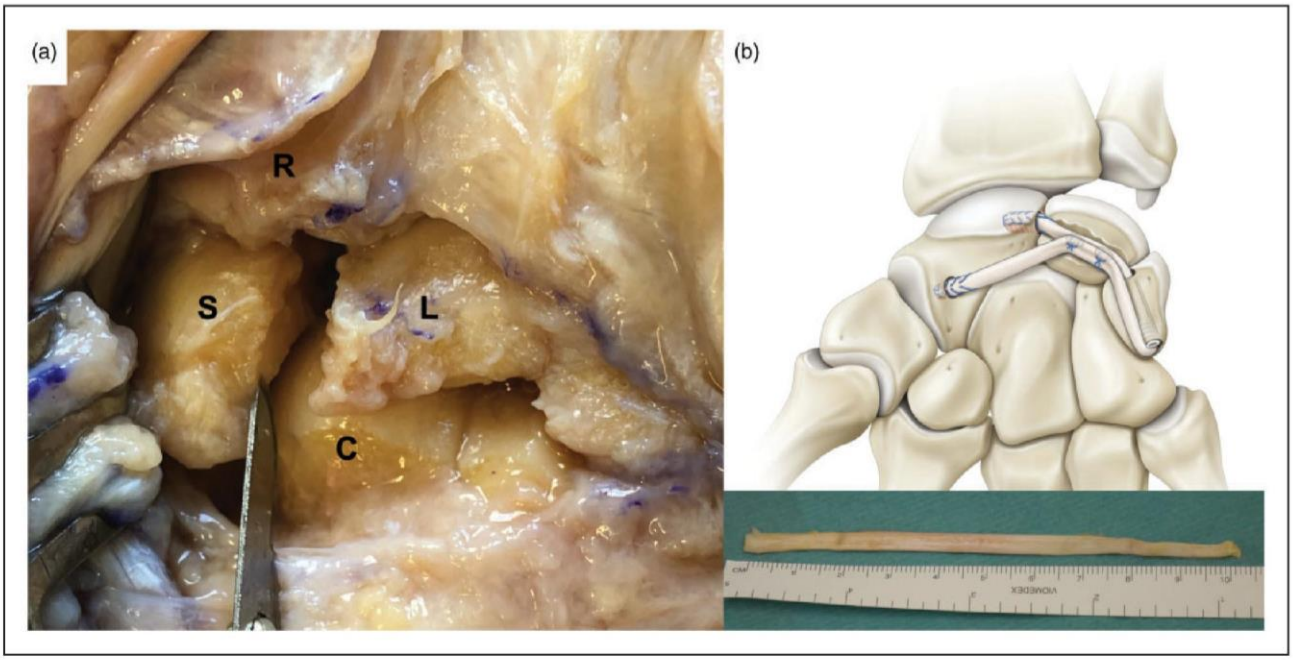

Figure 1. (a) Photograph showing a scapholunate dissociation created by sectioning the three segments of the scapholunate interosseous ligament, the dorsal radiocarpal ligament, dorsal intercarpal ligament and the dorsal capsulo-scapholunate septum with a scalpel blade. (b) Diagram illustrating the scapholunate intercarpal ligamentoplasty using a free palmaris longus graft to reduce scapholunate dissociation (Athlani et al., 2020a).
R: radius; S: scaphoid; L: lunate; C: capitate.

with absence of instability. We concluded that 4-DCT adds value to assessing chronic scapholunate instability, which allows the differentiation between patients with negative and those with positive instability, even in patients with an ambiguous diagnosis based on the initial radiographs. In this third study, we studied the effectiveness of SLICL using 4-DCT in a cadaver study.

A scapholunate instability was created in six fresh adult cadaveric wrists (three right and three left) by sectioning the scapholunate interosseous ligament, dorsal radiocarpal ligament, dorsal intercarpal ligament and dorsal capsulo-scapholunate septum. After dissection, all wrists showed a static scapholunate instability with a scapholunate diastasis, a lunate dorsiflexion and a posterior scaphoid subluxation (Figure 1(a)). Then, a SLICL was performed on each wrist (Figure 1(b)) as described by Athlani et al., (2020a). 4-DCT examinations were performed during radioulnar deviation in all specimens prior to dissection, after dissection and after ligamentoplasty. Systematically, 100 cycles of wrists flexion–extension were performed, simulating repetitive loading of the wrist and postoperative ligamentous loosening. For the three time points, specimens were moved in the scanner table using a dedicated device in acrylic glass (PLEXIGLAS®, Röhm GmbH, Weiterstadt, Germany) and ABS (Acrylonitrile butadiene styrene) for parts manufactured using a fused deposition modelling (FDM) three-dimensional printer (STREAM 30 Pro MK2,Volumic, France), which permitted a maximum of 30° in radial deviation and 30° in ulnar deviation (Figure 2). After ligament sectioning, the sizes of the scapholunate gap were significantly increased, corresponding to 36% for the mean, 22% for the maximal, 82% for the coefficient of variation and 67% for the range, respectively (Supplementary Video 1). After the SLICL, we noted a significant improvement in all those parameters, with a return to previous values, confirming reduction of scapholunate dissociation (Supplementary Video 2) (Table 1).

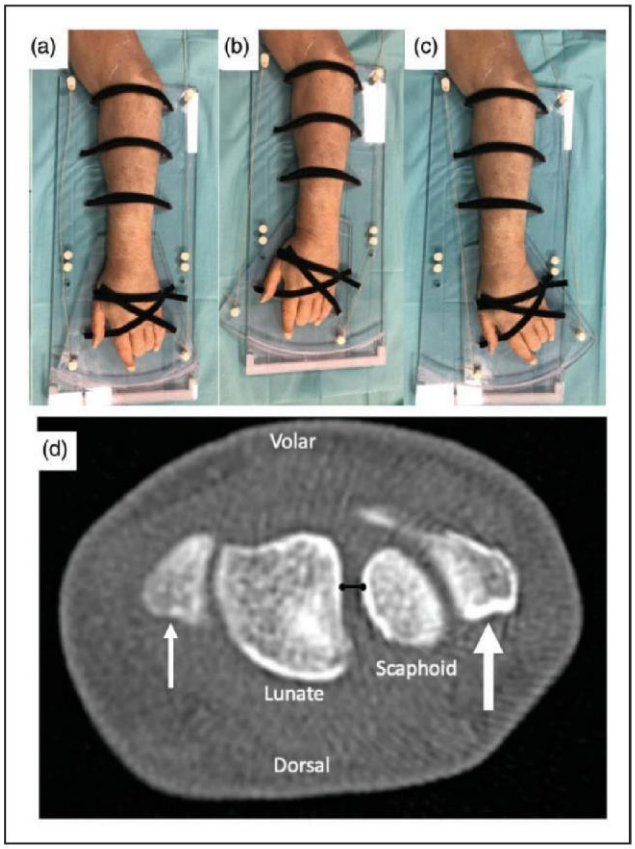

Figure 2. Photograph of the specific dedicated device and a cadaveric left wrist attached on the device and positioned in neutral (a), radial (b) and ulnar (c) deviation. For each wrist, an independent examiner performed passive movement in a continuous and homogenous manner, from maximum radial deviation to maximum ulnar deviation, and then to return to the starting point (full radioulnar deviation cycle) during an 8 second time frame. In the CT multiplanar images, for construction of scapholunate gap (d), two markers were placed on the scaphoid and lunate as the shortest distance between these two bones, in axial plane passing through the radial styloid (thin arrow) and ulnar styloid (thick arrow).

The findings from this cadaver study confirmed that SLICL corrected the anatomical features of scapholunate dissociation in all specimens evaluated. These results support the previous clinical study, that the SLICL procedure is effective for reducing scapholunate dissociation and restores scapholunate joint stability. 4-DCT demonstrated the anatomical impact of scapholunate interosseous and dorsal extrinsic ligaments sectioning on carpal stability during radioulnar deviation and more importantly, the positive impact of the SLICL in restoring CT kinematic parameters to normal and thus, scapholunate joint stability and normal carpal anatomy. This represents additional evidence of the effectiveness of the SLICL in correcting dissociation and supports the use of 4-DCT for the postoperative evaluation of patients with persistent symptoms and where radiographic evaluation may be non-contributory. Contrary to conventional radiographs, 4-DCT is not influenced by superimposition phenomenon and measurement errors related to the wrist position. This technique can quantify distances between carpal bones during motion with more precision and a better intra- and interobserver reproducibility than radiographs.

Further clinical studies with a kinematic 4-DCT assessment and SLICL reconstruction are required in order to ensure our results are reproduced in

Table 1. Outcomes for the gap sizes measured on 4-DCT.

Measurements of scapholunate gaps	Preligaments sectioning ($n=6$)	Postligaments sectioning ($n=6$)	Postligamentoplasty ($n=6$)
Mean (mm)	2.5 (2.3 to 3.9)	3.4 (3 to 4.8)	2.1 (1.9 to 3.1)
p value	0.01*	0.02**	NS***
Maximal (mm)	3.2 (2.6 to 4.5)	3.9 (3.6 to 5.3)	2.6 (2.5 to 3.5)
p value	0.03*	0.02**	NS***
Coefficient of variation (%)	8.1 (6.7 to 13.6)	14.7 (10.7 to 18.6)	6.6 (6 to 12.9)
p value	0.01*	0.02**	NS***
Range (mm)	0.9 (0.6 to 1.5)	1.5 (1.1 to 1.8)	0.8 (0.5 to 0.9)
p value	0.03*	0.02**	NS***

The data shown are median (interquartile range).
NS: no significant difference.
**p* values shown in this column are results compared between the preligaments sectioning and the postligaments sectioning.
***p* values shown in this column are results compared between the postligaments sectioning and the postligamentoplasty.
****p* values shown in this column are results compared between the postligamentoplasty and the preligaments sectioning.
The software measurement accuracy was estimated as 0.1 mm.

clinical practice, particularly in terms of reconstruction stability.

Acknowledgements The authors wish to thank Professor Marc Braun and Marine Krebs of the Department of Anatomy, Faculty of Medicine, University of Lorraine, for technical support. The authors wish to thank Dr Romain Detammaecker and Dr Jonathan Granero for their assistance in preparing the specimens

Declaration of conflicting interests The authors declared the following potential conflicts of interest with respect to the research, authorship, and/or publication of this article: two authors involved in this work (Pedro Augusto Gondim Teixeira and Alain Blum) participate on a non-remunerated research contract with TOSHIBA Medical Systems for the development and clinical testing of post-processing tools for musculoskeletal CT. The authors declare no potential conflicts of interest with respect to the research, authorship, and/or publication of this article.

Supplemental material Supplemental material for this article is available online.

References

Athlani L, Pauchard N, Dautel G. Intercarpal ligamentoplasty for scapholunate dissociation: comparison of two techniques. J Hand Surg Eur. Epub ahead of print 19 July 2020a. DOI: 10.1177/1753193420940498.

Athlani L, Rouizi K, Granero J et al. Assessment of scapholunate instability with dynamic computed tomography. J Hand Surg Eur. 2020b, 45: 375–82.

Lionel Athlani[1,2,*], Aymeric Rauch[3], Nicolas Weber[2], Alain Blum[2,3], Gilles Dautel[1] and Pedro Augusto Gondim Teixeira[2,3]

[1]Department of Hand Surgery, Plastic and Reconstructive Surgery, Nancy University Hospital, Nancy, France
[2]IADI, Université de Lorraine, Nancy, France
[3]Guilloz Imaging Department, Nancy University Hospital, Nancy, France
*Corresponding author: lionel.athlani@gmail.com

doi: 10.1177/1753193420973883 available online at http://jhs.sagepub.com

Supplementary Results

In this cadaveric study, 4DCT also allowed a dynamic and quantitative analysis of the LCA and the PRSA (Figure 3).

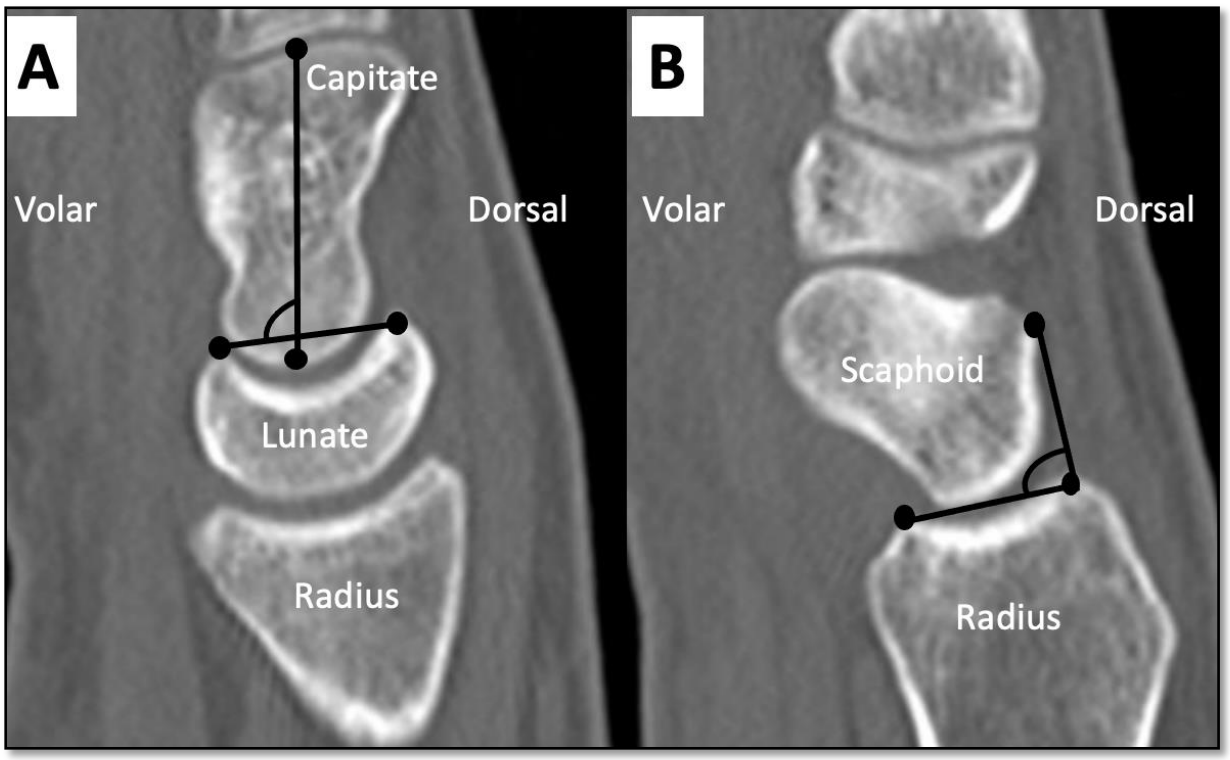

Figure 3. *In the CT multiplanar images, for construction of the LCA (A), two markers were placed in volar and dorsal horns of lunate bone and two other markers were positioned over capitate bone long axis, in sagittal plane located closest to the center of the lunate fossa of the radius. For construction of the PRSA (B), two markers were placed in posterior and anterior rims of scaphoid fossa of radius and two other markers were positioned in the posterior-most point of scaphoid and posterior rim of scaphoid fossa, in sagittal plane located closest to the center of the scaphoid fossa of the radius.*

Assessment of LCA

Between the three time points (before and after ligaments sectioning, after SLIC ligamentoplasty), we didn't note a significant difference in all median values of the LCA parameters ($p>0.05$) (Table 2).

Table 2. Outcomes for the LCA measured on 4DCT.

Measurements of LCA	Pre-ligaments sectioning (n=6)	Post-ligaments sectioning (n=6)	Post-ligamentoplasty (n=6)
Mean (mm)	79 (78 - 86) NS*	78 (76 - 80) NS**	81 (79 - 90) NS***
Maximal (mm)	84 (81 - 91) NS*	82 (79 - 87) NS**	85 (83 - 95) NS***
Coefficient of variation (%)	4.5 (4 – 5.1) NS*	3.7 (3 – 4.1) NS**	2.5 (1.8 – 4.5) NS***
Range (mm)	10 (9 - 11) NS*	10 (7 - 11) NS**	7 (5 - 10) NS***

The data shown are median (interquartile range)

NS: no significant difference

**p values shown in this column are results compared between the Pre-ligaments sectioning and the Post-ligaments sectioning.*

***p values shown in this column are results compared between the Post-ligaments sectioning and the Post-ligamentoplasty.*

****p values shown in this column are results compared between the Post-ligamentoplasty and the Pre-ligaments sectioning.*

The software measurement accuracy was estimated as 1°.

Assessment of PRSA

After ligaments sectioning, median values of the $PRSA_{mean}$ and $PRSA_{max}$ were significantly increased (p=0.04 and 0.03 with a 12% and 15% increase, respectively). After the SLIC ligamentoplasty, we noted a significant improvement in these parameters (p=0.03) with no statistically difference with median values before ligaments sectioning time (p>0.05) (Table 3).

Table 3. Outcomes for the PRSA measured on 4DCT.

Measurements of PRSA	Pre-ligaments sectioning (n=6)	Post-ligaments sectioning (n=6)	Post-ligamentoplasty (n=6)
Mean (mm)	108	121	106
	(99 - 122)	(117 - 128)	(103 - 111)
	0.04*	0.03**	NS***
Maximal (mm)	111	128	112
	(104 - 124)	(121 - 132)	(110 - 114)
	0.03*	0.03**	NS***
Coefficient of variation (%)	2.3	2.2	4.4
	(1.4– 4.7)	(1.3 – 3.4)	(2.8 – 4.9)
	NS*	NS**	NS***
Range (mm)	8	8	13
	(5 - 13)	(6 - 13)	(9 - 15)
	NS*	NS**	NS***

The data shown are median (interquartile range)

NS: no significant difference

**p values shown in this column are results compared between the Pre-ligaments sectioning and the Post-ligaments sectioning.*

***p values shown in this column are results compared between the Post-ligaments sectioning and the Post-ligamentoplasty.*

****p values shown in this column are results compared between the Post-ligamentoplasty and the Pre-ligaments sectioning.*

The software measurement accuracy was estimated as 1°.

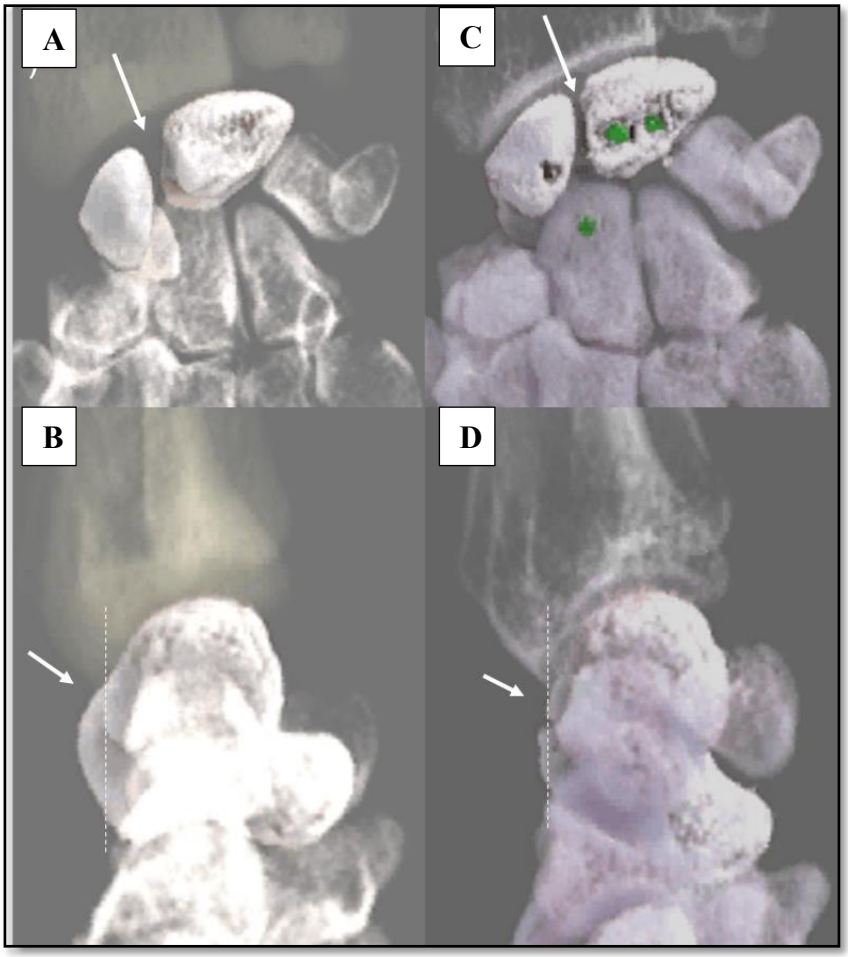

Figure 4. *Three-dimensional cinematic rendering images acquired in 4DCT at the level of the scapholunate joint after ligaments sectioning and after SLIC reconstruction. Frist, we observe the anatomical features of scapholunate dissociation (A, B). Then, we observe the correction of scapholunate dissociation (C, D).*

- *Comparaison des résultats avec la version initiale*

Full Length Article

JHS(E)

Journal of Hand Surgery
(European Volume)
0(0) 1–8

DOI: 10.1177/1753193420940498
journals.sagepub.com/home/jhs
SAGE

Intercarpal ligamentoplasty for scapholunate dissociation: comparison of two techniques

Lionel Athlani[1], Nicolas Pauchard[2] and Gilles Dautel[1]

Abstract

We modified our original surgical technique of scapholunate intercarpal ligamentoplasty for treating chronic scapholunate dissociation. The aim of this study was to compare the outcomes in patients treated by the same surgical team with the original method and the modified method over two different time periods. Nineteen patients with a mean age of 40 years were treated with the original method (mean follow-up of 34 months, range 12–54), and 21 patients with a mean age of 38 years were treated with the modified method (mean follow-up of 27 months, range 13–40). In both groups, we found a significant improvement in pain levels, grip strength, functional scores in terms of QuickDASH and Patient-Rated Wrist Evaluation, and radiographic scapholunate gap and scapholunate angle after surgery. There were no significant differences between the two groups in outcome measures except the scapholunate gap, which was significantly better controlled by the modified procedure. Between the immediate postoperative period and the last follow-up, there was a significant increase in the scapholunate gap and scapholunate angle after the original method, while there only a small increase after the modified method. We conclude that both versions of the scapholunate intercarpal ligamentoplasty yield satisfactory clinical and radiological results in the short to mid-term. The modified method makes the triquetral surgical step easier and seems to better optimize the tension across the ligamentoplasty, thus maintaining the intercarpal correction.

Level of evidence: III

Keywords

Scapholunate and intercarpal ligamentoplasty, scapholunate dissociation, scapholunate ligament, wrist instability

Date received: 25th April 2020; revised: 13th June 2020; accepted: 16th June 2020

Introduction

Scapholunate dissociation is a common cause of intracarpal instability. If left untreated, it contributes to the development of scapholunate advanced collapse (SLAC) osteoarthritis. Several tenodesis techniques have been described for treating symptomatic chronic reducible scapholunate dissociation when no chondral lesions are present. They all aim to reduce the scaphoid rotary subluxation and lunate extension (dorsal intercalated segment instability, DISI) to prevent SLAC wrist (Crawford et al., 2016). Recently, we described the scapholunate intercarpal ligamentoplasty (SLICL) that uses a free palmaris longus graft to reconstruct the dorsal segment of the scapholunate interosseous ligament (SLL) and the dorsal intercarpal ligament (DICL) in order to combat the scaphoid flexion deformity, the scapholunate gap (SLG) and DISI deformity (Athlani et al., 2018a). Indeed, biomechanical studies have highlighted the important stabilizing role of extrinsic dorsal ligaments (Mitsuyasu et al., 2004; Short

[1]Department of Hand Surgery, Plastic and Reconstructive Surgery, Centre Chirurgical Emile Gallé, CHU Nancy, France
[2]Service de Chirurgie de la Main – SOS main. Hôpital Privé Dijon Bourgogne, France

Corresponding Author:
Lionel Athlani, Department of Hand Surgery, Plastic and Reconstructive Surgery, Centre Chirurgical Emile Gallé, 49 rue Hermite, 54000 Nancy, France.
Email: lionel.athlani@gmail.com

et al., 2007). This finding corroborates the importance of reconstructing the DICL.

We have previously reported satisfactory clinical and radiological results with short- to mid-term follow-up. However, between the immediate postoperative period and the last follow-up, there was a significant increase in the SLG and scapholunate angle (SLA). The significant increase in these two radiographic parameters occurred in the subset of 15 wrists with static instability (Athlani et al., 2018a). Here, we report on a modification to our surgical technique that increases the tension in the ligamentoplasty. We then compare the results of the two versions with a minimum follow-up of 12 months.

Methods

Patients

From March 2013 to September 2016, we treated 19 patients (12 men and seven women, 15 from the previous study) with chronic scapholunate dissociation with the original SLICL procedure (2018a) (Figure 1(a)). From October 2016 to January 2019, we treated 21 patients (16 men and five women) with the modified procedure (Figure 1(b)). This was an institutional review board-approved study, in the same facility, over two different time periods.

All patients underwent a full imaging evaluation consisting of standard radiographs with posterior–anterior (PA) and lateral views, dynamic clenched fist views and CT arthrogram. All patients were diagnosed with chronic static reducible scapholunate instability (Watson et al., 1997) with no chondral damage, which corresponds to Stage 4 in the Garcia-Elias classification (Garcia-Elias et al., 2006). Before the ligament reconstruction, arthroscopy of the injured wrist was performed in all cases to confirm the scapholunate instability, quantify its magnitude (Dreant and Dautel, 2003), verify the scaphoid was easily reducible and confirm that no chondrosis was present.

Both groups of patients were reviewed twice, in person, using the same methodology by the same independent examiner of experience Level IV according to Tang (2009). After obtaining each patient's consent, a clinical and radiographic assessment was performed after a minimum follow-up of 12 months.

Surgical technique and postoperative protocol

The surgical procedures (Figure 2) were performed by senior surgeons of experience Level IV according to Tang (2009) and Tang and Giddins (2016) with the patient under regional anaesthesia and a tourniquet applied on the upper arm.

For both procedures, the objective was to create two segments: a scapholunatetriquetral segment that corrects the SLG and a triquetrolunatescaphoid segment that corrects the DISI deformity and scaphoid rotary subluxation. The use of a free palmaris longus graft allows for tendinous pretensioning to prevent ligamentous loosening.

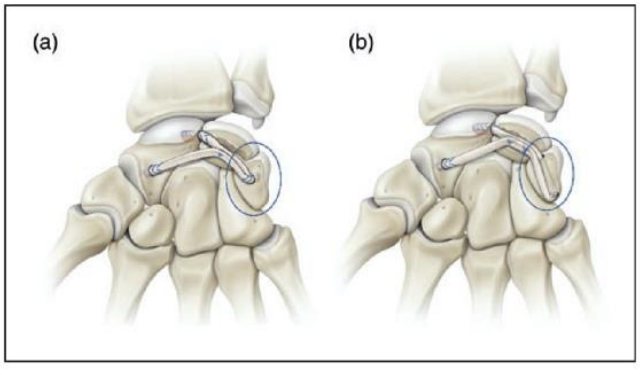

Figure 1. Diagram showing the original version (a) and the modified version (b) of the scapholunate intercarpal ligamentoplasty (SLICL).

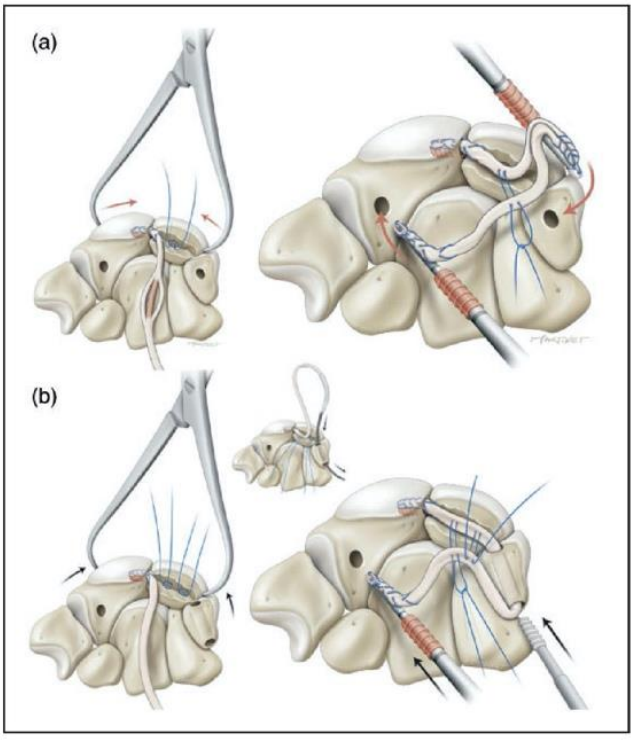

Figure 2. Diagram illustrating the different surgical steps of the both versions (a: original; b: modified) of the scapholunate intercarpal ligamentoplasty.

A dorsal incision was made along the axis of the third metacarpal centred on the midline of the radiocarpal joint. The extensor retinaculum was opened between the third and fourth compartments, and a dorsal capsulotomywas performed according to Berger et al. (1995). We then harvested a 10-cm free palmaris longus graft through a short incision. This graft was pretensioned with 3 kg for 2 minutes on a dedicated workstation (Arthrex®, Naples, FL, USA). The first scaphoid blind tunnel, 10 mm deep and 2.5 mm wide, was drilled at the site of the former scaphoid insertion of the dorsal segment of the SLL (proximal pole of the scaphoid). The posterior surface of the lunate was then reamed to create a shallow trench to serve as the interface for graft adhesion. A second scaphoid blind tunnel of the same depth and width was drilled at the level of the scaphoid isthmus near the scaphotrapezotrapezoidal (STT) joint surface. One of the two ends of the graft was then whip stitched over a length of 10 mm with non-absorbable Fiberloop™ 4-0 suture (Arthrex®), wedged into the first proximal scaphoid tunnel, and secured by interference fit with an impacted 2.5 absorbable Mini Bio-Pushlock™ anchor (Arthrex®). The dissociation was then reduced manually with the aid of pointed reduction forceps. Stabilization was achieved by scapholunate and scaphocapitate pinning (1.2 mm K-wires).

In the original SLICL procedure (Figure 2(a)), one 2.2-mm non-absorbable titanium MicroCorkscrew™ anchor (Arthrex®) was introduced into the lunate trench. Then, a triquetral blind tunnel, 10 mm deep and 2.5 mm wide, was drilled in the dorsal aspect of the bone near the radial side of the dorsal radiocarpal ligaments, following the axis of the lunate trench. Fixing the graft in the second triquetral tunnel meant both tapering it and performing a longitudinal plication. The central half was resected over 12 mm starting from the entry point in the second tunnel. The two resulting half strips were folded back onto themselves to create a new intermediary graft end as thick as the other two ends over a length of 6 mm. This new end was then whip stitched over 10 mm before inserting it into the second blind tunnel and attaching it with a Pushlock™ anchor.

We modified the original procedure because we felt this triquetral step contributed to fragility, and furthermore, it was difficult to generate optimal tension in the ligamentoplasty. The modification aimed to anchor the graft within the triquetrum (Figure 2(b)). First, we added a second 2.2 mm non-absorbable titanium MicroCorkscrew™ anchor into the lunate trench, one near the scapholunate joint space and another near triquetral joint space. Then, we drilled a 3.0-mm transosseus triquetral tunnel. Taking care to avoid damage to the triquetrum dorsal cortex, we placed the entry point of this tunnel directly distal to the lunotriquetral joint space with an axis parallel to the triquetrohamate joint. Then we passed the transplant through the tunnel using a QuickPass Tendon Shuttle™ (Arthrex®).

The scapholunate–triquetral graft segment was placed in the lunate trench, and the optimal tension was adjusted by pulling the remaining free graft. As soon as enough tension was obtained, we locked it in place with a 3.0 mm absorbable Tenodesis Screw™ (Arthrex®) through the ulnar side of the tunnel. The last step of the procedure was unchanged: the graft located between the first two intraosseous fixation points was fixed with the anchor sutures in the lunate trench.

To create the second segment, the remainder of the graft was again passed through the lunate trench and fixed by the same anchor sutures to superimpose the two segments in the tunnel. The remaining free end was resected at least 8 mm from the entry point in the second scaphoid blind tunnel and then inserted into the tunnel. To do so, this last end was whip stitched over 10 mm and fixed to the bottom of the second tunnel by impacting a Pushlock™ anchor. At this point, the tension of both segments was tested with a tendon hook. The final step consisted of suturing the capsule and retinaculum with absorbable PDS™ sutures (Ethicon®, One Johnson & Johnson Plaza, New Brunswick, NJ, USA) and the skin with non-absorbable sutures. The entire material-price is around 600 Euros for the original procedure and 700 Euros for the modified procedure.

Postoperative protocol

Immediately following surgery, the wrist was immobilized in a volar plaster cast for 2–3 days. Immobilization was extended for 2 months with a short-arm fibreglass cast. K-wires were removed 2 months postoperatively, and physiotherapy sessions were initiated. Heavy loading of the wrist was avoided for the first 6 months.

Clinical and functional evaluation

Pain at rest and during effort was evaluated using a visual analogue scale (0–10). Grip strength in the operated and contralateral side was collected using a Jamar® hydraulic hand dynamometer (Performance Health®, Charleville-Mézières, France). The active joint range of motion (ROM) in the operated wrist was measured in degrees with a goniometer (Prestige® Medical, Northridge, CA, USA) of accuracy up to 2° during wrist flexion, extension, radial deviation and ulnar deviation.

The functional outcomes were evaluated using standardized questionnaires: Quick version of the Disabilities of the Arm, Shoulder and Hand questionnaire (QuickDASH) (out of 100) and the Patient-Rated Wrist Evaluation (PRWE) (out of 100). The number of physiotherapy sessions attended and the time away from work were also recorded.

Radiologic evaluation

At the final review, standard radiographic views, standard neutral PA and lateral views, and a clenched fist PA view were taken in all patients. Immediately after surgery, only standard radiographic views were taken. The digital radiographs were viewed on J4care Smooth Viewer© (J4Care GmbH, Mödling, Austria). The static and dynamic SLG in millimetres as well as the SLA in degrees were calculated (0.1 mm accuracy for gaps and 1° for angles). SLG values greater than 3 mm were considered pathological, along with SLA greater than 70° (Larsen et al., 1991). Finally, the presence of posterior scaphoid subluxation was evaluated in the lateral view, as described by Athlani et al. (2018b). We also checked for narrowing in the radiocarpal and midcarpal joints.

Statistical analysis

Qualitative variables were described by their counts and percentages. Quantitative variables were summarized using mean values and ranges. Data were compared between groups using the paired Student's *t* test. The between-group characteristics were compared using the Fisher test or the chi squared test depending on the nature of the data. The significance level was set at $p < 0.05$.

Results

The two groups of patients had comparable preoperative characteristics (Table 1). In every patient, CT arthrogram revealed a full tear of the SLL with contrast leakage. Stage 3 instability was found in all cases arthroscopically. There was no chondral damage. The time to surgery was similar between the two groups. All the surgical procedures used a free palmaris longus graft. The surgical wound had healed in all patients after 2 weeks, and K-wires protecting the reconstruction were removed after a mean of 62 days (range 58–65).

Physiotherapy was initiated in all patients, and they attended an average of 30 sessions (range 20–60). The time away from work averaged 5 months (3–12) in the original SLICL procedure group and 4 months (1–10) in the modified procedure group. The mean follow-up time after surgery was 34 months (range 12–54) for the original SLICL procedure group and 27 months (range 13–40) for the modified procedure group (Figure 3). The results for both groups are listed in Table 2.

Clinical and functional outcomes

For both groups, pain levels at rest and during effort, grip strength and functional scores (QuickDASH and PRWE) were significantly improved at the final follow-up relative to the preoperative values ($p < 0.05$). The grip strength as a percentage of the contralateral side was 88% (55% preoperative) in the original SLICL procedure group and 90% (60% preoperative) in the modified procedure group. Comparatively with the preoperative period, there was no significant differences ($p > 0.05$) in ROM of the wrist for both groups at the review. There were no significant differences between groups ($p > 0.05$) for each clinical measurement.

Table 1. Patient characteristics.

Patients	Original ($n = 19$)	Modified ($n = 21$)
Average age (range), years	40 (22–50)	38 (26–49)
Sex	12 men7 women	16 men5 women
Wrist	11 right 8 left	14 right 7 left
Dominant side	13 (68%)	16 (76%)
Heavy manual labour	11 (58%)	10 (48%)
Time to surgery (range), months	12 (5–60)	10 (3–48)
Static instability	19 wrists	21 wrists
Staging (Garcia-Elias, 2006)	Stage 4	Stage 4
Arthroscopic classification (Dreant and Dautel, 2003)	Stage 3: 19 No chondral lesions: 19	Stage 3: 21 No chondral lesions: 21

Radiological outcomes

For both groups, there was a significant ($p < 0.05$) reduction in the mean static and dynamic SLG, as well as the SLA (Figure 4). At the final follow-up, all the mean values in the two groups were considered as non-pathological except for the dynamic SLG in the group of the original method (3.5 mm before versus 4.9 mm after surgery). Static and dynamic SLGs were reduced significantly more in the group of the modified method than that of the original method ($p < 0.05$). The difference in the SLA was not statistically significant between groups. In all cases, the posterior scaphoid subluxation was corrected in the lateral view. None of the patients had signs of SLAC osteoarthritis.

Between the immediate postoperative period and the last follow-up, there was a significant increase of 0.7 mm in the static SLG and of 9° in SLA for the group of the original method ($p < 0.01$). The corresponding increases of 0.3 mm and of 4° in the modified procedure group were not significant.

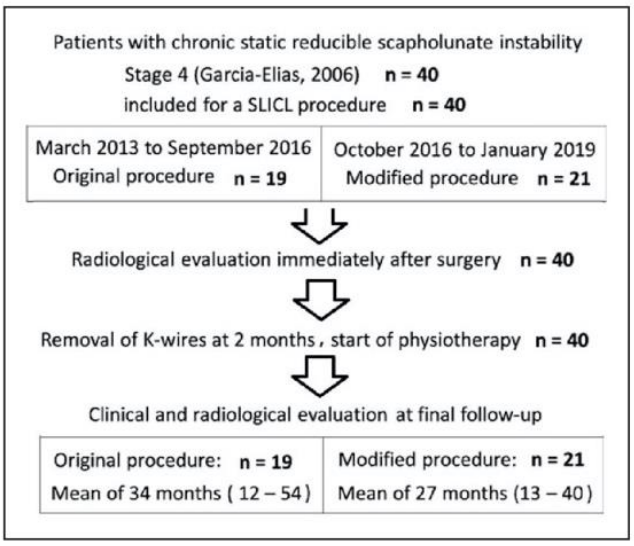

Figure 3. Flowchart of the study.

Complications and surgical revisions

Three patients receiving the original technique and one receiving the modified procedure developed De Quervain's tenosynovitis. All cases resolved with brace and corticosteroid injection. In the modified procedure group, one patient reported symptoms of type

Table 2. Clinical and radiographic outcomes (mean and range) for patients treated with two versions of methods.

	Original method ($n = 19$)				Modified method ($n = 21$)				Comparison of differences
Average values	Preop	Follow-up	Difference	*P* values	Preop	Follow-up	Difference	*P* values	*P* values
Pain at rest	4	0.5	−3.5	0.01	3.7	0.6	−3.1	0.01	0.17
Pain during effort	7	1.9	−5.1	0.01	6.5	2	−4.5	0.01	0.14
Grip strength (Kg/F)	24	40	+16	0.01	26	42	+16	0.01	0.89
Wrist flexion (°)	54	52	−2	0.68	56	52	−5	0.27	0.24
Wrist extension (°)	50	48	−2	0.59	52	48	−4	0.46	0.34
Ulnar deviation (°)	30	30	0	0.88	32	30	−2	0.76	0.45
Radial deviation (°)	16	16	0	0.73	15	14	−1	0.56	0.86
QuickDASH score	60	20	−40	0.01	53	18	−45	0.01	0.09
PRWE score	55	14	−41	0.01	52	13	−39	0.01	0.27
Static scapholunate gap (mm)	4.0	2.7	−1.3	0.01	4.3	2.3	−2	0.01	0.03
Dynamic scapholunate gap (mm)	4.9	3.5	−1.4	0.01	5.2	3.0	−2.2	0.01	0.02
Scapholunate angle (°)	81	65	−16	0.01	76	62	−14	0.01	0.14
	Immediate postoperative		Follow-up	P values	Immediate postoperative		Follow-up	P values	
Static scapholunate gap (mm)	2.0		2.7	0.009	2.0		2.3	0.57	
Scapholunate angle (°)	56		65	0.001	58		62	0.09	

Follow-up: 34 months (12–54) for original SLICL procedure and 27 months (12–40) for modified procedure.
PRWE: Patient-Rated Wrist Evaluation; SLICL: scapholunate intercarpal ligamentoplasty.

Figure 4. Posterior–anterior (a) and lateral (b) radiographs of a right wrist with a scapholunate dissociation. Posterior–anterior (c) and lateral (d) radiographs at 36 months' follow-up after treatment with the modified procedure.

one complex regional pain syndrome, which resolved with medical treatment. No patients in either group required additional wrist or hand surgery.

Discussion

Our results show that the two versions of the SLICL reconstruction significantly reduced pain and increase grip strength. We found no significant difference between two versions in terms of clinical outcomes at the final follow-up. The two versions of the procedure corrected the radiologic features of scapholunate dissociation. However, the modified version was more effective at controlling the SLG than the original one.

Several tenodesis techniques are designed to treat chronic, reducible scapholunate instability in the absence of chondral lesions (Crawford et al., 2016). Some use a distally based slip of the extensor carpi radialis brevis (Brunelli and Brunelli, 1995; Linscheid and Dobyns, 1992). Others use a slip of extensor carpi radialis longus (De Carli et al., 2011; Peterson and Freeland, 2010). The Brunelli technique modified by Van Den Abbeele et al. (1998) and the Garcia-Elias Three-ligament Tenodesis (3LT) (Garcia-Elias et al., 2006) use a pedicled slip of the flexor carpi radialis (FCR) to reconstruct the dorsal segment of the SLL and vertically reposition the scaphoid. The last two procedures were the basis for a number of clinical studies (Chabas et al., 2008; De Smet and Van Hoonacker, 2007; Elgammal and Lukas, 2016; Ellanti et al., 2014; Garcia-Elias et al., 2006; Links et al., 2008; Moran et al., 2006; Nienstedt, 2013; Pauchard et al., 2013; Talwalkar et al., 2006; Van Den Abbeele et al., 1998). The sample sizes in these studies are roughly comparable with that of our present study. Furthermore, these authors generally reported similar clinical findings with a remarkable reduction in pain levels and improvement in grip strength. Patients in both our groups had no significant differences in the wrist ROM before and after surgery. However, the average postoperative flexion–extension was 100°, comparable with that reported after FCR tenodesis procedures. Indeed, in these studies, the wrist flexion–extension ranged from 82° (Pauchard et al., 2013) to 103° (Garcia-Elias et al., 2006). Nevertheless, in most of these reports, the average wrist flexion was approximately 40°, while we found an average of 48°. Our relative preservation of wrist flexion can be attributed to not using a volar approach or the FCR.

The SLICL procedure does not disturb the wrist flexors or extensors, which are wrist stabilizers. Kauer (1980) speculated about muscular contributions in wrist stability. Linscheid and Dobyns (2002) and Short et al. (2007) suggested that the bowstringing force exerted by the FCR tendon on the scaphoid tuberosity may help prevent carpal collapse of wrists with dynamic instability. In a cadaver study, Esplugas et al. (2016) assessed the role of muscles in wrist stabilization. According to these reports, isometric contractions of some forearm muscles are likely to prevent scaphoid rotary subluxation in wrists with scapholunate ligament insufficiency. Isometric loading of the wrist flexors or extensors results in a consistent closure of the scapholunate joint gap and repositioning of the scaphoid proximal pole on the surface of the radioscaphoid fossa. In the same way, the 'blind' nature of the scaphoid tunnels also prevents the complications associated with the trans-scaphoid tunnel used in FCR tenodesis procedures, such as proximal pole necrosis (De Smet and Van Hoonacker, 2007).

In both groups, we found a significant reduction in SLG and SLA, with a return to normal values (Larsen et al., 1991) except for the dynamic SLG in the original SLICL procedure group (3.5 mm postoperatively). With the original SLICL procedure, the SLG and SLA increased significantly between the immediate postoperative period and the last follow-up. At similar average follow-up (27 versus 34 months), this did not occur with the modified

procedure, which we believe results from better tension in the ligamentoplasty. However, we still found a slight increase of 0.3 mm and 4° for the SLG and SLA, respectively. Some ligament loosening seems to have occurred despite preloading the palmaris longus graft, likely during that free graft's healing, particularly in these patients with static instability where high stresses occur. Therefore, it is essential to keep the K-wires in place for 2 months. As an alternative, Kakar and Greene (2018) propose using an InternalBrace™ Ligament Augmentation Repair (Arthrex®) with the scapholunate tenodesis. According to them, given the added stability afforded by intrinsic bracing, the ligament reconstruction may be mobilized earlier without the need for K-wire stabilization. However, the authors reported on only one patient with a year follow-up.

The reducible nature of the dissociation is the basic criterion that must be met to indicate scapholunate ligament reconstruction. An accurate assessment of the reducible nature of this dissociation is key. Performing dynamic manoeuvres during the arthroscopy and taking dynamic radiographic views during ulnar and radial deviation is the best way to do this preoperatively. Also, during the surgical procedure, it is essential to confirm the dissociation can be reduced 'easily' (repositioning of the scaphoid) right away. Unfortunately, there is no method to quantify the loads needed to reduce the scaphoid.

De Roo et al. (2019) used four-dimensional computerized tomography to study scaphoid motion in healthy wrists. They reported the scaphoid flexes 38° relative to the lunate between wrist extension and flexion. This new imaging modality could be used to assess the residual mobility of the scaphoid in the event of scapholunate instability. In all our patients, the posterior scaphoid subluxation was corrected in the lateral view, and there were no signs of SLAC osteoarthritis. This subluxation is considered the primary cause of radioscaphoid osteoarthritis. Chabas et al. (2008) reported SLAC osteoarthritis in 5% of cases, Nienstedt (2013) in 13%, Moran et al. (2006) in 13% and Garcia-Elias et al. (2006) in 23%.

Our study has its limitations. First, the sample size was limited in each group, although it was consistent with other published studies. We did not perform statistical power analysis as the mean differences in the variables between two groups were very small. Clinically, the differences are of no practical significance. Second, the surgical procedures were performed asynchronously. Nevertheless, the same surgical team was involved, and all the surgeons used the same standardized procedure. Lastly, we used the CT arthrogram for the assessment of SLL injuries. CT arthrogram has a high performance for the diagnosis SLL tears (95–100% sensitivity and 86–100% specificity) (Bille et al., 2007). However, MR arthrogram can be also performed to assess SLL tears with a good diagnostic performance (65–89% sensitivity and 90–100% specificity) (Lee et al., 2013). Lee et al. (2017) compared oblique axial planes on multidetector CT arthrogram and MR arthrogram to evaluate dorsal and volar parts of SLL. They determined that the accuracy of reformatted oblique axial imaging on CT arthrogram performed better than direct oblique axial imaging with MR arthrogram. This was most likely due to the improved spatial resolution and interactive nature of CT reformation.

The results of this study corroborate our previous clinical study's findings (Athlani et al., 2018a) that the SLICL procedure is effective for reducing scapholunate dissociation and restoring scapholunate joint stability. Our modified procedure makes the triquetral surgical step easier and seems to optimize the tension across the ligamentoplasty, thus retaining the intracarpal correction obtained during the intraoperative step. An additional study is needed to extend the follow-up period and ensure that these results are maintained long-term, and that SLAC osteoarthritis does not develop.

Acknowledgements The authors wish to thank Dr Joanne Archambault for English language editing assistance. The authors wish to thank Mr Cyrille Martinet for the illustrations.

Declaration of conflicting interests The authors declared the following potential conflicts of interest with respect to the research, authorship, and/or publication of this article: Nicolas Pauchard and Gilles Dautel declare a conflict of interest with Arthrex® (consultancies). Lionel Athlani declares no potential conflicts of interest.

Ethical approval This study was approved by our institutional review board and by the local ethics committee (Personal Protection Committee EST-III, Vandœuvre-les-Nancy, France). This study was registered with the no. NCT02401568.

Funding The authors received no financial support for the research, authorship, and/or publication of this article.

Informed consent All patients gave their informed consent for this study.

References

Athlani L, Pauchard N, Dautel G. Outcomes of scapholunate intercarpal ligamentoplasty for chronic scapholunate dissociation: a prospective study in 26 patients. J Hand Surg Eur. 2018a, 43: 700–7.

Athlani L, Pauchard N, Dautel G. Radiological evaluation of scapholunate intercarpal ligamentoplasty for chronic scapholunate dissociation in cadavers. J Hand Surg Eur. 2018b, 43: 387–93.

Berger RA, Bishop AT, Bettinger PC. New dorsal capsulotomy for the surgical exposure of the wrist. Ann Plast Surg. 1995, 35: 54–9.

Bille B, Harley B, Cohen H. A comparison of CT arthrography of the wrist to findings during wrist arthroscopy. J Hand Surg Am. 2007, 32: 834–41.

Brunelli GA, Brunelli GR. A new technique to correct carpal instability with scaphoid rotary subluxation: a preliminary report. J Hand Surg Am. 1995, 20: 82–5.

Chabas JF, Gay A, Valenti D, Guinard D, Legre R. Results of the modified Brunelli tenodesis for treatment of scapholunate instability: a retropective study of 19 patients. J Hand Surg Am. 2008, 33: 1469–77.

Crawford K, Owusu-Sarpong N, Day C, Iorio M. Scapholunate ligament reconstruction: a critical analysis review. J Bone Joint Surg Am. 2016, 4: 41–8.

De Carli P, Donndorff AG, Gallucci GL, Boretto JG, Alfie VA. Chronic scapholunate dissociation: ligament reconstruction combining a new extensor carpi radialis longus tenodesis and a dorsal intercarpal ligament capsulodésis. Tech Hand Up Extrem Surg. 2011, 15: 6–11.

De Roo MGA, Muurling M, Dobbe JGG, Brinkhorst ME, Streekstra GJ, Strackee SD. A four-dimensional-CT study of in vivo scapholunate rotation axes: possible implications for scapholunate ligament reconstruction. J Hand Surg Eur. 2019, 44: 479–87.

Dreant N, Dautel G. Development of an arthroscopic severity score for scapholunate instability. Chir Main. 2003, 22: 90–4.

De Smet L, Van Hoonacker P. Treatment of chronic static scapholunate dissociation with the modified Brunelli technique: preliminary results. Acta Orthop Belg. 2007, 73: 188–91.

Elgammal A, Lukas B. Mid-term results of ligament tenodesis in treatment of scapholunate dissociation: a retrospective study of 20 patients. J Hand Surg Eur. 2016, 41: 56–63.

Ellanti P, Sisodia G, Al-Ajami A, Ellanti P, Harrington P. The modified Brunelli procedure for scapholunate instablity: a single-centre study. Hand Surg. 2014, 19: 39–42.

Esplugas M, Garcia-Elias M, Lluch A, Llusá Pérez M. Role of muscles in the stabilization of ligament-deficient wrists. J Hand Ther. 2016, 29: 166–74.

Garcia-Elias M, Lluch AL, Stanley JK. Three-ligament tenodesis for the treatment of scapholunate dissociation: indications and surgical technique. J Hand Surg Am. 2006, 31: 125–34.

Kakar S, Greene RM. Scapholunate ligament internal brace 360 degree tenodesis (SLITT) procedure. J Wrist Surg. 2018, 7: 336–40.

Kauer JM. Functional anatomy of the wrist. Clin Orthop Relat Res. 1980, 149: 9e20.

Larsen CF, Mathiesen FK, Lindequist S. Measurement of carpal bone angles on lateral wrist radiographs. J Hand Surg Am. 1991, 16: 888–93.

Lee YH, Choi YR, Kim S, Song HT, Suh JS. Intrinsic ligament and triangular fibrocartilage complex (TFCC) tears of the wrist: comparison of isovolumetric 3D-THRIVE sequence MR arthrography and conventional MR image at 3T. Magn Reson Imaging. 2013, 31: 221–26.

Lee RK, Griffith JF, Ng AW et al. Intrinsic carpal ligaments on MR and multidetector CT arthrography: comparison of axial and axial oblique planes. Eur Radiol. 2017, 27: 1277–85.

Links AC, Chin SH, Waitayawinyu T, Trumble TE. Scapholunate interosseous ligament reconstruction: results with modified Brunelli technique versus four-bone weave. J Hand Surg Am. 2008, 33: 850–6.

Linscheid RL, Dobyns JH. Treatment of scapholunate dissociation. Rotatory subluxation of the scaphoid. Hand Clin. 1992, 8: 645–52.

Mitsuyasu H, Patterson RM, Shah MA, Buford WL, Iwamoto Y, Viegas SF. The role of the dorsal intercarpal ligament in dynamic and static scapholunate instability. J Hand Surg Am. 2004, 29: 279–88.

Moran SL, Ford KS, Wulf CA, Cooney WP. Outcomes of dorsal capsulodesis and tenodesis for treatment of scapholunate instability. J Hand Surg Am. 2006, 31: 1438–46.

Nienstedt F. Treatment of static scapholunate instability with modified Brunelli tenodesis: results over 10 years. J Hand Surg Am. 2013, 38: 887–92.

Pauchard N, Dederichs A, Segret J, Barbary S, Dap F, Dautel G. The role of three-ligament tenodesis in the treatment of chronic scapholunate instability. J Hand Surg Eur. 2013, 38: 758–66.

Peterson SL, Freeland AE. Scapholunate stabilization with dynamic extensor carpi radialis longus tendon transfer. J Hand Surg Am. 2010, 35: 2093–100.

Short WH, Werner FW, Green JK, Sutton LG, Brutus JP. Biomechanical evaluation of ligamentous stabilizers of the scaphoid and lunate: part III. J Hand Surg Am. 2007, 32: 297–309.

Talwalkar SC, Edwards AT, Hayton MJ, Stilwell JH, Trail IA, Stanley JK. Results of tri-ligament tenodesis: a modified Brunelli procedure in the management of scapholunate instability. J Hand Surg Br. 2006, 31: 110–7.

Tang JB. Re: levels of experience of surgeons in clinical studies. J Hand Surg Eur. 2009, 34: 137–8.

Tang JB, Giddins G. Why and how to report surgeons' levels of expertise. J Hand Surg Eur. 2016, 41: 365–6.

Van Den Abbeele KL, Loh YC, Stanley JK, Trail IA. Early results of a modified Brunelli procedure for scapholunate instability. J Hand Surg Br. 1998, 23: 258–61.

Watson HK, Weinzweig J, Zeppieri J. The natural progression of scaphoid instability. Hand Clin. 1997, 13: 39–49.

- *Une nouvelle capsulotomie comme approche dorsale du poignet : étude cadavérique*

Hand Surgery and Rehabilitation xxx (xxxx) xxx–xxx

Available online at ScienceDirect www.sciencedirect.com

Elsevier Masson France EM|consulte www.em-consulte.com

Technical note

A new capsulotomy-based dorsal approach to the wrist: A cadaver study

Une nouvelle capsulotomie comme abord dorsal du poignet: étude cadavérique

L. Athlani [a,*], M.-C. Sapa [a], Y.-K. De Almeida [a], M. Braun [b], G. Dautel [a]

[a] Department of Hand Surgery, Plastic and Reconstructive Surgery, Centre chirurgical Emile Gallé, CHU de Nancy, 49, rue Hermite, 54000 Nancy, France
[b] Department of Anatomy, Faculty of Medicine, University of Lorraine, 9, avenue de la Forêt de Haye, 54505 Vandœuvre-lès-Nanc, France

ARTICLE INFO

Article history:
Received 30 August 2020
Received in revised form 22 October 2020
Accepted 23 October 2020
Available online xxx

Keywords:
Capsulotomy
Carpal bones
Dorsal approach
Midcarpal joint
Radiocarpal joint
Wrist

ABSTRACT

Using a cadaver study, we described a new dorsal approach to the wrist joint using a "U-shaped with proximal base" capsulotomy. Six fresh adult cadaveric wrists were dissected after intra-arterial silicone injection. We did a dorsal approach to expose the dorsal joint capsule. It was then possible to identify the dorsal radiocarpal and intercarpal ligaments, the dorsal radiocarpal and intercarpal arterial arches, the dorsal branch of the anterior interosseous artery and the terminal branch of the posterior interosseous nerve. Wrist arthrotomy was done using our capsulotomy. In each dissected capsular flap, we always found the individual ligament, vascular, and nerve structures, implying they were intact over their trajectories. The mean surface area of the articular exposure was 945 mm^2 (range 725–1102 mm^2) allowing easy access to the carpal bones and the radiocarpal and midcarpal joint spaces. This surgical approach to the wrist is technically feasible and avoids damaging the dorsal extrinsic ligaments fibers. Keeping the vascularization intact could improve capsular healing, while preserving innervation could maintain wrist proprioception.

Mots-clés:
Abord dorsal
Articulation médiocarpienne
Articulation radio-carpienne
Capsulotomie
Os du carpe
Poignet

RÉSUMÉ

À l'aide d'une étude cadavérique, nous avons décrit un nouvel abord dorsal pour l'articulation du poignet en utilisant une capsulotomie en forme de "U" à base proximale. Six poignets de cadavres adultes frais ont été disséqués après injection intra-artérielle de silicone. Par une voie d'abord dorsale, nous avons exposé la capsule articulaire dorsale. Il a alors été possible d'identifier les ligaments radio-carpien et intercarpien dorsaux, les arcades artérielles radiocarpienne et intercarpienne dorsales, la branche dorsale de l'artère interosseuse antérieure et la branche terminale du nerf interosseux postérieur. L'arthrotomie du poignet a été réalisée à l'aide de notre capsulotomie. Dans chaque lambeau capsulaire disséqué, nous avons systématiquement trouvé les structures ligamentaires, vasculaires et nerveuses individualisées, ce qui implique qu'elles étaient intactes sur leurs trajets. La surface moyenne de l'exposition articulaire était de 945 mm^2 (range 725–1102 mm^2) permettant un accès facile aux os du carpe et aux espaces articulaires radio-carpien et médiocarpien. Cet abord chirurgical du poignet est techniquement réalisable et évite d'endommager les fibres des ligaments extrinsèques dorsaux. Garder la vascularisation intacte pourrait améliorer la cicatrisation capsulaire, tandis que la préservation de l'innervation pourrait maintenir la proprioception du poignet.

Introduction

Several traumatic, rheumatic or degenerative pathologies require a wrist joint approach. Most authors suggest using a dorsal approach rather than a palmar one for easier exposure [1]. Several capsulotomy techniques have been described such as longitudinal, transverse, oblique, "L-shaped", "T-shaped" or

* Corresponding author.
E-mail addresses: lionel.athlani@gmail.com (L. Athlani), mc.sapa14@gmail.com (M.-C. Sapa), dealmeida_yk@yahoo.fr (Y.-K. De Almeida), Marc.Braun@medecine.uhp-nancy.fr (M. Braun), gillesdautel@mac.com (G. Dautel).

https://doi.org/10.1016/j.hansur.2020.10.015
2468-1229/

"distally-based U-shaped" designs [2]. The "V-shaped" fiber-splitting capsulotomy described by Berger et al. is the most commonly used [3]. Its main advantage is that it provides good exposure of the radiocarpal and midcarpal joint spaces. However, in an anatomical study, Hagert et al. showed that it failed to maintain the integrity of the dorsal radiocarpal ligament (DRCL) and dorsal intercarpal ligament (DICL) fibers [4]. Similarly, the dorsal capsular innervation provided by the posterior interosseous nerve (PION) is always interrupted with the Berger procedure. Hagert et al. also highlighted the importance of preserving this nerve for its proprioceptive function, which is essential during postoperative rehabilitation [4]. In this cadaver study, we wanted to describe a new dorsal wrist capsulotomy procedure, its technical feasibility, and its advantages with regards to preserving anatomical structures and exposing the carpal joint spaces.

Materials and methods

Study protocol

Six upper limbs (three left and three right) from fresh, unembalmed adult cadavers were provided by our Medical School Anatomy Laboratory. The limbs had been disarticulated at the scapulohumeral joint and were prepared using the same protocol by a specialist surgeon (LA) [5]. The radial and ulnar arteries were dissected through an incision at the anterior aspect of the forearm and isolated to perform arteriotomy of each artery and then inject colored silicone rubber (Microfil®, Carver, Massachusetts). Each artery received 10 cc of radio-opaque silicone and was ligated to limit the silicone's effusion outside the vascular pedicles studied. After 1 week's rest in the refrigerator, we dissected the dorsal side of each wrist using the same surgical technique.

Capsulotomy technique

This technique was developed by one of the authors (LA), a specialist surgeon [5] who performed all the dissections.

A dorsal incision was made along the axis of the third metacarpal, centered on the midline of the radiocarpal joint. The extensor retinaculum was opened between the third and fourth compartments. The fifth compartment was also opened. To expose the dorsal joint capsule, the extensor pollicis longus was retracted on the radial side, while the fourth and fifth compartment extensors were retracted on the ulnar side. It was then possible to identify the DRCL and DICL, the dorsal radiocarpal arterial arch (DRCA) and the dorsal intercarpal arterial arch (DICA), the dorsal branch of the anterior interosseous artery (AIOA) and the terminal branch of the PION.

The next step consisted of drawing an outline of the capsulotomy with a surgical marker (Purple surgical International, Herts, England). The design was "U-shaped with proximal base". The ulnar border was a longitudinal axis located directly on the triquetral bone insertion of the DRCL and DICL, respecting the dorsal ulnocarpal ligament. The radial border was a longitudinal axis located in the extension of the medial edge of the radial styloid process. Finally, the distal transverse branch was located directly distal to the DICA (Fig. 1). Using a scalpel blade (Swann-Morton®, Sheffield, England), an arthrotomy was performed without elevating a bony chip from the dorsal aspect of the triquetrum. The capsular flap was raised to expose the carpal bones and the radiocarpal and midcarpal joint spaces. The final step was suturing the capsule and retinaculum with absorbable PDS™ sutures (Ethicon®, One Johnson & Johnson Plaza, New Brunswick, NJ).

Descriptive anatomy

For each wrist, an independent examiner (MCS) documented the anatomical configuration (origin, trajectory, and insertion) of the DRCL, DICL, DRCA, DICA, dorsal branch of the AIOA and the terminal branch of the PION. He also measured the width and length of each capsulotomy border in millimeters (accuracy 1 mm) with a graduated ruler (Purple surgical International™, Herts, England). This information was used to determine the average surface area in mm^2 of the capsular flap and thus its exposure capacity relative to the carpal bones and joint spaces. The last step was checking that all these individual anatomical structures were

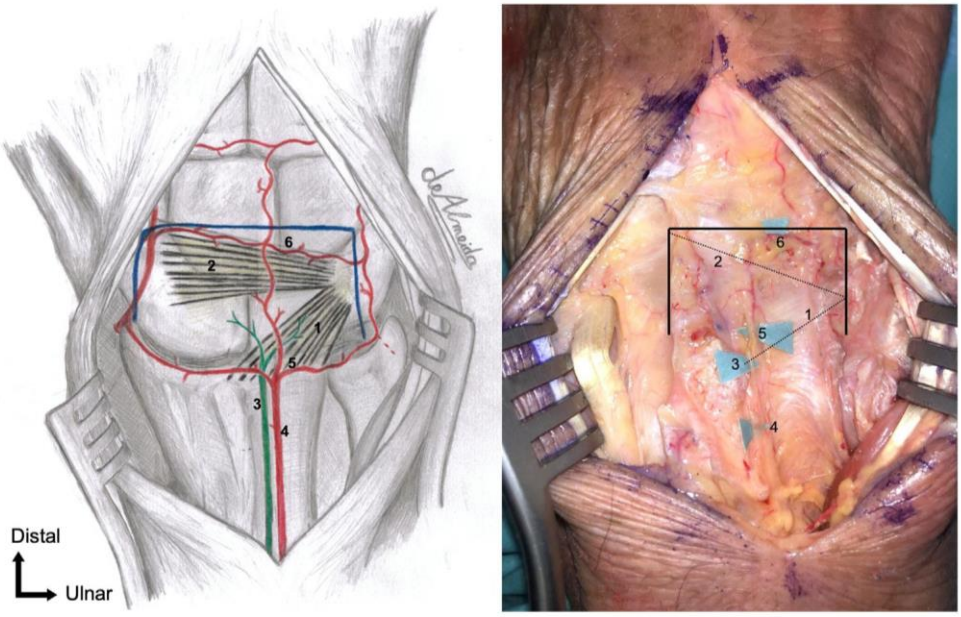

Fig. 1. Diagram and photograph of a posterior view of the wrist illustrating the anatomical structures and the outline of the capsulotomy (*black lines*). *1*: Dorsal radiocarpal ligament (DRCL) (*dashed line*); *2*: dorsal intercarpal ligament (DICL) (*dashed line*); *3*: terminal branch of posterior interosseous nerve (PION); *4*: dorsal branch of anterior interosseous artery (AIOA); *5*: dorsal radiocarpal artery arch (DRCA); *6*: dorsal intercarpal artery arch (DICA).

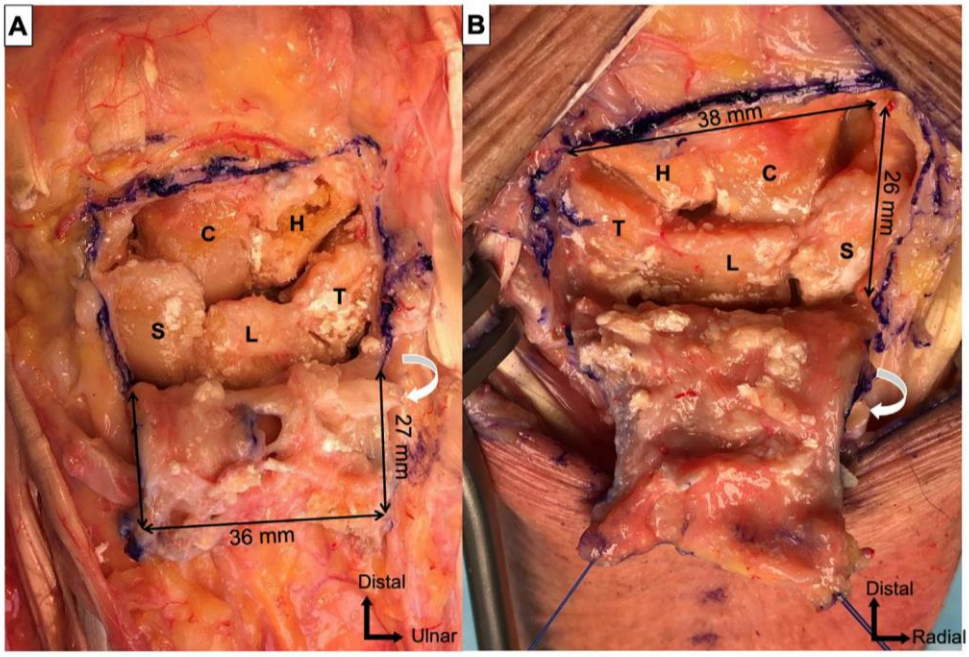

Fig. 2. Photographs of a posterior view of a right (A) and a left (B) wrist illustrating the carpal joint space exposure and its dimensions. The *black arrows* indicate the capsulotomy's outlines. *S*: Scaphoid; *L*: lunate; *T*: triquetrum; *C*: capitate; *H*: hamate.

present and intact within the capsular flap. Finally, we tested the capsular stitching using PDS slow-absorbing sutures (Ethicon®).

Statistical analysis

Quantitative parameters were described by their means and ranges and qualitative parameters by their counts and percentages.

Results

Six wrists were dissected in this study; each of them had the same anatomical configuration. The origin, trajectory, and insertion of the DRCL and DICL were consistent. The DRCL originated proximally from the dorsal rim of the distal radius, ulnar to Lister's tubercle. Next, the ligament had an oblique trajectory from

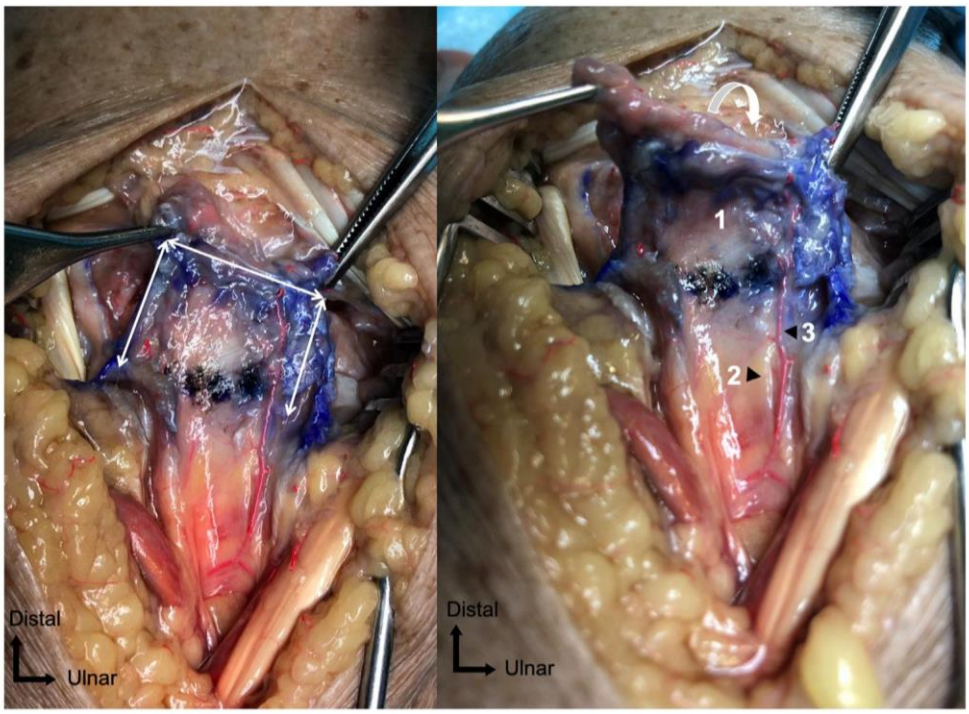

Fig. 3. Photograph of a posterior view of a right wrist illustrating the capsular flap. The *white arrows* indicate the capsulotomy's outline. *1*: capsular flap with the dorsal radiocarpal and dorsal intercarpal ligaments; *2*: terminal branch of posterior interosseous nerve; *3*: dorsal branch of anterior interosseous artery (AIOA).

proximal to distal and from lateral to medial. Its distal insertion was on the dorsal part of the triquetrum. The DICL originated proximally on the dorsal part of the triquetrum. Then, the ligament had a horizontal trajectory from medial to lateral. Its distal insertion was on the distal and dorsal part of the scaphoid and trapezium. The DCSS can be repaired by fixing it at its old bone insertion using an anchor.

The terminal branch of the PION ran longitudinally on the ulnar side of Lister's tubercle and was affixed to the floor of the fourth extensor compartment. At the level of the DRCL, the nerve penetrated the dorsal articular capsule at its surface. Both the DRCA and DICA were systematically found running perpendicular to the distal radius axis. The DRCA ran along the radiocarpal joint line while the DICA followed a trajectory parallel to the distal insertion of the DICL from medial to lateral. The dorsal branch of the AIOA had a longitudinal course, with its proximal part following the terminal branch of the PION along its ulnar edge. On the surface of the joint capsule, this branch was anastomosed perpendicularly to the two arterial arches.

The mean length of the capsular flap was 35 mm (range 29–38 mm) and its mean width was 27 mm (range 25–29 mm). The mean surface area of the articular exposure was 945 mm^2 (range 725–1102 mm^2). It systematically provided easy access to both rows of carpal bones, except the pisiform. It also provided good exposure of the radiocarpal and midcarpal joint spaces (Fig. 2). Access to the scaphotrapeziotrapezoid joint space was limited. In each dissected capsular flap, we found all the individual ligament, vascular, and nerve structures, implying that they were intact over their entire trajectories (Fig. 3) (Video 1). The capsular stitching was systematically easy to perform, including at the level of triquetral bone insertion of the DRCL and DICL by the ligament remnant on the bone.

Discussion

Our anatomical study confirmed the technical feasibility of this new dorsal capsulotomy and the resulting good carpal joint exposure. We also confirmed that the integrity of the dorsal extrinsic ligament fibers is maintained as well as the vascularization and innervation of the dissected capsular flap.

Several authors emphasize that the extrinsic ligaments are key stabilizers of the scapholunate complex. Viegas et al. [6], Mitsuyasu et al. [7] and Short et al. [8] showed that the DRCL and the DICL are important stabilizers, especially during the progression from dynamic to static scapholunate instability. More recently, Van Overstraeten et al. [9] described another stabilizer – the dorsal capsulo-scapholunate septum (DCSS) – which is a thickened portion of the capsule that joins the dorsal part of the scapholunate ligament and the DICL. This means that both the scapholunate interosseous ligament and extrinsic ligaments must be damaged for static scapholunate instability to develop [10].

With our capsulotomy, we were able to systematically preserve the DRCL and DICL fibers over their entire trajectories. We believe it is essential to preserve these stabilizers during intracarpal surgery, especially when doing intrinsic ligament reconstruction surgery. The objective is to avoid any intra-ligament scarring that could weaken its biomechanical properties.

The vascular anatomy of the wrist joint was described by Gelbermann et al. [11]. On the dorsal side, it consists of an anastomotic network including the DRCA, the DICA and the dorsal branch of the AIOA. The latter emerges dorsally after crossing the interosseous membrane near the proximal edge of the pronator quadratus. This dorsal branch runs with the PION affixed to the floor of the fourth extensor compartment. This nerve innervates the dorsal joint capsule [12]. Recently, in their histological study of the dorsal wrist capsule, Bonczar et al. showed the PION innervated 60% of the central portion; the remaining area was innervated by the superficial branch of the radial nerve and the medial antebrachial cutaneous nerve [13].

The design of this capsulotomy made it possible to preserve all these vascular and nerve structures in the capsular flap. Thus, in clinical practice, this could presage maintaining the dorsal joint capsule's vascularization and innervation. Vascular integrity would boost the capsule's healing which could in turn decrease retraction. The absence of intra-ligament scars in the radiocarpal area by preserving a proximal hinge could reduce joint stiffness secondary to any wrist arthrotomy.

Moreover, with a "U-shaped with proximal base" capsulotomy, the tension on the capsular closure can be adjusted by changing the location of distal anchorage points along a proximo-distal axis, such as an advancement flap, without filling the gap. This trick could be useful in cases of intracarpal osteoarthritis surgery in which restoring carpal height would require rebalancing the capsular closure tension to minimize stiffness in wrist's flexion-extension arc.

According to Hagert et al. [4] preserving the terminal branch of the PION would maintain wrist proprioceptive innervation. This could be useful for postoperative rehabilitation after performing wrist joint surgery. The recovery of grip strength and wrist mobility would be optimized. Given the anatomical configuration of this nerve branch, confirmed in our study, any capsulotomy with an incision on the radiocarpal joint line causes an iatrogenic lesion.

One of the aims of our study was to confirm how this dorsal capsulotomy can be done to expose carpal joint spaces. Omokawa et al. [14] described a longitudinal DICL preserving arthrotomy. The dorsal wrist capsule is opened between the DICL and DRCL, and the dorsal scapholunate joint space can be observed. The authors used this approach to treat scapholunate dissociation by transferring the DICL to reconstruct the dorsal scapholunate ligament. However, this procedure does not provide sufficient joint exposure to perform surgery on anything else than scapholunate pathologies. Based on our findings, our surgical approach provides access to the carpal bones as well as the radiocarpal and midcarpal joint spaces. Thus, this procedure could be suitable for many types of intracarpal bone or ligament surgeries. Nevertheless, access to the scaphotrapeziotrapezoid joint space remains difficult with this purely dorsal approach. A lateral or palmar approach seems to be better suited [2].

Our study has its limitations. Firstly, we had a limited sample size, which did not allow us to study this surgical procedure relative to the different anatomical variations of the wrist ligaments [15,16]. However, it was sufficient to assess the technical feasibility of this technique. Another limitation is the fact that a cadaver study, albeit with positive results, may not translate fully to the clinical scenario, particularly in terms of functional recovery. Likewise, we were not able to assess how well the capsular flap vascularization's was preserved with punctate bleeding. Finally, we did not compare our dorsal capsulotomy with other procedures such as Berger et al. [3] capsulotomy. A prospective clinical study would be the next step to validate our findings.

Ethical statement

The authors declare that the work described has been carried out in accordance with the Declaration of Helsinki of the World Medical Association revised in 2013 for experiments involving humans as well as in accordance with the EU Directive 2010/63/EU for animal experiments.

Funding statement

The authors received no financial support for the research, authorship, and/or publication of this article.

Conflict of interest

The authors declared no potential conflicts of interest with respect to the research, authorship, and/or publication of this article.

Informed consent

The participants had given informed consent for use of their bodies for medical research.

Acknowledgements

The authors wish to thank Dr. Joanne Archambault for English language support. The authors wish to thank Dr. Yoan-Kim De Almeida for the illustrations.

Appendix A. Supplementary data

Supplementary material related to this article can be found, in the online version, at doi:https://doi.org/10.1016/j.hansur.2020.10.015.

References

[1] Berger RA, Bishop AT, Bettinger PC. New dorsal capsulotomy for the surgical exposure of the wrist. Ann Plast Surg 1995;35:54–9.
[2] Anakwe RE, Middleton SD, Hayton MJ. A modified dorsal capsulotomy for improved radiocarpal exposure. J Hand Surg Eur 2013;38:805–6.
[3] Berger RA, Bishop AT. A fiber-splitting capsulotomy technique for dorsal exposure of the wrist. Tech Hand Up Extrem Surg 1997;1:2–10.
[4] Hagert E, Ferreres A, Garcia-Elias M. Nerve-sparing dorsal and volar approaches to the radiocarpal joint. J Hand Surg Am 2010;35:1070–4.
[5] Tang JB, Giddins G. Why and how to report surgeons' levels of expertise. J Hand Surg Eur 2016;41:365–6.
[6] Viegas SF, Yamaguchi S, Boyd NL, Patterson RM. The dorsal ligaments of the wrist: anatomy, mechanical properties, and function. J Hand Surg Am 1999;24:456–68.
[7] Mitsuyasu H, Patterson RM, Shah MA, Buford WL, Iwamoto Y, Viegas SF. The role of the dorsal intercarpal ligament in dynamic and static scapholunate instability. J Hand Surg Am 2004;29:279–88.
[8] Short WH, Werner FW, Green JK, Masaoka S. Biomechanical evaluation of the ligamentous stabilizers of the scaphoid and lunate: part II. J Hand Surg Am 2005;30:24–34.
[9] Van Overstraeten L, Camus EJ, Wahegaonkar A, Messina J, Tandare AA, Cambon-Binder A, et al. Anatomical Description of the Dorsal Capsulo-Scapholunate Septum (DCSS)-arthroscopic staging of scapholunate instability after DCSS sectioning. J Wrist Surg 2013;2:149–54.
[10] Laulan J. Rotatory subluxation of the scaphoid: pathology and surgical management. Chir Main 2009;28:192–206 [in French].
[11] Gelberman RH, Panagis JS, Taleisnik J, Baumgaertner M. The arterial anatomy of the human carpus. Part I: the extraosseous vascularity. J Hand Surg Am 1983;8:367–75.
[12] Wilhelm A. Denervation of the wrist. Hefte Unfallheilkd 1965;81:109–14 [in German].
[13] Bonczar T, Walocha JA, Bonczar M, Mizia E, Filipowska J. Assessing the innervation of the dorsal wrist capsule using modified Sihler's staining. Folia Morphol (Warsz) 2020;24 (Online ahead of print).
[14] Omokawa S, Ono H, Suzuki D, Shimizu T, Kawamura K, Tanaka Y. Dorsal intercarpal ligament preserving arthrotomy and capsulodesis for scapholunate dissociation. Tech Hand Up Extrem Surg 2020;24:43–6.
[15] Feipel V, Rooze M. The capsular ligaments of the wrist. Eur J Morphol 1997;35:87–94.
[16] Feipel V, Rooze M. The capsular ligaments of the wrist: morphology, morphometry and clinical applications. Surg Radiol Anat 1999;21:175–80.

Supplementary Figure

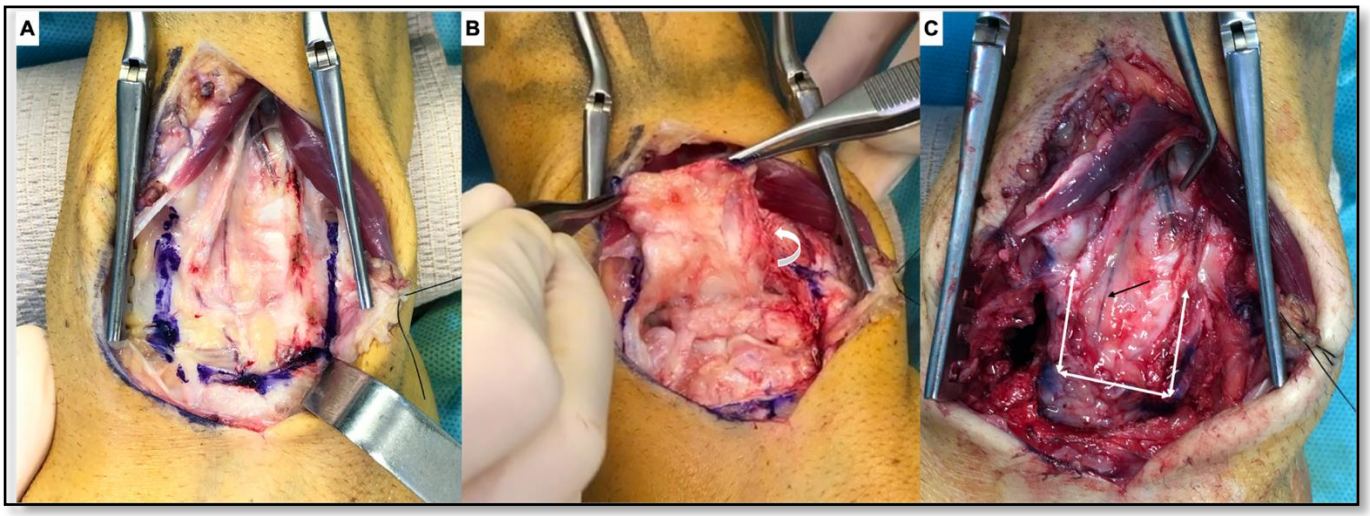

Fig. 4. *Photographs of a posterior view of the wrist illustrating the outline of the capsulotomy (blue line) (A); the carpal joint space exposure (B); the vascularization of the capsular flap (black arrow (C).*

Discussion et Conclusion

Nous avons vu qu'il existait plusieurs techniques de ligamentoplastie scapho-lunaire pour traiter l'ISL chronique, réductible, en l'absence d'arthrose (Crawford et al., 2016). Par l'utilisation d'un transplant tendineux, elles visent à reconstruire tout ou partie du complexe scapho-lunaire, et ainsi retrouver une synergie du couple scapho-lunaire et une cohérence spatiale des os du carpe. Leur objectif commun est donc de corriger les anomalies radiologiques afin de prévenir du risque à long terme d'arthrose SLAC. Ces procédures ont servi de base à plusieurs études cliniques (Athlani et al., 2018-1), et si toutes ces dernières partagent de bons résultats sur l'amélioration de la douleur et de la force de préhension, l'évaluation radiographique semble moins satisfaisante avec la récidive à court et moyen terme des anomalies radiologiques. Des complications iatrogènes osseuses, de type nécrose du pôle proximal du scaphoïde ou de collapsus arthrosique STT, ont également été soulignées. De même, l'évolution vers une arthrose SLAC était rapportée, avec un taux compris entre 5 et 25%, pour des études au recul d'au moins 2 ans.

Au vu des résultats obtenus dans nos différentes études anatomiques et cliniques, la ligamentoplastie « SLIC » semble corriger les différentes composantes de la dissociation scapho-lunaire et ainsi restituer une biomécanique normale du carpe.
Cette technique réduit considérablement la douleur et augmente la force de préhension, principaux motifs de consultation. Cependant, comme les autres ligamentoplasties, elle est source d'enraidissement du poignet en flexion-extension. Toutefois, nous avons pu constater deux données capitales. Premièrement, il n'existait pas de différence significative dans les mobilités pré- et post-opératoires pour le poignet opéré ; la différence étant significative lors de la comparaison avec les valeurs du côté controlatéral. Deuxièmement, la flexion moyenne de poignet retrouvée dans la littérature, toutes ligamentoplasties confondues, était d'environ 30° à 40°. Dans notre étude clinique, nous avons trouvé une moyenne de 50° avec la ligamentoplastie « SLIC ». Cette préservation relative de la flexion du poignet peut être attribuée à la non-utilisation d'une approche palmaire ou du tendon Flexor Carpi Radialis. De même, un des avantages de la « SLIC » est d'éviter la morbidité et les difficultés techniques d'un tunnel transfixiant trans-scaphoïdien. De plus, avec un recul moyen de plus de 2 ans, nous ne déplorons, à ce jour, aucun cas d'arthrose SLAC.

Les différents paramètres radiologiques se sont améliorés significativement avec un retour à des valeurs considérées comme normales, à l'exception du contrôle durable du diastasis scapho-lunaire chez les patients porteurs d'une ISL statique, et opérés d'une « SLIC » dans sa version initiale. Toutefois, il semble que nous contrôlons mieux la gestion de la tension de la ligamentoplastie dans sa version modifiée, conservant ainsi la correction intra-carpienne obtenue en per-opératoire, notamment dans ces cas d'ISL statique où les contraintes sont importantes. Un enseignement de ces différentes études est la correction systématique de la SPS grâce à cette technique. Cette déformation, rarement recherchée dans les autres études cliniques, représente le point de départ de l'arthrose radio-scaphoïdienne ; le diastasis étant considéré comme non arthrogène.

Nous avons également appris au fil du temps, à préciser le spectre d'efficacité de la ligamentoplastie « SLIC ». En effet, le caractère réductible de la dissociation est le critère indispensable pour poser l'indication de reconstruction ligamentaire scapho-lunaire. Une évaluation précise de la nature réductible de cette dissociation est essentielle. Réaliser des radiographies en inclinaison ulnaire et effectuer des manœuvres dynamiques lors de l'arthroscopie exploratrice est la façon la plus courante de le faire en pré-opératoire. Malgré tout, lors de l'intervention chirurgicale, il est essentiel de confirmer que la dissociation peut être réduite sans difficulté par une manœuvre de pression postéro-antérieure sur le capitatum et d'inclinaison ulnaire du poignet. Une résistance au repositionnement du scaphoïde ou la nécessité d'un geste de libération de l'articulation STT, sont prédictifs d'un caractère irréductible de l'instabilité et source d'échec de la reconstruction ligamentaire. Dans ces situations, il semble plus légitime de récuser la ligamentoplastie et proposer un geste d'arthrodèse partielle intra-carpienne.
Néanmoins, il n'existe aucune méthode permettant de quantifier les charges nécessaires pour réduire le scaphoïde. Ainsi, le 4DCT pourrait apporter satisfaction sur ce point en évaluant précisément l'amplitude de mobilité du scaphoïde. La quantification de cette donnée contribuerait à préciser les limites d'indication des ligamentoplasties.

Enfin, nous pensons bénéfique de ne pas prélever les fléchisseurs ou extenseurs du poignet, couramment utilisés comme transplant, qui semblent être des stabilisateurs du complexe scapho-lunaire (Esplugas et al., 2016; Short et al., 2007). L'utilisation du Palmaris Longus évite cela et sa précontrainte en tant que transplant libre prévient de sa distension secondaire et donc de la détente ligamentaire en résultant.

Notre étude prospective a certaines limites. Premièrement, la taille de l'échantillon reste limitée même si cohérente avec celle des autres études publiées. Deuxièmement, les interventions chirurgicales ont toutes été effectuées par l'équipe chirurgicale conceptrice de la procédure, facilitant ainsi sa réalisation optimale. Néanmoins, cette technique est standardisée et chacune des étapes détaillées permettant sa reproductibilité inter-opérateurs. L'abord dorsal pur évite la complexité d'une double approche. Pour finir, cette étude doit être poursuivie à long terme afin de s'assurer de la stabilité de nos résultats, et de la prévention du risque arthrosique. De plus, nous avons seulement réalisé une analyse radiographique ne permettant pas d'apprécier réellement la restauration d'une cinématique physiologique des os du carpe, notamment du couple scapho-lunaire.

L'étude cadavérique 4DCT a démontré l'impact anatomique de la section des ligaments interosseux scapho-lunaire et extrinsèques dorsaux, sur la stabilité du complexe scapho-lunaire ; et surtout l'impact positif de la ligamentoplastie « SLIC » dans la restauration d'une synergie et stabilité articulaire scapho-lunaire. Cela représente une preuve supplémentaire de l'efficacité de cette technique dans la correction de la dissociation et soutient l'utilisation du 4DCT pour l'évaluation post-opératoire des patients présentant des symptômes persistants et une évaluation radiographique non contributive.

De nombreux auteurs ont souligné l'importance des ligaments extrinsèques, notamment les ligaments DIC et DRC, dans la stabilité du couple scapho-lunaire. La capsulotomie transligamentaire en « V » à charnière radiale décrite par Berger et al. (1995) que nous utilisons couramment pour la chirurgie du carpe, a soulevé des interrogations sur l'absence du respect de l'intégrité des fibres longitudinales de ces ligaments. De même, l'innervation capsulaire, représentée par le nerf interosseux postérieur, est systématiquement sectionnée. Ce nerf, par sa fonction proprioceptive du poignet, jouerait un rôle non négligeable lors de la rééducation post-opératoire d'une chirurgie du poignet. Cela nous a amené à concevoir une nouvelle capsulotomie dorsale permettant une bonne exposition du carpe, tout en préservant les fibres des ligaments DIC et DRC. L'objectif est d'éviter toute cicatrisation ligamentaire qui pourrait affaiblir leurs propriétés biomécaniques stabilisatrices. De même, la conservation d'une vascularisation de la capsule articulaire dorsale pourrait présager d'une meilleure cicatrisation capsulaire, et à son tour diminuer la rétraction fibreuse. Enfin, le respect de l'innervation, notamment en cas de nerf d'aspect non névromateux, ne pourrait qu'être bénéfique lors de la rééducation proprioceptive. La prochaine étape serait de valider nos résultats et hypothèses en pratique clinique.

CHAPITRE 4.
DÉVELOPPEMENT D'UN DISPOSITIF DE GUIDAGE DU MOUVEMENT DU POIGNET POUR L'IMAGERIE DYNAMIQUE

Introduction

Très peu d'études rapportent l'utilisation d'un dispositif permettant de guider le mouvement du poignet d'un sujet, afin d'analyser la cinématique du carpe en imagerie dynamique. Mat Jais et Tay (2017) ont utilisé, sur des poignets cadavériques, un dispositif de simulation du mouvement de DRU. Ils ont analysé les changements dans la cinématique du scaphoïde en 4DCT. Selon eux, cette analyse scanographique des mobilités du scaphoïde lors des mouvements du poignet représente un argument de faisabilité pour le diagnostic des instabilités carpiennes dynamiques. De Roo et al., (2019), dans une étude sur sujet sain, se sont intéressés à analyser la cinématique du couple scapho-lunaire lors des mouvements du poignet en 4DCT. Les auteurs ont utilisé un autre dispositif permettant un mouvement actif du poignet en flexion-extension ou en DRU. Ceci a permis de définir le positionnement de l'axe de rotation scapho-lunaire (pôle proximal dorsal du scaphoïde) afin d'optimiser les techniques de reconstruction ligamentaires. En ce qui concerne le type de manœuvre à utiliser, Kakar et al. (2016) allaient dans le même sens qu'Abou Arab et al. (2018), en précisant que la manœuvre de DRU permettait de mieux déceler les lésions du LIOSL par rapport aux manœuvres de poing serré ou de flexion-extension.

Afin d'homogénéiser la reproductibilité du mouvement de DRU du poignet, mais également d'en calculer l'amplitude lors de l'acquisition en imagerie dynamique, nous nous sommes intéressés, avec Nicolas Weber et Jacques Felblinger du *Laboratoire IADI INSERM U1254 – Université de Lorraine,* à la conception d'un dispositif de recherche permettant de répondre à cette problématique.

Le document ci-dessous est rédigé conformément à l'Arrêté du 16 août 2006 relatif au contenu et aux modalités de présentation d'une brochure pour l'investigateur d'une recherche biomédicale portant sur un dispositif médical de diagnostic. Il contient les informations nécessaires pour qu'un investigateur puisse les comprendre et effectuer sa propre évaluation impartiale sur le bien-fondé de la recherche proposée, en se basant sur le rapport des bénéfices et des risques de celle-ci.

Présentation générale du dispositif de recherche

Nom du dispositif	Guided Wrist Motion Device (GWMD)
Fabricant	IADI Laboratory
Marquage CE	Non
Objectif	Ce prototype a pour objectif de guider le poignet (articulations du carpe) des sujets selon un mouvement de DRU afin de permettre une acquisition en imagerie dynamique quatre dimensions.
Destination	Ce prototype est destiné à la recherche clinique. Il doit permettre l'observation et l'analyse des amplitudes de DRU du poignet en vue d'un diagnostic précis des instabilités intra-carpiennes.
Justification de la recherche	Améliorer le diagnostic et pronostic des instabilités intra-carpiennes, qui n'est pas optimal à l'heure actuelle.
Indication attendue à l'issue de la recherche	Bilan diagnostic et pronostic des instabilités intra-carpiennes. Bilan d'évaluation de l'efficacité des techniques chirurgicales intra-carpiennes.

Description complète du dispositif de recherche

Le Dispositif GWMD permet la réalisation par le sujet d'un mouvement volontaire de DRU homogène et harmonieux, d'amplitudes maximales en inclinaison radiale puis ulnaire, tout en permettant de neutraliser les mouvements de flexion-extension et prono-supination. Il est conçu pour être utilisé en imagerie dynamique centrée sur le carpe. Il doit permettre de mettre en évidence des signes d'instabilités intra-carpiennes apparaissant lors de la cinématique du carpe. La stabilisation de l'avant-bras afin d'éviter tout mouvements parasites de translation, nécessite une fixation de celui-ci sur le dispositif. Les risques de blessures liées à une compression trop importante sont à anticiper.

- *Conception 3D*

Les plans de conception du dispositif GWMD ont été entièrement conçus sur le logiciel 3D Inventor® Professional 2021 (Autodesk®, San Rafael, Californie, États-Unis). Ceci nous a permis d'avoir une vision globale du dispositif avant de lancer sa fabrication (Figure 26). Le dispositif GWMD est composé d'une quarantaine de pièces mécaniques découpées et/ou imprimées, de six éléments mécaniques de type roulement et de nombreuses vis, écrous et guiches (Figure 27). Toutefois, nous pouvons décrire deux parties distinctes : la partie fixe ou support, et la partie mobile ou amovible (Figures 28 et 29). À cela, s'ajoute le capteur d'enregistrement des amplitudes de mouvement du poignet (Figure 30).

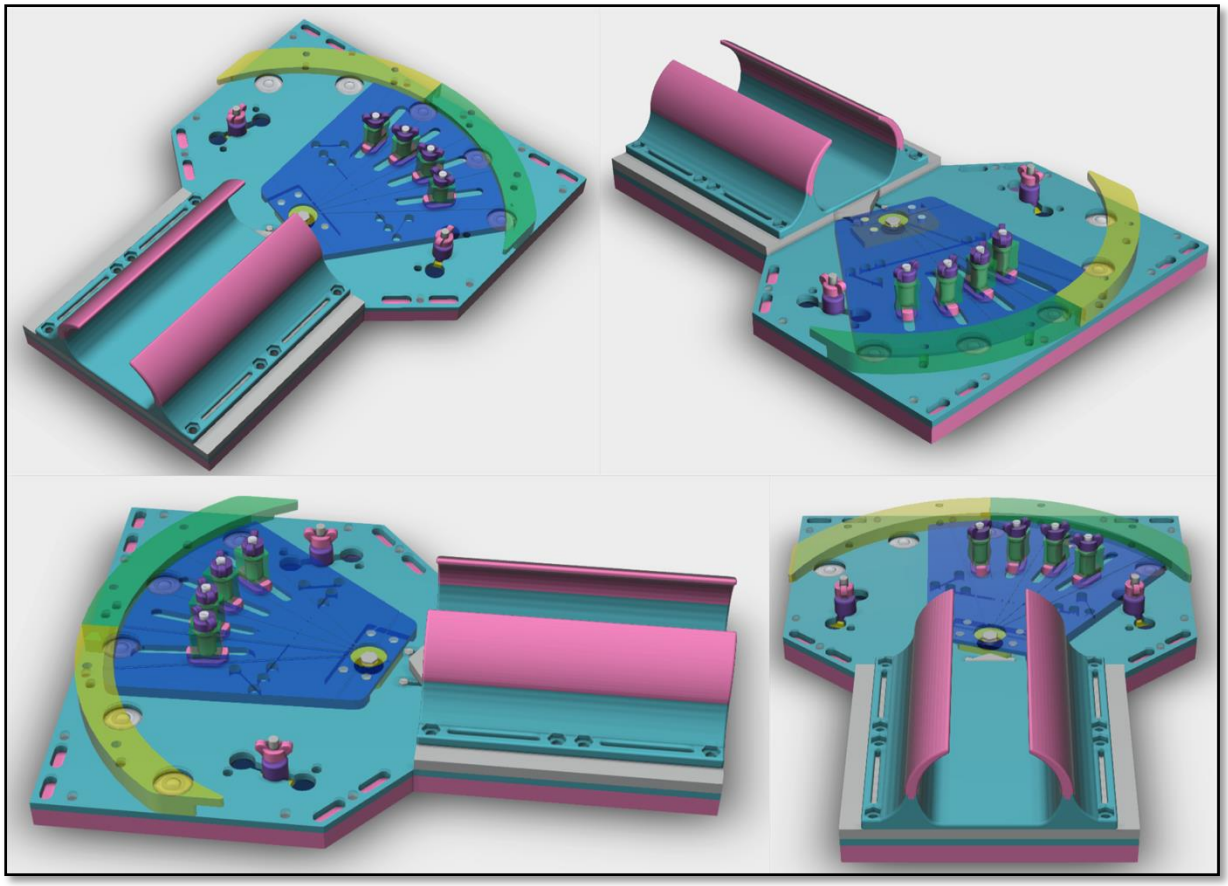

Figure 26. *Vues 3D du dispositif GWMD.*

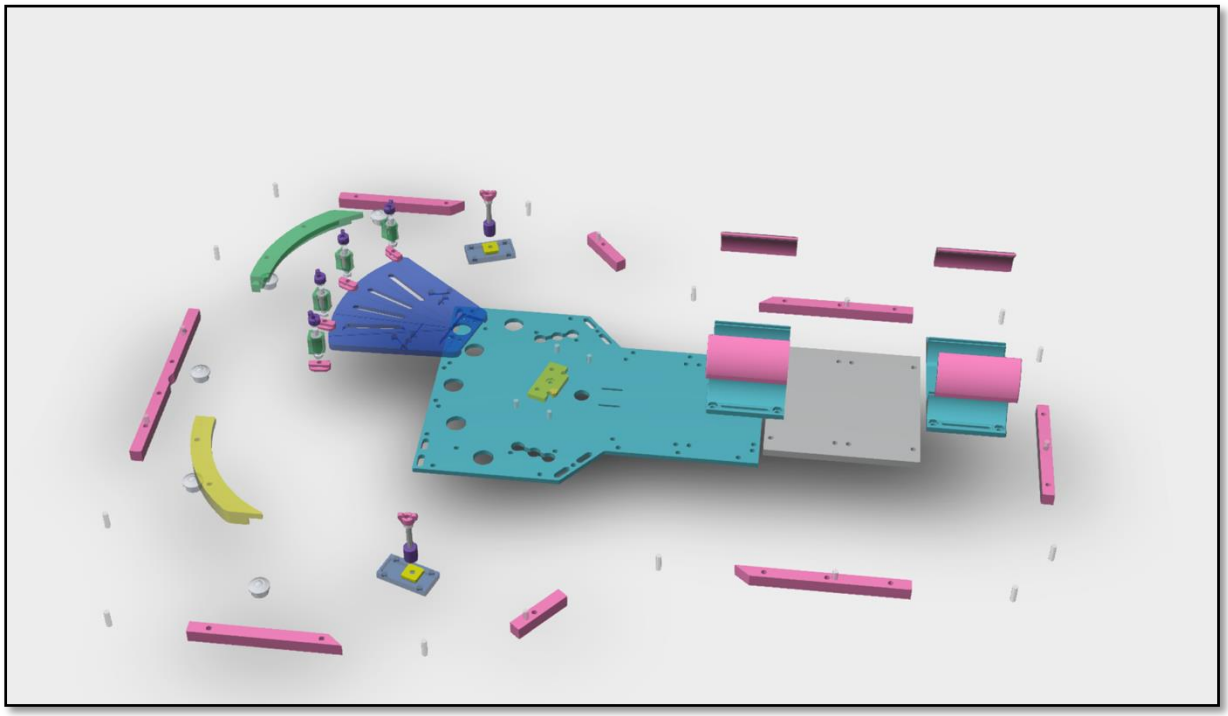

Figure 27. *Vue 3D de l'ensemble des pièces constituant le dispositif GWMD.*

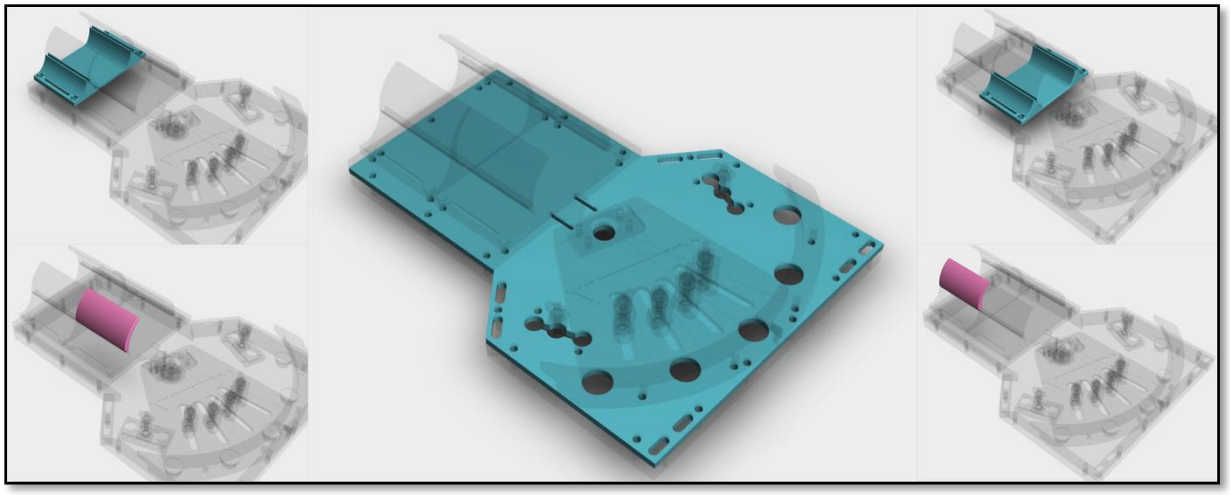

Figure 28. *Vues 3D de la partie fixe ou support du dispositif GWMD.*

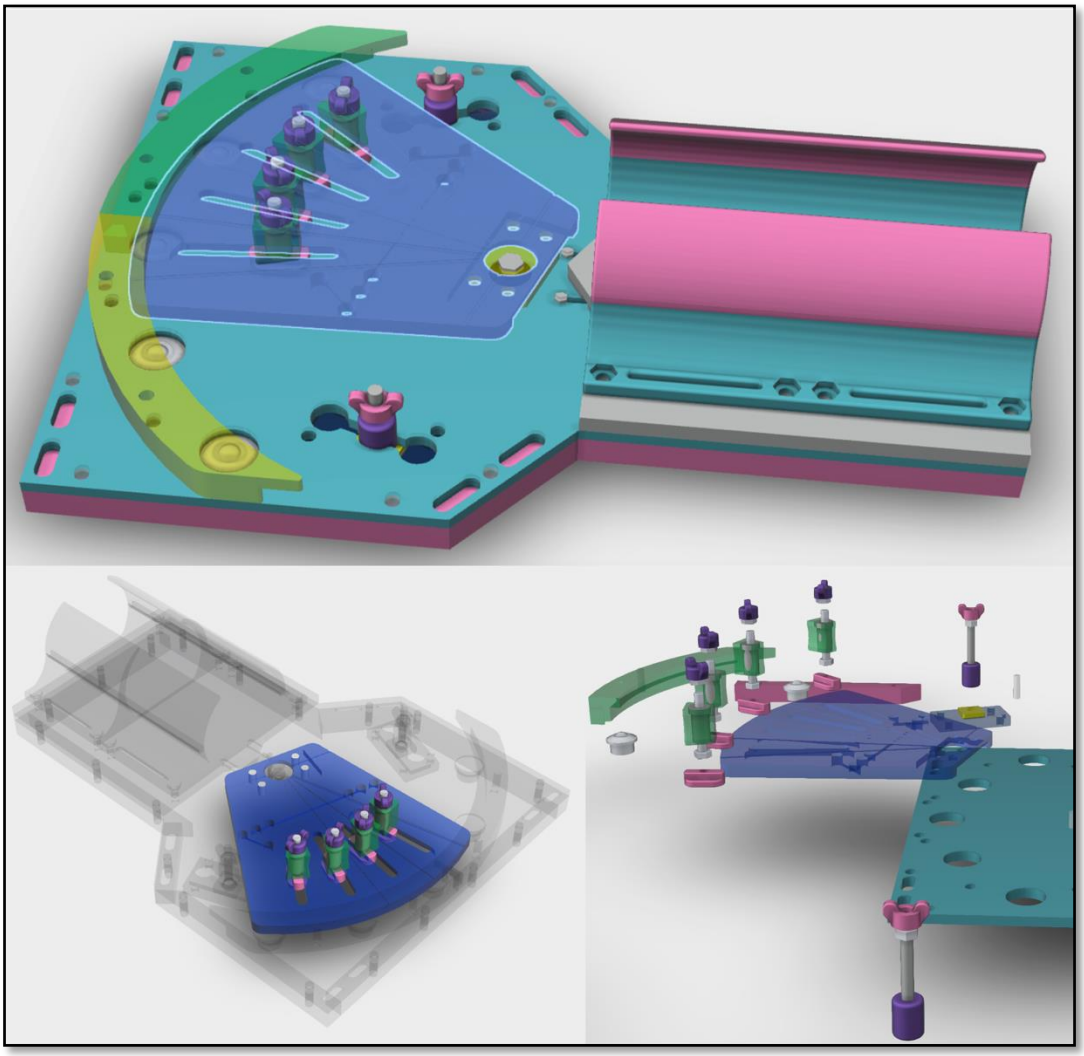

Figure 29. *Vues 3D de la partie mobile ou amovible du dispositif GWMD.*

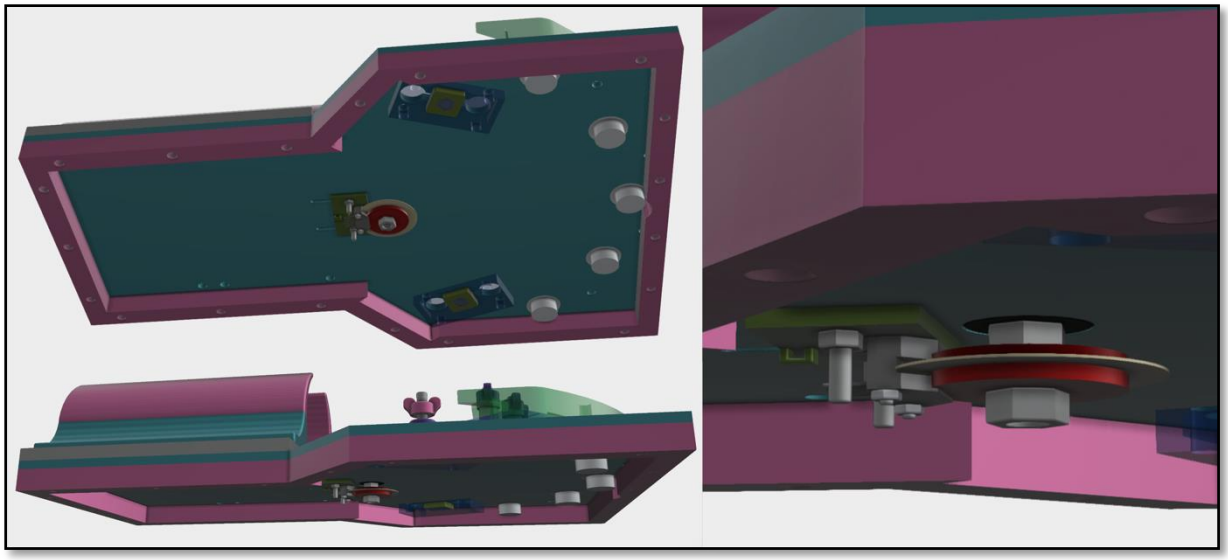

Figure 30. *Vues 3D du capteur d'enregistrement des amplitudes de mouvement du poignet.*

- ***Composition et Fabrication***

Le dispositif GWMD (Figure 31) est majoritairement composé de verre polyméthacrylate de méthyle (PMMA) ALTUGLAS® (Altuglas International SAS, Groupe Akerma, France), d'acrylonitrile butadiene styrene (ABS) et de thermoplastic polyurethane (TPU), NinjaFlex® Flexible 3D (TPU 85A) (NinjaTek®, Manheim, Pennsylvanie, États-Unis). Les pièces en PMMA ont été usinées à la main, celles en ABS et en TPU, imprimées en utilisant une imprimante 3D FDM (Fused Deposition Modeling) STREAM 30 ULTRA (Volumic 3D, Nice, France) (Figure 32). Les sangles de maintien du membre ont été conçues en utilisant des rubans auto-agrippant (VELCRO®). Pour finir, le capteur d'analyse des amplitudes du mouvement est composé d'une roue encodeuse en Mylar (Broadcom®, Irvine, Californie, États-Unis), d'un encodeur incrémental (Broadcom®, Irvine, Californie, États-Unis) et d'une carte de contrôle compatible IRM développé par le *laboratoire IADI, INSERM U1254 - Université de Lorraine* (Figure 33).

La transmission des données est assurée par un câble fibre optique plastique de 1 mm. Les données sont acquises par le Signal Acquisition and Event Controller (SAEC) développé par le *laboratoire IADI, INSERM U1254 - Université de Lorraine*.

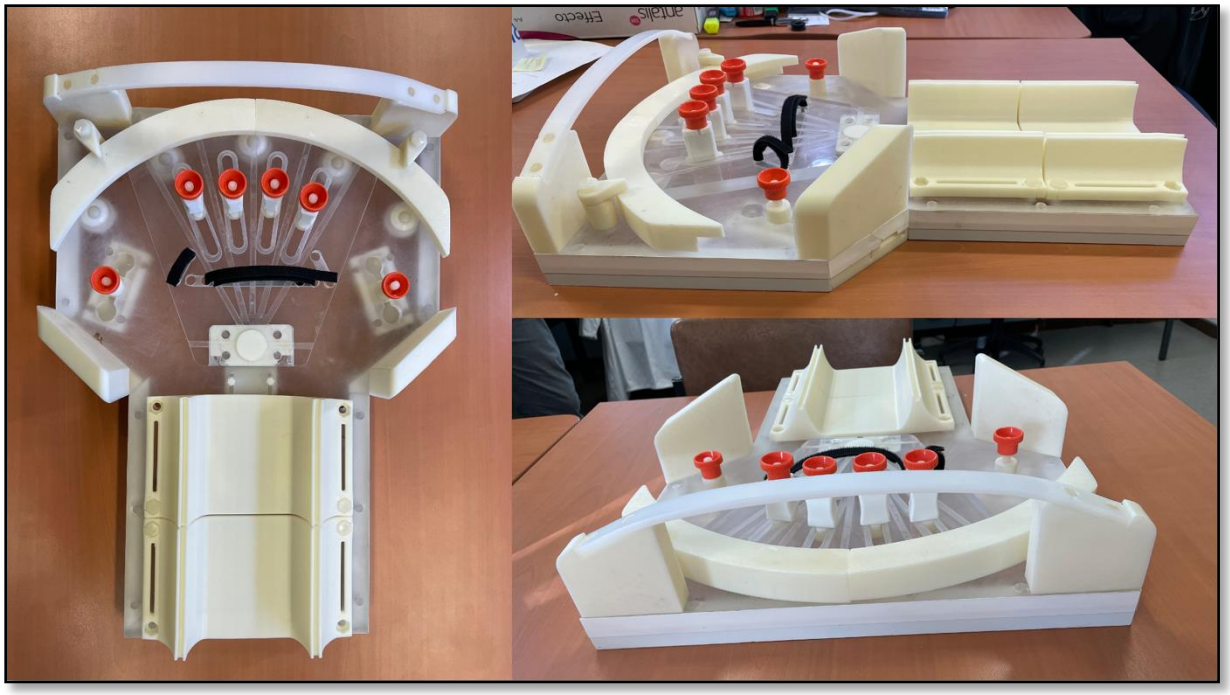

Figure 31. *Vues globales du dispositif GWMD.*

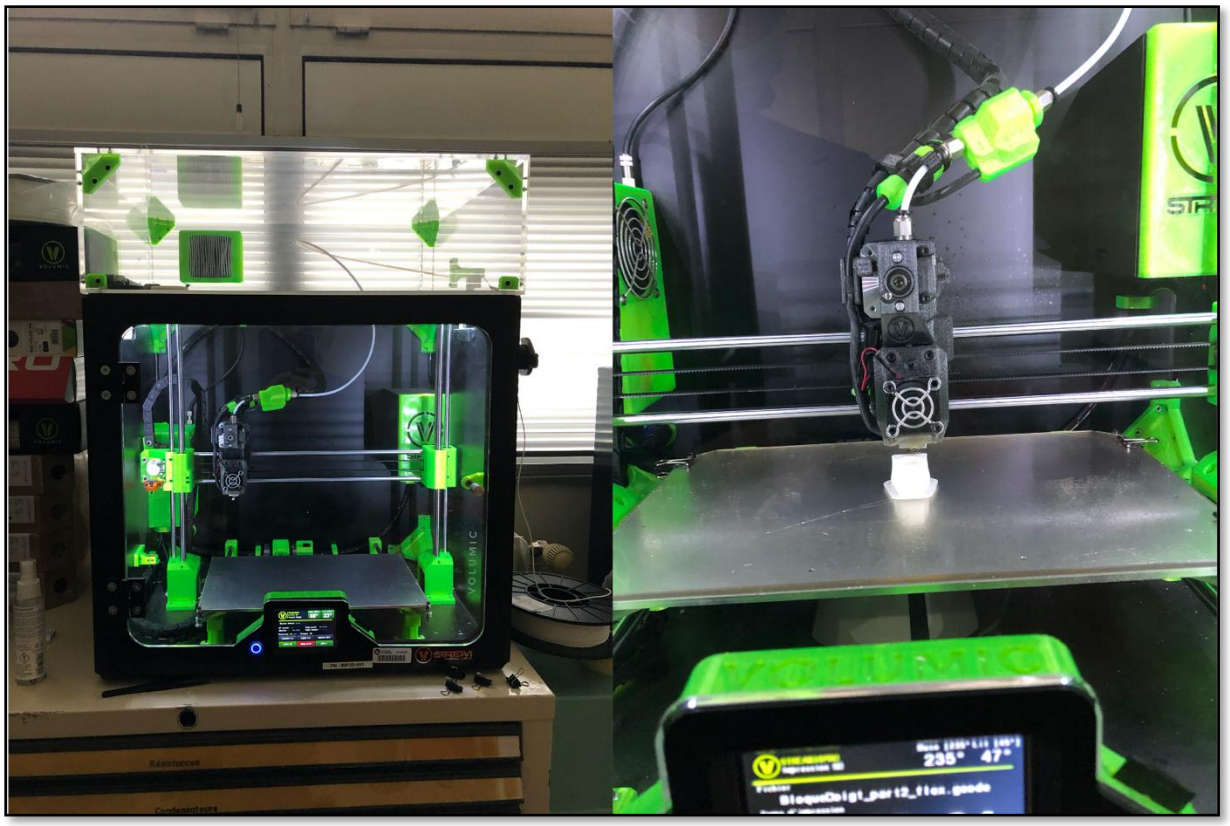

Figure 32. *Photographies de l'imprimante 3D STREAM 30 ULTRA (Volumic, France).*

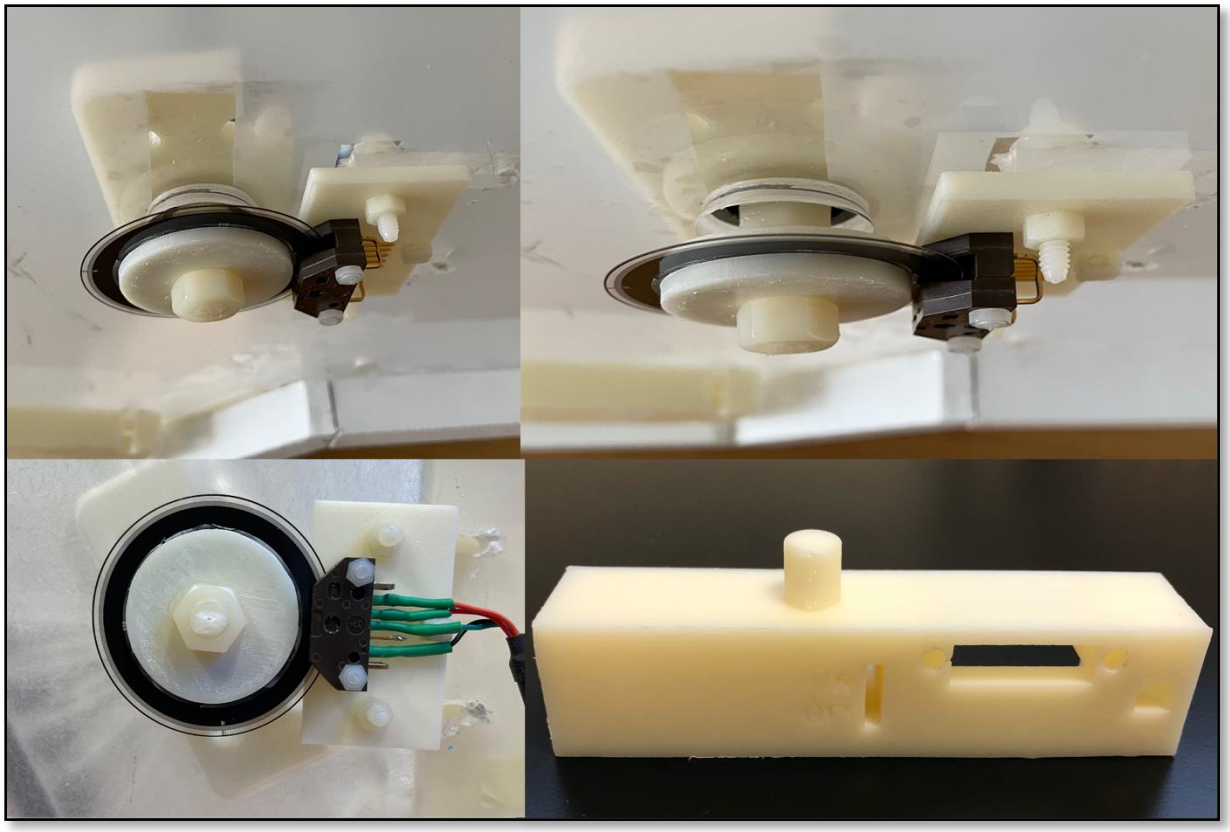

Figure 33. *Photographies du capteur d'analyse des amplitudes du mouvement. À noter en bas à droite, l'impression 3D de la pièce servant de support à l'interrupteur ON/OFF et au passage du câble de liaison du capteur à la console TDM ou IRM.*

La partie amovible est destinée au positionnement et à la stabilisation de la main. Il s'agit d'un élément pouvant s'adapter à la latéralité et aux dimensions du membre à analyser (Figures 34 et 35).

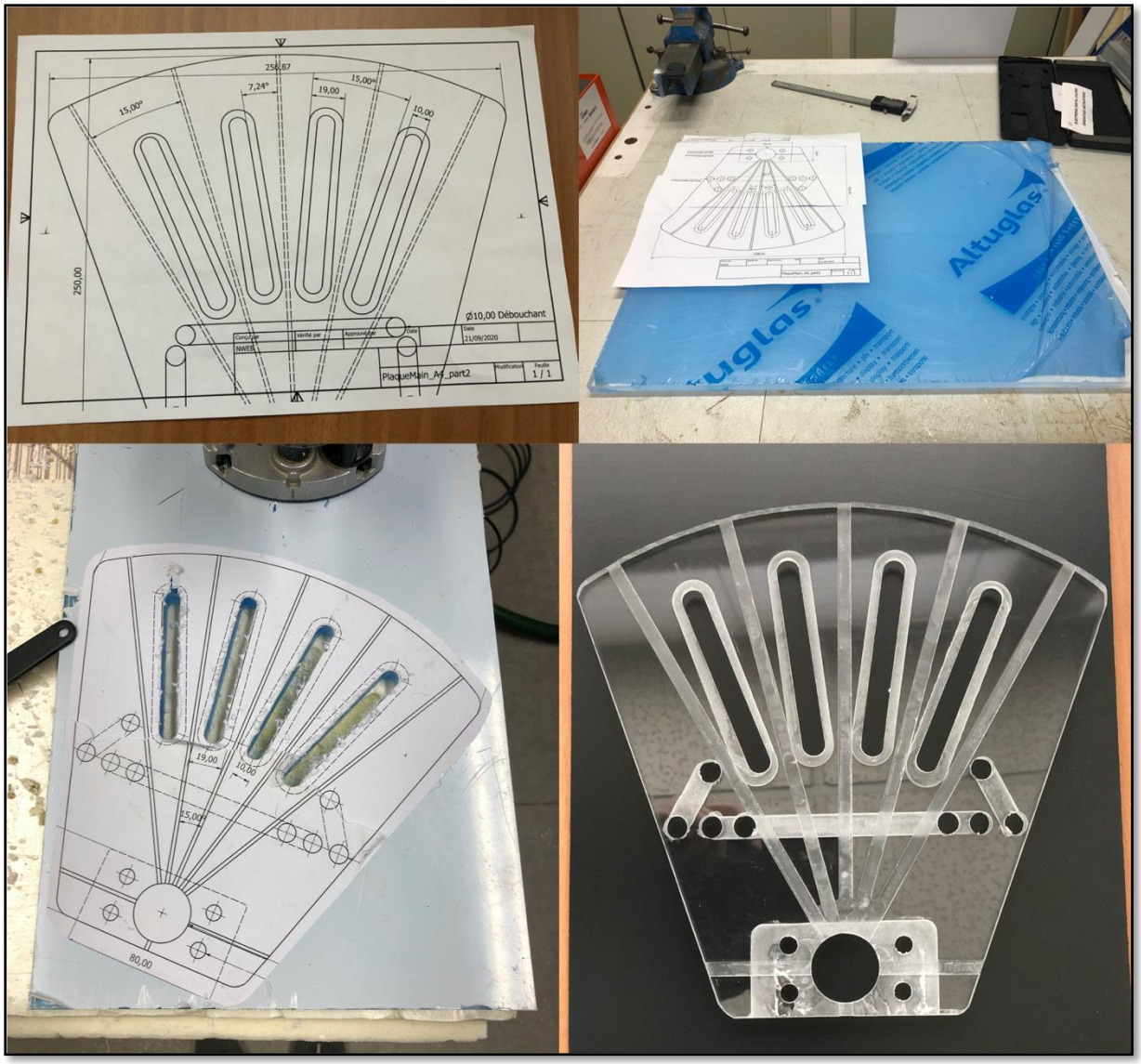

Figure 34. *Photographies illustrant les grandes étapes de l'usinage de la base de la partie mobile amovible.*

Figure 35. *Photographies de la partie mobile amovible avec son système de stabilisation de la main. À noter l'adaptabilité selon la latéralité et les dimensions du membre.*

La partie fixe contient le support de maintien de l'avant-bras (gouttière) et le socle recevant la partie amovible (encliquetage rapide). Il contient la rotule autorisant le mouvement du poignet en DRU (Figures 36 et 37). Au verso, on y retrouve également le boitier électronique pour le recueil des données. Deux loquets sont disponibles de part et autre afin de limiter les amplitudes de mouvement pour chacune des inclinaisons (10°, 20° ou 30°) (Figure 38).

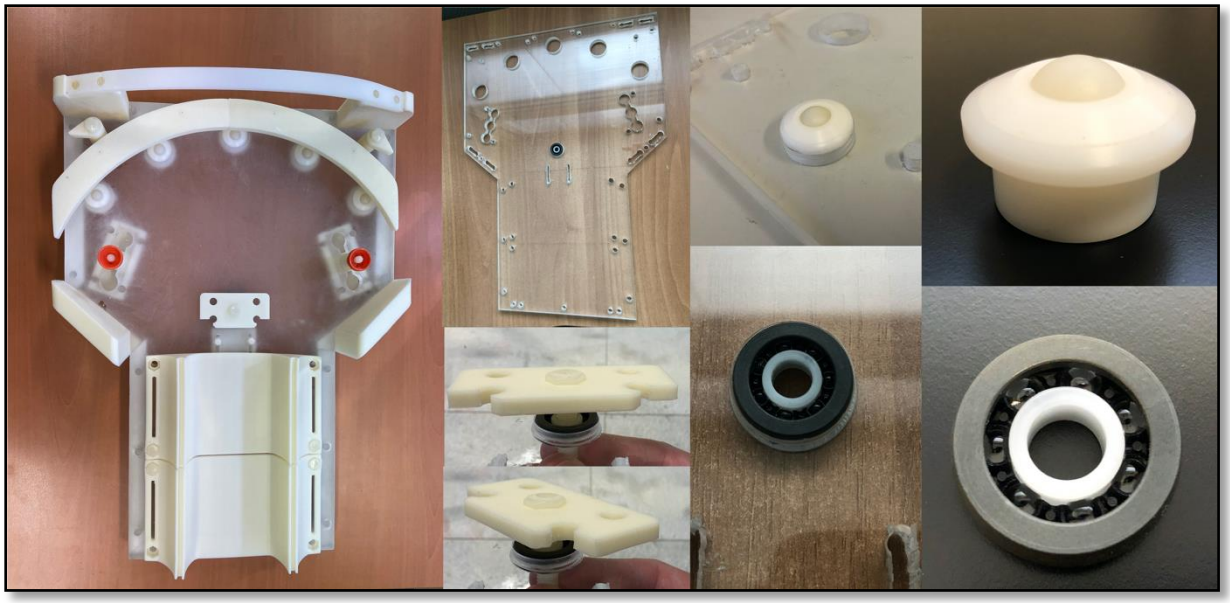

Figure 36. *Photographies de la partie fixe avec son système de rotule permettant le mouvement de rotation. À noter les supports de roulement assurant le déplacement de la partie mobile sur la partie fixe.*

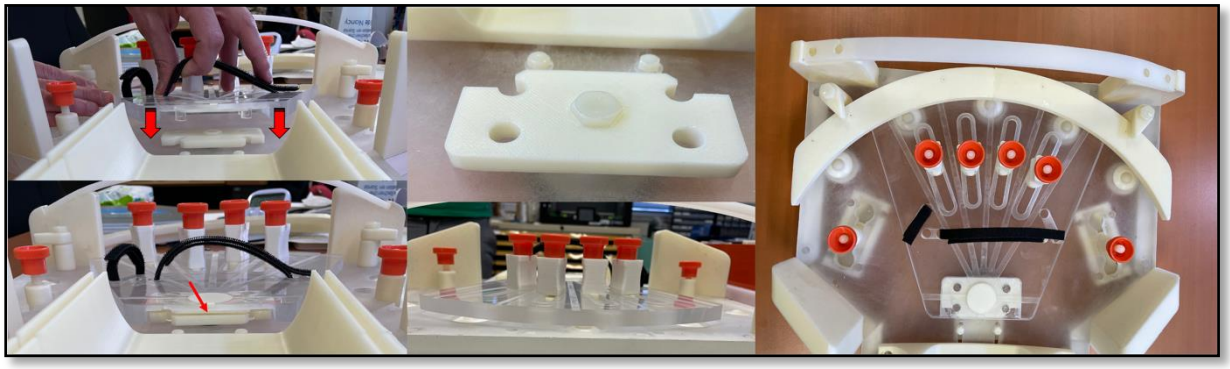

Figure 37. *Photographies illustrant le système d'encliquetage rapide présent sur la partie fixe et destiné à accueillir la partie amovible.*

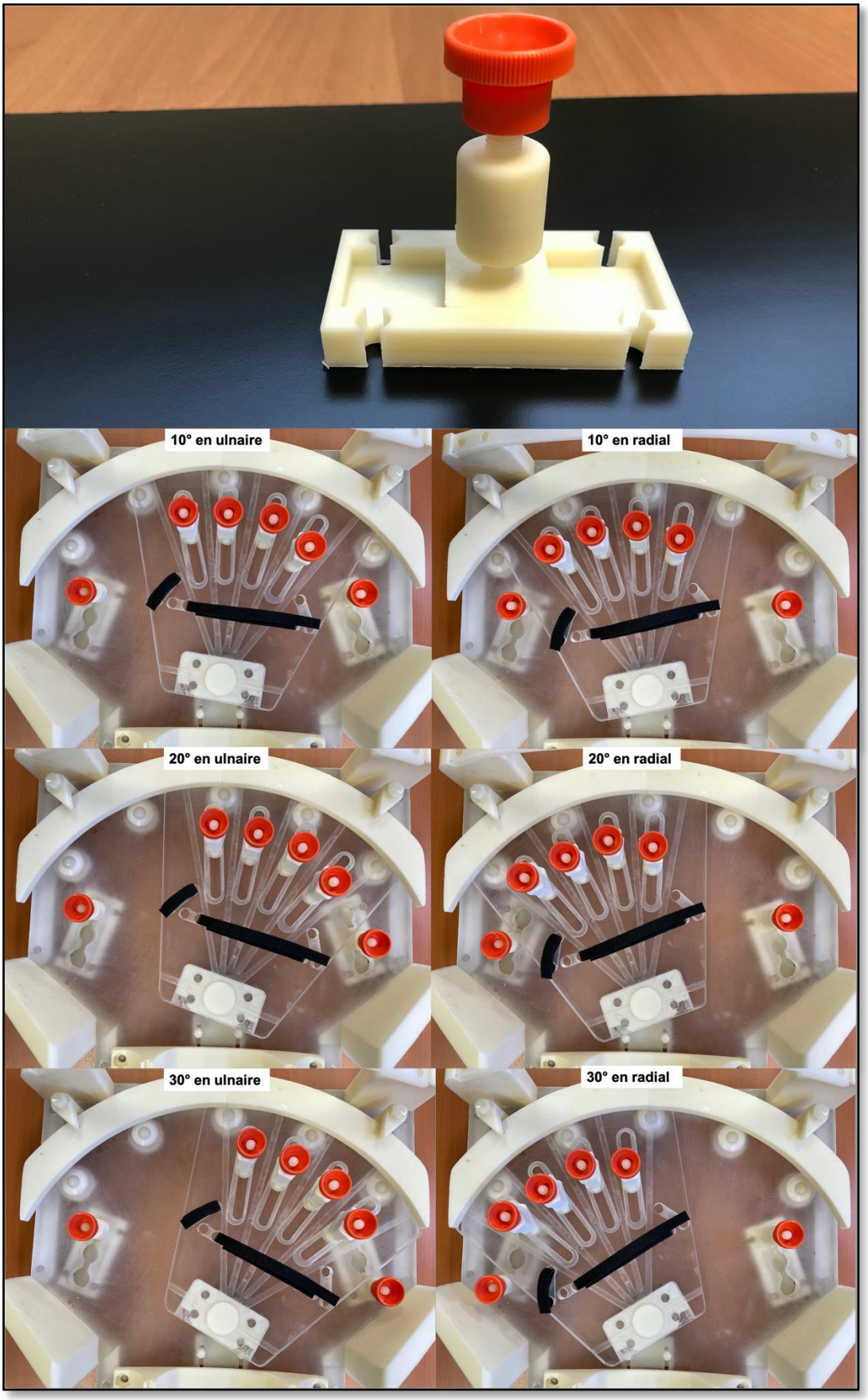

Figure 38. *Photographies du système de réglage des amplitudes d'inclinaisons radiale et ulnaire, comprises entre 10° et 30°.*

Afin d'éviter tout mouvement parasite, il est recommandé que le sujet soit en contact direct avec les matériaux du dispositif.

- ***Destination***

Le GWMD est destiné à être utilisé par toute personne formée à son fonctionnement afin d'observer en imagerie dynamique, les articulations du carpe lors des mouvements de DRU, en vue d'un diagnostic précis d'instabilité du carpe et notamment d'ISL.

- ***Contre-indications, avertissements, risques possibles***

Ce dispositif n'a pas été conçu pour être compatible avec d'autres dispositifs médicaux.

- ***Instructions d'utilisation ou d'installation***

Avant l'installation, il est recommandé de procéder à une désinfection du dispositif.

Installation du dispositif sur la table d'examen du scanner :

Le dispositif est entièrement indépendant de la table d'examen. Il est positionné sur celle-ci, dans le sens longitudinal, au niveau de la partie têtière. Sa stabilité est assurée par des patins antidérapant en caoutchouc (3M) disposés à son verso et directement en contact avec la table. Suivant les spécificités anatomiques de chaque sujet, il est indispensable de placer l'axe de rotation de la partie mobile du dispositif (centrage du poignet) en regard de l'antenne d'acquisition du scanner. Le dispositif ne doit ensuite plus pouvoir bouger au niveau de sa partie fixe. Une fois le dispositif installé, appuyez sur les cliquets distaux afin de détacher la partie mobile sur laquelle va être positionnée et fixée la main du sujet.

Installation du sujet sur le dispositif :

Durant la mise en place de la main sur la partie mobile du dispositif, le sujet peut être à distance de la table d'examen. Avant de placer la main, il faut s'assurer du bon fonctionnement du système de verrouillage des doigts longs (coulissement de chacun des cinq plots dans leurs rails respectifs). Une fois cette vérification faite, la main du sujet doit être placée à plat sur la partie mobile libre, les doigts écartés de manière à disposer chacun des plots en regard des commissures interdigitales. Les plots sont ensuite déplacés le long de leurs rails jusqu'à obtenir une fixation solide et stable de la main et des doigts.

Le sujet, muni de la partie mobile solidarisée à la main, doit venir s'installer à côté de la table d'examen, en position débout ou assise, protégé par un tablier de plomb et cache thyroïde. Puis, l'avant-bras vient se positionner naturellement au niveau de la partie fixe du dispositif, restée en place sur la table d'examen.

La partie mobile accueillant la main, va venir s'encliqueter sur la rotule de la partie fixe. Il est indispensable d'assurer le maintien de l'avant-bras afin d'éviter tout mouvement parasite, grâce à la gouttière et à ses sangles destinées à cet usage. Ainsi, les seuls mouvements autorisés seront ceux de la rotule du dispositif et donc de l'articulation du poignet située juste à ce niveau.

Avant de débuter l'examen, vérifiez que le câble du boitier électronique renfermant le capteur de mesure d'angulation du mouvement, est raccordé à l'antenne d'acquisition.

L'installation finie, le sujet peut simuler un cycle de mouvement DRU à titre de vérification ultime avant l'acquisition. Une fois que le mouvement est compris et reproduit correctement par le sujet, celui-ci doit essayer de réaliser un aller-retour (de la position neutre du poignet à l'inclinaison radiale puis à l'inclinaison ulnaire et retour à la position neutre) en un nombre de secondes définies par la durée d'acquisition que l'on souhaite effectuer. Une fois cet entrainement réalisé, le sujet est prêt à passer l'examen.

Lorsque l'examen est terminé, débranchez le câble puis détacher les sangles de fixation afin libérer le membre du sujet. Appuyez ensuite sur les cliquets qui bloquent la partie mobile du dispositif afin de la désolidariser de son support. La partie fixe peut ensuite être retirée de la table d'examen.

Précautions à prendre après utilisation

Après désinfection et nettoyage du dispositif, celui-ci est rangé dans la mallette prévue à cet effet. Vérifier régulièrement la rotule ainsi que l'ensemble des éléments de fixation.

Entretien et stockage

Stocker le dispositif dans une pièce où la température ne varie pas et où celle-ci n'est ni trop haute, ni trop basse (environ 20°C)

Le dispositif GWMD ne nécessite pas de stérilisation puisqu'il entre en contact uniquement avec la peau du sujet. Il peut être nettoyé avec des produits dédiés à l'entretien des dispositifs médicaux.

La rotule du dispositif glisse, aidée par de la graisse de silicone. Compte tenu de l'importance de cette pièce sur le bon fonctionnement du dispositif, il est possible d'en remettre au besoin.

- ***Formation nécessaire***

L'utilisation du dispositif nécessite une rapide formation rappelant les principes de base. Son utilisation est sous la supervision d'un médecin qui contrôle l'installation du dispositif et du sujet.

- ***Mécanisme d'action de l'inclinaison radio-ulnaire***

Cette partie est destinée à appliquer un mouvement guidé de DRU par le poignet du sujet, sans mouvement de la main ni de l'avant-bras. Le mouvement d'inclinaison est autorisé par la rotation de la rotule. Sa limitation en amplitude, dans les deux sens, est appliquée par les loquets d'arrêt. Ils sont disposés de part et d'autre de la partie fixe du dispositif et autorise une amplitude de 10°, 20° ou 30° pour chacune des deux inclinaisons latérales (Figure 38).

- ***Normes appliquées***

Nous nous sommes référés à la Directive Européenne 93/42/CE pour garantir la sécurité du patient, du personnel et de l'environnement hospitalier, pendant l'utilisation du dispositif GWMD. Cette directive énonce les exigences essentielles auxquelles un prototype doit répondre avant sa mise à disposition au personnel soignant, que ce soit dans un contexte clinique ou d'études cliniques. Notre dispositif possède une partie mécanique, électronique, de mesure et est utilisé en association avec un dispositif médical pouvant émettre des rayonnements.

La directive (D.E. 93/42/CE) exige sur ces parties que nous veillons à :

Mécanique :	Protéger le patient et l'utilisateur des risques liés, par exemple, à la résistance, à la stabilité et aux pièces mobiles.
Mesure :	Que la mesure soit réalisée par un système conçu et fabriqué de telle sorte ▪ Que la mesure soit exacte et donnée avec une constance de mesure suffisante, dans la limite d'exactitude appropriée. ▪ Qu'elle respecte des principes ergonomiques. ▪ Que les mesures effectuées soient exprimées en unités légales (sous-entendu exprimée en Unité du Système International).
Electronique :	▪À prévoir les moyens nécessaires pour supprimer ou réduire autant que possible les risques pouvant découler d'un défaut. ▪À éviter, dans la mesure du possible, les risques de chocs électriques accidentels dans des conditions normales d'utilisation. ▪À réduire à un minimum les risques de création de champ électromagnétiques susceptibles d'affecter le fonctionnement d'autres dispositifs ou équipements placés dans l'environnement habituel.
De rayonnement :	À concevoir le dispositif de façon à réduire l'exposition des patients, de l'utilisateur et des autres personnes, aux émissions de rayonnements au minimum compatible avec le but recherché.

Pour atteindre les exigences essentielles de la directive susmentionnée, nous nous sommes référés à la norme ISO 14971.

Pour appliquer cette norme nous avons procédés selon le schéma suivant :

1. Le risque est recensé, défini et décrit.

2. La criticité initiale de ce risque est calculée. Pour cela, la gravité et la probabilité de survenue sont estimées sur une échelle de 1 à 5 et la criticité initiale est calculée en multipliant la probabilité de survenue du risque par sa gravité.

3. Les moyens de réduction ou de résolution du risque mis en œuvre sont définis et décrits.

4. La criticité résiduelle est calculée en estimant la gravité et la probabilité de survenue du risque avec l'application des mesures définies en amont.

- ***Évaluation du risque***

Afin d'évaluer le risque, chacune des étapes de l'utilisation du dispositif GWMD a été analysée et des moyens de maitrise du risque ont été mis en place. Pour chaque étape, le risque résiduel a ainsi été évalué et placé dans le tableau 4. Chaque moyen de maitrise du risque est décrit dans la liste suivante.

Identification des risques selon la norme ISO-14971 :

1. Mouvement

Risque 1 : Amplitude d'inclinaisons autorisée trop importante pour le sujet entraînant des douleurs.

- Résolution : Des loquets permettent de limiter les angulations de l'articulation observée, bloquant les mouvements selon une angulation maximale autorisée. Ces amplitudes maximales autorisées sont définies par le praticien avec le patient lors de la phase test pré-acquisition. L'amplitude autorisée est donc adaptable en fonction des douleurs articulaires du sujet.

Risque 2 : Ne pas connaître le degré d'amplitude d'inclinaisons du poignet du sujet pendant l'examen.

- Résolution : L'amplitude autorisée est limitée dans ses extrêmes par les deux loquets. La mesure de l'amplitude durant l'examen est recueillie par le boitier électronique relié à la console.

2. Mise en place

Risque 3 : Douleurs à la base des doigts induites par les plots.

- Résolution : Chaque plot coulisse le long d'un rail respectif permettant de gérer la hauteur nécessaire à la fixation des doigts sans occasionner de douleurs. De plus, les plots ont été imprimés en utilisant un plastique souple évitant ainsi les appuis douloureux.

Risque 4 : Les douleurs d'avant-bras induites par la gouttière et ses sangles.

- Résolution : Chaque partie de la gouttière est recouverte d'un coussin souple permettant une compression totalement indolore sur l'avant-bras. Les sangles de serrage ne sont pas en contact direct avec l'avant-bras mais passe par-dessus les rebords de la gouttière.

3. Le sujet

Risque 5 : Le sujet présente des douleurs au repos ou une raideur importante de poignet.

- Résolution : Le médecin formé à l'utilisation du dispositif GWMD prend la responsabilité de son utilisation ou non, en fonction de l'examen clinique du patient et des résultats qu'il attend de l'examen d'imagerie.

Risque 6 : Le sujet possède une immobilisation du poignet.

- Résolution : L'utilisation du dispositif GWMD est contre-indiquée.

Risque 7 : Le sujet rapporte des allergies de contact.

- Résolution : L'utilisation ou non du dispositif GWMD est sous la responsabilité du médecin.

4. Compatibilité électromagnétique

Risque 8 : Le capteur interfère avec le bon fonctionnement de l'environnement d'imagerie.

- Résolution : Le capteur utilisé a été choisi pour son marquage CE et le dispositif n'est pas utilisé avec un dispositif médical autre que l'antenne d'acquisition de l'outil d'imagerie.

Risque 9 : Le dispositif possède des pièces incompatibles avec les champs magnétiques de l'IRM.

- Résolution : L'ensemble des pièces du dispositif sont non métalliques et compatibles avec l'IRM.

Tableau 4. Évaluation des risques du dispositif GWMD.

		Étendue des dommages (ED)			
		Faible	Substantielle	Importante	Très importante
Probabilité de survenue (P)	Presque certaine				
	Très importante		R1 R2		
	Importante		R8		
	Modérée	R1 R2	R3 R4	R5	R7
	Improbable	R3 R4 R5 R8	R6 R7 R9	R6	R9
Légende	R Évaluation du risque avec mise en place de moyens de maitrise du risque R Évaluation du risque sans mise en place de moyens de maitrise du risque R1 : Mauvais réglage de l'amplitude R2 : Absence d'indication de l'amplitude R3 : Absence de support pour les doigts R4 : Absence de support pour l'avant-bras R5 : Patient avec des douleurs ou une raideur du poignet R6 : Patient avec une immobilisation du poignet R7 : Patient avec des allergies de contact R8 : Capteur interférent R9 : Dispositif IRM non compatible				

La plupart des risques identifiés dans le tableau ci-dessus sont classifiés avec une probabilité de survenance « improbable ». Les risques classifiés avec une probabilité de survenance « modérée » sont liés à une mauvaise utilisation du dispositif GWMD.

- Le risque R1 correspond à l'application d'une amplitude d'inclinaisons autorisée trop grande. Ce risque est limité dans sa dangerosité par deux points : le premier est qu'en l'absence de tout réglage des loquets, le seuil maximal d'amplitude autorisée sera de 30° en inclinaison radiale et 30° en inclinaison ulnaire, soit 60°. Physiologiquement, la déviation radiale du poignet a une amplitude d'environ 15° à 25° et la déviation ulnaire d'environ 40° à 50°, soit 55° à 75°. Ainsi, le seuil maximal en l'absence de réglage sera dans les normes physiologiques. Le deuxième point est que le patient spontanément limitera son amplitude maximale afin de ne pas déclencher des douleurs et donc éviter des potentiels dommages.
- Le risque R2 correspond à un mauvais recueil de l'angulation en degrés. Ce risque présente un dommage pour les données récoltées par l'opérateur mais n'a aucun impact sur le patient.

Ainsi, malgré les deux risques ayant une probabilité de survenance « modérée », le bénéfice tiré d'un examen utilisant le dispositif GWMD et permettant le diagnostic d'instabilité du carpe en imagerie dynamique, dépasse largement les risques encourus.

Essais précliniques

Pour l'évaluation du dispositif GWMD, deux types de test ont été réalisés :

Type de test	**Schéma du test**	**Conclusions attendues**
Préclinique en Scanner	Nous avons réalisé une acquisition scanographique du dispositif en utilisant le scanner Aquilion One du *service d'imagerie Guilloz.* Le but était de vérifier la compatibilité en termes d'encombrement du dispositif sur la table d'examen ainsi que sa stabilité notamment lors du déplacement de la partie mobile. Nous avons également vérifié l'absence d'artéfact provoqué par les composants du dispositif.	- Les dimensions du dispositif sont compatibles avec une utilisation en scanner. - Le dispositif est stable sur la table d'examen, notamment lors du déplacement latéral gauche – droite de sa partie mobile. - Le dispositif ne provoque pas d'artéfact, y compris au niveau de son capteur électronique.
Préclinique sur volontaires sains	Nous avons réalisé des essais sur volontaires sains en conditions réelles dans la salle du scanner Aquilion One du *service d'imagerie Guilloz*, sans acquisition scanographique. Le but était de valider le fonctionnement du dispositif (installation et maintien du membre, faisabilité du mouvement de DRU, recueil des données du boitier électronique sur le logiciel, compatibilité de l'encombrement du dispositif membre installé avec la table d'examen)	- Le membre supérieur (main, poignet, avant-bras) se positionne correctement sur le dispositif avec un confort pour le sujet. - La main et l'avant-bras sont parfaitement stabilisés ; seul le poignet peut être le siège d'un mouvement. - Les sangles du dispositif résistent à un usage répétitif. - Le dispositif permet la réalisation d'un mouvement actif bidirectionnel axial d'amplitudes maximales, tout en évitant les autres mouvements parasites. - Le logiciel affiche les données recueillies par le boitier électronique sur l'amplitude de mouvement. - L'utilisation du dispositif est compatible avec un environnement de scanner.

- ***Test de compatibilité avec le scanner***

Le dispositif GWMD a été placé dans l'environnement du scanner Aquilion One du *service d'imagerie Guilloz* afin de vérifier que ses dimensions étaient compatibles avec la table d'examen, et que sa composition n'entrainait pas de gêne pour la réalisation et la lecture de l'acquisition scanographique. Ainsi, le dispositif a été installé de façon à simuler une acquisition centrée sur la zone d'intérêt à analyser. Le test s'est déroulé avec les paramètres d'acquisition décrit par Gondim Teixeira et al., 2017 (Tableau 3). Préalablement au lancement de l'acquisition scanographique, un médecin volontaire a simulé l'installation de son membre supérieur droit sur le dispositif, telle qu'elle pourrait avoir lieu en pratique courante.

Nous avons pu confirmer, d'une part, le bon rapport entre les dimensions du dispositif et la taille de la table d'examen. D'autre part, l'installation du poignet du médecin volontaire n'a présenté aucune difficulté permettant à ce dernier de réaliser un cycle de DRU (Figure 39).

De plus, le dispositif GWMD est resté parfaitement stable lorsque le sujet mobilisait son poignet. Nous avons ensuite procédé à la séquence d'acquisition du dispositif. Les résultats ont montré que le dispositif GWMD n'occasionnait ni artéfact, ni gène à la réalisation et à la lecture de chacune des séquences (Figure 40).

Figure 39. *Photographie montrant la compatibilité en termes d'encombrement du dispositif avec la table d'examen du scanner Aquilion One du service d'imagerie Guilloz. À noter la simulation hors acquisition scanographique, de l'installation sur le dispositif du membre supérieur droit d'un médecin volontaire.*

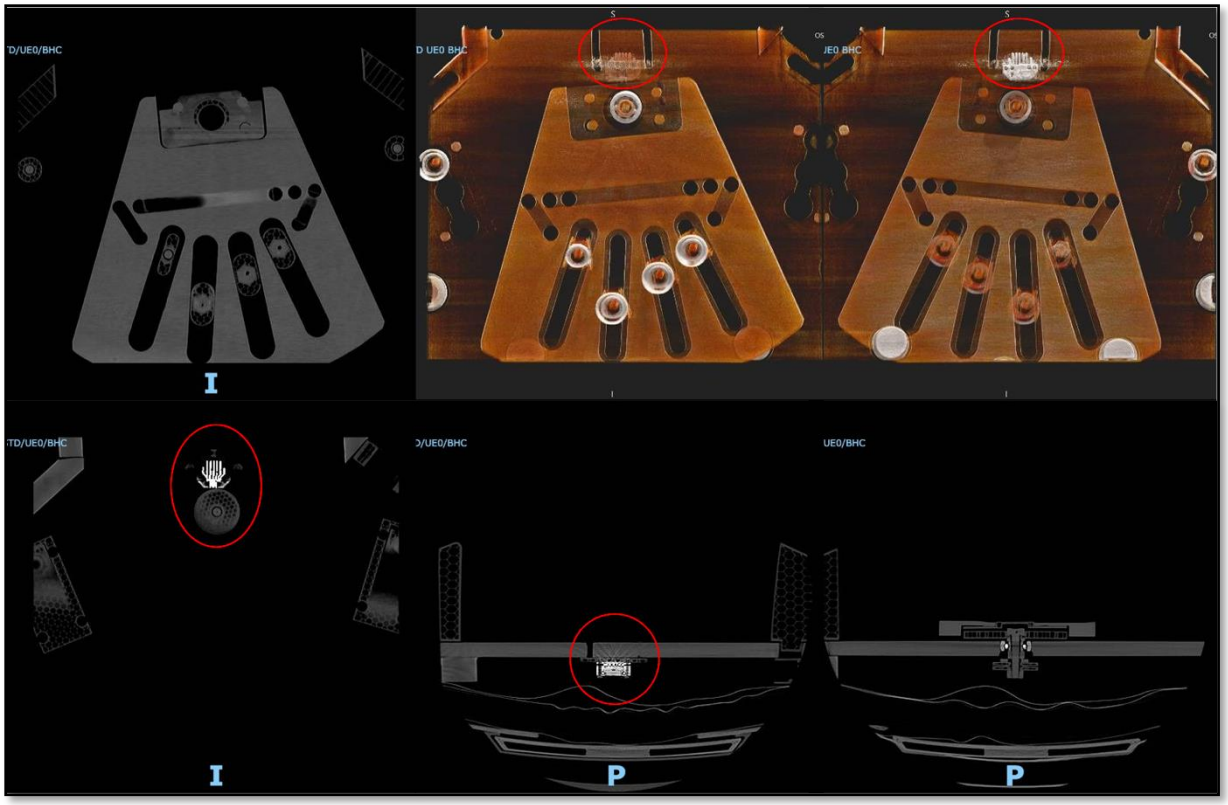

Figure 40. *Acquisition scanographique (scanner Aquilion One du service d'imagerie Guilloz) du dispositif, centrée sur la zone d'intérêt à analyser, montrant l'absence d'artéfact induit par le capteur électronique (cercles rouges).*

- ***Test de fonctionnement sur sujets sains***

Le but de ce test était de valider le fonctionnement du dispositif GWMD en simulant des conditions réelles mais sans acquisition. Plusieurs éléments ont été testés :

- Le positionnement du membre supérieur : la main, poignet et avant-bras se sont systématiquement positionnés correctement. La partie mobile s'est adaptée à tout type d'anatomie, la fixation des doigts se faisant sans difficulté ni gène pour le sujet. La partie mobile est venue s'encliqueter sans aucun mouvement forcé. L'avant-bras prenait une position axiale naturellement et sa stabilisation était excellent sans aucune gêne pour le patient.
- La mise en mouvement de DRU : le dispositif a permis au sujet d'effectuer, avec une totale indolence, un mouvement volontaire axial bidirectionnel d'amplitudes radio-ulnaires maximales (variables d'un sujet à l'autre), avec neutralisation des mouvements de translation et de prono-supination de l'avant-bras. Les loquets latéraux limitaient parfaitement le degré d'amplitude en inclinaisons radiale et ulnaire maximales.
- L'enregistrement et la visibilité des données du capteur : un enregistrement de l'amplitude de mouvement a été permis par le capteur avec une lecture directe sur le logiciel. Nous n'avons pas retrouvé de différences notables entre l'amplitude maximale (inclinaison radiale maximale + inclinaison ulnaire maximale) mesurée cliniquement avec un goniomètre (Prestige® Medical, Northridge, USA, précision 1°) poignet disposé sur le dispositif, de celle enregistrée par le capteur (Tableau 5) (Figure 41).
- L'installation du sujet en salle d'examen : Chaque sujet a pu s'installer à côté de la table d'examen et positionner son poignet, fixé au dispositif, au centre de l'antenne d'acquisition. Lors du mouvement du poignet, aucune gêne n'a été rapportée en rapport avec l'environnement du scanner.

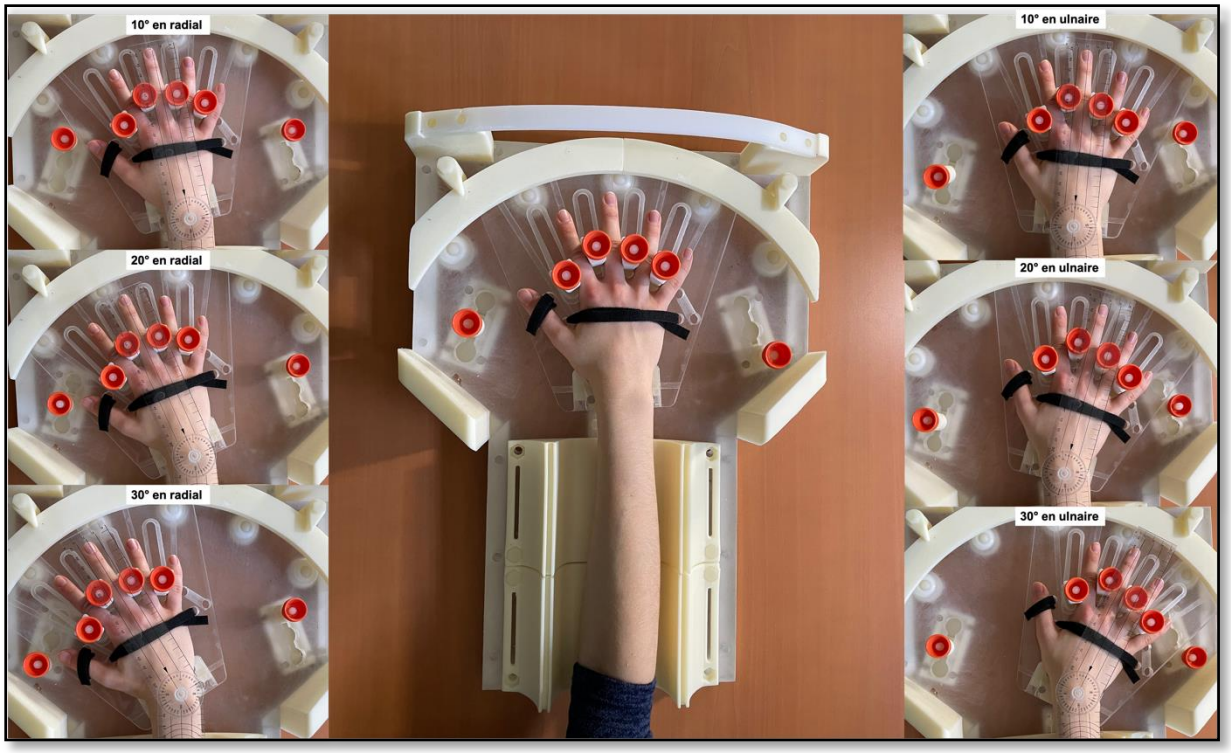

Figure 41. *Photographies illustrant l'installation du membre droit d'un volontaire sain sur le dispositif GWMD avec son poignet positionné à 0° puis en inclinaison radiale à 10°, 20°, 30° et en inclinaison ulnaire à 10°, 20°, 30°.*

Tableau 5. Comparaison des mesures clinques et des enregistrements électroniques des amplitudes inclinaisons radio-ulnaires maximales.

Sujet	Sexe	Mesure clinique de l'amplitude maximale	Enregistrement électronique de l'amplitude maximale
1	F	60°	60°
2	F	40°	40°
3	H	50°	50°
4	H	60°	60°
5	H	50°	50°

F : Femme, H : Homme

Les résultats de ce test démontrent le bon fonctionnement du dispositif dans l'environnement scanner et sa compatibilité chez le sujet sain.

Conclusion et résumé des recommandations pour l'investigateur

Le dispositif de recherche GWMD représente une aide à la réalisation d'une acquisition en imagerie dynamique quatre dimensions du poignet, par l'homogénéisation et la reproductibilité d'un mouvement de DRU. Il permet également de palier à d'éventuels mouvements parasites, notamment induit par la prono-supination de l'avant-bras. Le recueil des données enregistrées sur l'amplitude d'inclinaisons apporte une valeur ajoutée pour l'analyse des images acquises par l'outil d'imagerie. Ce dispositif de guidage du mouvement du poignet devrait permettre d'apporter confort et précision dans le bilan diagnostic et pronostic en imagerie dynamique des pathologies du carpe et notamment l'ISL. Le dispositif GWMD doit être utilisé seul et ne peut être associé à un dispositif médical autre que l'outil d'imagerie (TDM ou IRM). Seul le personnel formé à son fonctionnement peut l'utiliser et ce, sous la tutelle d'un médecin responsable.

CONCLUSION ET PERSPECTIVES

Dans ce travail de thèse, nous avons tenté d'apporter et d'évaluer des solutions pertinentes pour la prise en charge diagnostique et thérapeutique des ISL chroniques au stade pré-arthrosique. Plusieurs outils ont été sollicités dans ce travail particulièrement collaboratif. Le 4DCT (scanner Aquilion One du *service d'imagerie Guilloz)* s'est avéré être un outil d'imagerie dynamique essentiel tout au long de ce travail, à la fois pour son rôle dans l'évaluation diagnostic et pronostic des patients suspectés d'ISL, mais également dans l'évaluation de l'efficacité biomécanique de notre technique chirurgicale de reconstruction du complexe scapho-lunaire.

- Nous avons, dans un premier temps, évalué la contribution du 4DCT dans le bilan d'imagerie diagnostique des patients avec une suspicion clinique d'ISL. Nos résultats ont montré la bonne performance de cet examen pour confirmer l'état d'ISL, y compris chez les patients présentant une évaluation radiographique initiale non contributive. Le 4DCT, par son analyse quantitative et dynamique des distances et des angles interosseux, a rendu possible la mise en évidence et la quantification des caractéristiques anatomiques rencontrées lors d'un état d'ISL. L'évaluation du SLG s'est avérée être le meilleur paramètre pour confirmer le diagnostic d'ISL. Les évaluations des PRSA et LCA sont apparues comme pertinentes pour apporter une valeur pronostic en termes de gravité lésionnelle. De plus, la corrélation que nous avons pu établir entre l'exploration chirurgicale arthroscopique pré-thérapeutique, considérée comme « gold standard » par la plupart des auteurs, et l'analyse en 4DCT, de l'articulation scapho-lunaire, a conforté nos conclusions sur l'intérêt clinique de ce nouvel outil. Nous pouvons également en ressortir des avantages en faveur du 4DCT, tels que l'absence de risque de complications post-opératoires, la reproductibilité inter- et intra-observateurs, ainsi que la possibilité de quantification. Ces études prospectives s'intègrent dans le cadre du protocole de recherche clinique « **Étude EDLIS** ». Notre perspective future est d'augmenter les inclusions afin de pouvoir confirmer nos résultats, et ainsi intégrer le 4DCT dans notre protocole d'imagerie proposé aux patients suspectés d'ISL avec doute persistant à l'issue du bilan radiographique. Nous pensons qu'il pourra être possible, à terme, de proposer une classification des stades d'ISL en 4DCT, probablement plus précise que les classifications actuelles radiographiques ou arthroscopiques. Nous soulevons également la question de l'intérêt de maintenir l'étape chirurgicale d'arthroscopie exploratrice pré-thérapeutique.

➢ Dans un deuxième temps, nous avons abordé l'aspect thérapeutique de cette pathologie au stade pré-arthrosique. De multiples techniques de reconstruction ligamentaires scapho-lunaires sont présentes dans la littérature, et toutes ont en commun de reconstruire à la fois le LIOSL mais aussi un ou plusieurs stabilisateurs extrinsèques. Néanmoins, notre revue de la littérature nous a amené à constater qu'il n'existait pas de « gold standard » à ce jour, et que majoritairement, les auteurs rapportaient une discordance radio-clinique. En effet, ces différentes ligamentoplasties apportent généralement grande satisfaction sur le plan de l'amélioration symptomatique, mais il persiste dans la majorité des cas des anomalies radiographiques d'ISL. De plus, aucune étude de la littérature propose une évaluation de l'efficacité de la chirurgie en utilisant un outil d'imagerie performant tel que le 4DCT. Dernièrement, plusieurs auteurs ont souligné l'existence de complications iatrogènes, induites par le caractère trans-scaphoïdien d'un grand nombre de ces techniques de reconstruction. Il nous a donc semblé pertinent de proposer une nouvelle technique de ligamentoplastie avec un double objectif : corriger les imperfections des ligamentoplasties retrouvées dans la littérature et répondre aux concepts actuels sur les différents stabilisateurs ligamentaires incriminés dans la genèse de l'ISL.

Dans un souci de précision et rigueur scientifique, notre ligamentoplastie « SLIC » a pu faire l'objet d'une évaluation à la fois cadavérique et clinique. Nous avons comparé son efficacité clinique et radiographique à la Triple ténodèse de Garcia-Elias (Garcia-Elias et al., 2006), la plus fréquemment utilisée dans la littérature. Nos premiers résultats ont permis de montrer d'une part l'impact positif de la « SLIC » sur la correction de la dissociation, et d'autre part, sa supériorité par rapport à la Triple ténodèse en termes d'amélioration des anomalies radiographiques. Toutefois, des limitations sont apparues dans la version initiale de cette ligamentoplastie. Nous avons constaté des difficultés techniques portant sur l'étape intermédiaire de la procédure. Une réalisation parfois aléatoire de celle-ci aboutissait à une gestion imparfaite de la tension de la ligamentoplastie, responsable d'une absence de maintien de la correction de la dissociation obtenue en per-opératoire et de ce fait, une altération radiographique secondaire. Ainsi, nous avons amélioré notre ligamentoplastie « SLIC » afin de répondre à ces constatations. Une évaluation cadavérique en 4DCT a été réalisée permettant de montrer l'efficacité de notre version modifiée, notamment en ce qui concerne la restauration de l'alignement intra-carpien. Nos constatations cadavériques se sont confirmées lors de la comparaison des résultats cliniques prospectifs de nos deux versions.

La modification technique a permis d'obtenir le maintien de la correction per-opératoire. Ces études prospectives s'intègrent dans le cadre du protocole de recherche clinique « **Étude SLIC** ».

Nous souhaitons maintenant évaluer l'efficacité de notre reconstruction ligamentaire scapho-lunaire chez nos patients opérés, en faisant appel au 4DCT. Ainsi, nous avons récemment déposé un projet de recherche « **Étude EDLIS 2** », dont l'objectif principal sera d'évaluer la variation des paramètres biomécaniques du poignet avant et après chirurgie. Il sera intéressant de corréler les résultats en 4DCT avec l'évolution clinique du patient. Les données que nous recueillerons permettront de préciser l'algorithme décisionnel chirurgical basé sur les paramètres en 4DCT. Par exemple, il est acquis que la ligamentoplastie « SLIC », comme les autres ligamentoplasties, doit être réservée aux ISL réductibles, c'est-à-dire avec un scaphoïde pouvant se reverticaliser lors des mouvements du poignet. Au vu des résultats post-opératoires en 4DCT que nous obtiendrons, nous espérons pouvoir préciser différents stades de réductibilité de l'instabilité.

Pour finir, nous avons également proposé un nouvel abord dorsal de l'articulation du poignet. Notre objectif était de développer une capsulotomie respectueuse des structures capsulaires vasculo-nerveuses et ligamentaires extrinsèques, tout en permettant une bonne exposition des os du carpes. Notre étude anatomique a confirmé la faisabilité technique de cette nouvelle approche et ses avantages en termes d'exposition osseuse, du maintien de l'intégrité des fibres des ligaments extrinsèques dorsaux ainsi que la vascularisation et l'innervation du lambeau capsulaire disséqué. Une étude clinique prospective serait la prochaine étape pour valider nos résultats.

- Nous avons enfin conçu un dispositif de guidage du mouvement de DRU du poignet pour les acquisitions en imagerie dynamique. Ce dispositif de recherche a fait l'objet d'essais précliniques confirmant sa compatibilité avec l'environnement du scanner et son fonctionnement hors acquisition scanographique sur volontaires sains. Par ailleurs, l'ensemble des composants du dispositif est compatible IRM. Son utilisation en pratique courante simplifiera la réalisation des acquisitions en imagerie dynamique, par sa facilité de reproductibilité du mouvement de DRU, et par l'absence de mouvements parasites de l'avant-bras. Nous souhaitons l'inclure dans le projet de recherche clinique « **Étude EDLIS 2** ».

➢ Pour finir, Boutin et al., (2013) et Shaw et al., (2019) ont rapporté des résultats intéressants sur l'utilisation de l'IRM dynamique dans l'évaluation de la cinématique du carpe, et ainsi des possibles applications dans le cadre du diagnostic des instabilités intra-carpiennes. Les auteurs se sont notamment intéressés à l'analyse de plusieurs séquences d'acquisitions, afin d'obtenir une bonne résolution spatiale mais aussi temporelle.

L'un des avantages de l'IRM est l'absence de caractère irradiant. Toutefois, nous souhaitons préciser que le 4DCT reste faiblement irradiant. L'autre avantage de l'IRM est la possibilité d'avoir une analyse qualitative morphologique ligamentaire. Nos premiers essais réalisés sur volontaires sains ont permis de poser les bases des paramètres d'acquisitions. Nous avons utilisé un système IRM 1.5T Signa HDxt (General Electric, Milwaukee, Wisconsin, États-Unis). La figure 42 illustre la qualité de précision des structures analysées que nous avons pu obtenir. Sur cette base, nous souhaitons prolonger ce travail afin de définir un protocole d'acquisition, permettant d'allier résolution spatiale et temporelle. La question du choix de l'antenne surfacique représente également un enjeu indispensable avant de pouvoir proposer cette technique d'imagerie dynamique en pratique clinique.

Telles sont nos conclusions de ce travail et les perspectives que nous envisageons pour le poursuivre.

Figure 42. *Acquisition en IRM dynamique du poignet droit d'un volontaire sain pendant un mouvement de DRU. Images coronales du poignet dans les positions d'inclinaison radiale (A), neutre (B) et ulnaire (C) lors de la manœuvre continue de déviation. Il s'agit d'une séquence RF-Spoiled Radial FLASH : voxel size (mm^3) = 0.62x0.62x5, temporal resolution (ms) = 600, TR/TE (ms) = 4.65/2.27.*

RÉFÉRENCES

Adolfsson L. Arthroscopic diagnosis of ligament lesions of the wrist. *J Hand Surg Br*. 1994, 19:505-512.

Almquist EE, Bach AW, Sack JT, Fuhs SE, Newman DM. Four-bone ligament reconstruction for treatment of chronic complete scapholunate separation. *J Hand Surg Am.* 1991, 16:322-7.

Anakwe RE, Middleton SD, Hayton MJ. A modified dorsal capsulotomy for improved radiocarpal exposure. *J Hand Surg Eur Vol. 2013, 38:805-6.*

Andersson JK, Andernord D, Karlsson J, et al. Efficacy of magnetic resonance imaging and clinical tests in diagnostics of wrist ligament injuries: a systematic review. *Arthroscopy*. 2015, 31:2014–2020.

Abou Arab W, Rauch A, Chawki M et al. Scapholunate instability: improved detection with semi-automated kinematic CT analysis during stress maneuvers. *European Radiology*. 2018, 28:4397-4406.

Athlani L, Pauchard N, Detammaecker R et al. Treatment of chronic scapholunate dissociation with tenodesis: A systematic review. *Hand Surg Rehabil*. 2018, 37:65-76.

Athlani L, Pauchard N, Dautel G. Radiological evaluation of scapholunate intercarpal ligamentoplasty for chronic scapholunate dissociation in cadavers. *J Hand Surg Eur Vol*. 2018, 43:387-393.

Athlani L, Pauchard N, Dautel G. Outcomes of scapholunate intercarpal ligamentoplasty for chronic scapholunate dissociation: a prospective study in 26 patients. *J Hand Surg Eur Vol*. 2018, 43:700-707.

Athlani L, Pauchard N, Dautel G. Intercarpal ligamentoplasty for scapholunate dissociation: comparison of two techniques. *J Hand Surg Eur Vol.* 2020, 19;1753193420940498.

Bain GI, Krishna SV, MacLean S et al. "Locked" Scapholunate Instability Diagnosed with 4D Computed Toography Scan. *J Wrist Surg*. 2019, 8:321-326.

Bain GI, Watts AC, McLean J, Lee YC, Eng K. Cable-augmented, quad ligament tenodesis scapholunate reconstruction: rationale, surgical technique, and preliminary results. T*ech Hand Up Extrem Surg.* 2013, 17: 13-9.

Baxamusa TH, Williams CS. Capsulodesis of the wrist for scapholunate dissociation. *Tech Hand Up Extrem Surg*. 2005, 9:35–41.

Berger RA, Bishop IT. A fiber-splitting capsulotomy technique for dorsal exposure of the wrist. *Tech Hand Up Extrem Surg.* 1997, 1:2-10.

Berger RA, Bishop AT, Bettinger PC. New dorsal capsulotomy for the surgical exposure of the wrist. *Ann Plast Surg*. 1995, 35: 54-59.

Berger, RA. The ligament of the wrist. A current overview of anatomy with considerations of their potential functions. *Hand Clin*. 1997, 13:63–82.

Bille B, Harley B, Cohen H. A comparison of CT arthrography of the wrist to findings during wrist arthroscopy. *J Hand Surg Am*. 2007, 32:834 – 841.

Blatt G. Capsulodesis in reconstructive hand surgery. Dorsal wrist capsulodesis for the unstable scaphoid and volar capsulodesis following excision of the distal ulna. *Hand Clin.* 1987, 3:81–102.

Blevens AD, Light TR, Jablonsky W et al. Radiocarpal articular contact characteristics with scaphoid instability. *J Hand Surg Am.* 1989, 14:781–790.

Boutin RD, Buonocore MH, Immerman I et al. Real-time magnetic resonance imaging (MRI) during active wrist motion--initial observations. *PLoS One*. 2013, 8:e84004.

Brunelli GA, Brunelli GR. A new technique to correct carpal instability with scaphoid rotary subluxation: a preliminary report. *J Hand Surg Am.* 1995, 20: 82-5.

Burgess RC. The effect of rotatory subluxation of the scaphoid on radio-scaphoid contact. *J Hand Surg Am.* 1987, 12:771-774.

Carlsen, BT, Shin, AY. Wrist Instability. *Scandinavian Journal of Surgery*. 2008, 97:324–332.

Carr R, MacLean S, Slavotinek J et al. Four-Dimensional Computed Tomography Scanning for Dunamic Wrist Disorders: Prospective Analysis and Recommendations for Clinical Utility. *J Wrist Surg*. 2019, 8:161-167.

Cautilli GP, Wehbé MA. Scapho-lunate distance and cortical ring sign. *J Hand Surg Am*. 1991, 16:501–503.

Chabas JF, Gay A, Valenti D, Guinard D, Legre R. Results of the modified Brunelli tenodesis for treatment of scapholunate instability: a retropective study of 19 patients. *J Hand Surg Am.* 2008, 33:1469-77.

Cognet JM, Baur P, Gouzou S. Un ligament scapholunaire bombé, signe arthrotomodensitométrique d'instabilité scapholunaire traumatique. *Rev Chir Orthop Reparatrice Appar Mot*. 2008, 94:182-187.

Corella F, Del Cerro M, Ocampos M et al. Arthroscopic ligamentoplasty of the dorsal and volar portions of the scapholunate ligament. *J Hand Surg Am*. 2013, 8:2466–2477.

Crawford K, Owusu-Sarpong N, Day C, Iorio M. Scapholunate Ligament Reconstruction: A Critical Analysis Review. *J Bone Joint Surg Am*. 2016, 4:41-8.

Cueno P. Osteoligamentoplasty and limited dorsal capsulodesis for chronic scapholunate dissociation. *Ann Chir Main*. 1999, 18:38–53.

Dautel G, Goudot B, Merle M. Arthroscopic diagnosis of scapho-lunate instability in the absence of X-ray abnormalities. *J Hand Surg Br*. 1993, 18:213–218 .

De Carli P, Donndorff AG, Gallucci GL, Boretto JG, Alfie VA. Chronic scapholunate dissociation: ligament reconstruction combining a new extensor carpi radialis longus tenodesis and a dorsal intercarpal ligament capsulodésis. *Tech Hand Up Extrem Surg.* 2011, 15:6-11.

De Roo MGA, Muurling M, Dobbe JGG et al. A four-dimensional-CT study of in vivo scapholunate rotation axes: possible implications for scapholunate ligament reconstruction. *J Hand Surg Eur Vol*. 2019, *44*:479–487.

De Smet L, Van Hoonacker P. Treatment of chronic static scapholunate dissociation with the modifed Brunelli technique: preliminary results. Acta Orthop Belg. 2007, 73:188-91.

Dréant N, Dautel G. Development of an arthroscopic severity score for scapholunate instability. *Chir Main*. 2003, 22:90–94.

Dréant N, Mathoulin C, Lucchetti R et al. Comparison of two arthroscopic classifications for scapholunate instability. *Chir main*. 2009, 28:74–77.

Dornberger JE, Rademacher G, Mutze S et al. Accuracy of simple plain radiographic signs and measures to diagnose acute scapholunate ligament injuries of the wrist. *European Radiology*. 2015, 25:3488-98.

Elgammal A, Lukas B. Mid-term results of ligament tenodesis in treatment of scapholunate dissociation: a retrospective study of 20 patients. *J Hand Surg Eur.* 2016, 41:56-63.

Ellanti P, Sisodia G, Al-Ajami A, Ellanti P, Harrington P. The modified Brunelli procedure for scapholunate instablity: a single-centre study. *Hand Surg.* 2014, 19:39-42.

Esplugas M, Garcia-Elias M, Lluch A, Llusá Pérez M. Role of muscles in the stabilization of ligament-deficient wrists. *J Hand Ther.* 2016, 29:166-74.

Gajendran VK, Peterson B, Slater RR, Szabo RM. Long-term outcomes of dorsal intercarpal ligament capsulodesis for chronic scapholunate dissociation. *J Hand Surg Am*. 2007, 32:1323–33.

Garcia-Elias M, Alomar Serrallach X, Monill Serra J. Dart-throwing motion in patients with scapholunate instability: a dynamic four- dimensional computed tomography study. *J Hand Surg Eur Vol*. 2014, 39:346–352.

Garcia-Elias M, Geissler WB. Carpal instability. In Green, Hotchkiss, Pederson, Wolfe (eds.) Green's operative hand surgery. Fifth edition. Elsevier Churchill Livingstone. Volume 1 : 2005; pp. 535-604.

Garcia-Elias M, Lluch AL, Stanley JK. Three-ligament tenodesis for the treatment of scapholunate dissociation: Indications and surgical tech- nique. *J Hand Surg Am*. 2006; 31:125–134.

Garcia-Elias M, Puig de la Bellacasa I, Schouten C. Carpal Ligaments: A Functional Classification. *Hand Clin*. 2017, 33:511-520.

Geissler WB. Arthroscopic management of scapholunate instability. *J Wrist Surg*. 2013, 2:129-135.

Geissler WB, Freeland AE, Savoie FH et al. Intracarpal soft-tissue lesions associated with an intra-articular fracture of the distal end of the radius. *J Bone Joint Surg*. 1996, 78:357-365.

Gilula LA, Weeks PM. Post-traumatic ligamentous instabilities of the wrist. *Radiology*. 1978, 129:641–651.

Gondim Teixeira PA, De Verbizier J, Aptel S et al. A. Posterior Radioscaphoid Angle as a Predictor of Wrist Degenerative Joint Disease in Patients With Scapholunate Ligament Tears. *AJR Am J Roentgenol*. 2016, 206:144-50.

Gondim Teixeira PA, Formery AS, Hossu G et al. Evidence-based recommendations for musculoskeletal kinematic 4D-CT studies using wide area-detector scanners: a phantom study with cadaveric correlation. *European Radiology*. 2017, 27:437–446.

Gondim Teixeira PA, Blanc JB, Rauch A, Abou Arab W, Hossu G, Athlani L, Blum A. Evaluation of dorsal subluxation of the scaphoid in patients scapholunate ligament tears: a four-dimensional CT study. *AJR Am J Roentgenol*. 2021, 216:141-149.

Guss MS, Bronson WH, Rettig ME. Acute Scapholunate Ligament Instability. *J Hand Surg Am*. 2015, 40:2065-2067.

Hafezi-Nejad N, Carrino JA, Eng J et al. Scapholunate interosseous ligament tears: diagnostic performance of 1.5 T, 3 T MRI, and MR arthrography-a systematic review and meta-analysis. *Acad Radiol*. 2016, 23:1091–1103.

Hagert E, Forsgren S, Ljung BO. Differences in the presence of mechanoreceptors and nerve structures between wrist ligaments may imply differential roles in wrist stabilization. *J Orthop Res*. 2005, 23:757–763.

Hagert E, Persson JK, Werner M et al. Evidence of wrist proprioceptive reflexes elicited after stimulation of the scapholunate interosseous ligament. *J Hand Surg Am*. 2009, 34:642–665.

Hagert E, Ferreres A, Garcia-Elias M. Nerve-sparing dorsal and volar approaches to the radiocarpal joint. J Hand Surg Am 2010, 35:1070-4.

Johnstone DJ, Thorogood S, Smith WH et al. A comparison of magnetic resonance imaging and arthroscopy in the investigation of chronic wrist pain. *J Hand Surg Am*. 1997, 22:714–718.

Kakar S, Breighner RE, Leng S et al. The role of dynamic (4D) CT in the detection of scapholunate ligament injury. *J Wrist Surg*. 2016, 5:306–310.

Kamal RN, Starr A, Akelman E. Carpal kinematics and kinetics. *J Hand Surg Am*. 2016, 41:1011–1018.

Kani K.K, Mulcahy H, Chew FS. Understanding carpal instability: a radiographic perspective. *Skeletal Radiol*. 2016, 45:1031-1043.

Kijima Y, Viegas SF. Wrist anatomy and biomechanics. *J Hand Surg Am*. 2009, 34: 1555–1563.

Kitay A, Wolfe SW. Scapholunate Instability: Current Concepts in Diagnosis and Management. *J Hand Surg Am*. 2012, 37:2175-2196.

Koh KH, Lee HI, Lim KS, Seo JS, Park MJ. Effect of wrist position on the measurement of carpal indices on the lateral radiograph. *J Hand Surg Eur Vol*. 2013, 38:530-41.

Kwong Y, Mel AO, Wheeler G et al. Fourdimensional computed tomography (4DCT): a review of the current status and applications. *J Med Imaging Radiat Oncol*. 2015, 59:545-54.

Larsen CF, Amadio PC, Gilula LA et al. Analysis of carpal instability: I. Description of the scheme. *J Hand Surg Am*. 1995, 20:757–764.

Laulan J. Rotatory subluxation of the scaphoid: Pathology and surgical management. *Chir main*. 2009, 28:192–206.

Laulan J. Le poignet traumatique. Le Nen D, Laulan J, editors. Sémiologie de la main et du poignet. Montpellier: Sauramps Médical; 2001. p. 247-67.

Lawland A, Foulkes GD. The “clenched pencil” view:a modified clenched fist scapholunate stress view. *J Hand Surg Am*. 2003, 28:414-418.

Leclercq C, Mathoulin C. Complications of Wrist Arthroscopy: A Multicenter Study Based on 10,107 Arthroscopies. *J Wrist Surg.* 2016, 5:320–326.

Lee SK, Desai H, Silver B et al. Comparison of radiographic stress views for scapholunate dynamic instability in a cadaver model. *J Hand Surg Am*. 2011, 36:1149 –1157.

Lee YH, Choi YR, Kim S et al. Intrinsic ligament and triangular fibrocartilage complex (TFCC) tears of the wrist: comparison of isovolumetric 3D- THRIVE sequence MR arthrography and conventional MR image at 3 T. *Magn Reson Imaging*. 2013, 31:221–226.

Leng S, Zhao K, Qu M et al. Dynamic CT technique for assessment of wrist joint instabilities. *Med Phys*. 2011, 38:S50–S56.

Links AC, Chin SH, Waitayawinyu T, Trumble TE. Scapholunate interosseous ligament reconstruction: results with modified Brunelli technique versus four-bone weave. J Hand Surg Am. 2008, 33:850-6.

Linscheid RL, Dobyns JH. Treatment of scapholunate dissociation. Rotatory subluxation of the scaphoid. Hand Clin. 1992, 8:645-52.

Linscheid RL, Dobyns JH, Beabout JW et al. Traumatic carpal instability of the wrist. Diagnosis, classification and pathomechanics. *J Bone Joint Surg*. 1972, 54:1612–32.

Löw S, Erne H, Strobl U, et al. Significance of Scapholunate Gap Width as Measured by Probe from Midcarpal. *J Wrist Surg*. 2017, 06:316-324.

Magee T. Comparison of 3-T MRI and arthroscopy of intrinsic wrist ligament and TFCC tears. *AJR Am J Roentgenol.* 2009, 192:80–85.

Mahmood A, Fountain J, Vasireddy N et al. Wrist MRI arthrogram v wrist arthroscopy: what are we finding? *Open Orthop J*. 2012, 6:194–198.

Mat Jais IS, Tay SC. Kinematic analysis of the scaphoid using gated four-dimensional CT. *Clin Radiol*. 2017, 72:794.e1–794.e9.

Mataliotakis G, Doukas M, Kostas I, et al. Sensory innervation of the subregions of the scapholunate interosseous ligament in relation to their structural composition. *J Hand Surg Am*. 2009, 34:1413–1421.

Meade TD, Schneider LH, Cherry K. Radiographic analysis of selective ligament sectioning at the carpal scaphoid: a cadaver study. *J Hand Surg Am*. 1990, 15:855–862.

Megerle K, Pöhlmann S, Kloeters O et al. The significance of conventional radiographic parameters in the diagnosis of scapholunate ligament lesions. *European Radiology*. 2011, 21:176–181.

Messina JC, Van Overstraeten L, Luchetti Ret al. The EWAS classification of scapholunate tears: an anatomical arthroscopic study. *J Wrist Surg*. 2013, 2:105–109.

Mitsuyasu H, Patterson RM, Shah MA et al. The role of the dorsal intercarpal ligament in dynamic and static scapholunate instability. *J Hand Surg Am.* 2004, 29:279–88.

Moran SL, Cooney WP, Berger RA, Strickland J. Capsulodesis for the treatment of chronic scapholunate instability. *J Hand Surg Am*. 2005, 30:16–23.

Moran SL, Ford KS, Wulf CA, Cooney WP. Outcomes of dorsal capsulodesis and tenodesis for treatment of scapholunate instability. *J Hand Surg Am.* 2006, 31:1438-46.

Morley J, Bidwell J, Bransby-Zachary M. A comparison of the findings of wrist arthroscopy and magnetic resonance imaging in the investigation of wrist pain. *J Hand Surg Am*. 2001, 26:544–546.

Murphy BD, Nagarajan M, Novak CB et al. The Epidemiology of Scapholunate Advanced Collapse. *Hand (N Y).* 2018, 01:1558944718788672.

Nienstedt F. Treatment of static scapholunate instability with modified Brunelli tenodesis: results over 10 years. *J Hand Surg Am.* 2013, 38: 887-92.

Obdeijn MC, Tuijthof G JM, Van Der Horst C et al. Trends in Wrist Arthroscopy. *J Wrist Surg*. 2013, 2:239–24.

Overstraeten LV, Camus EJ, Wahegaonkar A et al. Anatomical description of the dorsal capsulo-scapholunate septum (DCSS)-arthroscopic staging of scapholunate instability after DCSS sectioning. *J Wrist Surg*. 2013, 2:149–154.

Özkan S, Kheterpal A, Palmer W et al. Dorsal Extrinsic Ligament Injury and Static Scapholunate Diastasis on Magnetic Resonance Imaging Scans. *J Hand Surg Am*. 2019, 44:641-648.

Pauchard N, Dederichs A, Segret J, Barbary S, Dap F, Dautel G. The role of three-ligament tenodesis in the treatment of chronic scapholunate instability. *J Hand Surg Eur Vol.* 2013, 38:758-66.

Picha BM, Konstantakos EK, Gordon DA. Incidence of bilateral scapholunate dissociation in symptomatic and asymptomatic wrists. *J Hand Surg Am*. 2012, 37:1130–1135.

Pliefke J, Stengel D, Rademacher G et al. Diagnostic accuracy of plain radiographs and cineradiography in diagnosing traumatic scapholunate dissociation. *Skeletal Radiol*. 2008, 37:139–145.

Pomerance J. Outcome after repair of the scapholunate interosseous ligament and dorsal capsulodesis for dynamic scapholunate instability due to trauma. *J Hand Surg Am*. 2006, 31:1380–6.

Rajan PV, Day CS. Scapholunate Interosseous Ligament Anatomy and Biomechanics. *J Hand Surg Am*. 2015, 40:1692-1702.

Rauch A, Arab WA, Dap F, Dautel G, Blum A, Gondim Teixeira PA. Four-dimensional CT Analysis of Wrist Kinematics during Radioulnar Deviation. *Radiology*. 2018, 289:750-758.

Ross M, Loveridge J, Cutbush K, Couzens G. Scapholunate reconstruction. *J Wrist Surg.* 2013, 2:110-5.

Salva-Coll G, Garcia-Elias M, Hagert E. Scapholunate instability: proprioception and neuromuscular control. *J Wrist Surg*. 2013, 3:136-140.

Slater RR, Szabo RM, Bay BK, Laubach J. Dorsal intercarpal ligament capsulodesis for scapholunate dissociation: biomechanical analysis in a cadaver model. *J Hand Surg Am*. 1999, 24:232–9.

Saupe N, Prussmann KP, Luechinger R et al. MR imaging of the wrist: comparison between 1.5 and 3 T MR imaging—preliminary experience. *Radiology.*2005, 234:256–264.

Schädel-Höpfner M, Böhringer G, Gotzen L et al. Traction radiography for the diagnosis of scapholunate ligament tears. *J Hand Surg Br*. 2005, 30:464–467.

Schadel-Hopfner M, Iwinska-Zelder J, Braus T et al. MRI versus arthroscopy in the diagnosis of scapholunate ligament injury. *J Hand Surg Am*. 2001, 26:17–21.

Scheck RJ, Kubitzek C, Hierner R et al. The scapholunate interosseous ligament in MR arthrography of the wrist: correlation with non-enhanced MRI and wrist arthroscopy. *Skeletal Radiol*. 1997, 26:263–271.

Schmid MR, Schertler T, Pfirrmann CW et al. Interosseous ligament tears of the wrist : a comparaison of mulit-detector row CT arthrograpgy and MR imaging. *Radiology*. 2005, 237:1008-1013.

Schweizer A, Steiger R. Long-term results after repair and augmentation ligamentoplasty of rotary subluxation of the scaphoid. *J Hand Surg Am*. 2002, 27:674–84.

Shahabpour M, De Maeseneer M, Pouders C et al. MR imaging of normal extrinsic wrist ligaments using thin slices with clinical and surgical correlation. *Eur J Radiol*. 2011, 77:196-201.

Shapeero LG, Dye SF, Lipton MJ et al. Functional dynamics of the knee joint by ultrafast, cine-CT. *Invest Radiol*. 1988, 23:118–123.

Shaw CB, Foster BH, Borgese M et al. Real-time three-dimensional MRI for the assessment of dynamic carpal instability. *PLoS One*. 2019, 14:e0222704.

Short WH, Werner FW, Green JK et al. Biomechanical evaluation of ligamentous stabilizers of the scaphoid and lunate. *J Hand Surg Am*. 2002, 27:991–1002.

Short WH, Werner FW, Green JK at al. Biomechanical evaluation of the ligamentous stabilizers of the scaphoid and lunate: Part II. *J Hand Surg Am*. 2005, 30:24–34.

Short WH, Werner FW, Green JK et al. Biomechanical evaluation of the ligamentous stabilizers of the scaphoid and lunate: part III. *J Hand Surg Am*. 2007, 32:297–309.

S**zabo RM, Slater RR, Palumbo CF, Gerlach T**. Dorsal intercarpal ligament capsulodesis for chronic, static scapholunate dissociation: clinical results. *J Hand Surg Am.* 2002, 27:978–84.

Taleisnik J. The wrist. Edinburgh: Churchill Livingstone; 1985.

Taleisnik J. Carpal instability. Current concepts review. *J Bone Joint Surg.* 1988, 70:1262–8.

Talwalkar SC, Edwards AT, Hayton MJ, Stilwell JH, Trail IA, Stanley JK. Results of tri-ligament tenodesis: a modified Brunelli procedure in the management of scapholunate instability. *J Hand Surg Br*. 2006, 31:110-7.

Totterman S, Tamez-Pena J, Kwok E et al. 3D visual presentation of shoulder joint motion. *Stud Health Technol Inform*. 1998, 50:27–33.

Van Den Abbeele KL, Loh YC, Stanley JK, Trail IA. Early results of a modified Brunelli procedure for scapholunate instability. *J Hand Surg Br.* 1998, 23:258-61.

Van Overstraeten L, Camus E. Arthroscopic Classification of the Lesions of the Dorsal Capsulo-Scapholunate Septum (DCSS) of the Wrist. *Tech Hand Up Extrem Surg*. 2016, 20:125–128.

Viegas SF, Yamaguchi S, Boyd NL et al. The dorsal ligaments of the wrist: Anatomy, mechanical properties, and function. *J Hand Surg Am*. 1999, 24:456–468.

Ward PJ, Fowler JR. Scapholunate Ligament Tears: Acute Reconstructive Options. *Orthop Clin North Am*. 2015, 46:551-559.

Wassilew GI, Janz V, Heller MO et al. Real time visualization of femoroacetabular impingement and subluxation using 320-slice computed tomography. *J Orthop Res*. 2013, 31:275–281.

Watson H, Ottoni L, Pitts EC et al. Rotary subluxation of the scaphoid: a spectrum of instability. *J Hand Surg Br*. 1993, 18:62–64.

Watson HK, Ashmead D IV, Makhlouf MV. Examination of the scaphoid. *J Hand Surg Am*. 1988, 13:657–660.

Watson HK, Brenner LH. Degenerative disorders of the wrist. *J Hand Surg Am*.1985, 10:1002-6.

Watson HK, Ballet FL. The SLAC wrist: scapholunate advanced collapse pattern of degenerative arthritis. *J Hand Surg Am*.1984, 9: 358 –365.

Wright TW, Dobyns JH, Linscheid RL et al. Carpal instability non-dissociative. *J Hand Surg Br*.1994, 19:763–73.

Zhao K, Breighner R, Holmes D III et al. A technique for quantifying wrist motion using four-dimensional computed tomography: approach and validation. *J Biomech Eng*. 2015, 137:074501–1–5.

ANNEXES

Annexe 1 : Questionnaire Quick Dash® en langue Française

1

Quick DASH

Veuillez évaluer vos possibilités d'effectuer les activités suivantes au cours des 7 derniers jours en entourant le chiffre placé sous la réponse appropriée

		Aucune difficulté	Difficulté légère	Difficulté moyenne	Difficulté importante	Impossible
1.	Dévisser un couvercle serré ou neuf	1	2	3	4	5
2.	Effectuer des tâches ménagères lourdes (nettoyage des sols ou des murs)	1	2	3	4	5
3.	Porter des sacs de provisions ou une mallette	1	2	3	4	5
4.	Se laver le dos	1	2	3	4	5
5.	Couper la nourriture avec un couteau	1	2	3	4	5
6.	Activités de loisir nécessitant une certaine force ou avec des chocs au niveau de l'épaule du bras ou de la main. (bricolage, tennis, golf, etc..)	1	2	3	4	5

		Pas du tout	Légèrement	Moyennement	Beaucoup	Extrêmement
7.	**Pendant les 7 derniers jours**, à quel point votre épaule, votre bras ou votre main vous a-t-elle gêné dans vos relations avec votre famille, vos amis ou vos voisins ? (entourez une seule réponse)	1	2	3	4	5

		Pas du tout limité	Légèrement limité	Moyennement limité	Très limité	Incapable
8.	Avez-vous été limité dans votre travail ou une de vos activités quotidiennes habituelles en raison de problèmes à votre épaule, votre bras ou votre main?	1	2	3	4	5

Veuillez évaluer la sévérité des symptômes suivants **durant les 7 derniers jours.** (entourez une réponse sur chacune des lignes)		Aucune	Légère	Moyenne	Importante	Extrême
9.	Douleur de l'épaule, du bras ou de la main	1	2	3	4	5
10.	Picotements ou fourmillements douloureux de l'épaule, du bras ou de la main	1	2	3	4	5

		Pas du tout perturbé	Un peu perturbé	Moyennement perturbé	Très perturbé	Tellement perturbé que je ne peux pas dormir
11.	**Pendant les 7 derniers jours**, votre sommeil a-t-il été perturbé par une douleur de votre épaule, de votre bras ou de votre main ? (entourez une seule réponse)	1	2	3	4	5

Le score QuickDASH n'est pas valable s'il y a plus d'une réponse manquante.

Calcul du score du QuickDASH = ([somme des n réponses] - 1) X 25, où n est égal au nombre de réponses.

1 *Questionnaire DASH*

Annexe 2 : Questionnaire PRWE® en langue Française

PRWE
Evaluation du poignet par le patient

Nom: _____ **Signature:** _____ **Date:** _____

Les questions ci-dessous vont nous permettre de comprendre les difficultés que vous avez rencontrées avec votre poignet la semaine dernière. Sur une échelle de 0 à 10, vous décrirez l'intensité moyenne des symptômes de votre poignet durant la semaine dernière. Veuillez répondre à TOUTES les questions. Si vous n'avez fait aucune des activités, veuillez ESTIMER la douleur ou la difficulté à laquelle vous vous seriez attendue. Si vous n'avez jamais fait l'activité, vous pouvez laisser l'item en blanc.

DOULEUR – Veuillez évaluer l'intensité moyenne de la douleur à votre poignet durant la semaine dernière en entourant le chiffre qui correspond le mieux votre douleur sur une échelle de 1 à 10. Le zéro (0) signifie que vous n'avez ressenti aucune douleur et le dix (10) signifie que vous avez ressenti la pire douleur jamais éprouvée ou que vous n'avez pas pu faire l'activité à cause de la douleur.

Evaluer votre douleur :

	Pas de douleur										Pire douleur jamais ressentie
Au repos	0	1	2	3	4	5	6	7	8	9	10
Lorsque vous faites une tâche avec un mouvement répétitif du poignet	0	1	2	3	4	5	6	7	8	9	10
Lorsque vous soulevez un objet lourd	0	1	2	3	4	5	6	7	8	9	10
Lorsque la douleur est à son comble	0	1	2	3	4	5	6	7	8	9	10
Avez vous souvent mal?	0	1	2	3	4	5	6	7	8	9	10
	Jamais										Toujours

FONCTION

A. ACTIVITES SPECTIFIQUES - Veuillez évaluer le niveau de difficulté que vous avez éprouvé à accomplir avec votre main atteinte chacun des gestes listés ci-dessous – au cours de la semaine dernière, en entourant le chiffre qui correspond le mieux à la difficulté éprouvée sur une échelle de 1 à 10. Le zéro (0) signifie que vous n'avez rencontré aucune difficulté et le dix (10) signifie que c'était tellement difficile que vous ne pouviez pas le faire du tout.

	Aucune difficulté										Incapable de faire
Tourner une poignée de porte	0	1	2	3	4	5	6	7	8	9	10
Couper de la viande	0	1	2	3	4	5	6	7	8	9	10
Boutonner ma chemise	0	1	2	3	4	5	6	7	8	9	10
Se lever d'une chaise	0	1	2	3	4	5	6	7	8	9	10
Porter un objet de 5 Kg	0	1	2	3	4	5	6	7	8	9	10
Utiliser du papier toilette	0	1	2	3	4	5	6	7	8	9	10

B. ACTIVITES HABITUELLES - Veuillez évaluer le niveau de difficulté que vous avez éprouvé à accomplir vos activités habituelles dans chacun des domaines listés ci-dessous, au cours de la semaine dernière, en entourant le chiffre qui correspond le mieux à la difficulté éprouvée sur une échelle de 1 à 10. Par activités habituelles, nous entendons les activités que vous faisiez avant d'avoir des problèmes avec votre poignet. Le zéro (0) signifie que n'avez rencontré aucune difficulté et le dix (10) signifie que c'était tellement difficile que vous ne pouviez pas faire vos activités habituelles.

	Aucune difficulté										Incapable de faire
Soins personnels (s'habiller, se laver)	0	1	2	3	4	5	6	7	8	9	10
Tâches ménagères (nettoyage, entretien)	0	1	2	3	4	5	6	7	8	9	10
Travail (votre emploi ou tâches quotidiennes habituelles)	0	1	2	3	4	5	6	7	8	9	10
Loisirs	0	1	2	3	4	5	6	7	8	9	10

Page 1 sur 1

Titre : L'intérêt de l'imagerie dynamique 4-Dimensions dans la prise en charge chirurgicale des instabilités scapho-lunaires

Résumé : L'instabilité scapho-lunaire est difficile à diagnostiquer et à traiter. En l'absence de traitement, elle évolue vers l'arthrose du poignet. Au stade statique, le diagnostic est évident lorsqu'une analyse radiographique minutieuse est effectuée, mais le choix du traitement chirurgical n'est pas aussi simple. Au stade dynamique, le diagnostic est plus difficile à poser sur la base unique de méthodes d'imagerie statiques (radiographies, tomodensitométrie ou IRM), ce qui justifie qu'une arthroscopie exploratoire puisse être nécessaire avant le traitement chirurgical. Bien qu'il s'agisse d'une procédure invasive, l'arthroscopie est considérée par de nombreuses équipes chirurgicales comme le gold standard pour explorer l'espace articulaire scapho-lunaire. L'imagerie dynamique, telle que le scanner dynamique quatre dimensions (4DCT), peut analyser les modifications des espaces articulaires du carpe lors des mouvements du poignet. Au vu des résultats de notre étude prospective, le 4DCT est apparu comme un outil pertinent multiparamétrique quantitatif et reproductible pour le diagnostic et le pronostic de l'instabilité scapho-lunaire suspectée, y compris pour les patients présentant des résultats radiographiques douteux. Les valeurs anormales des paramètres cinématiques semblent indiquer des changements biomécaniques significatifs dans les poignets dissociés. De plus, l'analyse 4DCT a démontré une correspondance avec l'analyse dynamique arthroscopique de l'espace articulaire scapho-lunaire. Plusieurs techniques de ligamentoplastie ont été décrites pour traiter l'instabilité scapho-lunaire réductible, chronique et sans lésions chondrales. Leur objectif commun est de corriger les anomalies radiologiques afin de prévenir des risques d'arthrose. Ces procédures ont servi de base à plusieurs études cliniques, et si ces dernières partagent de bons résultats cliniques similaires, l'aspect radiographique est très variable, où la récidive des anomalies radiologiques est fréquente. Ainsi, nous avons mis au point la ligamentoplastie scapho-lunaire et inter-carpienne (SLIC) qui utilise un transplant libre de Palmaris Longus pour reconstruire le complexe scapho-lunaire. Avec un suivi à court et moyen terme, nous rapportons des résultats cliniques et radiologiques satisfaisants, et aucun cas d'arthrose. Dans une étude cadavérique, nous avons évalué en 4DCT cette ligamentoplastie et fourni des preuves supplémentaires de son efficacité dans la réduction de l'instabilité scapho-lunaire et la restauration de la stabilité articulaire de ce couple. Enfin, nous avons conçu un dispositif de guidage des mouvements du poignet, afin d'augmenter la reproductibilité et l'homogénéité du mouvement lors de l'acquisition d'imageries dynamiques.

Mots-clés : Carpe, Instabilité scapho-lunaire, Ligamentoplastie, Poignet, Scanner dynamique quatre dimensions.

Title: Value of kinematic four-dimensional imaging in the surgical management of scapholunate instabilities

Abstract: Scapholunate instability is challenging to diagnose and to treat. If left untreated, it contributes to the development of wrist osteoarthritis. In the static stage, diagnosis is obvious when a careful radiographic analysis is performed, but the choice of surgical treatment is not as straightforward. In the dynamic stage, diagnosis is harder to make solely based on static imaging methods (radiographs, CT or MR arthrogram), which means exploratory arthroscopy may be required prior to surgical treatment. Despite it is an invasive procedure, arthroscopy is considered by many surgical teams, as the gold standard to explore the scapholunate joint space. Dynamic imaging, such as the four-dimensional computed tomography (4DCT), can analyze changes in the carpal joint spaces during wrist movements. Given our prospective study's findings, 4DCT appeared as a quantitative multiparametric and reproductible relevant tool for the diagnosis and prognosis of suspected scapholunate instability, including for patients with questionable radiography findings. Abnormal kinematic parameters values seem to be indicative of significant biomechanical changes in the dissociated wrists. Moreover, 4DCT analysis demonstrated correspondence with the arthroscopic dynamic analysis of the scapholunate joint space. Several ligamentoplasty techniques have been described to treat chronic reducible scapholunate instability without chondral lesions. Their common objective is to correct radiological anomalies in order to prevent risk of osteoarthritis. These procedures have served as the basis for several clinical studies and while all the latter share similar good clinical results, the radiographic aspect varies widely, with frequently the recurrence of radiological anomalies. Thus, we described the scapholunate intercarpal ligamentoplasty (SLIC) which uses a free Palmaris Longus graft to reconstruct the scapholunate complex. At short to mid-term follow-up, we report satisfactory clinical and radiological results, and no osteoarthritis wrist case. In a cadaver study, we reported the 4DCT evaluation of that ligamentoplasty and provided additional evidence of its effectiveness in reducing scapholunate instability and restoring scapholunate joint stability. Finally, we designed a device for guiding wrist movements in order to increase the reproducibility and homogeneity of the movement during dynamic imaging acquisition.

Keywords: Carpus, Four-dimensional computed tomography, Ligamentoplasty, Scapholunate instability, Wrist.